NAGOYA UNIVERSITY AFRICAN RIFT VALLEY EXPEDITION 1968 REPORT

DECEMBER 1969

Association for African Studies, Nagoya University
(Department of Earth Sciences)
Nagoya, Japan

SPECIAL VOLUME OF THE JOURNAL OF
EARTH SCIENCES, NAGOYA UNIVERSITY
DECEMBER 1969

CONTENTS

Nagoya University African Rift Valley Expedition (NUARVE) in 1968

Isao MATSUZAWA

Head of Nagoya University African Rift Valley Expedition
President of Association for African Studies, Nagoya University
Emeritus Professor of Nagoya University

(Received 21 April 1969)

PURPORT OF THE EXPEDITION

The African Great Rift System, traversing in the north-south direction from the north of Syria in the Middle East to Mozambique in southeastern Africa, with a total extension of 7,000 km or more, is an enormous chasm which deeply cuts the continent, and is indeed the world's greatest rift valley. This is a markedly unstable zoue of the earth, frequently subjected to volcanic and seismic activities and crustal movements even to this day, which accounts for all kinds of anomalies such as gravity, geomagnetism and the like. In contrast with this great rift system, there are the circum-Pacific tectogenic belts including our Japanese Islands, and the Alpine-Himalayan tectogenic belt. Though differing from rift valleys in the mechanism of formation, these belts are also affected by volcanic and seismic activities as well as by crustal movements, and are the most unstable parts of the earth.

In the study of the earth, it is of vital importance that the construction and development of continents, the problem of continental drift, and the relationship between the earth's crust and mantle are elucidated. Elucidation of these problems would be achieved only with the researches on tectogenic belts and rift systems that have undergone, and are still undergoing, many changes. From this viewpoint, study of the African Great Rift System, which is the largest of all rift systems of the continental crust and is located adjacent to the typical Alpine-Himalayan tectogenic belt, is the most important and requisite.

The writer has lately presented a new theory on the process and mechanism of formation of the African Great Rift System in his paper "A Study on the Formation of the African Rift Valley* (1966)", which has attracted attention of scientists home and abroad. According to his theory, the African Great Rift System was formed and developed in the tensional field due to the mantle's convection current, in a close relation to the formation and development of the Alpine-Himalayan tectogenic belt, under the influence of the construction of Arabia-African continental crust.

In order to develop the study based on this theory, on-the-spot investigations in the Great Rift System region and researches on the obtained results have to be accomplished. The Ministry of Education highly esteemed the significance of this study and granted a fund for overseas scientific researches. Also, several corporations of economic circles in Nagoya subscribed to the investigation fund. These valuable helps have enabled Nagoya University to organize the African Rift Valley Expedition for the purpose of field investigations.

The major object of the expedition is to develop the study of the African Great Rift System from the standpoint of comparative tectonics, by means of field work referring to the researches on the formation of great fault systems, the aspect of volcanic activity, the constitution and structure of the Precambrian basement, the deformation of basement rocks caused by crustal movements, and other phenomena.

Highly unstable parts of the earth's crust are represented by tectogenic belts and rift valleys. As already mentioned, a comparative tectonic study of stable land masses and unstable zones is important for elucidating the mechanism of development of continents.

PROGRESS OF THE PROJECT

In 1962, Nagoya University dispatched the Eastern Africa Scientific Investigation Commission, consisting of two investigators and several assistants, to four countries of northeastern Africa, namely Egypt, Sudan, Ethiopia and French Somaliland (Afars and Issas), for field investigations of geology and medical plants, and gained many valuable results. In the same year the Association for African Studies, Nagoya University made a start, supported by the late Dr. Seizo Katsunuma, former president of the university. Since then, the Eastern Africa Scientific Investigation Commission has continued the researches on the survey data and specimens obtained during the field trips, and has already published some twenty papers.

In April 1964, the writer took part in the committee for organizing the Japanese Association of Africanists. By appealing to the nation-wide re-

* Jour. Earth Sci., Nagoya Univ., **14**, 89-115 (1966).

searchers, the committee succeeded to establish the association. The second general meeting of the association of May 1965 and also the sixth general meeting of May 1969 were held at Nagoya University. At the meeting of April 1967, the Association for African Studies, Nagoya University invited Dr. Jean Dresch, President of the African Society of France and Professor of the University of Paris, as a guest lecturer.

Ever since its foundation, the Association for African Studies, Nagoya University has been in touch not only with the corresponding associations in Japanese universities but also with overseas universities and institutions concerned with African studies, such as the African nations, U.K., U.S.A. and France, in order to maintain and strengthen the mutual relations. In this way, the Association has come to set up the present project of expedition to the African Great Rift System region.

OUTLINE OF INVESTIGATIONS IN 1968

(1) *Object of the Expedition*

Based on the purport of the project the expedition party was to carry out field investigations with special reference to tectonic geology, petrology and geophysics in and around Tanzania and in southern Kenya for about four months of the dry season from July 1968.

The framework of the eastern African continent is composed of the extremely hard and massive large cratons and the less solid metamorphic belts which are zonally distributed with a marked linear structure of a dominant north-south trend. The African Great Rift System lies in these metamorphic belts.

According to the writer's theory, the African Great Rift System was formed in the tensional field on account of the mantle's convection current under a strong influence of the constitution and geologic structure of the continental crust, inclusive of the cratons and the metamorphic belts, and the formation of the rift system was contemporaneous with the compression of the Alpine-Himalayan tectogenic belt. The resultant lateral tensile movement of the continental crust caused depression belts by faulting to form rift valleys, and these valleys are fault systems and depression rifts as observed today. The fault systems occur in a discontinuous chain of échelon-arrangement, representing a series of shear fractures of elastic solid.

The Great Rift System which is represented by the chain of fault systems, *viz.* the chain of depression rifts, is divided into two zones, the Eastern Rift Valley (or Gregory Rift Valley) and the Western Rift Valley, showing a large scale échelon-arrangement on east and west sides of Tanganyika Shield (Craton).

As mentioned before, the greater part of the African Great Rift System

stretches roughly along the linear structure of the zonally distributed metamorphic belts out of the area of cratons. This suggests that the formation of the African Great Rift System was controlled and affected by the structure of the pre-existing metamorphic belts and cratons of the continental crust. In order to verify such relations it is requisite that the construction of the basement be clarified and the structure of each metamorphic belt and craton that constitute the basement be measured.

The region centering on Tanzania and southern Kenya is provided with these geologic elements and is located where the Eastern Rift Valley and the Western Rift Valley are developed in contiguity with Tanganyika Craton. The Tanganyika Craton and metamorphic belts, such as the Mozambique, Burundian-Karagwe-Ankolean and Rusizi-Ubendian Belts, are developed and well exposed in this region. Since the region is also characterized by Cretaceous kimberlite in Mwadui in the south of Lake Victoria, various volcanic rocks effused from late Cretaceous to Quaternary volcanoes as seen in Kenya and northern Tanzania, and post-Tertiary carbonatite in the Oldoinyo-Lengai volcanic area, the geotectonic and petrological studies are of special importance. Development of Tertiary and Quaternary rocks is better in this region than in other regions and, with the recent discovery of fossil man and stone implements in the Olduvai Gorge, it has become an important region for the late Tertiary to Quaternary chronology, which would also reveal the subsequent history of the African Great Rift System.

From the viewpoint of geophysics, too, this region presents many important problems characteristic to rift valleys, such as earthquakes, gravity anomaly, geomagnetic anomaly and anomalous high heat flow.

Thus, no other parts of Africa can rival this region in furnishing a suitable stage for the study of formation and development of the African Great Rift System. This is the reason the region was chosen for the expedition.

(2) *Subjects of field investigations*

In the field investigation, the tectonic geology party examined the fault systems forming rifts and associated fractures on either side of rift valleys, and the structure and interrelations of geologic units of basement rocks, with reference to the formation of rift valleys, so as to elucidate the formation mechanism and the process of development of fault systems that account for the rift valleys. Further, the party investigated the mutual relations between the structure of rift valleys and the geologic structures of basement framework and overlying volcanic series.

The petrology party studied the character and constitution of cratons and metamorphic belts of the basement that served as the stage of formation of the African Great Rift System, for the purpose of finding the relation of the construction of basement rocks to the rift valleys in the light of the formation

mechanism. The party also investigated the process and aspect of volcanic activities that are closely related to the formation of rift valleys.

The geophysical party carried out gravimetric measurements since gravity anomaly is found to be related to the structure of the Great Rift System. Characteristics of gravity anomaly accompanying the development of rift valleys have been revealed by various investigation parties, chiefly from England. However, many of these investigations were for explaining the relationship between the gravity anomaly on the whole and the underground structure. Consequently, the obtained results failed to reflect sufficiently the regional character and geologic structure of the rift valleys. Our investigation aimed at precise measurement of gravity anomaly, so far as the limits of accuracy permit, in certain areas of the Great Rift System, by referring to the data of tectonic geology and petrology.

(3) *Circumstances of field investigations*

Before the field work was commenced, the base of operations was set up in each of the following towns; Naivasha, Dodoma, Kigoma, Mbeya, Iringa, Arusha and Moshi. Field investigations were carried out in and around each base town, making full use of motor-vehicles. For base-to-base transportation, railways, cars and airplanes were utilized.

Major constituents of the basement which was the stage of formation of the African Great Rift System are Precambrian metamorphic rocks associated with granitic rocks. They are found as massive solid cratons and zonally distributed banded metamorphic belts, and the rift valleys are developed in the latter without exception. The region including Tanzania and Kenya is the most ideal field for investigation, where the Eastern Rift Valley and the Western Rift Valley run side by side in an échelon pattern with the Tanganyika Craton sandwiched between the two.

The investigation of fault systems as the principal elements of the structure of rift valleys and associated geologic series was performed chiefly in areas of Lake Naivasha, Lake Eyasi and Lake Manyara Rifts of the Eastern Rift Valley zone, and along Lake Tanganyika, Lake Rukwa, and in the Mbeya area of the Western Rift Valley zone. The petrological and structural studies of the basement rocks were also made in several areas such as Dodoma, Mwadui, Kigoma, Mbeya, Iringa and Morogoro, Arusha, and Moshi. The party paid special attention to the geologic structure, stratigraphy, lithologic facies and interrelations of the respective rock series, and examined macroscopic character of rocks and rock-forming minerals in the field.

The activity of the African Great Rift System was accompanied by several events of volcanism, which resulted in the extensive distribution of great quantities of basic volcanic rocks in and around the rift valleys, where the characteristic carbonatite and alkali volcanic rocks are known. There are

two types of development of volcanic rocks, one is a horizontal spread of volcanic series thickly accumulated on a very large scale as seen mostly in Kenya and Ethiopia, and the other is a vertical accumulation as exemplified by the volcanoes of Kilimanjaro, Meru, Kenya, Longonot, Susua and Oldoinyo-Lengai volcanoes group in the Eastern Rift Valley zone. The former type is generally older than the formation of rift valleys, and the latter is ascribed to subsequent volcanic activities. In the Western Rift Valley zone, however, there is scarcely detected any volcano except for two or three patches of volcanic rocks as seen in the environs of Lake Edward, Lake Kivu and in the Mbeya area. The elucidation of the nature of volcanic activities and the character of volcanic rocks may throw a new light on the formation mechanism and process of development of rift valleys. The investigation of volcanic series was made mainly along the eastern margin of the Lake Naivasha Rift, in the Kilimanjaro volcano area, in the area of Oldoinyo-Lengai volcanoes group, and in the Mbeya area.

Several cycles of tectogeny took place in the Precambrian period. In relation to these cycles the rocks of the Dodoman, Nyanzian, Kavirondian, Rusizi-Ubendian, Usagaran, Ukingan, Burundian-Karagwe-Ankolean, Bukoban series and 'Mozambique metamorphic belt', and several granite bodies were formed. On the whole, it would be possible to discriminate the cratons which were folded and metamorphosed 2,500–2,600 m.y. ago or earlier, such as Dodoman, Nyanzian, Kavirondisn and related granitic intrusions, from the metamorphic belts of later formation, such as the other Precambrian folded and metamorphosed series and associated granitic bodies. In the Cretaceous period, the activity of kimberlite and igneous carbonate rocks took place. Kimberlite is concentrated in the Tanganyika Craton, whereas igneous carbonate are distributed in the rift valley zones. In the period of late Cretaceous to early Tertiary, thickly accumulated volcanic series spread out horizontally to a large extent overlying the basement mostly in Kenya and Ethiopia. This volcanic series originated probably in large scale eruptions from great fissures, so the writer considers that these fissures might be forerunners of the African rift valleys. In the Tertiary and Quaternary periods, volcanic activities of a number of cones following the formation of rift valleys become cospicuous.

In the course of the field investigation, approximately 1,000 rock specimens were collected. After returning to Japan, the expedition party has been conducting optical, physical and chemical analyses of the collected rocks and minerals. Also, the party has entrusted the related institutions, such as the University of Tokyo, Tohoku University, Tokyo University of Education, Kyoto University and Kyushu University, with the radiometric age determination of the specimens, so as to clarify the relativity of the African Great Rift System and its basement rocks from the viewpoint of the formation mechanism.

When the data of the radiometric age determination are completed, we would be able to discuss the mechanism of continental growth and formation of the Great Rift System in a less abstract way.

The gravity anomaly investigation was focussed on the Kigoma-Lake Tanganyika area and the Mbeya area. Making use of all available roads and transport facilities, gravimetric measurements were carried out at intervals of about 3 km on an average. The interval of 3 km is rather large for precise investigation, but this was decided after taking into account the accuracy of the altimeter, the size of the area to be investigated, and the number of days to be spent. Thus, measurements were done at about 50 stations in the Kigoma-Lake Tanganyika area and about 100 stations in the Mbeya area, with Woldon's gravimeter. The gravity itself is accurate enough when the error in the altitude measurement is considered. Measurement of altitudes on the basis of atmospheric pressure usually involves error of 10 m or more, but by jointly using triangulation the party succeeded to lessen the error to several meters.

According to the result of the gravity investigation, the gravity anomaly in the rift valleys is very large, ranging from several tens to 100 mgal (with about 3 mgal error), which will suffice to prove the relation between gravity anomaly and geologic structure. The party believes that the character of the Great Rift System will be elucidated in detail, by correlating the combined results of the structural and petrological studies with the gravity anomaly map which is in preparation.

ADDITIONAL REMARKS

1. On the Birth of Mankind

It is reasonably presumed that the African continent is the birthplace of man. The presumption has been justified by the discovery of fossil man, *Zinjanthropus* and *Homo habilis*, in the Olduvai Gorge in the northern part of Tanzania, preceded by the finding of *Australopithecus* in Transvaal, Republic of South Africa. Through field investigations the expedition party attempted to reveal archaeologically the history of man, who was born some two million years ago in the natural environment of the Great Rift System which was subjected to crustal movement, several volcanic and seismic activities, and who ever since kept on developing by adapting himself to the circumstances.

2. On the Pathological Geography of Disease

In Africa are found a number of diseases, especially the infectious diseases that are either unknown or seldom found in other continents. Epidemiological statistics of these infectious diseases are very few, and little has been known about the cause, the frequency and the mode of decline of such diseases in various parts of Africa. Particularly in East Africa centering around

Tanzania, available information is next to nothing. Therefore, the expedition party intended to make a study of epidemiology of these specific disorders in Tanzania. It was hoped that the study would prove helpful to deduce the nature of diseases that must have affected pre-historic man, and would contribute as well to prevention of infectious diseases in this part of Africa.

MEMBERS OF THE EXPEDITION PARTY

D. Sc. Isao Matsuzawa:	Head of the Expedition: Professor of Tectonic Geology, Nagoya Univrsity
D. Sc. Isao Shiida:	Professor of Physical Geology, Nagoya University
D. Sc. Kanenori Suwa:	Assistant Professor of Petrology, Nagoya University
D. Sc. Kunihiko Miyakawa:	Associate Professor of Petrology, Nagoya Institute of Technology
D. Sc. Shinjiro Mizutani:	Associate Professor of Tectonic Geology, Nagoya University
M. Sc. Kenji Yairi:	Assistant Professor of Tectonic Geology, Nagoya University
D. Sc. Harumi Aoki:	Assistant Professor of Geophysics, Nagoya University
B. A. Giichi Ohmi:	Assistant Professor of Archaeology, Nagoya University
B. M. Hidehiko Kurimoto:	Assistant Professor of Medicine, Nagoya University

PROGRESS OF THE INVESTIGATION TRIPS

Date	*Course and Surveying Area*	*Matters*
July 19 21	Tokyo–Bombay–Nairobi	Leave Japan by air
July 22 23	Nairobi	Exchange of research informations
July 24 29	Nairobi–Naivasha Naivasha–Nairobi	Investigation of Naivasha Rift area
July 30 31	Nairobi–Dar es Salaam	Leave Nairobi by air
Aug. 1 6	Dar es Salaam	Exchange of research information and preparation of field survey in Tanzania
Aug. 7 12	Dar es Salaam–Mwadui Mwadui–Dar es Salaam	Investigation of Mwadui area
Aug. 13 21	Dar es Salaam	Exchange of research informations and preparation of field survey
Aug. 22 27	Dar es Salaam–Dodoma	Investigation of Dodoma area

Aug. 28 Sept. 7	Dodoma–Kigoma Kigoma–Dar es Salaam	Investigation of Kigoma area
Sept. 8 12	Dar es Salaam	Arrangement of data and preparation of field survey
Sept. 13 16	Dar es Salaam–Morogoro–Iringa–Mbeya	Transference to Mbeya and investigation along the way
Sept. 17 Oct. 8	Mbeya	Investigation of Mbeya area
Oct. 9 12	Mbeya–Iringa	Investigation of Iringa area
Oct. 13 29	Iringa–Dodoma–Arush and Moshi	Investigation en route and of Oldoinyo–Lengai volcanic area, Arusha and Moshi area, Kilimanjaro volcano area, Pare Mts. and Usambara Mts.
Oct. 30 Nov. 9	Moshi–Dar es Salaam	Arrangement of data and preparation of returning to Japan
Nov. 10 16	Nairobi–Cairo–Tokyo	Return to Japan

Members of the Expedition Party

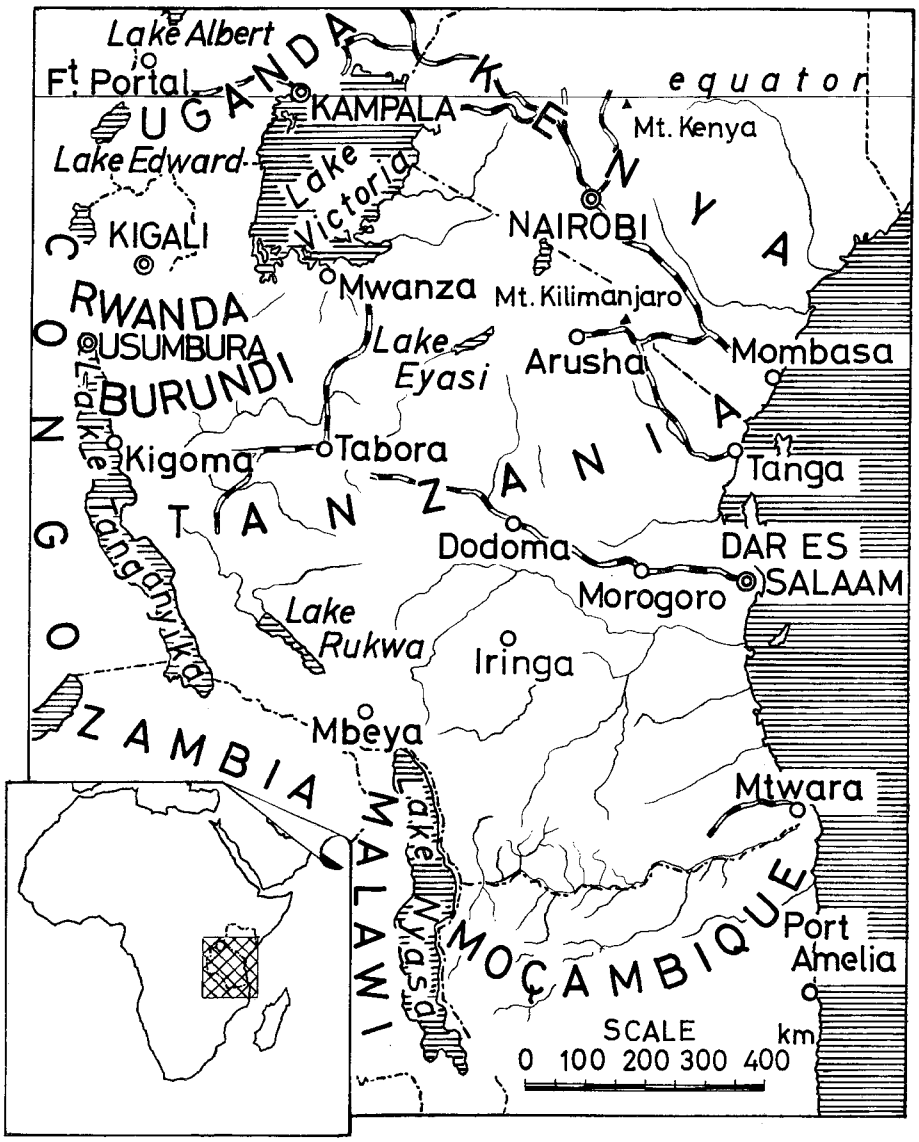

Map of Tanzania and its vicinity

Formation of the African Great Rift System

Isao MATSUZAWA*

(Received 16 August 1969)

CONTENTS

* Emeritus Professor of Nagoya University
President of Association for African Studies, Nagoya University
Haed of Nagoya University African Rift Valley Expedition (NUARVE)

ABSTRACT

Tectogenic belts and rift valleys, or fracture belts, are weakest and unstable zones of the earth, the former resulting from crustal compression and the latter by crustal tension. Motive force of such crustal disturbances is most reasonably attributed to convection current in the mantle. Since the continental crust has very complex construction and structure, the influence of stress caused by the mantle's convection current would be variable, and as a result the zones of disturbance would assume different shapes.

The Alpine-Himalayan tectogenic belt and the African Great Rift System are of contemporaneous formation, and the former reflecting compression and the latter reflecting tension are intersecting at right angles in a T shape. In view of the scope of disturbance, however, the former is the greatest diastrophic belt on the earth and the latter is only an auxiliary belt. Therefore, it is duly presumed that at the time of formation of these belts, the convection current in the uppermost part of the mantle was converging toward the Alpine-Himalayan tectogenic belt, and in that case the Arabia-African continental mass must have been placed in the field of tension. In elucidating the formation mechanism of the African Great Rift System, it is of great importance to find out how the tensile force affected the construction and structure of the continental crust. From this viewpoint the writer previously published "A study on the Formation of the African Rift Valley" as a tentative theory. The theory has been re-examined through the recent field observations in East Africa, and a supplemented and corrected theory on the formation mechanism of the African Great Rift System is presented in this paper.

INTRODUCTION

In the study of our earth, one of the most interesting problems would be an elucidation of the mechanism that formed diastrophic belts and of the

causative crustal movements. Tectogenic belts and great rift systems are the notable diastrophic belts of the earth's crust. The present writer believes that investigations of the formation mechanism of such diastrophic belts, the character of related crustal movements, and the interrelations between the two are of a great importance in elucidating the problems concerning the crust and the mantle.

The Alpine-Himalayan tectogenic belt, formed by the Alpine tectogenic cycle, is the most typical tectogenic belt. Since it has been studied by a large number of geologists, its features are fairly well known. The African Great Rift System, which is the largest rift system in the continental crust, extends in the N–S direction and abuts on the E–W trending Alpine-Himalayan tectogenic belt, thus forming a T-shaped intersection.

The writer has been deeply interested in the study of diastrophic belts and crustal movements. This is the reason he selected the African Great Rift System as a field of his study, with an intention of elucidating its geological and geophysical characters, and its correlation with the Alpine-Himalayan tectogenic belt which is located at a right angle to this rift system.

After publishing the paper entitled "A Study on the Formation of the African Rift Valley" (1966) [55], the writer visited East Africa in 1968 and, in collaboration with six researchers, he carried out geological and geophysical surveys in various parts of the great rift system covering Kenya and Tanzania, for four months from July to November. During this period, the writer found many new facts and collected great quantities of materials for study. Although the previous paper may need revision in some points, the results obtained through these trips have strongly supported his theory on the formation of the Rift Valley System, and he has become more convinced of his theory.

The followings were the principal points of discussion in the writer's previous paper:

1) The writer maintains the idea that the crustal movements that form diastrophic belts are attributed to the mantle's convection current. Especially he emphasizes that a tectogenic belt is formed where the mantle's convection current moving laterally converged from the convection cells on two sides and then headed downward, so that the crust of this part would be dragged in and compressed by the lateral pressure from both sides, thus resulting in a tectogenic belt there.

2) A prevalent view up to now has been that the African Rift Valley was formed where the mantle's convection current ascended and diverged into convection cells on both sides, causing tension of the crust toward both sides. However, the writer is against the view for the reasons given below.

3) The writer attached importance to the fact that the African Great Rift System was formed contemporaneously with the Alpine-Himalayan tectogenic belt. In this connection, he regarded it also important that the Alpine-

Himalayan tectogenic belt, which is an E-W trending compression zone of the crust, abuts on the African Great Rift System, which was formed by tension of the crust and extends N-S, so that a T-shaped intersection was produced. He explained the mechanism by which these two belts were formed contemporaneously within the same region.

4) The Alpine-Himalayan tectogenic belt ranks among the greatest diastrophic belts of the crust. Compared with this, the African Great Rift System is much smaller in scope. Although the two are of synchronous formation, the latter is only subordinate to the former.

5) Should the Alpine-Himalayan tectogenic belt be reflecting a converged zone of the mantle's convection current, a reasonable explanation must be given by which the location of this belt, representing a compression zone, and the African Great Rift System, which was formed by tensional movement, are well harmonized with the shape and arrangement of the mantle's convection cells, as well as with the direction of the convection current.

According to the writer's theory, the African Great Rift System was formed under strong control and influence of the geologic structure of the continental crust—the foliated structure of the Mozambique metamorphic belt showing a definite trend, and its structural position against craton. That is to say, although the African Great Rift System was formed in the tensional field under the influence of tension, its structural form and the direction of its extension are not reflecting the diverged zone of the mantle's convection current, but are exemplifying the result of such effects. In other words, formation of the African Great Rift System is attributed to the construction and the remarkable directivity of geologic structure of the continental crust.

6) As to the field of tension in which the African Great Rift System was formed, the writer explained as follows: During the Alpine tectogenic cycle, the lateral movement of the convection current within the mantle beneath the African continental crust had created a tensional field extending toward the converged zone of current where the tectogenic belt was formed along the margin of the Gondwanaland of those days.

The above-mentioned points of discussion in the writer's theory were re-examined during the recent four-month long field work by which various parts of the Rift System were investigated and numerous new facts were gained.

The field observation proved especially fruitful as it confirmed the construction and geologic structure of the "Tanganyika Shield"—a craton located between the Eastern Rift Valley (Gregory Rift Valley) and the Western Rift Valley constituting the African Great Rift System and being deviated largely from each other in an echelon pattern—and also clarified the relationship between the Eastern Rift Valley and the Western Rift Valley by comparing their construction and geologic structure.

Therefore, in many parts this paper overlaps the previous one, but the results of later studies and the materials obtained through the field work are included here, and the writer's viewpoints are emphasized all the more.

I. GENERAL ASPECT OF THE AFRICAN GREAT RIFT SYSTEM

The African Great Rift System is a great chasm of the crust, running north-south in the Arabian Peninsula and the eastern part of the African continent from the north of Syria in the Middle East to Mozambique in southeastern Africa [1]. With a nearly constant width, generally between 30 km and 60 km, and with a total extension exceeding 7,000 km or more, this system presents a remarkable zone of depression caused by faulting. This is indeed the greatest of all rift systems incised into the continental crust.

In the north it extends northward to southern Turkey near the northeastern corner of the Mediterranean Sea, and abuts on the Alpine-Himalayan tectogenic belt. Then it stretches along the coast of the Mediterranean Sea to pass through the Gulf of Aqaba and enter into the Red Sea. After that, it turns southwestward, via the Red Sea Rift, passes through the Abyssinian Rift of Ethiopia, and advances farther south extending over Kenya and Tanzania. The part so far mentioned is called the Eastern Rift Valley (Gregory Rift Valley). The Western Rift Valley is largely deviated to the west, and shows an echelon arrangement against the Eastern Rift Valley. It is seen to stretch southward from the Lake Albert Rift in western Uganda to the Lake Tanganyika Rift and, passing through the Lake Malawi Rift*, it extends farther to the south of the Zambezi River of Mozambique and reaches the southwestern Indian Ocean (Fig. 1) [1, 12, 34, 35].

A detailed observation of the African Great Rift System would reveal that, in addition to the conspicuous echelon arrangement of the Eastern Rift Valley and the Western Rift Valley, minor breaks and changes of trend are found everywhere, presenting irregular echelon patterns; the rift valleys are also branching off locally. Consequently, the African Great Rift System can be regarded as a long chain of fault-depressed zone formed by several discontinuous fault systems. In many places, the margins of the great rift system are bounded with echelon faults, and the rift system itself is broken into echelon-arranged parts. The form of this echelon chain is similar to that of a certain kind of fracture system in an elastic solid body caused by shearing. Special attention should be paid to this fact.

Topographically speaking, high mountains of the African continent occur mostly in the eastern part, except the Atlas Range that stretches along the Mediterranean coast over a distance about 2,500 km. Thus, eastern Africa,

* Lake Nyasa is lately renamed Lake Malawi, so that the Lake Nyasa Rift is called the Lake Malawi Rift in this paper.

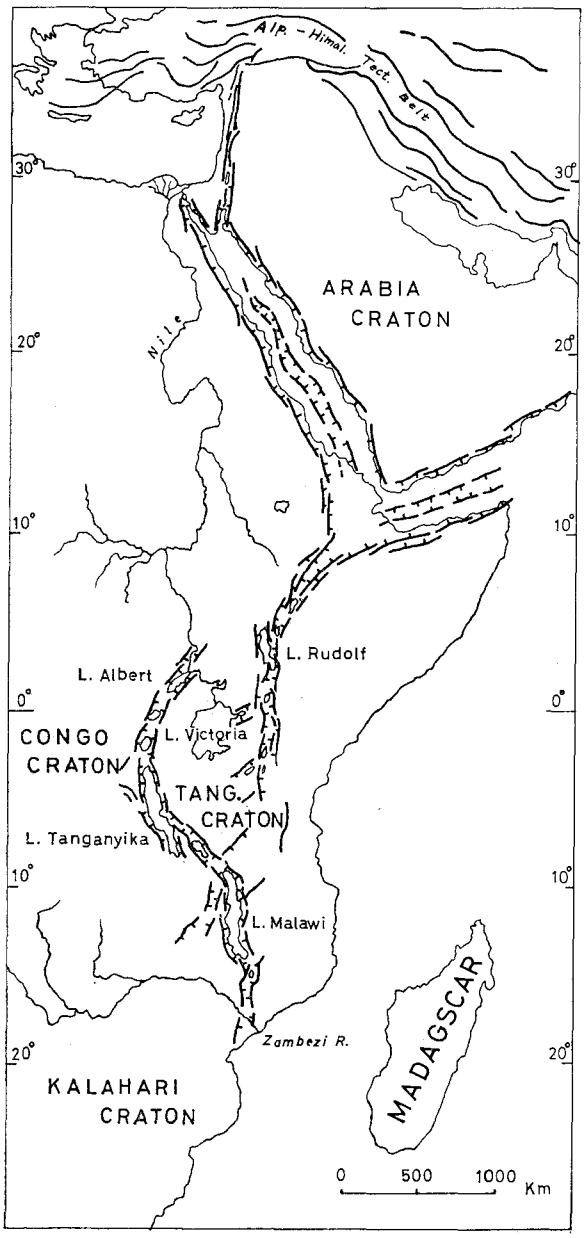

FIG. 1. Distribution map of the African Great Rift System.

except for the coastal regions, is characterized by the topography of tablelands and mountains higher than 1,200 m above sea level. The African Great Rift System runs lengthwise through these highlands, and is bounded on both sides always with distinct fault scarps. The relative height of the highlands is as great as several hundred to two thousand and several hundred meters from the bottom of the rift valley. The bottom of the rift valley has a considerable relief on account of deposition of later sediments and formation of younger volcanoes and lakes.

A large number of old and young volcanoes are found to concentrate in

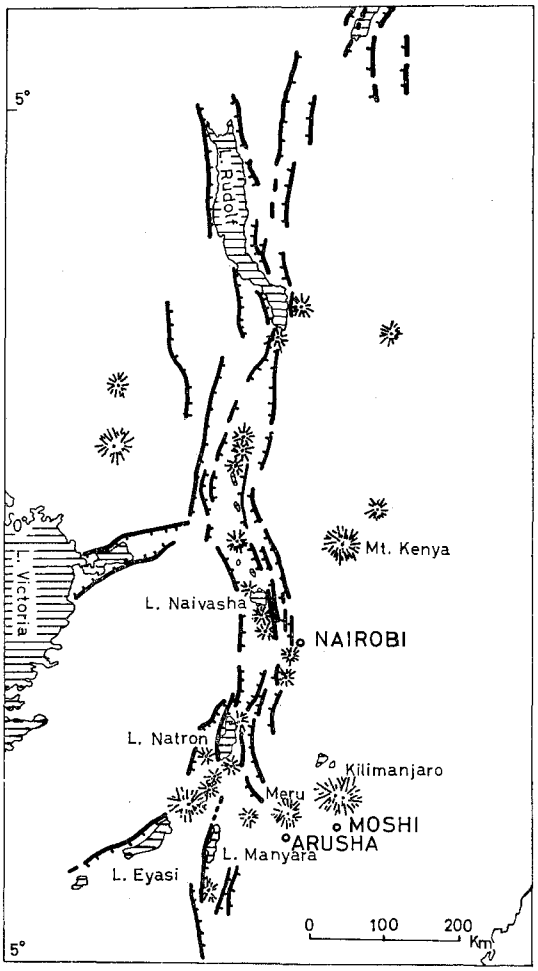

FIG. 2. Map showing the distribution of younger volcanoes located in and around the African Great Rift System from the Ethiopian border to the northern part of Tanzania.

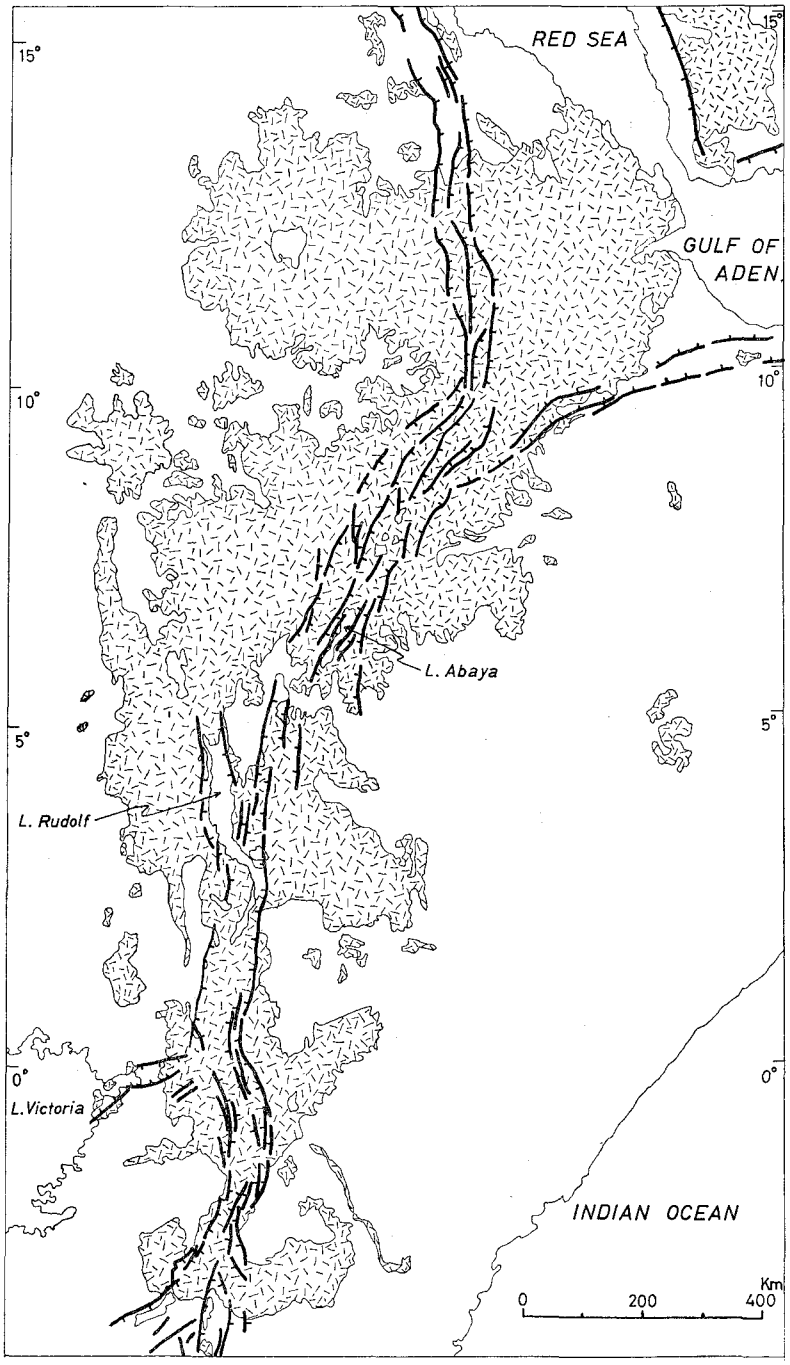

FIG. 3. Distribution of old and young volcanic series in the region of the Eastern Rift Valley.

and around the rift valley (Figs. 2 and 3). Issue of vapor and gush of hot spring along cracks are also noticed in places. These features suggest that volcanic activity is intimately connected with the formation of the great rift system. Shallow-focus earthquakes are frequent also in and around the rift valley. In some areas it seems that crustal movement is taking place along faults.

As indicated by the above-mentioned phenomena, the African Great Rift System is an unstable belt of the earth, and volcanic activity [27], crustal movement and earthquake [10] are still occurring at present. Another noticeable fact is that in the rift valley the geothermal flux is high and anomaly of gravity and geomagnetism [6, 29, 32, 64] is particularly conspicuous.

Judging from these phenomena and the nature of volcanic rocks, which indicate vigorous activity of dense basic magma [5, 27, 29], it would be reasonable to consider that the formation of the African Great Rift System was closely related to some movement within the mantle.

The character of the African Great Rift System is not entirely uniform throughout its extension over 7,000 km. As a matter of fact, (a) the rift system in the African continent, (b) the Red Sea Rift and the Gulf of Aden Rift, and (c) the rift system of Arabia are more or less different in character and in formation mechanism. Nevertheless, since all these were formed in the same period and constitute one chain, the cause of their formation must have been the same. Therefore, a theory to elucidate their formation mechanism and the process of their development ought to be comprehensive enough to explain inclusively the above-named three regions.

II. GEOPHYSICAL CHARACTER OF THE AFRICAN GREAT RIFT SYSTEM

Remarkable anomaly of gravity is commonly observed in rift valleys [6, 29, 31, 43]. Gravity measurement was carried out in various parts of the African Great Rift System. As a result, negative Bouguer anomaly of −50 mgal was recorded from the Lake Albert Rift in the northernmost part of the Western Rift Valley (Figs. 4 and 5) [6, 29]. Also in the Lake Tanganyika Rift, Lake Rukwa Rift and Lake Malawi Rift, negative Bouguer anomaly around −50 mgal was recorded [23. 29, 31]. In the Eastern Rift Valley, too, about −50 mgal anomaly was recorded from the Lake Rudolf Rift, Lake Magadi Rift and Lake Eyasi Rift [6, 14]. Negative Bouguer anomaly in the Gulf of Suez Rift was −50 mgal, and in the Gulf of Aqaba Rift it was −80 to −90 mgal [29]. Thus, except for some special cases, the value around −50 mgal or more may be regarded as a general value of negative gravity anomaly amplitude in the African Great Rift System. According to the result of the gravity investigation through our field work, the negative gravity anomaly in the rift valleys in Tanzania is very large, ranging from several tens to 100

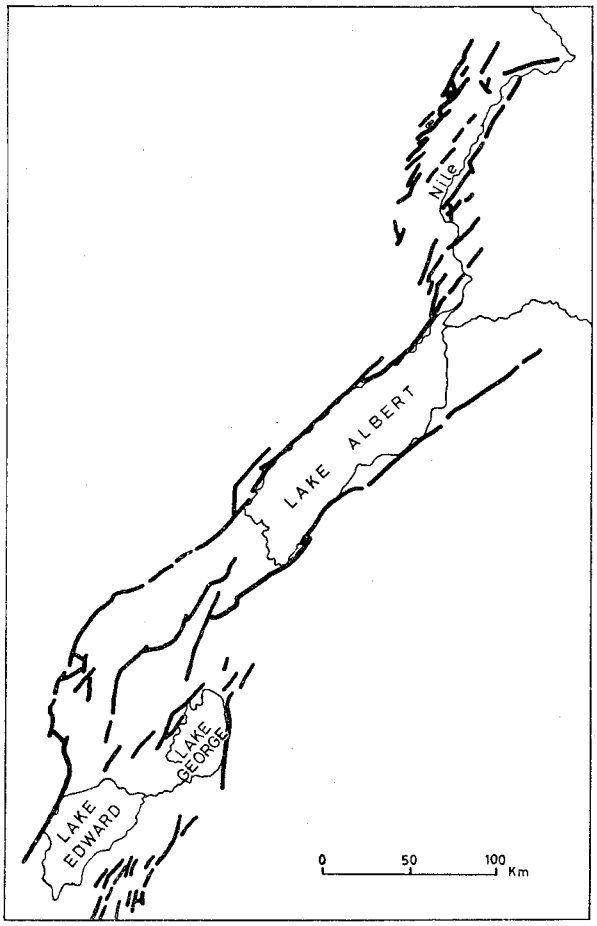

FIG. 4. Structural sketch map of the Lake Albert Rift and the Lake Edward Rift.

mgal.

The fact that the rift valleys in the continental crust show negative gravity anomaly means that the underground portion of the rifts is composed of a relatively light material down to a greater depth, as compared with the portion on either side. In other words, it suggests that a part of the crust (continental crust), whose density is smaller than other parts, was depressed under the ground deeper than other parts on either side.

However, the gravity anomaly in the Red Sea Rift and the Gulf of Aden Rift is markedly different in aspect from that in the above-mentioned continental areas [13, 26, 30, 65, 91]. The Red Sea extends for about 2,000 km from NW to SE. Its width is one hundred and several tens of kilometers in the northern part, and becomes wider southward until it attains to about 300 km, but the

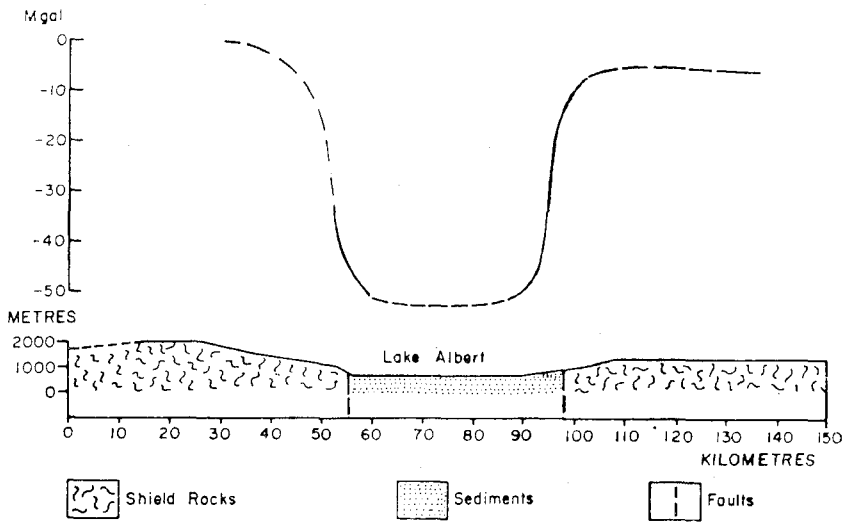

FIG. 5. Gravity profile over the Lake Albert Rift (after Girdler, 1964).

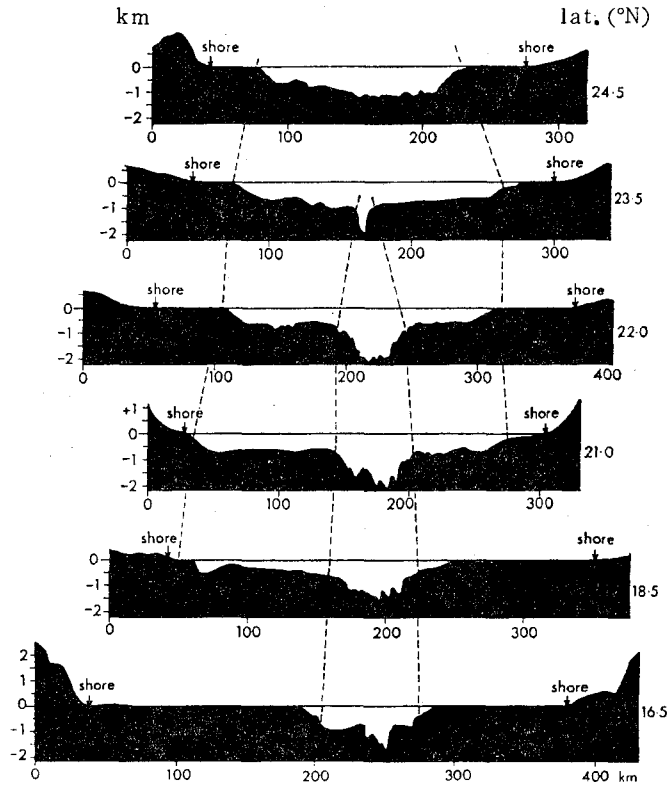

FIG. 6. Bottom topography of the Red Sea (after Drake and Girdler, 1964).

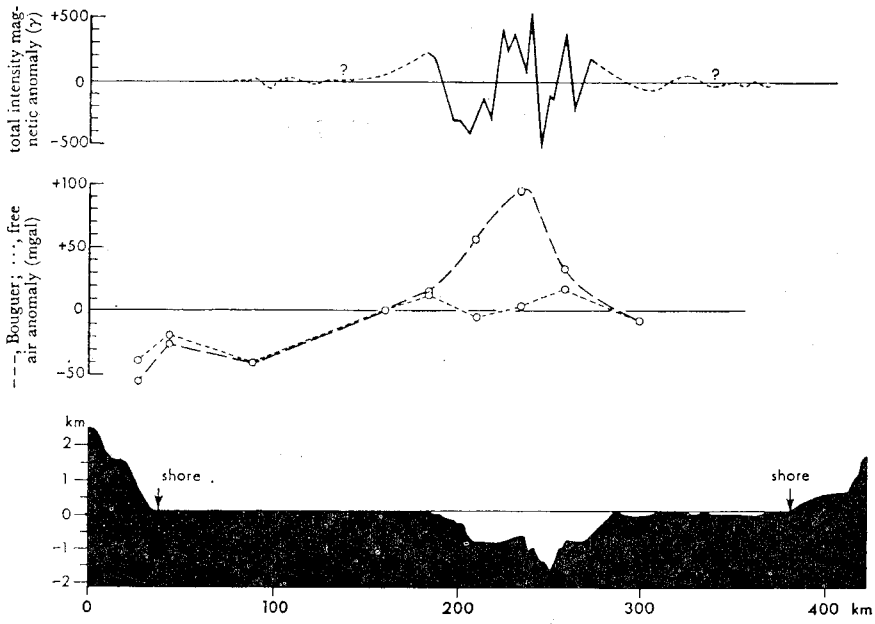

FIG. 7. Gravity and magnetic profiles for the Red Sea at latitude 16°N (after Drake and Girdler, 1964).

depth is generally uniform, being about 600 m or less, thus forming a shallow sea bottom on the whole. But its central part, south of lat. 24°N, is deeply incised by a narrow trough running in the same direction as the Red Sea. This narrow deep trough also increases its width from 10-odd km in the north to about 60 km in the south, with a depth ranging from about 1,000 m to about 2,000 m. The writer calls this double trough the Red Sea Rift (Figs. 6 and 20). In the central narrow deep trough of the Red Sea Rift, remarkable positive Bouguer anomaly, ranging from +80 to +100 mgal in amplitude, has been observed (Fig. 7) [13, 29, 30]. It is noteworthy that the anomaly is positive there, reverse to the negative anomaly in the continental rifts. The Gulf of Aden Rift, southeast of the Red Sea, also has a double trough structure (Fig. 20) and in the central narrow deep trough, 50–60 km wide, conspicuous positive anomaly has been recorded [65, 91].

The fact that the marked positive gravity anomaly is observed in the area from the Red Sea Rift to the Gulf of Aden Rift suggests that a relatively heavy material, namely, a rock body of high density, as compared with the material on both sides, exists below the central deep trough in these rifts.

The central deep trough in the Red Sea Rift and another in the Gulf of Aden Rift show also remarkable magnetic anomaly [13, 29, 30, 65]. In the former, the magnitude of anomaly is 1,200 gamma and the gradient is 200 gamma/

km (Fig. 7), and in the latter the amplitude is as large as 2,200 gamma. The geothermal flux, too, is unusually high in these deep troughs.

All the above facts support the idea that intrusive igneous bodies of a large density had filled the fissure on a large scale and then ascended to a very shallow depth of the crust beneath the central deep troughs. The calculated value of the magnetic intensity of the uppermost limit of the intrusive bodies is in the order of approximately 2×10^{-3} E.M.U./cm^3. This value agrees well with the value of basic igneous bodies. Hence it would be reasonable to assume that the rock bodies underlying the central deep troughs are simatic basic intrusives similar to the oceanic crust material.

The cross section of the underground structure of the southern part of the Red Sea, divided by the refraction velocity of seismic waves, reveals a remarkable difference in construction between the part beneath the central deep trough and the part beneath the shallow shelves on both sides (Tables 1 and 2) [30]. As seen in Table 1, the part below the 1,320 m deep bottom of the central deep trough is composed of sediments as thick as 3,980 m, locally interbedded with lava flows (?) (2.2–2.4 g/cm^3 in density), and a basic intrusive body (3.0 g/cm^3 in density) is inferred to underlie the sediments. On the other hand,

TABLE 1. STRUCTURAL PROFILE BENEATH THE CENTRAL TROUGH OF THE RED SEA (after Girdler, 1965)

	Velocity (km/sec)	Density (g/cm^3)	Thickness (km)	Pressure (10^2 kg/cm^2)
Sea water	1.54	1.1	1.32	1.45
Sediments	3.00	2.2	0.86	1.90
Lava? and Sediments	4.25	2.4	3.12	7.48
Basic intrusives	7.08	3.0	29.70	87.91
Total			35.00	98.74

TABLE 2. STRUCTURAL PROFILE BENEATH THE SHELVES OF THE RED SEA RIFT (after Girdler, 1965)

	Velocity (km/sec)	Density (g/cm^3)	Thickness (km)	Pressure (10^2 kg/cm^2)
Sea water	1.54	1.1	0.28	0.30
Loose sediments	1.85	1.8	0.14	0.26
Coral reef (?)	2.62	2.1	0.66	1.39
Evaporites	3.73	2.3	2.85	6.55
Granitic shield rocks	5.89	2.8	13.57	38.00
Basic intrusives		3.0	17.50	52.50
Total			35.00	99.00

as Table 2 shows, the part below the 280 m deep bottom of the shallow shelves is composed of 3,650 m thick sediments (1.8–2.3 g/cm^3 in density), which seem to be underlain by a granitic body (continental crust) of 13,570 m thick (with density 2.8 g/cm^3), and farther below by a basic body (with density 3.0 g/cm^3).

If the underground density to a depth of 35 km below the sea level, which roughly corresponds to the Mohorovičić discontinuity, was compared between the central deep trough and the shelves on both sides (Tables 1 and 2), it would reveal a conspicuous difference between the two. For instance, at a depth of some 15 km the disparity of about 0.2 g/cm^3 in density seems to be brought about between the two.

Thus, it is a noticeable fact that the Red Sea Rift and the Gulf of Aden Rift have the nature different from the continental rifts of Africa. Accordingly, even though all these rifts may have formed under the identical conditions, their formation mechanism should be different.

III. GEOTECTONIC FEATURES IN RELATION TO FORMATION OF THE GREAT RIFT SYSTEM

1. Relations between continental rift system and oceanic rift system

On the floor of the Indian Ocean, Atlantic Ocean and Pacific Ocean, enormous ranges of submarine mountains (ocean ridges) are stretching over a great distance on a global scale, and along their crestline, almost without exception, runs a deep cleft, generally 15 km to 50 km wide and 800 to 1,800 m deep [39, 40, 43]. In this cleft, the geothermal flux is unusually high and anomaly of gravity and geomagnetism is also remarkable. Besides, shallow-focus earthquakes are frequent in and around the cleft. Thus, the cleft makes a conspicuous shallow earthquake zone along the ocean ridges.

On the other hand, a shallow earthquake zone is noticeable also along the continental rift system [10, 30, 51, 78], as mentioned already. The similarity between the continental rift system and the submarine cleft, in the anomaly of gravity and geomagnetism as well as in the shape, may lead many geophysicists to a belief that these two are a result of the same mechanism, and in this connection they maintain that the African Great Rift System is continuous, via the Gulf of Aden Rift, with the Carlsberg Ridge and farther extends to join the Mid-Indian Ridge in the Indian Ocean [17, 26, 40].

However, in spite of the close similarity of shape, a problem remains as to whether the continental rift system and the submarine cleft were originated from the same cause and were formed by the same mechanism, since the continental rift system is a fracture of the continental crust (sialic crust) whereas the submarine cleft is that of the oceanic crust (simatic crust). At the present stage it is not known for a fact that the Gulf of Aden Rift is directly connected with the Carlsberg Ridge Rift to a certainty.

Therefore, it would be desirable to discriminate the continental rift system from the oceanic rift system and study the character of these two kinds of rifts before their relationship is discussed.

2. Convection current and its relation to the formation of continental rift system

It is said that thermal convection is taking place within the mantle, moving in several convection cells (mantle convection theory). Heat energy of the convection turns into kinetic energy and, in the uppermost part of the mantle where the ascending convection current diverges to right and left, the kinetic energy affects the overlying crust and causes a great fracture; but where the convection currents from two directions converge into one descending flow, the energy works to drag in the overlying crust, and the resultant compressive force will build up a tectogenic belt. This theory is supported by many scientists today. Laying aside the numerical values of thermodynamic calculations concerning heat flow and velocity of convection current and its stress, the most fascinating and noteworthy point of the mantle convection theory is that the theory can explain well the formation of tectogenic belts and rift valleys. For the theory to be substantiated, however, the shape and phenomena of diastrophic belts of the crust ought to have a correlativity with the form of convection current in the mantle. But, no relevant view has ever been expressed on such correlationship.

Supposing the theory is acceptable, it must clarify that the trend and location of the tectogenic belts which reflect the zone of compression where the lateral convection currents from two directions converge into one descending flow, and the rift systems which reflect the field of tension where the ascending flow of convection current diverges right and left, are correlative with the form and arrangement of convection cells in the mantle.

The writer, attaching importance to the facts to be mentioned in the following section, and also to the form and arrangement of convection cells, has reached a judgement that the African Great Rift System is not reflecting the location of diverged zone of ascending convection current, and he has deduced a mechanism of formation of the rift system as will be explained later.

3. Relationship between the Alpine-Himalayan tectogenic belt and the African Great Rift System

The major tectogenic movement, by which the Alpine-Himalayan tectogenic belt was formed, began in the Miocene epoch and continued to the Pliocene epoch of the Tertiary period. But its forerunning movement had started as early as Jurassic of the Mesozoic era. Crustal deformation originating from this tectogenic movement is still going on. The African Great Rift System was formed also during the period from Miocene to Pliocene, but precursory movements, such as subsidence and upheaval, associated with large scale volcanic activities, already took place since Mesozoic to early Tertiary;

earthquakes and volcanic activities are taking place even at the present time.

Attaching importance to the fact that the Alpine-Himalayan tectogenic belt and the African Great Rift System are contemporaneous, that the two are intersecting at right angles in a T shape, and that the latter is a smaller scale diastrophic belt subordinate to the former, the writer maintains as follows: Assuming the form and arrangement of convection cells within the mantle at the time of formation of the Alpine-Himalayan tectogenic belt, the African Great Rift System is considered to have been formed in the field of tension, but its location does not necessarily reflect the diverged zone of ascending convection current. In the following section the writer will explain the formation of the African Great Rift System.

4. Character of faults of the great rift system

Concerning the type of faults that were causative of the African Great Rift System there have been two different views. Some people maintain that tension in the crust had produced parallel normal faults and the intermediate area was depressed, forming this great rift system. Others insist on compression of the crust by which parallel reversed faults were developed and the both sides were upraised relatively, resulting in the rift valley in the intermediate area. In other words, whether the faults were normal or reversed has been the subject of controversy. However, it would not be proper to decide whether the great rift system is a result of crsutal compression or of tension, merely from the character or form of faults observable on the surface.

According to the latest geological observation in the field, all the faults on either side of the rift valley have the features of gravity-fault due to tensional force, and none shows a compression-fracture structure of thrust-fault type. In many cases the faults on both sides of the rift valley comprise several normal faults that step down toward the inner side. In topography, too, these faults present conspicuous fault scarps as will be described later.

R. W. Girdler holds a view that the African Great Rift System is a fault-depression belt due to tension, for the following reasons: Presuming the both sides of the rift are normal faults, the values of gravity anomaly calculated from various data obtained in the Lake Albert Rift agree quite well with the values of that actually measured in this rift, but if the faults are presumed to be reversed, no such good agreement is found between the calculated values and the measured values [29]. His theory involves several assumptions on the dip of fault plane, depth of faults and so forth. From the results of our geological observation and from various other data, it seems reasonable to think that the great rift system was formed under the influence of tension.

IV. CHARACTERISTICS OF THE STAGE OF FORMATION OF THE AFRICAN GREAT RIFT SYSTEM

1. Continental rift system

The continental crust and the oceanic crust are markedly different in nature. The former comprises sial (granitic) layer in the upper part and sima (basaltic) layer in the lower part; the latter is composed of the basaltic layer, devoid of the granitic layer, and is continuously distributed below the ocean floor. Accordingly, there is a conspicuous difference of physical properties between the two kinds of crust. This is a very important point. In considering the mechanism of formation, the continental rift system should be treated separately from the oceanic rift system.

Suppose the kinetic energy of the lateral movement of the convection current in the uppermost part of the mantle had brought forth the tension to the overlying crust to form the rift system, then the resultant rift system can be regarded as a series of fractures, namely, a shear-fracture zone. Therefore, the formation and shape of the fracture zone must have been largely influenced by the properties and structure of the materials constituting the crust. The continental rift system and the oceanic rift system must have been formed by different mechanism, as the properties of the crust are different between the two.

Accordingly, before the formation of the great rift system of the African continent is discussed, it is necessary to elucidate the construction and geologic structure of the crust of this continent where the great rift system was formed. The writer believes that the behavior and process of formation of the African Great Rift System are closely related to, and greatly influenced by, the construction and geologic structure of the Arabia-African continental crust. In this connection, the average thickness of the earth's crust is supposed to be 30-odd km, but in the eastern part of Africa where the great rift system is present, the crust, especially the granitic layer, is very thick, probably 50–60 km or more, because it is a plateau region higher than one thousand and several hundred meters above sea level.

2. Crustal construction and structure of the region of the African Great Rift System

Older rocks of the Precambrian age are the most important component of the geologic construction and structure of the African continental crust. These rocks occupy more than 57% of the whole surface area of the African continent [1, 22]. Such an extensive distribution of Precambrian rocks is not known in other continents. The petrographic study of the Precambrian rocks in South Africa and East Africa has made a great progress lately. In particular, the dating of absolute age by means of radioactive elements has been carried out [8], and the results have revealed a wide range of ages, some being as old as 3,000–3,665 million years. According to A. Holmes (1960), the age of the standard

Cambrian base is limited between 600 and 620 million years [43], so that the Precambrian period of the African continent may cover a duration of about 3,000 million years.

Along with the absolute age dating, the stratigraphic position of the Precambrian rocks has been studied, and the period of the tectogenic movements, their character and areal extension have been clarified to a certain extent. According to the result, the African continent underwent several tectogenic phases during the Precambrian period, and in each phase the continent suffered folding, metamorphism and granitization repeatedly. The Precambrian rocks, formed in deep parts of the crust, constitute the framework of the basement of the African continent. However, a remarkable change is noticed in the tectogenic phases after about 2,500 million years.

The rock masses, broadly affected by the tectogenic phases older than about 2,500 million years, remained locally as several cratons that are very hard and compact. In the later tectogenic phases, the areas between these cratons were affected and produced several zones of foliated metamorphic rocks showing a distinct trend. Thus, the cratons older than 2,500 m.y. and the younger foliated metamorphic rocks in the basement are tectonically distinguishable.

Four cratons existent in the region from the Arabian Peninsula to the eastern part of the African continent. The Arabia craton is existence in the Arabian Peninsula in the north. In the central part of the continent, there is the Congo craton, and to its east is found another craton known as the Tanganyika Shield. In the southern part there is the Kalahari craton (Fig. 8) [48]. Between these cratons, or around them, foliated metamorphic rocks are zonally distributed with a roughly N-S trend, mostly NE-SW or NW-SE, and constitute the foliated complex having a distinct meridional trend. The African Great Rift System traverses the eastern part of the African continent in a roughly N-S direction. At about the middle it is separated into the Eastern Rift Valley (Gregory Rift Valley) and the Western Rift Valley, with the Tanganyika craton (shield) in between. It is a noticeable and very important fact that the Great Rift System was formed within the zone of foliated metamorphic rocks generally along the foliation and avoiding the cratons (Figs. 1 and 8).

3. Cratons and foliated metamorphic rock belts

In the African continent, especially in its eastern part, tectogenic movement took place five or six times during the Precambrian period [1, 22]. The location and range of each movement have been revealed to some extent. With regard to the cratons of this continent, there are two different views. One of the views is that the entire area of the Precambrian system, which was formed through disturbances caused by the Precambrian tectogenic movements, is

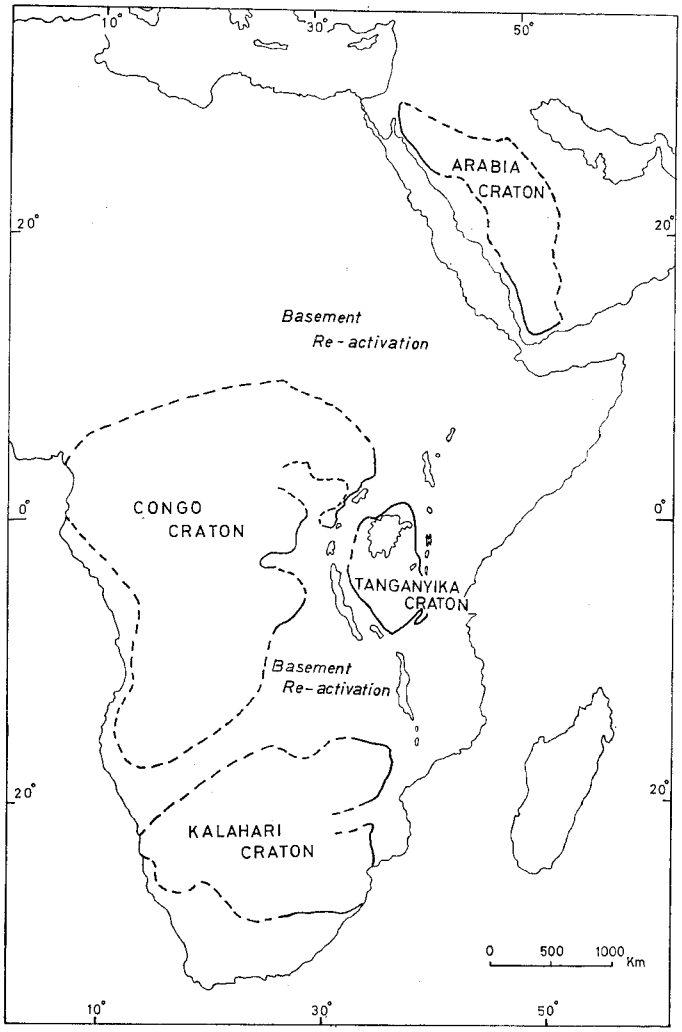

FIG. 8. Cratons in the eastern African continent and the Arabian Peninsula.

regarded as a craton. The other view maintains that some parts of the area survived the later tectogenic disturbances in Precambrian age and remained as stable masses to be called cratons. In the present paper, the latter view is adopted for the convenience of discussion. That is, the area of the Precambrian system is divided into two categories; one is the craton, referring to the stable mass consisting of rocks older than about 2,500 m.y., and the other is the belt of foliated metamorphic rocks, affected by later tectogenic movements.

In the remote past, some 2,500 m.y. ago, the tectogenic movements affected these cratons with metamorphism, accompanied by marked granitization and

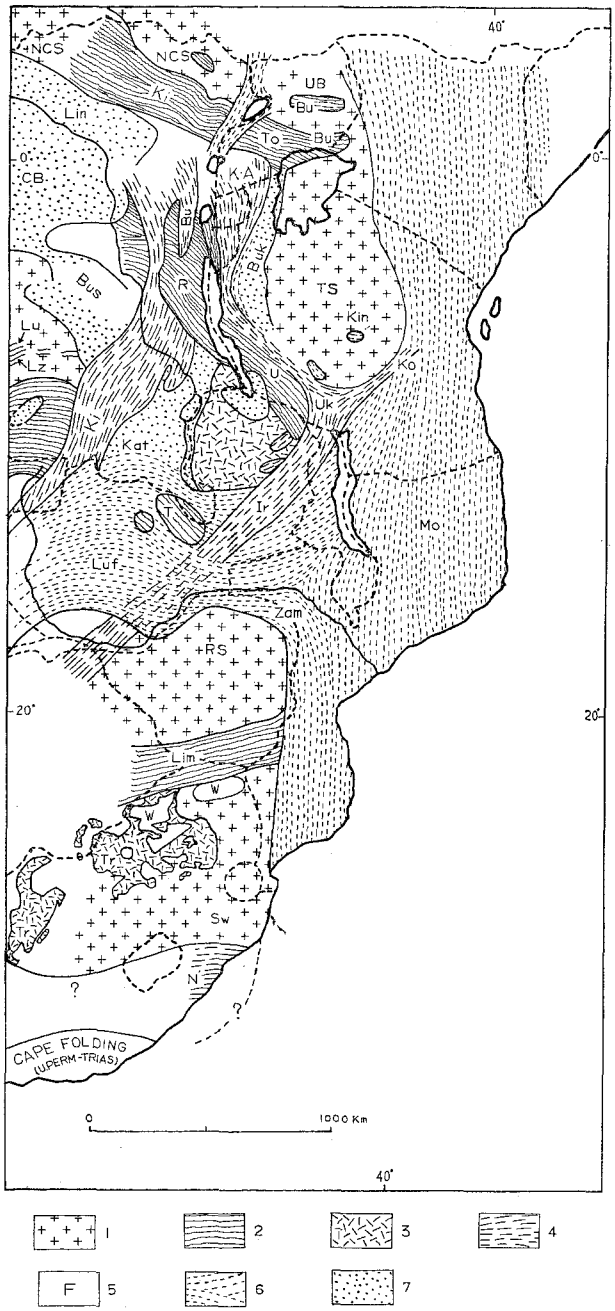

1. Folded and metamorphosed areas older than 2,500 m.y. ago. TS: Tanganyika craton; RS and SW: Kalahari craton.
2. Belts, folded and metamorphosed about 2,100 to 1,950 m.y. ago: Post-tectogenic events can be as young as 1,650 m.y. ago. R-U: Rusizi-Ubendian metamorphic belt.
4. Belts, folded and metamorphosed about 1,300 to 1,100 m.y. ago: Post-tectogenic events can be as young as 850 m.y. ago. BU-K•A-UK-Ko: Burundian-Karagwe-Ankolean metamorphic belt.
6. Belts, folded and metamorphosed about 730 to 600 m.y. ago: Post-tectogenic events can be as young as 450 m.y. ago. Mo and Zam: Mozambique (Katangan) metamorphic belt.
7. Beds, more or less tabular, corresponding to 6. Buk: Bukoban System.

FIG. 9. Structural sketch map of the Precambrian basement of East Africa. (after Cahen and Snelling, 1966).

migmatitization. After that, the cratons remained stable as hard and compact masses, in spite of later intrusions of granite and other igneous rocks. In fact, the cratons are the hardest and most solid masses in the continental crust of today. The foliated metamorphic rocks, presenting a steeply dipping foliated structure, are zonally distributed among the cratons or along their margins.

In the region of the great rift system of eastern Africa, there are recognized at least three belts of foliated metamorphic rocks; (1) Rusizi-Ubendian metamorphic belt, (2) Burundian-Karagwe-Ankolean metamorphic belt, and (3) Mozambique (Katangan) metamorphic belt. The foliated structure of each belt is developed roughly in the meridional trend (Fig. 9). Namely, between the Tanganyika craton and the Congo craton are found the Rusizi-Ubendian metamorphic belt trending roughly NW–SE, and the Burundian-Karagwe-Ankolean metamorphic belt trending N–S or NW–SE, and in the northern part the Mozambique metamorphic belt stretches NE–SW; these belts locally overlap one another. The Western Rift Valley is situated in this region and extends farther southward into the Mozambique metamorphic belt. The Mozambique (Katangan) metamorphic belt has a considerable width and extends almost N–S from the southwestern margin of the Arabia craton to the south along the eastern margin of the Tanganyika craton and the Kalahari craton (Figs. 1 and 9). The Eastern Rift Valley is located in this region.

The geochronometric data have revealed the following [8]: The Rusizi-Ubendian metamorphic belt was formed in the processes of folding and metamorphism caused mainly by the Ubendian tectogenic cycle (about 2,100 to 1,950 m.y. ago) and by the post-tectogenic events that continued till about 1,650 m.y. ago. The Burundian–Karagwe-Ankolean metamorphic belt is a result of folding and metamorphism caused by the Kibaran tectogenic cycle (about 1,300 to 1,100 m.y. ago) and by the post-tectogenic events that continued till about 850 m.y. ago. This belt is connected with the one extending from the south of the Tanganyika craton to the north of the Kalahari craton in a NE–SW direction. The Mozambique metamorphic belt was formed through folding and metamorphism of the Katangan tectogenic cycle (about 730 to 600 m.y. ago). This belt, stretching between the Tanganyika and Congo cratons and the Kalahari craton, branches off southwestward and seemingly joins the Damaran metamorphic belt. The post-tectogenic events are continuous with the Damaran tectogenic cycle of a later age (about 550 to 450 m.y. ago; probably corresponding to the Caledonian tectogenic cycle).

The above-mentioned cratons and the belts of foliated metamorphic rocks were formed in deep parts of the crust as a result of the folding and metamorphism of the Precambrian tectogenic movements and related granitization and migmatitization. Due to the remarkable uplift which took place later and the intensive erosion of the overlying strata, these deep-seated rocks came to be found near the ground surface. The cratons and the belts of metamorphic

rocks represent the construction of the basement of eastern Africa, and the setting of these two different rock types has an intimate conncetion with the formation of the Great Rift System, as will be mentioned later.

4. Component rocks of cratons and metamorphic belts, and their major geologic structure

a. Tanganyika craton

The Tanganyika craton occupies the area between the Eastern Rift Valley and the Western Rift Valley where they are largely deviated from each other in an echelon pattern. This area was first named Tanganyika Shield by McConnell (1948) [59]. The Tanganyika craton spreads widely from the north of Lake Victoria to its south, with a N-S extension about 1,200 km and a maximum width more than 500 km E-W.

This craton is composed of metamorphic rocks belonging to at least two or more tectogenic cycles of old ages (before about 2,500 m.y. ago), much older than the Ubendian tectogenic cycle [1, 8, 22]. Among the rocks the Dodoman, Nyanzian and Kavirondian Systems* of sedimentary and volcanic origin are recognized, but these are merely relics distributed sporadically as enclaves or xenoliths or lenses in the migmatitic rocks, granitic gneisses and older granites. The Dodoman System is typically distributed near Dodoma of central Tanzania. The Nyanzian and Kavirondian Systems are found in the northern part of this craton; with the neighborhood of Kavirondo Gulf as the type locality, they show sporadic distributions along Lake Victoria, from the northeast to the east and to the south.

The Dodoman System consists of banded and ferruginous quartzites and various kinds of schists, such as sericite-schists, quartz-schists, ironstones, hornblende-schists, epidiorites, talcose and chloritic schists, associated with injection gneisses. These rocks occur as enclaves or lenses in unfoliated or weakly foliated granites and migmatitic rocks, and their fold axes strike roughly WNW-ESE or E-W.

Component rocks of the Nyanzian System are as follows: Metamorphic rocks originated in gritty and muddy sediments, accompanied by conglomerates; quartzites (ironstones) containing fine bands of magnetite and chlorite; metamorphic rocks originated in volcanic rocks such as rhyolites, trachytes, andesites, basalts, dolerites, and corresponding acidic and basic tuffs, lavas and agglomerates. These rocks occur as enclaves or lenses, and their fold axes strike mostly NE-SW and NW-SE.

The Kavirondian System consists of conglomerates and metamorphic rocks originated from arenaceous and argillaceous sedimentary rocks, and often contains sediments supposedly derived from the Nyanzian System. The strike

* The name Dodoman System was given by A. M. Quennell *et al.* (1956) [25, 69], and the Nyanzian and Kavirondian Systems were designated by R. M. Stockley (1943) [78].

of their fold axes is almost always E–W.

When the Nyanzian and Kavirondian Systems are developed together, the latter overlies the former with an unconformable relation, which indicates that the former is older and that a period of crustal deformation existed between the deposition of the former and that of the latter. From the facts that the latter contains materials which seem to have been derived from the former, that the strike of the fold axes is different between the two systems, and that the latter is also affected by intense folding and metamorphism, the post-Nyanzian to Pre-Kavirondian deformation can be distinguished from the post-Kavirondian deformation. As to the relation between the Dodoman System and the Nyanzian and Kavirondian Systems, J. R. Harpum says that the Dodoman is older and that the Dodoman's migmatitization and granitization took place prior to the deposition of the Nyanzian [38]. But, his explanation is mere guesswork. The relation between the Dodoman and the Nyanzian and Kavirondian remains unclarified.

So far mentioned is the outline of the construction of the Tanganyika craton. The situation is just about the same in the Congo and Kalahari cratons.

b. Rusizi-Ubendian metamorphic belt

Located between the Tanganyika craton and the Congo craton, the Rusizi-Ubendian metamorphic belt runs with a NW–SE trend, stretching from the north of Lake Malawi to the northwest and obliquely traversing Lake Tanganyika at about the middle, and then along the northern half of the lake it diverges northward to reach the north of Lake Kivu (Fig. 9). It presents an aspect of a strongly folded zone along its trend, dipping steeply, with the extension roughly 1,000 km and the width about 100 to 200 km. This metamorphic belt is called the Ubendian System in Tanzania, and the Rusizian Group in the Congo, Burundi and Rwanda.

This metamorphic belt was formed chiefly under the influence of the Ubendian diastrophism (about 2,100 m.y. to 1,950 m.y. ago) [8]. The constituent rocks are, for the most part, metamorphics originated from various kinds of pelitic and volcanic rocks. These metamorphic rocks comprise quartzites, crystalline limestones, gneisses, schists, phyllites, phyllitic conglomerates, amphibolites, migmatites and anorthosites or calcic granulites. Granitic rocks range from migmatites to intrusive granites, and are accompanied by porphyry as chilled roof of granites; these are distributed as narrow and long dyke-like intrusive bodies generally along the extension of the metamorphic belt. Thus, they show that granitization took place in association with the tectogenic movement of folding and metamorphism.

The metamorphic condition of the above-mentioned belts corresponds roughly to the amphibolite and hornblende-granulite facies. They are characteristically developed as a foliated complex parallel to the NW–SE fold axes

along the extension of the metamorphic belt, and another parallel to the fold axes along the arcuate northerly-directed branch of the former.

c. Burundian–Karagwe-Ankolean metamorphic belt

The Burundian–Karawe-Ankolean metamorphic belt occurs between the Congo craton and the Tanganyika craton. It is located on the east side of the Rusizi-Ubendian metamorphic belt and extends for about 1,400 km. It is represented by the Burundian Belt extending from Burundi to the southern part of Uganda in the west of Lake Victoria, and by the Karagwe-Ankolean Belt extending from the north-western part of Tanzania to the southern part of Uganda. These belts running side by side attain a maximum width of about 300 km, with folding axes of NNW–SSE or NNE–SSW, sometimes NW–SE, trend. Decreasing in width in the east of Lake Tanganyika, these bend southeastward along the west margin of the Tanganyika craton, and stretch in a narrow belt until it finally joins the Ukingan Belt which runs NE–SW along the south margin of the Tanganyika craton (Fig. 9).

The Burundian–Karagwe-Ankolean metamorphic belt was formed chiefly due to the Kibaran diastrophism (about 1,300 m.y. to 1,100 m.y. ago) [8]. It consists mostly of shales, slates, phyllites and low-grade sericite-schists of argillaceous material origin, sandstones and quartzites of arenaceous material origin, and phyllitic conglomerates. It also contains gneissic granites and porphyritic granites which resulted from granitization.

The grade of metamorphism of this belt ranges from shales or slates to phyllites and, passing through the muscovite and muscovite-biotite-schists stage, to migmatitic gneisses. The metamorphic condition roughly corresponds to the amphibolite facies. The trend of fold axes is variable from area to area, but the main fold axes coincide with the trend of the extension of the metamorphic belt, and the rocks are all foliated, forming a steeply dipping foliated complex along the said trend.

d. Mozambique metamorphic belt

The Mozambique (Katangan) metamorphic belt is a vast zone of steeply dipping foliated metamorphic rocks, being about 5,280 km in extension with a considerably large width. It stretches in the eastern part of eastern Africa with a N-S trend, running along the east side of the Kalahari craton and the Tanganyika craton. In the north it reaches the southwestern margin of the Arabia craton, and in the south it goes as far as the southern part of Mozambique, passing through Kenya and Tanzania; along the west coast of the Red Sea it extends over Ethiopia, Sudan, United Arab Republic and Somalia (Fig. 9). A. Holmes called this belt "Mozambique Belt" for the first time (1948) [42], and since then this name has been widely used.

The Mozambique metamorphic belt resulted from folding and metamorphism chiefly due to the Katangan diastrophism (about 730 m.y. to 600 m.y. ago)[8].

The constituent rocks are biotite-gneisses, migmatites, pelitic schists and psammitic granulites, associated with marbles and amphibolites. The conspicuous foliation of these rocks agrees on the whole with the strike of the metamorphic belt, and the rocks make up a steeply dipping foliated complex with a distinct meridional trend. The metamorphic condition of this belt corresponds largely to the amphibolite facies and partly to the granulite facies. The belt is locally intruded by later granites and pegmatites. Along the upper reaches of the Zambezi River north of the Kalarari craton, the belt branches away to the west and seems to continue with the Damaran metamorphic belt between the Kalahari craton and the Congo craton. As mentioned already, the post-tectogenic events of the Mozambique metamorphic belt (the Katangan diastrophism) may have continued even during the Damaran diastrophism (about 550 to 450 m.y. ago).

The Mozambique metamorphic belt constitutes part of the basement of eastern Africa. On the ground it is locally covered by Palaeozoic-Mesozoic and Tertiary sediments and volcanics. Especially in the Eastern Rift Valley region volcanics are widely covering the belt, so that the basement rocks are only sporadically exposed as enclaves (Fig. 3).

5. Foliated metamorphic belt and great rift system

The cratons and the foliated metamorphic belts so far mentioned make the fundamental framework of the continental crust of eastern Africa and Arabia. These were formed in the Precambrian period as parts of tectogenic belts in a considerably deep part of the crust, and were later upraised toward the ground surface. The African Great Rift System is located, for the most part, in the region of foliated metamorphic belts, namely, the Eastern Rift Valley occurs in the Mozambique metamorphic belt and the Western Rift Valley stretches over several metamorphic belts, as exemplified by Lake Albert and Lake Edward in the Mozambique metamorphic belt, Lake Kivu, Lake Tanganyika and Lake Malawi in the Rusizi-Ubendian metamorphic belt and Burundian-Karagwe-Ankolean metamorphic belt, and the area south of Lake Malawi in the Mozambique belt, stretching roughly along their foliated structure.

V. FORMATION OF BASEMENT OF AFRICAN CONTINENTAL CRUST AND LATER DEVELOPMENTS

The Mozambique metamorphic belt branches, in its southern part, off toward the west and seems to become continuous with the Damaran metamorphic belt which extends in a NE–SW direction along the northwestern margin of the Kalahari craton. Many geologists regard these two metamorphic belts as contemporaneous, but the present writer thinks that the Damaran tectogenesis (about 550 m.y. to 450 m.y. ago) which formed the Damaran metamorphic belt corresponds to the Caledonian tectogenesis of Europe. On the other hand,

the post-tectogenic events of the Katangan tectogenesis (about 730 m.y. to 600 m.y. ago), which formed the Mozambique metamorphic belt, seem to have lasted until about 450 m.y. ago (according to the geochronometric data), and this is perhaps the reason many geologists misinterpreted the ages of the two metamorphic belts as contemporaneous.

From the above-mentioned viewpoint it can be concluded that the basement of the African continent was completed in the period of the early Palaeozoic Damaran tectogenesis. After that period up to the present, the greater part of the African continent was free from severe tectogenic deformation, except for the area of the Atlas Range that was affected by the Alpine tectogenesis along the Mediterranean Sea.

The basement composed of the cratons and the foliated metamorphic rocks constituted part of the tectogenic belts at a considerable depth of the crust. Then, due to intense upheaval, erosion and denudation, the basement came to appear near the ground surface. During the period from late Palaeozoic to early Mesozoic, an extensive epeirogenic subsidence of the basement took place. The area of the Mozambique metamorphic belt, in particular, was subjected to gentle epeirogenic subsidence of warp type, giving rise to transgression by which the thick marine (?) sediments of the Karroo System (Carboniferous to Triassic or Jurassic) were deposited. In the Cretaceous period, however, the epeirogenic movement changed to an uplifting movement. The upheaval became conspicuous since about the Eocene epoch of Tertiary. Accompanying the upheaval, volcanism became active in Kenya and Ethiopia, effusing basalt and other laves on a large scale and forming the Abyssinian plateau, etc. This volcanic series, thickly accumulated and spread out horizontally to a large extent in the period of late Cretaceous to early Tertiary, might be originated probably in large scale effusions from great fissures. So, the writer considers that these fissures might be forerunners of the African Great Rift System.

Thus it is evident that, in comparison with the areas of cratons, the Mozambique metamorphic belt and other areas of foliated metamorphic rocks were repeatedly affected by gentle uplift and subsidence since Mesozoic to Palaeogene, and volcanic activities accompanied these movements. Such events are supposed to be the forerunning phenomena of the crustal movement that formed the great rift system during the Miocene and later period.

VI. CONFIGURATION OF RIFT VALLEYS

The Eastern Rift Valley, or Gregory Rift Valley, and the Western Rift Valley are more or less different from each other in their geological setting. And in their character they again differ from the Red Sea Rift and the Gulf of Aden Rift.

The Eastern Rift Valley was formed by fault that deeply cut into the almost

horizontal thick beds of volcanic rocks which rest on the foliated metamorphic rocks of the Mozambique belt of basement. These volcanic rocks consist chiefly of lavas produced by large scale effusions probably during the period from late Cretaceous to early Tertiary, covering a wide region extending from Ethiopia to Kenya. Younger volcanoes, ranging in age from late Tertiary to Quaternary, are also numerous in this region, and effusive rocks are widespread [49] (Figs. 2 and 3). In other words, the greater part of the Eastern Rift Valley is in the region of volcanic rocks that thickly cover the basement [80, 84].

On the other hand, the Western Rift Valley for the most part directly cuts the Precambrian basement rocks, and extends through the western borders of Uganda, Rwanda, Burundi and Tanzania to the vicinity of the Zambezi River in Mozambique.

Accordingly, the Eastern Rift Valley would be best suited for the study of configuration and structure of rift valleys relating to faulting movement and geological setting, on the basis of the horizontally accumulated stratigraphy of volcanic rocks. For this purpose the writer and his collaborators chose southern Kenya as their field. The Western Rift Valley, on the other hand, is a good object of the study of structural relationship between the foliated metamorphic belts of basement and the rift valleys. Therefore, investigations were carried out in various parts of Tanzania.

1. Rift valleys in southern Kenya

The area of the Eastern Rift Valley is covered, for the most part, with volcanic rocks that make almost horizontal strata. Distributed below these is the Mozambique metamorphic belt, characterized by the N-S trending foliation. The features of the Eastern Rift Valley are best observed in Kenya, where the Lake Rudolf Rift, Lake Naivasha Rift and Lake Magadi Rift are aligned nearly N-S, to pass through the west of Nairobi and join the Lake Natron Rift in northern Tanzania (Figs. 3, 10, 11 and 12).

The African Great Rift System is dotted with some thirty lakes of various sizes that are aligned like a string of beads. Lake Naivasha is one of them, and is located at about 70 km northwest of Nairobi. To its north are found Lake Elementeita and Lake Nakuru. The area covering these lakes is ideal for observation of configuration and structure of rift valleys, and the writer calls it the Lake Naivasha Rift (Fig. 10). Investigations were made in various parts of the Lake Naivasha Rift. In order to reveal the character of fault which is one of the most important structural elements of rift valleys, the fault scarp on the eastern margin of the Lake Naivasha Rift is described below.

In a distant view this is a great continuous fault scarp, but getting closer it is seen to comprise several stepped fault scarps, each of which is of a rather small scale. In a plane figure several faults, usually 2 to several kilo-

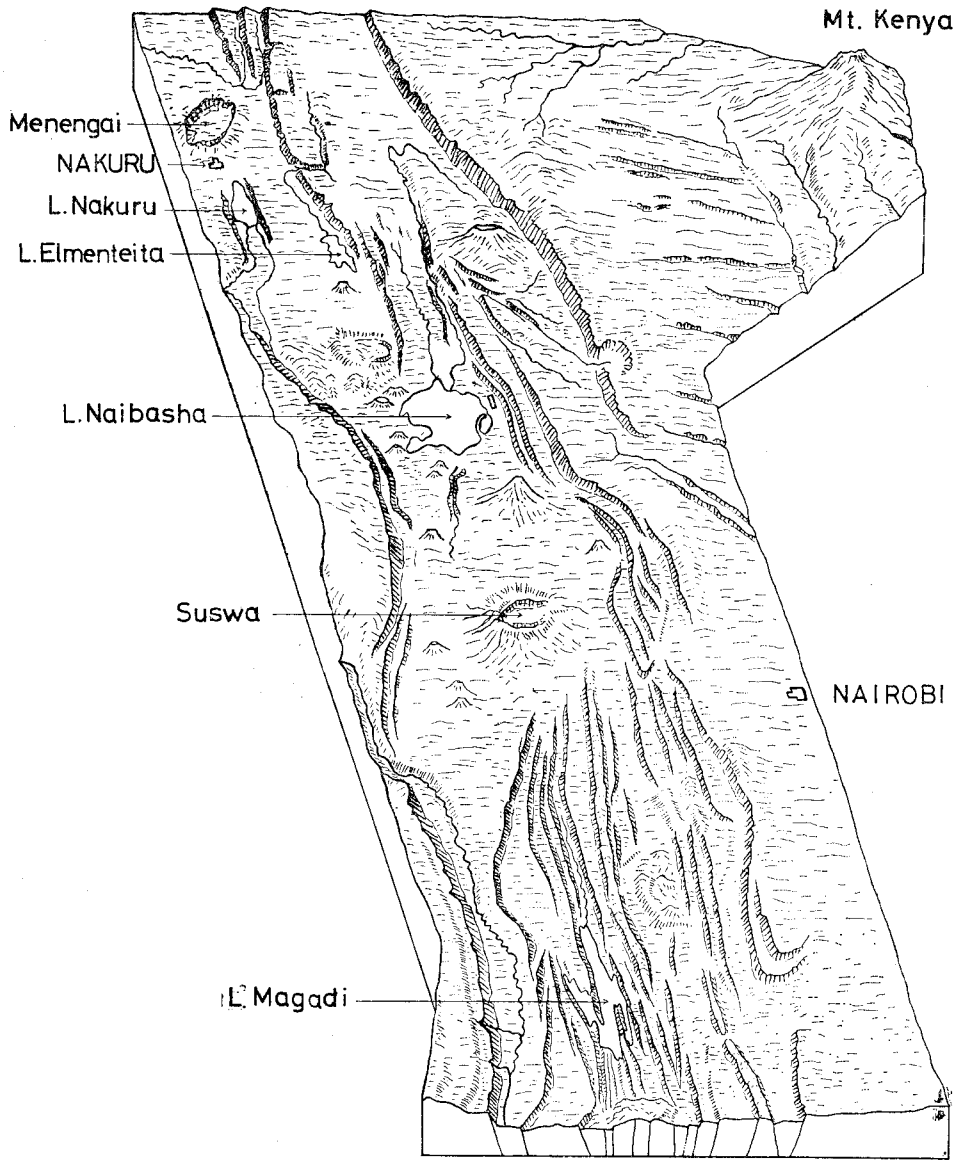

FIG. 10. Schematized block diagram of the great rift system in southern Kenya (after Busk, 1939; partly modified by Matsuzawa).

meters long, sometimes as long as 20 km, make up fault zones in an irregular echelon arrangement and the zones themselves are again deviated in places to present another echelon pattern. Four zones of fault run nearly parallel with one another, in a NNW–SSE direction, each forming a conspicuous fault scarp. With a throw 50 m to about 300 m, the fault scarps rise in four steps from

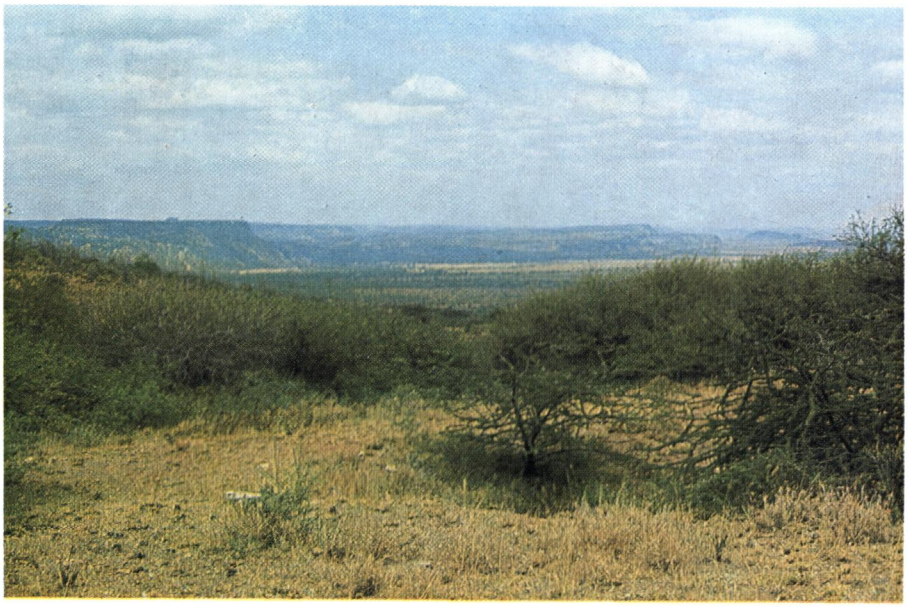

FIG. 11. Distant view of the western fault scarps of the great rift system from near Olorgesaille, southwest of Nairobi (photo by Ohmi, member of our party).

FIG. 12. Bird's-eye photograph of the stepped fault scarps of the great rift system (the Lake Magadi Rift), north of Lake Magadi (photo by Suwa, member of our party).

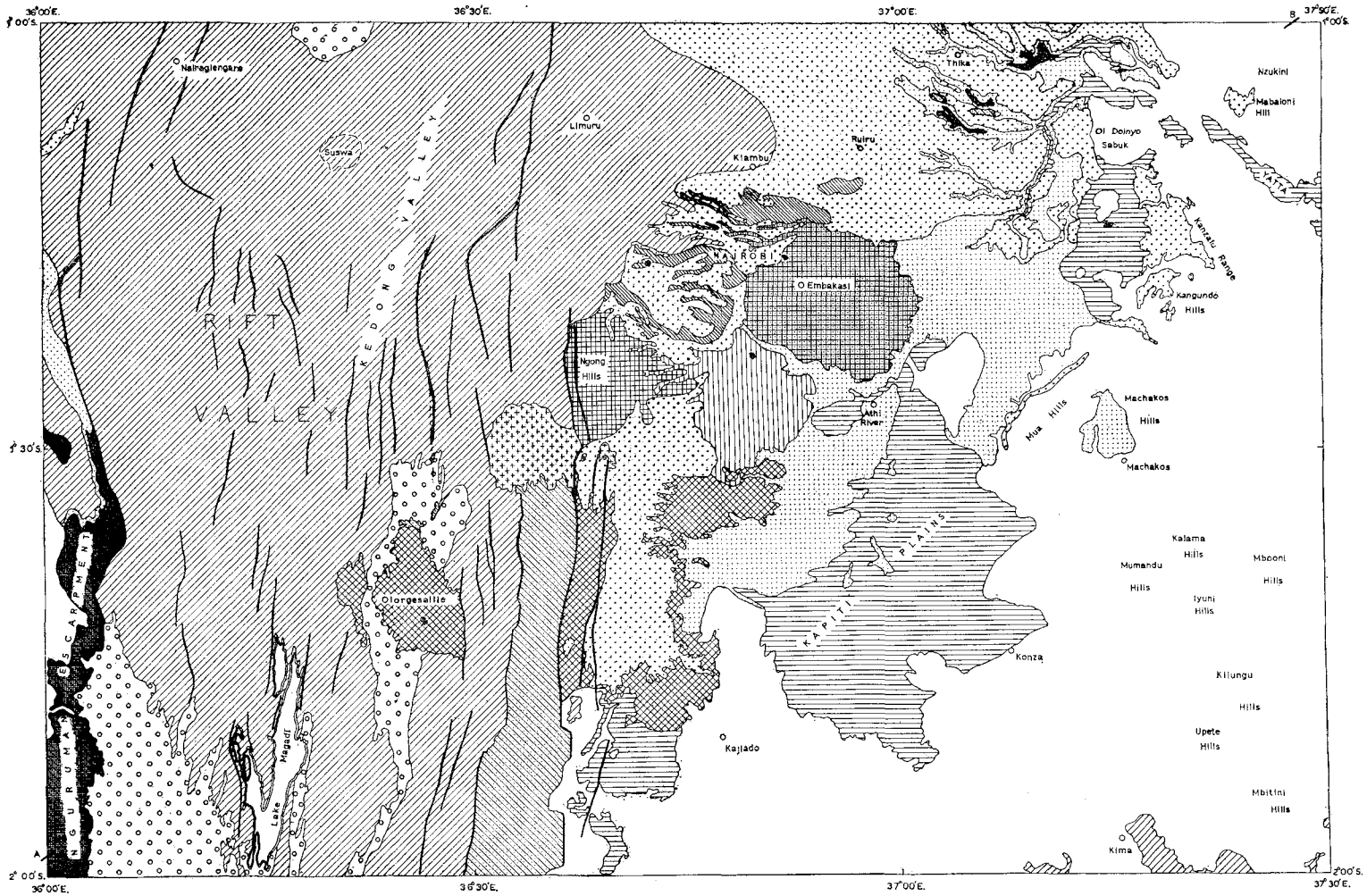

FIG. 13. Geologic map of the Lake Magadi Rift and the Nairobi area (after Williams, 1967).

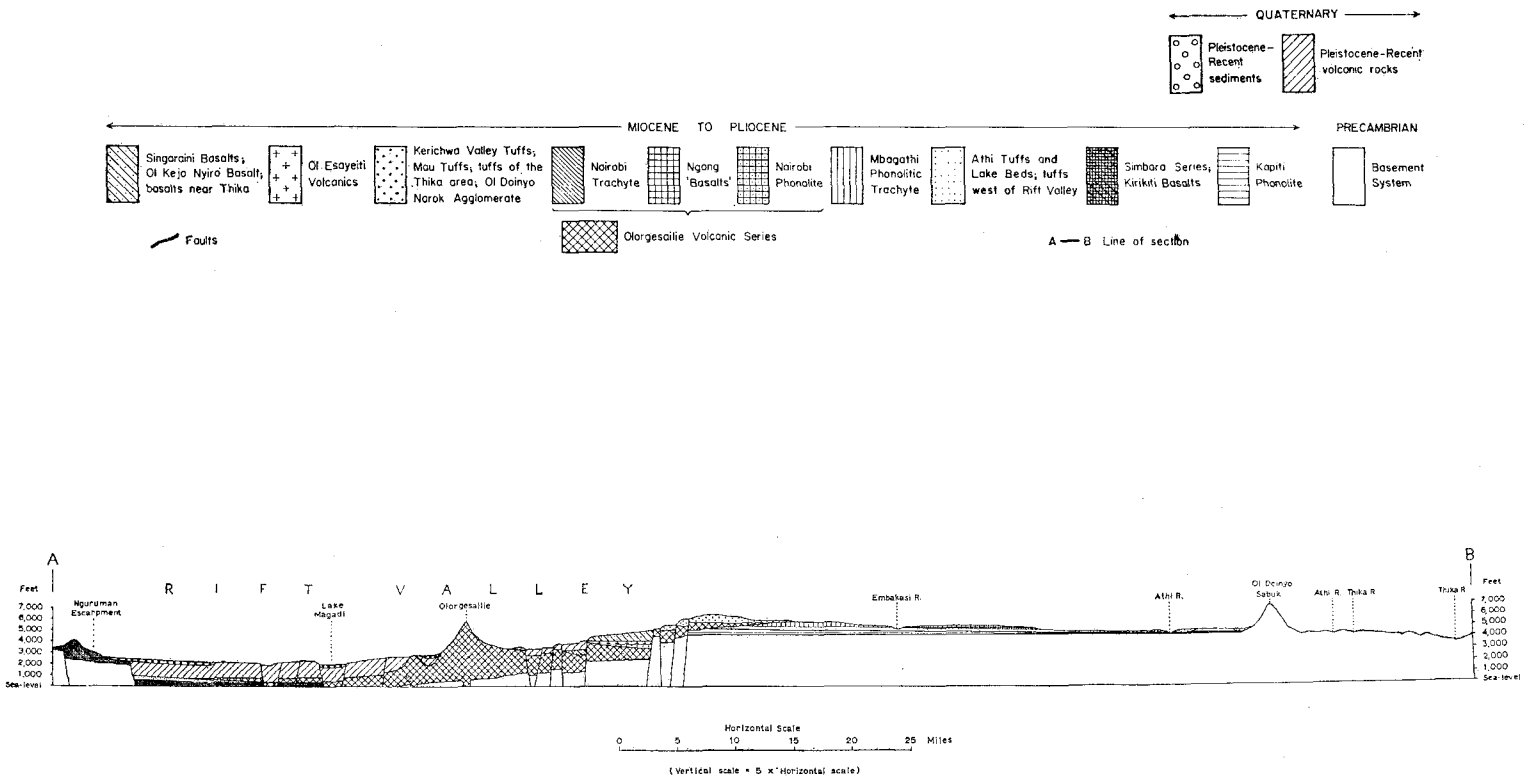

FIG. 14. Geologic profile of the Lake Magadi Rift (the area of Fig. 13) (after Williams, 1967).

the plain on the rift bottom to the plateau. Each step is a level strip of land, its width ranging from 3 km to 9 km according to the position of the fault zone. The level plane around Lake Naivasha is 1,850 m above sea level, the first step lies at 1,950 m, the second step at 2,000–2,050 m, the third step 2,160 m, and the last step is the surface of the plateau at 2,450–2,500 m above sea level. The throw is largest between the plateau and the third step, and the scarp between them marks the outer margin of the Lake Naivasha Rift. The difference in altitude between the plateau surface and the rift bottom is 600–650 m. Width of the level surface of each step varies with the position of the fault zone in the echelon arrangement, and the steps are locally displaced.

The eastern margin of the Lake Naivasha Rift, consisting of four distinct steps of fault scarps of normal fault type, has a width of more than 10 km. The total width of the Lake Naivasha Rift is over 50-odd kilometers or more 60 km. The western margin of the rift is also marked with fault zones trending NNW–SSE, and conspicuous fault scarps facing east are developed (Mau Escarpment is the most remarkable one of these). To show the general structure of this rift in southern Kenya, the geologic map and cross-section of the vicinity of Nairobi, compiled by L. A. J. Williams [98], are reproduced here (Figs. 13 and 14).

The observations of the Lake Naivasha Rift revealed the following facts: (1) The margin of the rift is bounded not by one great fault but by several small faults that constitute fault zones of echelon arrangement, and the fault zones themselves are also arranged in an echelon pattern. (2) The faults are normal faults, lowering toward the inside of the rift in several distinct steps. These facts are especially important as they show a format of formation mechanism of the African Great Rift System, and they may suggest that rift valleys were formed in the tensional field due to depression caused by tension. Some geophysicists and geologists used to attribute the formation of a rift valley to a compressive force, holding a view that the blocks on either side were thrust up and the area in between became the rift valley. However, the field observations have disclosed no structure to verify thrust movement, and no evidence to support a thrust origin has been found.

2. Southern end of Eastern Rift Valley in northern Tanzania

The Eastern Rift Valley stretches southward from Kenya and connects with the Lake Natron Rift in northern Tanzania. In the south of the Lake Natron Rift it seems to bifurcate. Although the location of the forking point is not clear because of the extensive cover of ejecta from several younger volcanoes, one branch advances southwestward and forms the Lake Eyasi Rift that trends NE–SW, whereas the other branch extends southward to form the Lake Manyara Rift with a trend N by E–S by W and farther goes to the south along the west side of Kondoa north of Dodoma (Fig. 15).

The Eastern Rift Valley presents a typical form of depression, with its margins on either side cut by faults, only in the area from the north of Kenya to the Lake Natron Rift. After bifurcating into the Lake Eyasi Rift and the Lake Manyara Rift, the rift valley comes to have an aspect suggestive of tilting. One side of the rift valley is composed of tilted blocks that are cut by faults or fault zones and are deeply inclined toward them, but no corresponding conspicuous faults or fault zones are found on the opposite side. In other words, the rift valley in this part shows an irregular configuration due to tilting and depression of one side only. In the Lake Eyasi Rift the block on the southeast side of the fault zone was tilted northwestward, and depression was greatest along the fault zone so that Lake Eyasi was formed in this lowered part. In the Lake Manyara Rift the block on the east side of the fault zone was tilted westward, and Lake Manyara was formed where the depression became deepest along the fault zone. In either case, any remarkable corresponding faults are not found on the opposite side.

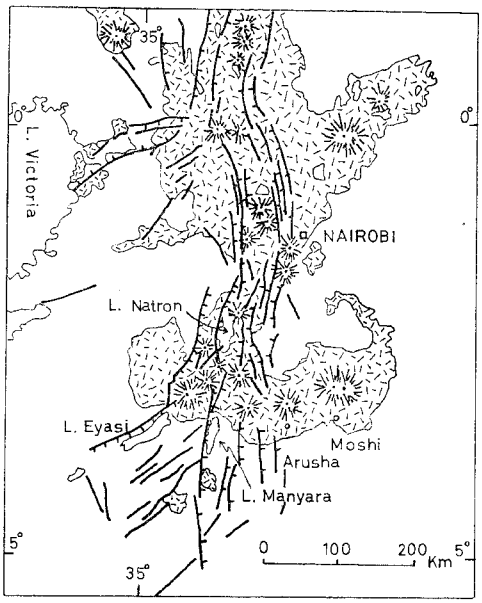

FIG. 15. Structural sketch map of the great rift system of the area of Lake Natron Rift, Lake Eyasi Rift and Lake Manyara Rift.

The Lake Eyasi Rift, with the NE–SW trending normal fault whose scarp faces southeast, traverses the Serengeti plateau. The difference in altitude between the plateau and the lowland on the south (where the altitude of the surface of Lake Eyasi is about 1,030 m above sea level) is 500 m or more. The Lake Manyara Rift is marked with two or three normal faults, separate about 10 km from each other, trending parallel in a N by E-S by W direction. These faults are distinctly stepped toward the lowland on the east, with the fault scarps facing east. The first step (about 1,280 m above sea level) is some 320 m above the lowland around Lake Manyara (the surface of which is 960 m above sea level), and the scarp between the lowland and the first step is called the Mto Wa Mbu Escarpment. The second step is about 280 m above the first, bounded with the Klima Cha Tembo Escarpment. The second step has a width of about 20 km; between this step and the Ngorongoro Forest Resort (about 2,250 m above sea level) in the rear, presence of a fault, with a throw probably several hundred meters, is inferred. The tilted block on the

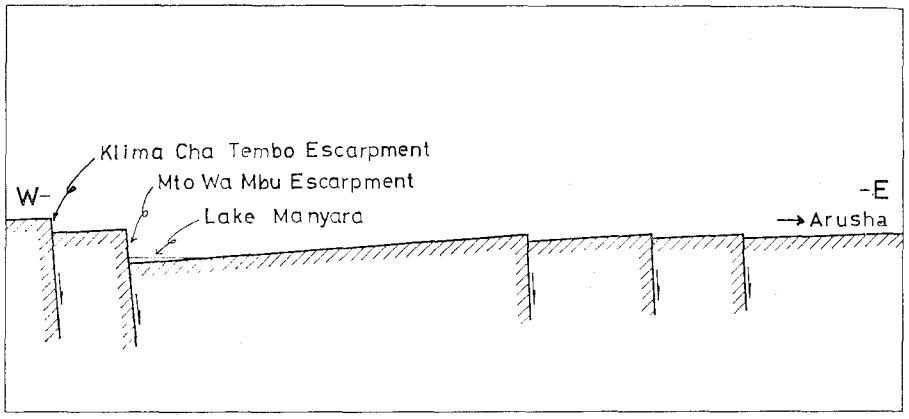

FIG. 16. Simplified profile of the Lake Manyara Rift and its east.

east side, bounded with the Mto Wa Mbu Escarpment, increases its elevation gradually toward east from the lowland of Lake Manyara until it ends with the plateau around Arusha (Fig. 16). Over a distance of about 100 km between Lake Manyara and Arusha, there are found three or four rows of faults, roughly running N–S. These faults are responsible for the repeated tilting of three or four west-inclined blocks. Each row of the faults presents a distinct escarpment, with a throw several tens of meters, facing east.

The area to the south has no typical rift valleys, although faults of N–S system or NE–SW system are often observed around the Tanganyika craton and within the Mozambique metamorphic belt (Fig. 18).

According to the observations mentioned so far, the following points are important in the Eastern Rift Valley of northern Tanzania:

(1) The Eastern Rift Valley occupies the region where the Mozambique metamorphic belt constitutes the basement, and extends from Ethiopia to Tanzania through Kenya, but in the area between southern Kenya and northern Tanzania it is developed where the Mozambique metamorphic belt contacts the Tanganyika craton. It is noticeable that the Lake Manyara Rift and its southern extension stretch along the above-mentioned contact, and the Lake Eyasi Rift extends into the craton.

(2) The typical features of the Eastern Rift Valley, that is, the both sides are cut by faults and the area in between is depressed to form a typical rift valley, are observed only from the north to the Lake Natron Rift, and in the south of the Lake Natron Rift the rift valley bifurcates into the Lake Eyasi Rift trending NE–SW and the Lake Manyara Rift trending roughly N–S. These two branch rifts no longer exhibit the typical rift valley features, but are characterized by tilting blocks which are separated by faults or fault zones and deeply depressed on one side.

(3) The area where the Eastern Rift Valley bifurcates into two rifts is widely covered by volcanic rocks erupted from several younger volcanoes including Oldoinyo Lengai volcano, so that the state of the bifurcation point is little known (Fig. 15). However, the concentrative distribution of very dense basic effusive rocks suggests that the bifurcation has some connection with a deep part of the crust.

(4) In the southernmost part of the Eastern Rift Valley, where the Mozambique metamorphic belt comes in contact with the Tanganyika craton, the typical form of the rift valley is lost, because the rift forks to fracture zones due to fault, and assumes an irregular shape with one side being composed of tilted and sunk blocks. This fact may be regarded as an evident reflection of the marked contrast between the foliated metamorphic rocks and the cratons, in both strength and structure.

3. Lake Tanganyika Rift

The northern half of the Western Rift Valley lies in the area of foliated metamorphic rocks, as represented mainly by the Rusizi-Ubendian metamorphic belt and the Burundian-Karagwe-Ankolean metamorphic belt, running between the Tanganyika craton and the Congo craton. The Lake Tanganyika Rift is situated where the above two belts and other structures are intersecting or contacting or overlapping, and so the rift exhibits complex features (Fig. 17).

Almost the whole area of the Lake Tanganyika Rift is filled with water, forming Lake Tanganyika. The lake is 30 km to 70 km in width, 660 km in extension, and the surface is at 773 m above sea level. The bottom of the lake is lower than the sea level, and in places the depth is as great as six hundred and several tens of meters below sea level.

Thus, the Lake Tanganyika Rift, including Lake Tanganyika, has a remarkably narrow and elongate form, with its northern half stretching roughly N–S and the southern half NNW–SSE, bending at about the middle. Near the bending point, the northern half joins the southern half in a zigzag pattern (Fig. 17). The southeastern extension of the bend of the northern half corresponds to the extension of the Lake Rukwa Rift which runs southeast of the Lake Tanganyika Rift in echelon. In the geologic structure, too, the two rifts are continuous.

In the Lake Tanganyika Rift and its vicinity, the Rusizi-Ubendian metamorphic belt, the Burundian-Karagwe-Ankolean metamorphic belt, and the Precambrian Bukoban System which is unconformable with those belts, are seen to adjoin or overlap and make up a complex structure of the basement (Fig. 9). The rift owes its form to the basement structure, particularly to the foliation. Various kinds of metamorphic rocks constituting the Rusizi-Ubendian metamorphic belt have their foliation trending NNW–SSE or N by W–S by E in the northern part, and turn SE in the middle part to head for the extension

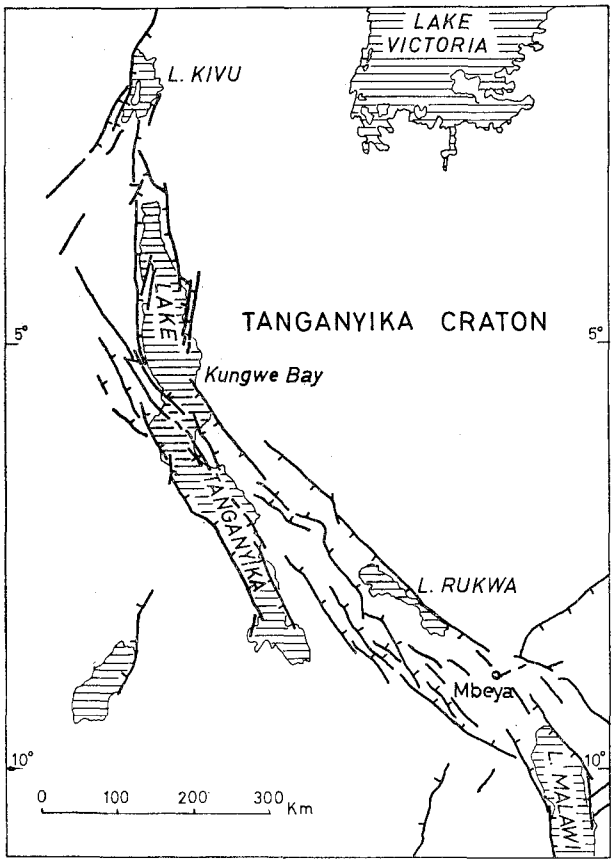

FIG. 17. Structural sketch map of the Lake Tanganyika Rift and the Lake Rukwa Rift.

of the Lake Rukwa Rift. Some of the rocks stretch southeastward with the same trend as the southern half of the rift, and become continuous with migmatites, gneisses and other foliated metamorphic rocks in the south, which were formed chiefly by granitization (Fig. 9). Foliated rocks of the Burundian-Karagwe-Ankolean metamorphic belt are distributed along the east side of the former belt, or overlapping it, with their trend roughly N-S in the north, bending southeastward in the middle to extend toward the extension of the Lake Rukwa Rift. The Bukoban System, covering the Tanganyika craton and the Burundian-Karagwe-Ankolean metamorphic belt in a flat-lying cover, is seen to extend southwestward from the west shore of Lake Victoria. Then it reaches Kungwe Bay at about the middle of Lake Tanganyika, and goes southeastward until it gets to the north of the Lake Rukwa Rift (Fig. 9). The Bukoban System is the youngest of all Precambrian formations, and consists

essentially of unmetamorphosed rocks*. The system is folded only slightly, and undulates gently, but is cut by many faults. Development of fissures along joints is remarkable. In the area south of Ujiji on Kungwe Bay the system has a part in the rift valley construction. The structure of the rift valley, especially the marginal structure, becomes all the more complex in this area, as the foliation of metamorphic rocks and the fault zones, that are responsible for the main trend of the rift valley, are intersecting numerous faults and fissures of the Bukoban System at right angles or oblique angles [100].

In the Western Rift Valley, the state of the rift directly cutting into the Precambrian basement can be observed. The observation of the Lake Tanganyika Rift, representative of the Western Rift Valley, reveals that the basement structure is complicated with the adjoining or overlapping foliated metamorphic rocks of different ages and non-schistose unmetamorphosed rocks, where the rift valley was formed under the strong influence of, and in close relation to, the foliated structure, the faults and fissures in the basement, and the geologic structure of the area. The Western Rift Valley presents a conspicuous echelon arrangement where the Lake Rukwa Rift is deviated eastward from the southern part of the Lake Tanganyika Rift.

4. Fault system in the southeastern part of the Tanganyika craton

The rift valley extends farther from the Lake Rukwa Rift to the Lake Malawi Rift, and from about the middle of this extension, where Mbeya is located, a fault system runs northeastward at a right angle to the rift valley. This fault system cuts the southeastern margin of the Tanganyika craton for a distance of about 400 km. It corresponds to the Fufu Escarpment between Dodoma and Iringa, with its remarkable fault scarp facing southeast. The southeast side of the fault is deeply depressed forming an irregular rift valley due to tilting and sinking of blocks (Fig. 18).

In this area the foliated metamorphic rocks of the Burundian-Karagwe-Ankolean metamorphic belt are zonally distributed with a NE-SW trend along the Tanganyika craton (Fig. 9). The above-mentioned irregular rift valley due to tilting is supposed to have been formed under the strong influence of the orientation of those foliated metamorphic rocks. In the area to the southeast as far as Iringa and Ifakara, faults of a NE-SW or NNE-SSW trend are developed remarkably. It is worthy of note that the Usagara Mountains near Iringa and the Kilombero Valley near Ifakara are elongated in this direction. Development

* The Bukoban System is composed of a varied assortment of rock types including conglomerates, sandstones, quartzites, greywackes, shales, dolomitic limestones and basalts. The rocks showing more or less tabular beds have suffered slight folding and a considerable amount of faulting but are virtually unmetamorphosed. The system rests unconformably on a variety of older rocks of the Burundian-Karagwe-Ankolean belt and the Tanganyika craton, and its age is considered to be corresponded to that of the Mozambique belt.

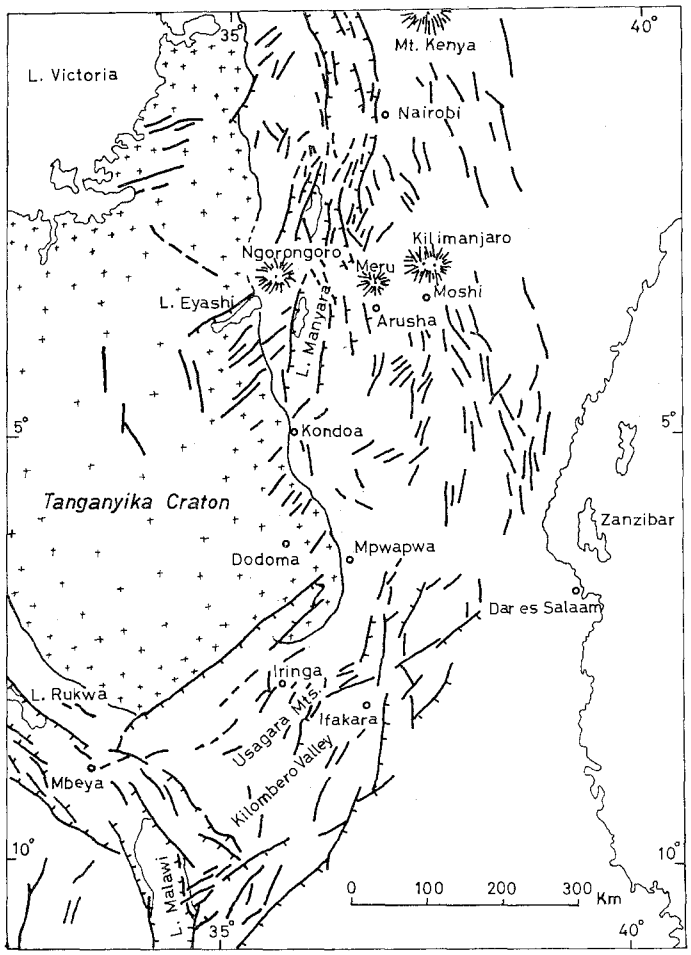

FIG. 18. Structural sketch map of fault systems in the eastern and southeastern parts of the Tanganyika craton.

of such a directional structure line is probably ascribed to the influence of the interrelations of the Tanganyika craton and the foliated metamorphic rocks in the basement.

5. Width of rift valleys

With the exceptions of the Red Sea Rift and the Gulf of Aden Rift, the rift valleys in Africa are usually extremely long, and it is quite interesting that the width of those rift valleys is almost uniform generally between 30 km and 60 km. The consistent width is a characteristic of rift valleys in other continents, too.

Width of rift valleys is an important subject for future study, and the present writer has no definite view for its elucidation as yet. It involves

various questions to be answered, as follows: Why do faults occur on two sides and why is an intermediate area depressed to form a rift valley when a certain stress works? Why, in some cases, does only one side of the faulted area undergo tilting and sinking block movements, resulting in an anomalous type of rift valley? Why does the depression take place always with a nearly uniform width in spite of its great length? What is the reason that the width is usually between 30 km and 60 km or so? Is the uniformity of the width related to the construction or physical properties of the crust, particularly of the granitic layer of continental crust? Or, is it related to the intensity of the exerted stress?

Hans Cloos in his experiments succeeded to make a model rift by giving slow upheaval to moist clay layers (crust) (Fig. 19) [9]. According to him, the surface width of the rift is in the same order as the total thickness of the clay "crust".

The region of the African Great Rift System is mostly occupied by plateau higher than 1,000 m or more above sea level, so the thickness of the continental crust in that part may be 50 to 60 km or so. Should the width of rift valleys is related to the thickness of the continental crust, the experiment by Cloos is of great significance. At any rate, the width of rift valleys awaits further researches.

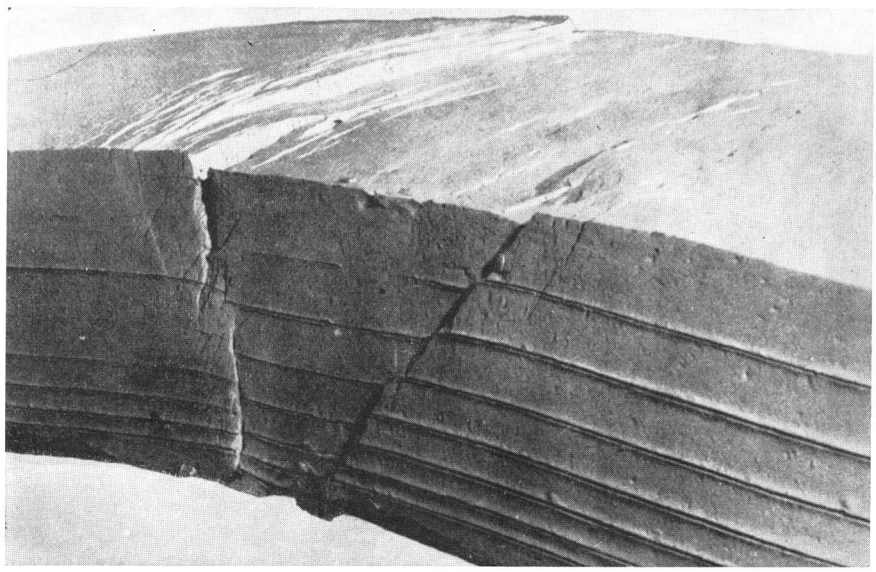

FIG. 19. Experimental production of a rift valley by slow upheaval of layers of moist clay by Hans Cloos. Note that the surface width of the rift valley is of the same order as the total thickness of the clay "crust" (after Hans Cloos, 1939).

VII. PECULIARITY OF RIFTS AROUND ARABIA CRATON

Between the African continent and the Arabian Peninsula lie the Red Sea Rift and the Gulf of Aden Rift. There is also a chain of rifts, extending northward from the Gulf of Aqaba Rift in the northern part of the Red Sea Rift and, passing through the Dead Sea Rift, it runs along the western margin of the Arabian Peninsula roughly parallel with the coast of the Mediterranean Sea. At its northern extremity, the chain intersects the Alpine-Himalayan tectogenic belt at a right angle. Since these rifts occur around the Arabia craton, the writer includes them in the African Great Rift System, considering that they were formed contemporaneously with other rifts in the African continent by the same causative force, although they differ from the latter in the mechanism of formation.

1. Red Sea Rift and Gulf of Aden Rift

The Red Sea Rift and the Gulf of Aden Rift have a double-rift feature [30]. Their geophysical character and geologic setting have been described already. Both the Red Sea and the Gulf of Aden are the depressed zones due to faults along the coast of Africa and Arabia. The width of the Red Sea is 140–150 km in the northern part, and gradually widens toward south attaining to 300 km or more in the southern part. At its southern end, the Red Sea makes an L-shape bend to be connected with the Gulf of Aden. Coastal plains of Eritrea and northeastern Ethiopia fringe the Red Sea, where the width of the sea suddenly decreases. A fault system along the southwest coast of the Red Sea is found to encircle the west margin of the lowland, and extends southward from the east of Massawa on the Eritrea coast. From the vicinity of Addis Ababa it turns eastward and, encircling the south margin of the lowland, it stretches over the south coast of the Gulf of Aden. All this while, the fault system exhibits conspicuous fault scarps. Thus, it is evident from the topography also that the fault-depressed belt of the Red Sea continues to that of the Gulf of Aden (Fig. 20). These depression belts are, unlike other rifts of the continent, very wide and have another deeper rift in the median zone along their trend. In other words, they are double rifts. The central deep trough begins to appear at about lat. 24°N, some 700 km from the northwestern end of the Red Sea Rift. In the beginning, its width is very narrow, some 10-odd km, but it gradually widens and attains to 50–60 km in the southeastern part. Since the southernmost part of the Red Sea is covered with younger sediments and lavas, and coral reef is developed along coast, the connection of this central deep trough with that of the Gulf of Aden is not clear. Under the sediments, however, it is most likely continuous with the latter which stretches roughly E–W with a width of 50–60 km, just as the outer rifts are continuous with each other.

The noticeable facts are that the double rift is found to extend over the

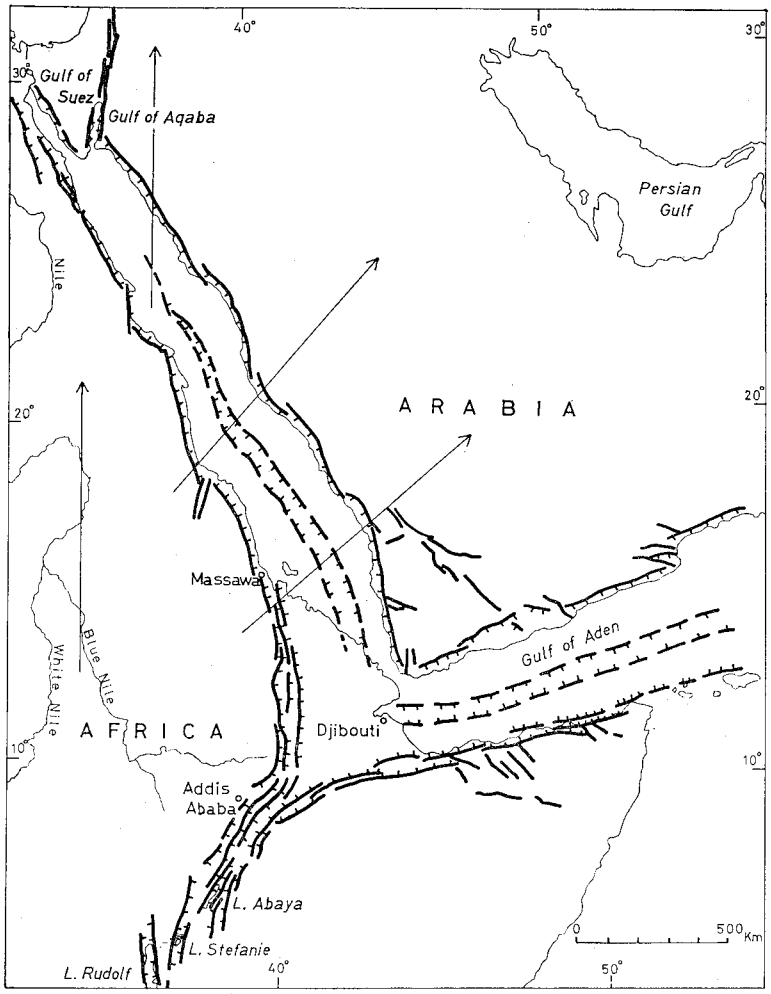

FIG. 20. Structural sketch map of the Red Sea Rift and the Gulf of Aden Rift.

Red Sea Rift and the Gulf of Aden Rift, encircling the southwestern to southern margin of the Arabia craton, and the outer rift gradually widens from northwest to southeast, and that the central trough, or fracture, appears at about lat. 24°N and becomes gradually wider toward southeast into the Gulf of Aden. Some geophysicists and geologists hold a view that the width of the central trough represents the amount of separation of the two land-masses and that the Arabian Peninsula drifted with an anticlockwise rotation of about 6–9° against the African continent. The writer supports this view, but as to the mechanism of land split he thinks differently.

According to R. W. Girdler, the ascending convection current within the

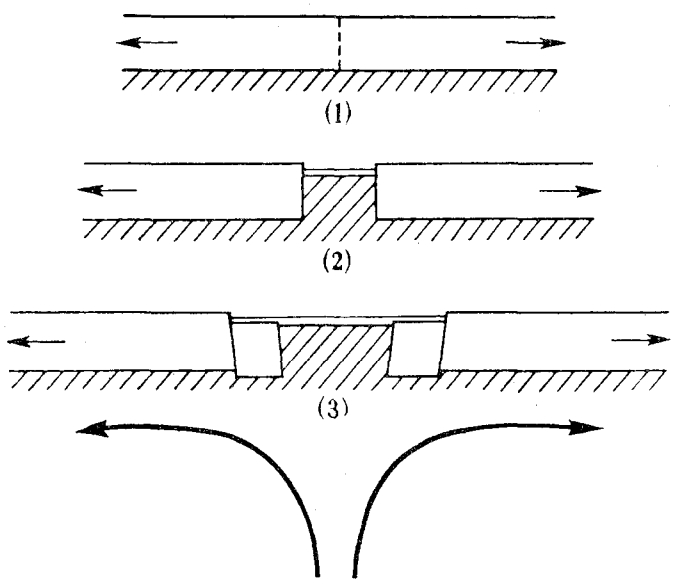

FIG. 21. Girdler's theory—A possible mechanism for the formation of the Red Sea structure and crustal separation. He considered that the tensional stresses are a consequence of a region of rising mantle convection (after Girdler, 1965).

mantle diverged right and left in the uppermost part, giving rise to tension which worked on the overlying crust in opposite directions so that the African continent in the southwest and the Arabian Peninsula in the northeast came to be separated from each other, thence the formation of the Red Sea Rift (Fig. 21) [26, 29, 30]. His theory, however, does not sound plausible when the relationship between the African Great Rift System and the Alpine-Himalayan tectogenic belt and the shapes and arrangement of convection cells within the mantle are taken into account.

The writer's theory is as follows: On the north side of the Arabian Peninsula the Taurus tectogenic belt belonging to the Alpine-Himalayan tectogenic belt runs roughly E–W in Turkey, and its extension in Iran turns to southeast and stretches NW–SE along the northeast side of the Persian Gulf (Fig. 1). Accordingly, at the time of formation of the African Great Rift System which is contemporaneous with the Alpine-Himalayan tectogenic belt, that is, when the Arabian Peninsula was separated from the African continent, the lateral movement of the convection current in the uppermost part of the mantle must have created a field of strong tension in the crust and the tensional force must have worked northward or northeastward, namely, toward the above-mentioned tectogenic belts. So far as the Arabian Peninsula is concerned, the tensional force worked stronger to the northeast and produced a great influence on the crust.

In this tensional field the tension worked differentially on the Arabia craton and on the Mozambique metamorphic belt because of their difference in strength and construction. Along the boundary between the two, a fault system was developed encircling the outer margin of the Red Sea Rift and the Gulf of Aden Rift, and produced a fault-depression belt. Then, a remarkable fracture occurred in the median zone of this depression belt. The cause of the fracture is attributed to crustal displacement by the northward, particularly northeastward, tensional force, as well as to the orientation of the Arabia craton against the depression belt and to the differential drift according to the structure of the crust. As the fracture opens wider toward southeast, the simatic basic rock body made a fluidal ascending movement until it reached a hydrostatic equilibrium, and filled the lower part of the fracture (Fig. 22). The writer does not think that the Arabian Peninsula made an independent anticlockwise rotation, but he believes that the interrelation between the

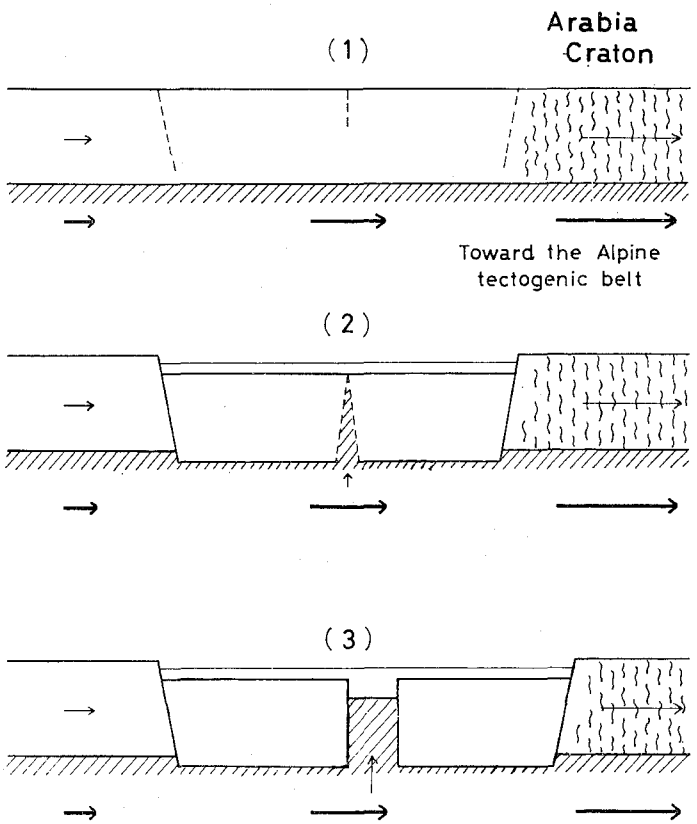

FIG. 22. Simplified diagram to illustrate the formation of the double rifts of Red Sea Rift by the lateral tensional stresses.

differential structure of the crust and the northward or northeastward tensional force is responsible for the apparently rotational aspect, open to the southeast.

The fact that the Red Sea Rift and the Gulf of Aden Rift show various kinds of anomalies different from the continental rifts has been already mentioned. The central deep trough, in particular, shows conspicuous positive Bouguer anomaly and strong anomaly of geomagnetism, and the geothermal flux is especially large. These phenomena may indicate that the afore-said basic intrusive body is situated at a relatively shallow depth. A granitic layer, 13.75 km thick, is inferred to exist beneath the shallow outer rift, but no such evidence is found in the central deep trough (Tables 1 and 2). This is also an element to support the writer's theory.

2. Rifts along the west margin of Arabia craton

The Red Sea Rift bifurcates at its northwestern end into the northwestward-proceeding Gulf of Suez Rift and the northerly-bound Gulf of Aqaba Rift; the latter stretches farther north along the Mediterranean coast on the west side of the Arabia craton for a distance of about 1,100 km. This rift is the northernmost member of the African Great Rift System. In the southern part of Turkey it adjoins, in a T shape, the Taurus tectogenic belt which is a part of the Alpine-Himalayan tectogenic belt.

The Dead Sea Rift, located at about the middle of the above-mentioned

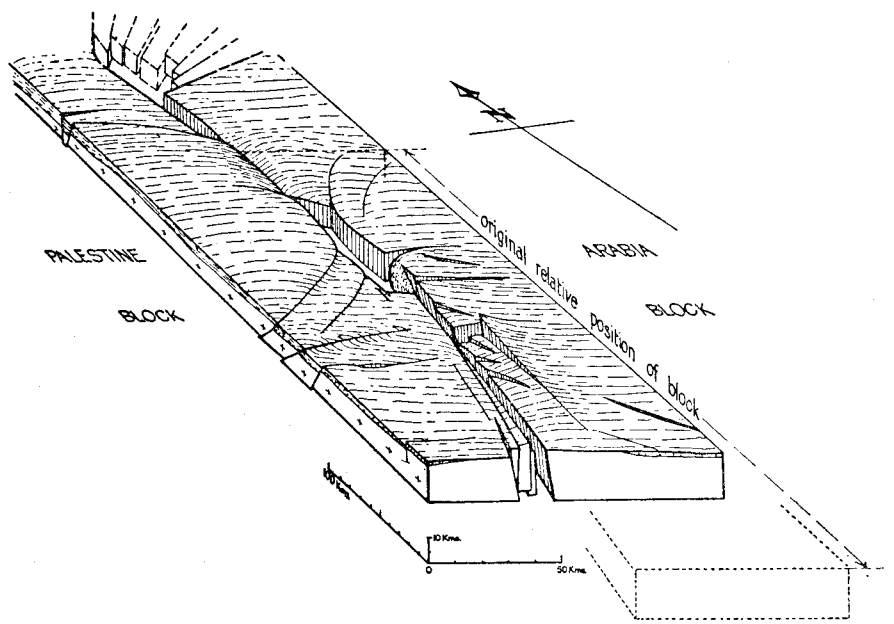

FIG. 23. Isometric block diagram to illustrate the formation of the Dead Sea Rift. Original relative position shown in broken lines (after Quennell, 1958).

rift, was studied by A. M. Quennell [68] whose conclusion is worthy of special mention as it elucidates well the status of formation of this rift. According to him, in the making of the Dead Sea Rift the Arabia block on the east was remarkably displaced horizontally, about 107 km northward, against the Sinai-Palestine block on the west, and the displacement was accompanied by about a 5.5° rotational drift of the Arabia block. This movement took place in two phases. In the first phase, ranging in age from early Miocene to early Pliocene, the Arabia block underwent a horizontal displacement of about 62 km northward, accompanied by 3° rotation; in the second phase, mostly during middle Pleistocene, the block was further displaced horizontally about 45 km northward, with 2.5° rotation, and the displacement is still in progress. In this movement, of course, warping, tilting and local uplift occurred concurrently, but the horizontal component of the movement was more prominent than the vertical component (Fig. 23).

The writer is greatly interested in Quennell's theory in the points that the Arabia block made a northward drift relative to the western block, and the drift was rotational, and that the formation of the Dead Sea Rift was contemporaneous with the culminant period of the Alpine tectogenic cycle.

3. Formation of rifts around Arabia craton

The Arabia craton is encircled on the west by the Gulf of Aqaba Rift and its northern extension, on the southwest by the Red Sea Rift, and on the south by the Gulf of Aden Rift. These rifts are considered to have been formed almost contemporaneously. On the north to northeast side of the Arabia craton, a tectogenic belt produced by the Alpine tectogenic cycle stretches. Formation of all these rifts is supposed to be roughly contemporaneous with that of the Alpine-Himalayan tectogenic belt, but in scope they are by far smaller than the latter. Therefore, it is most likely that the above-named rifts were formed as accessory diastrophic belts of the Alpine-Himalayan tectogeny.

Should one assume that the Alpine-Himalayan tectogenic belt was formed where the crust had undergone a strong compressive stress caused by the downward convergence of the lateral convection current coming from two sides in the uppermost part of the mantle, the convection current must have worked toward the tectogenic belt. Since the tectogenic belt on the north to northeast of the Arabia craton extends in an E-W to NW-SE direction, the convection current at that time is believed to have flowed northward and northeastward (Figs. 20 and 22). Such a convection movement in the uppermost part of the mantle would have exerted strong tension to the overlying crust, giving rise to strong dragging of the crust toward the tectogenic belt. On the other hand, the basement construction of this region reveals that the massive and very hard Arabia craton is markedly different from the surrounding

foliated metamorphic rocks (Mozambique metamorphic belt) in strength of rock and in geologic structure. Accordingly, the two land-masses made differential drifting movements, and the weakest part of the crust near the boundary between the two was fractured. On account of the shape and location of the Arabia craton and its relation to the northward or northeastward stress, the crust made the noticeable northward and northeastward horizontal drift, as seen along the west side of the Arabia craton, *i.e.*, Arabia block, and the anticlockwise rotational drift as seen on the southwest and south sides. Thus, the fracture, to be called the central deep trough, was developed in the Red Sea Rift and the Gulf of Aden Rift.

VIII. CONDITIONS RESPONSIBLE FOR FORMATION OF THE AFRICAN GREAT RIFT SYSTEM

As is obvious from what has been mentioned in the preceding chapters, an elucidation of the circumstances of formation of the African Great Rift System must satisfy at least the following facts:

(1) The basement of the African Great Rift System (extending over the eastern region of the African continent and the Arabian Peninsula) is composed of cratons, which are great massive bodies of extremely hard and compact rocks, and less hard foliated metamorphic rocks that are zonally distributed meandering through the cratons. The foliation of the metamorphic rocks shows a generally N-S trend which is also the trend of their distribution. The great rift system lies in the region of these foliated rocks. Where the rift valleys lie adjacent to the cratons or stretch into the cratons, a typical rift shape is often deformed and rift valleys assume irregular shapes.

(2) The great rift system, having an almost uniform width of 30 to 60 km, shows a typical shape of rift valley, with both sides cut by faults and the median zone depressed. However, this typical shape does not continue throughout the whole length of the rift system, because the system comprises many discontinuous rift valleys and many discontinuous faults in rows of irregular echelon arrangement, presenting fracture systems caused by shearing of elastic solid.

(3) The trend of the great rift system roughly coincides with the direction of the zonal distribution of the foliated metamorphic rocks. The fault system on either side of the rift system also corresponds to the trend of the foliation, or obliquely intersects the latter at low angles less than 45°.

(4) The fault system is usually accompanied by several accessory faults, which are all normal faults, stepped inward with a steep dip. No reverse faults are present. Judging from the shape of the rift valley and the character of the fault system, it would be reasonable to consider that the great rift system was formed in the tensional field. No evidence to support the com-

pression origin as maintained by some geologists has been found.

(5) The fact that faults and rift valleys constituting the African Great Rift System occur in discontinuous chains of echelon arrangement suggests that the causative tensional force, namely stress, had worked in an oblique direction against the structural trend of the foliated metamorphic rocks, not at a right angle to the latter.

(6) Topographically, the land on both sides of the great rift system shows mostly the aspect of tilting movement, where each block is upheaved in the part contacting the rift and gradually lowers outward.

(7) The African Great Rift System is a belt of fracture deeply cutting into the continental crust. In petrological character, the field where a continental rift system was formed is markedly different from the field where an oceanic rift system (submarine cleft) was formed. Since the former is the sialic crust whereas the latter is the simatic crust, the mechanism of formation of rift valleys should be naturally different between the two.

(8) Formation of the African Great Rift System took place mostly during a period from early Miocene to Pliocene, and the movement is still continuing to the present. However, ever since the latter part of Mesozoic or Cretaceous up to Palaeogene, the region of Precambrian foliated metamorphic rocks, in which the rift system was formed, had been affected by somewhat vigorous crustal movement, repeating gentle downwarping and upwarping, accompanied by volcanic activities. These disturbances may be regarded as forerunning phenomena of the formation of the great rift system. In other words, formation of the African Great Rift System was synchronous with that of the Alpine-Himalayan tectogenic belt. The writer, attaching importance to this point, considers that the African Great Rift System was formed as a link in the chain of the Alpine tectogenic cycle.

(9) The Alpine-Himalayan tectogenic belt extends roughly E-W, locally bending in NW-SE, or NE-SW, direction, on the north side of the African continent and Arabian Peninsula. The African Great Rift System, on the other hand, trends N-S and intersects the former at a right angle. The former is a folded tectogenic belt by lateral compression of the crust whereas the latter is a fault-depressed belt ascribed to lateral tension of the crust, and the two are of synchronous formation as mentioned above.

(10) Like other continental rifts the African Great Rift System usually shows conspicuous negative Bouguer anomaly. However, in some parts of the rift system, such as the Red Sea Rift and the Gulf of Aden Rift, the width is much greater and remarkable positive Bouguer anomaly is recorded in the central deep trough. Geomagnetic anomaly and geothermal flux are also larger in the central deep trough. These facts suggest that the Red Sea Rift and the Gulf of Aden Rift are structurally different from other rifts.

(11) In the period of late Cretaceous to early Tertiary, thickly accumulated

volcanic series spread out horizontally to a large extent overlying the Mozambique metamorphic rocks of the basement mostly in Kenya and Ethiopia. This volcanic series originated probably in large scale eruptions from great fissures, so the writer considers that these fissures might be forerunners of the African Great Rift System.

IX. CONCLUDING REMARKS ON FORMATION MECHANISM OF THE AFRICAN GREAT RIFT SYSTEM

Paying special attention to the fact that the African Great Rift System was formed as a link of the chain of the Alpine tectogenic cycle through synchronous diastrophic movements, the writer considered that the motive force of the movements was convection current within the mantle. From the fact that blocks on both sides of the great rift system are tilted outward, he recognized the ground upheaval of the region and ascribed it to isostasy which occurred as post-tectogenic events in the process of the rift system formation. In this chapter the writer attempts an elucidation of the formation mechanism of the great rift system, by taking into account those conditions described in the preceding chapter.

1. Interpretation by means of convection current

The African Great Rift System is a zone of shear fracture due to crustal tension, while the Alpine-Himalayan tectogenic belt is a zone of folding due to compression. In the great rift system, as well as in the tectogenic belt, gravity anomaly, geomagnetic anomaly and large geothermal flux are conspicuous. The great rift system is also characterized by shallow-focus earthquakes and effusion of dense basic volcanic rocks. These features lead one to deduce that the crustal compression and tension reflect deep-seated movements. Accordingly, the formation mechanism of the great rift system must have an intimate relation to the movements in the underlying mantle. It seems to be most reasonable to seek the cause of the formation of such large scale diastrophic belts of the crust in the thermal convection current within the mantle.

Thermal flow in the mantle comprises several convection cells which move in upward, downward and sideward currents. Where the ascending current diverges laterally in two directions in the uppermost part of the mantle, the area becomes a field of tension and the stress of the current movement exerts a tensional force to the overlying crust. Where the convection current in the uppermost part of the mantle moves sideward its stress would cause a tensional or dragging stress to the crust above. On the other hand, when lateral currents coming from two directions converge into one current and goes downward, the lateral and downward compressive stress would work to compress the overlying crust and drag it downward.

The Alpine tectogenic cycle reached its culmination during the period from

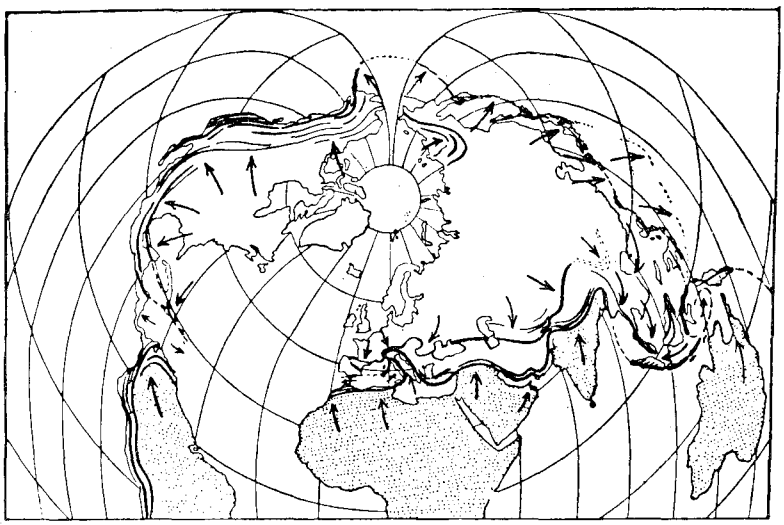

FIG. 24. Map showing the interrupted tectogenic ring peripheral to the continental masses of Laurasia (after Holmes, 1965).

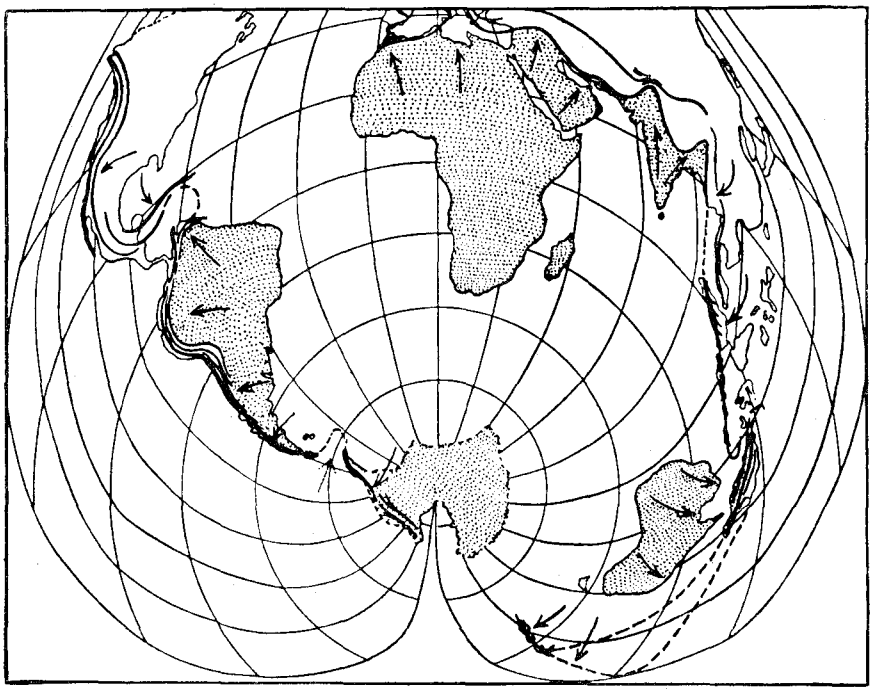

FIG. 25. Map showing the interrupted tectogenic ring peripheral to the continental masses of Gondwanaland (after Holmes, 1965).

early Miocene to Pliocene. In this period, the continental mass on the earth (Pangaea was one and the only continent in the late Palaeozoic era) was split into two masses, Laurasia continent and Gondwanaland, around which large scale tectogenic belts were formed (Figs. 24 and 25). Supposing these great tectogenic belts reflect the location where the convection currents coming from two directions had converged into a downward flow during the Alpine tectogenic cycle, the scope of the two continents would be helpful in inferring the approximate shape and position of the convection cells at that time. Thus, a field of compression and a field of tension or lateral drag can be imagined in the uppermost part of the mantle of those days. The Laurasia continent later was split into the Eurasian and North American continents, and the Gondwanaland was split into the South American, African, Indian, Australian and Antarctic continents [28, 71].

Before these continents became separate, the Alpine-Himalayan tectogenic belt lied along the Tethys Sea, serving as a boundary between the Laurasia continent and the Gondwanaland. It ran between Europe and Africa and to the north of India, stretching generally in an E–W direction. The African Great Rift System, which was formed roughly contemporaneous with the former, extended almost N–S and intersected the former in a T-shape. In view of the diastrophic scope, however, the African Great Rift System was of a much smaller scale, being only subordinate to the former which is the largest tectogenic belt on the earth.

The amount of the crustal contraction in the Alpine-Himalayan tectogenic belt varies with calculator and with the standard value employed for the calculation. The amount calculated for the Alps region is 480 km or 250 km. At any rate, it is evident that by this tectogenic movement the continental crust of Europe and Africa was largely dragged toward the tectogenic belt.

Should a tectogenic belt be reflecting a belt of compression due to convection current, then the inner area encircled by the tectogenic belt must reflect a field of tensile stress or lateral stress. At the present stage it is almost impossible to trace the direction and intensity of lateral stress within the area and divide them by region, but it is evident at least that the crust in the area extending from the African continent to the Arabian Peninsula was once placed in a field of tensile stress or lateral stress which was exerted toward the Alpine-Himalayan tectogenic belt on the north. When viewed from the present geographical distribution, the Alpine-Himalayan tectogenic belt is found to run generally E–W along the Mediterranean Sea, and partly bends southeastward in the east of Turkey (the Taurus tectogenic belt), at the base of the Arabian Peninsula. In the area over the southern part of Iran it stretches in a NW–SE direction and continues to the Himalayan Mountains. Such distribution seems to indicate that the lateral convection current in the uppermost part of the mantle flowed northward or northeastward beneath the crust of Africa and

Arabia, and thermal energy of the current turned kinetic energy, causing tensile stress to the overlying crust and dragging it toward the Alpine-Himalayan tectogenic belt.

In other words, the crust of the African continent and the Arabian Peninsula was placed in a field of maximum tensile stress during the Miocene-Pliocene period about 25 million years or less ago, as a link of the chain of the Alpine tectogenic cycle. To elucidate how the continental crust was affected by the lateral convection current in the mantle, and how the stress worked to form the African Great Rift System, we must examine the construction and structure of the continental crust of Africa and Arabia which served as the stage of formation of the rift system.

2. Explanation of influence by construction and structure of continental crust

In case the convection current in the mantle produces influence on the crust above the Mohorovičić discontinuity plane, the mode of propagation of stress and the resultant features would vary with construction and structure of the crust. Since the simatic, or basaltic, crust right above the discontinuity plane is a homogeneous layer of basic rocks, the stress would spread uniformly, but the sialic, or granitic, crust overlying the simatic layer is a layer of highly unhomogeneous construction and complex structure, so that the exerted stress would be greatly variable. The continental crust is mostly composed of this sialic layer.

The basement of the African continental crust, especially the portion extending from the Arabian Peninsula to eastern Africa, is composed of the extremely hard and compact massive cratons and the less hard and zonally distributed metamorphic rocks structurally controled by the marked steeply dipping foliation. After the late Precambrian tectogenic movements, these rock bodies remained stable, forming the basement of the continent. Separation of the above-mentioned two different types of rocks accounts for the different construction of the African continental crust. The cratons distinguished by the writer are great massive rock bodies that have suffered little from any of the tectogenic movements since about 2,500 m.y. ago and have remained stable as the hardest and most compact parts of the crust. The belts of foliated metamorphic rocks, on the other hand, were formed through the tectogenic movements since about 2,500 m.y. ago, and are characterized by zonal distribution meandering among cratons, by marked foliation, and by folded structure in the Precambrian age. As the cratons and the foliated metamorphic rock belts were formed at great depths of the crust, their segregation must have started at a still greater depth, probably at the base of the continental crust.

The cratons constituting the crust of the Arabian Peninsula and eastern Africa are as follows: Arabia craton in the north, Tanganyika craton and Congo craton in the middle of the continent, and Kalahari craton in the south

(Fig. 8). From the southwestern and southern margin of the Arabia craton to the south the Mozambique metamorphic belt runs roughly N–S. From the middle to the southern parts the belt is bounded on the west by Tanganyika and Kalahari cratons. The Burundian-Karagwe-Ankolean metamorphic belt and the Rusizi-Ubendian metamorphic belt run between Tanganyika craton and Congo craton, extending in a NNE–SSW or N–S or NW–SE direction.

The belts of foliated metamorphic rocks present N–S, NW–SE or NE–SW fold, and the steeply dipping foliation along the direction of their zonal distribution, well manifesting the remarkable meridional trend of the geologic structure.

These foliated rocks are just like a straight-grained board. They are resistant to compression or tension in the direction of their extension, but are weak against the force exerted at right or oblique angles and are easily split along the foliation. In other words, markedly foliated rock bodies are easy to be broken or fractured in the direction of their structure. As a result, the rock bodies show cracks or fractures parallel or slightly oblique to the prominent foliation structure.

The African Great Rift System was formed in the region of the foliated metamorphic rocks, generally along their extension, and avoiding the region of hard and compact cratons. Faults and rift valleys constituting the great rift system are arranged in an echelon pattern, either parallel or slightly oblique to the foliation. No faults or rift valleys are found to intersect the foliated structure at right angles or high oblique angles. As mentioned before, the African Great Rift System is not continuous throughout its whole length but is composed of numerous discontinuous fault systems and long irregular chains of rift valleys in an echelon arrangement. The aspect reminds us of a certain kind of fracture system in elastic solid.

Therefore, the writer holds a view that the African Great Rift System is a result of elastic shearing of the continental crust due to the stress of convection current in the uppermost part of the mantle, under the strong control of the construction and structural orientation of the crust. That is to say, the great rift system is not reflecting a diverge zone of the convection current, or does not comply only with the direction of the diverging current or with the scope of the exerted stress. The writer considers that the formation of the great rift system was governed by the differences between the two types of component rocks of the continental crust, namely the cratons and the foliated metamorphic rocks, differing in location, hardness and geologic structure. In particular, influence of the foliated structure of the metamorphic rocks was prominent. The rift system was produced when shear fracture occurred in a structurally weak part of the crust where the hard cratons and the less hard metamorphics come into contact. Our present knowledge of the direction and the scope of laterally moving convection current in the uppermost part of the mantle cannot

go beyond conjecture. It is possible, however, that the current did not move in a definite direction but diffused in various directions in the form of a turbulent flow.

During the Alpine tectogenic cycle the convection current in the uppermost part of the mantle is considered to have flowed ultimately toward the location of the Alpine-Himalayan tectogenic belt. Along with the formation of this tectogenic belt, the African and Arabian continental crust was affected by the convection current, and the relatively weak part in the foliated metamorphic belts, where the belts and the crations meet, suffered shearing, largely under the influence of the foliation, and resulted in the formation of the great rift system. In this case, sicne the fault systems are arranged in chains of an echelon pattern, the stress must have been most effective in the components of oblique directions against the trend of the prominent foliated structure.

Thus, the writer is against the past theory of some scientists that the African Great Rift System reflects a diverging zone of the ascending convection current into right and left.

3. Crustal movement due to isostasy after formation of the African Great Rift System

As has been mentioned already, the land blocks on either side of the great rift system are found to be highest in the part adjacent to rift valley and become gradually lower outward, presenting a topography apparently resulted from tilting movement. This aspect is explained by the writer as follows.

The outer shell of the continental crust is made of a sialic layer whose average density is 2.7, and the underlying shell is a simatic layer which is 3.0 to 3.3 in density. The great rift system, having a width of 30 to 60 km and a depth several hundred to more than 2,000 meters, stretches zonally over a great length. Whatever may the mechanism of its formation be, the isostasy of the crust beneath the great rift system must have been disturbed and the balance level should have sunk deeper. The strength of the crust may be able to bear the load of local blocks, but it cannot be large enough to hold the load of materials over a wide area.

When the great rift system was formed, the causative force pressed down the lighter sialic material, shoving aside the heavier simatic material. Thus, the balance level of load at a certain depth was disturbed. To keep the isostasy, that is, to recover the lost balance, the region of the rift valley was upheaved, resulting in the aspect of tilted blocks that are higher along the margin of the rift valley and lower in the outer side.

This assumption may sound vague because of deficient numerical data, but the writer believes that this is the most reasonable explanation of the land features as observed today.

4. Formation of Red Sea Rift and Gulf of Aden Rift

The unique features of the Red Sea Rift and the Gulf of Aden Rift, differing

from other rifts of the African continent, have been described already. In the following paragraphs the writer explains the formation of these characteristic rifts.

The Arabian Peninsula was originally continuous with the African continent on the south side of the Tethys Sea, but was later separated from the latter. In the process of the separation, rift valleys were formed around the Arabia craton. Although the African Great Rift System was formed contemporaneously with the Alpine-Himalayan tectogenic belt, its scope was much smaller, being a subordinate diastrophic belt of the latter, but the geographical positions of the two belts are worthy of notice.

In a general aspect, the African Great Rift System trending N–S intersects the E–W trend of the Alpine-Himalayan tectogenic belt in a T shape in the southern part of Turkey. However, the rift system bends around the Arabia craton, as shown by the N–S trend of the part north of the Gulf of Aqaba Rift, the NW–SE trend of the Red Sea Rift, and the W by S–E by N trend of the Gulf of Aden Rift. In the eastern part of Turkey the E–W trending Alpine-Himalayan tectogenic belt turns southeastward to the southern part of Iran (that is, the Taurus tectogenic belt), extending in a NW–SE direction on the northeast side of the Arabia craton (Fig. 1).

The Alpine tectogenic cycle culminated from early Miocene to Pliocene, and in this period the convection current that was laterally moving in the uppermost part of the mantle is considered to have converged intensely toward the area of the Alpine-Himalayan tectogenic belt. As a result, the continental mass of Arabia and Africa was strongly dragged northward, and especially the part including the Arabian Peninsula must have been dragged to the northeast, too.

When the Arabian Peninsula was affected by the northward and northeastward tensile force, the tension caused differential drift of the Arabia craton and the surrounding belt of foliated metamorphic rocks, thus producing the fault system between the Arabian Peninsula and the African continent. The median zone of the fault system sunk and formed the fault-depression zone of the present Red Sea and the Gulf of Aden. A zone of fracture was formed also in the north of the Gulf of Aqaba Rift. Due to a strong tensile force, fracture occurred in the median zone of the Red Sea Rift and the Gulf of Aden Rift. As the fracture opened gradually wider, a simatic basic rock body ascended in a fluidal movement and filled the fracture, and when it reached a hydrostatic equilibrium the central deep trough was formed in each of the rifts (Fig. 22).

It is conceivable that the tension was relatively larger as it neared the tectogenic belt, but in the case of the Arabia block the tension worked fairly strongly northeastward as well as northward, that is, the block was dragged toward north and northeast, so that the width of the central deep trough of the Red Sea became wider from northwest to southeast and the central deep

trough of the Gulf of Aden widened in the east than in the west, thus showing an anticlockwise rotational drift of the Arabia block at an angle of 6–9°. In the vicinity of the Dead Sea Rift, the Arabia block drifted northward against the Sinai-Palestine block on the west, over a distance of about 107 km with a rotational movement at an angle of about 5.5° (Fig. 23).

The unusually large width of the Red Sea Rift and the Gulf of Aden Rift, and their double-rift structure with the noticeable central deep trough, can be reasonably explained by the following assumption: The Arabia-Africa continental crust was located in the field of lateral tension that was caused by the convection current in the uppermost part of the mantle at the time of conversion of the descending current. The lateral tension thus caused was greater in the converged zone, namely, the area of the Alpine-Himalayan tectogenic belt which extends E–W but bends in a NW–SE direction on the north to northeast side of the Arabian Peninsula. The differences between the Arabia craton and the surrounding belt of foliated metamorphic rocks, in construction, geologic structure and strength of component rocks, gave rise to differential drift of land against the tension. In short, either the Red Sea Rift or the Gulf of Aden Rift does not reflect a diverged zone of ascending convection current in the uppermost part of the mantle (Figs. 20 and 22).

POSTSCRIPT

The tectogenic belts and the great rift systems are the largest weak and unstable lines on the earth, the former is ascribed to crustal compression and the latter to crustal tension. So far as the present knowledge goes, the writer thinks that the convection current in the mantle is the most reasonable motive force of such great disturbances. The crust, especially continental crust, is extremely intricate in construction and geologic structure, so that the influence of stress caused by the convection current would naturally vary with them. Formation mechanism of diastrophic belts can be elucidated only through detailed geophysical and geological studies of the interrelations between tectogenic belts, such as represented by the Alpine-Himalyan tectogenic belt, and fracture belts, such as represented by the African Great Rift System. Based on this viewpoint, the writer is proceeding with his study.

The writer paid special attention to the fact that the Alpine-Himalayan tectogenic belt reflecting crustal compression and the African Great Rift System reflecting crustal tension are of contemporaneous formation in a T shape intersection, and he considered these regions are the best stage for the above-mentioned study. On the Alpine-Himalayan tectogenic belt a great many works have been published and its general aspect is fairly well known, whereas on the African Great Rift System many problems remain unsolved. The writer previously published his tentative theory in "A Study on the Formation of

the African Rift Valley" [55]. It has been supplemented this time with the data and knowledge gained from the recent field work in East Africa, and the result is presented here in the form of a theory on formation mechanism of the African Great Rift System. The writer would appreciate criticism from the reader.

REFERENCES

[1] Association des Services Geologique Africains and United Nations Educational, Scientific, and Cultural Organization, Carte tectonique internationale de l, Afrique: 1 : 5,000,000 (1968).

[2] BAKER, B. H., An outline of the geology of the Kenya rift valley: *Rept. Geol. Geophys. East Afr. Rift System*, 1-19 (1965).

[3] ——, The rift system in Kenya: *Rept. UMC/UNESCO Seminar East Afr. Rift System*, 82-84 (1965).

[4] BISHOP, W. W. and TRENDALL, A. F., Erosion surfaces, tectonics and volcanic activity in Uganda: *Quart. J. Geol. Soc. London*, **122**, 385-420 (1966).

[5] BOWEN, N. L., Lavas of the African Rift Valleys and their tectonic setting: *Am. J. Sci.*, **35-A**, 19-33 (1938).

[6] BULLARD, E. C., Gravity measurements in East Africa: *Phil. Trans. Roy. Soc. London*, **253-A**, 445-531 (1936).

[7] BUSK, H. G., Explanatory note on the block diagram of the Great Rift Valley from Nakuru to Lake Magadi: *Quart. J. Geol. Soc. London*, **95**, 231-233 (1939).

[8] CAHEN, L. and SNELLING, N. J., The geochronology of equatorial Africa: North Holland Pub. Co., 195 pp. (1966).

[9] CLOOS, H., Hebung-Spaltung-Vulkanismus: *Geol. Rund.*, **30**, 405-527 (1939).

[10] DE BREMAECKER, J. CL., Seismicity of the Western Rift Valley: *J. Geophys, Research*, **64**, 1961-1966 (1959).

[11] DE SWARDT, A. M. J., Rift faulting in Zambia: *Rept. UMC/UNESCO Seminar East Afr. Rift System*, 105-114 (1965).

[12] DIXEY, F., The East African Rift System: *Overseas Geol. Miner. Resurces Bull.*, H. M. Stationery Office (1956).

[13] DRAKE, C. L., East African Rift System: *Geotimes*, **10**, 13-14 (1965).

[14] ——, GIRDLER, R. W. and LANDISMAN, M., Geophysical measurements on the Red Sea: *Reprints Intern. Oceanogr. Congr.*, 21 pp. (1959).

[15] DUNDAS, D. L., Review of rift faulting in Tanzania: *Rept. Geol. Geophys. East Afr. Rift System*, 95-103 (1965).

[16] EAST AFR. COMMIT. COOPR. GEOPHYS., Structural sketch map of part of the rift zone of eastern Africa (Scale 1 : 5,000,000): *Rept. Geol. Geophys. East Afr. Rift System* (1965).

[17] EWING, M. and HEEZEN, B. C., Continuity of Mid-Oceanic Ridge and Rift Valley in the southwestern Indian Ocean confirmed: *Science*, **131**, 1677-1679 (1960).

[18] FOZZARD, P. M. H., Quarter degree sheet 124, "Kelema", 1 : 125,000: Geol. Surv. Tanganyika (1960).

[19] ——, Quarter degree sheet 123, "Kwa Mtoro", 1 : 125,000: Geol. Surv. Tanganyika (1961).

[20] FOZZARD, P. M. H., Quarter degree sheet 182, "Kimamba", 1 : 125,000: Geol. Surv. Tanzania (1965).

[21] FURON, R. and DAUMAIN, G., Notice explicative, Carte esquisse structurale provisoire de L'Afrique (1 : 10,000,000): *Congr. Geol. Intern. Assoc. serv. geol. africains* (1959).

[22] —— and LOMBARD, J., Notice explicative, Carte géologique de L'Afrique (1:5,000,000): UNESCO-ASGA (1963).

[23] GARSON, M. S., Summary of present knowledge of the rift system in Malawi: *Rept. UMC/UNESCO Seminar East Afr. Rift System*, 94-104 (1965).

[24] Geological Map of East Africa (1 : 4,000,000), with Table I (Stratigraphical table showing lithology) and Table II (Principal tectonic events in East Africa): East African Literature Bureau, Nairobi (1961).

[25] GEOLOGICAL SURVEY of TANGANYIKA, Geological Map of Tanganyika (Scale 1 : 2 000,000) with Summary of the Geology of Tanganyika: Geol. Surv., Minist. Mines and Comm., Tanganyika (1959).

[26] GIRDLER, R. W., The relationship of the Red Sea to the East African Rift System: *Quart. J. Geol. Soc. London*, **114**, 79-102 (1958).

[27] ——, Geophysical evidence on the nature of magmas and intrusions associated with Rift Valleys: *Abstr., Intern. Assoc. Volc., Meet., Tokyo, Japan*, May, 1962.

[28] ——, Initiation of continental drift: *Nature*, **194**, 521-524 (1962).

[29] ——, Geophysical studies of rift valleys: *Physics and Chemistry of the Earth*, **5**, 121-156 (1964).

[30] ——, The formation of new oceanic crust: A Symposium on Continental Drift, organized by P. M. S. Blackett *et al.* Chapt. XI, 123-136 (1965).

[31] GOGUEL, J., La structure des fossés Africains et la gravimétrie: *Ann. Geophys.*, **5**, 174 (1949).

[32] GOUIN, P., Magnetic measurements in Southern Ethiopia: *Bull. Geophys. Obs. Univ. Coll. Addis Ababa*, **2**, 21-22 (1960).

[33] GRAINGER, D. J. and FOZZARD, P. M. H., Quarter degree sheet 199, "Mikumi", 1 : 125,000: Miner. Resour. Div. Tanzania, (1966).

[34] GREGORY, J. W., The great rift valley: London, John Murray (1896).

[35] ——, The Rift Valleys and geology of East Africa: London, Seeley, Service and Co., 479 pp. (1921).

[36] ——, The structure of the Great Rift Valley: *Nature*, **12**, 514-516 (1923).

[37] HALDEMANN, E. G., Quarter degree sheet 274, "Milo (Njombe south)", 1 : 125,000: Geol. Surv. Tanganyika (1961).

[38] HARPUM, J. R., Some problems of pre-Karroo geology in Tanganyika: *Congr. Geol. Intern. Compt. Rend. 19e, Algiers, 1952*, **20**, 209-239 (1954).

[39] HEEZEN, B. C., The rift in the ocean floor: *Sci. Am.*, **203**, 99-110 (1960).

[40] ——, The world rift system: *Reft. UMC/UNESCO Seminar East Afr. Rift System*, 116-118 (1965).

[41] HEPWORTH, J. V., KENNERLEY, J. B. and SHACKLETON, R. M., Photogeological investigation of the Mozambique front in Tanzania: *Nature*, **216**, 146-147 (1967).

[42] HOLMES, A., The sequence of Precambrian orogenic belts in south and central Africa: *Intern. Geol. Congr. 18th, Great Britain, 1948, Rept.*, **14**, 254-269 (1951).

[43] ——, Principles of Physical Geology, Rev. ed.: Thomas Nelson (1965).

[44] IVANHOE, L. F., Crustal movements in the Arabia region: *Geotimes*, Dec. 1967, 12-13

(1967).

[45] JACOBS, J. A., RUSSELL, R. D. and TUZO WILSON, J., Physics and Geology: McGraw-Hill, N.Y. (1959).

[46] JAMES, T. C., Degree sheet 92-Mbamba bay, N. E. Quarter and part of S. E. Mbamba bay-south C 36/W II and part of W IV, "Tanganyika" 1 : 125,000: Geol. Surv. Tanganyika (1956).

[47] ——, Degree sheet 85-Manda, S. E. Quarter, Litembo-south C 36/Q IV, "Tanganyika" 1:125,000: Geol. Surv. Tanganyika (1956).

[48] KENNEDY, W. Q., The structural differentiation of Africa in the Pan-African (±500 m.y.) tectonic episode: *Univ. Leeds, Research Inst. Afr. Geol., 8th Ann. Rept.*, 48-49 (1964).

[49] KENT, P. E., The age and tectonic relationships of East African volcanic rocks: *Geol. Mag.*, **81**, 15-24 (1944).

[50] KÔNO, Y., Stress distribution within the mantle convection cell and stirring of the mantle by the convection (in Japanese with English abstract): *Zisin (Earthquake)*, Ser. II, **19**, 176-186 (1966).

[51] LOUPEKINE, I. S., Seismology in East Africa: *Rept. UMC/UNESCO Seminar East Afr. Rift System*, 85 (1965).

[52] MACDONALD, R., The status of rift valley studies in Uganda: *Rept. Geol. Geophys. East Afr. Rift System*, 53-82 (1965).

[53] ——, The status of rift valley in Uganda: *Rept. UMC/UNESCO Seminar East Afr. Rift System*, 52-81 (1965).

[54] MACFARLANE, A., MACDONALD, A, S., GRANTHAM, D. R. and SKERL, A., Quarter degree sheet 227, "Luika", 1 : 125,000: Geol. Surv. Tanzania (1964).

[55] MATSUZAWA, I., A study on the formation of the African Rift Valley: *J. Earth Sci., Nagoya Univ.*, **14**, 89-115 (1966).

[56] ——, Some considerations on the formation of the African rift valley (in Japanese with English abstract): *Africa Kenkyu (J. Afr. Stud., Japan. Assoc. Africanists)*, **4**, 1-24 (1967).

[57] MIZUTANI, S. and YAIRI, K., Tectonic sketch of the Mbeya area, southern Tanzania: *J. Earth Sci. Nagoya Univ.*, **17**, 107-124 (1969).

[58] MCCALL, B. J. H., Geology of the Nakuru-Thomsois Falls—Lake Hannington Area (Degree sheet 35, S. W. Quarter and 43, N. W. Quarter, 1 : 125,000): *Minist. Nat. Resour., Geol. Surv. Kenya, Rept.*, **78**, pp. 122 (1967).

[59] MCCONNELL, R. B., Rift and shield structure in East Africa: *Intern. Geol. Congr. 18th, Great Gritain 1948, Reft.*, **14**, 199-207 (1951).

[60] ——, The East African rift system: *Nature*, **215**, No. 5101, 578-581 (1967).

[61] MOHR, P. A., The Ethiopian Rift System: *Bull. Ceophys. Obs. Univ. Coll. Addis Ababa*, **3**, 33-62 (1962).

[62] ——, Transcurrent Faulting in the Etiopian Rift System: *Nature*, **218**, 938-940 (1968).

[63] MUDD, G. C. and ORRIDGE, G. R., Quarter degree sheet 85, "Babati", 1 : 125,000: Miner. Resour. Div. Tanzania (1966).

[64] MUSSETT, A. E., REILLY, T. A. and RAJA, P. K. S., Palaeomagnetism in East Africa: *Rept. Geol. Geophys. East Afr. Rift System*, 83-94 (1965).

[65] NAFE, J. E., HENNION, J. F. and PETER, G., Geophysical measurement in the Gulf of Aden: *Reprints Intern. Oceanogr. Congr.*, 42 pp. (1959).

[66] ORRIDGE, G. R., Quarter degree sheet 69, "Mbulu", 1 : 125,000: Mine. Resour. Div. Tanzania (1965).

[67] PALLISTER, J. W., The rift system in Tanzania: *Rept. UMC/UNESCO Seminar East Afr. Rift System.*, 86-91 (1965).

[68] QUENNELL, A. M., The structure and geomorphic evolution of the Dead Sea rift: *Quart. J. Geol. Soc. London*, **114**, 1-19 (1958).

[69] ——, MCKINLAY, A. C. M. and AITKEN, W. G., Summary of the geology of Tanganyika: *Geol. Surv. Tanganyika, Mem.*, **1** (1956).

[70] REILLY, T. A., East African palaeomagnetism: *Rept. Geol. Geophys. East Afr. Rift System*, 40-43 (1965).

[71] RUNCORN, S. K., Towards a theory of continental drift: *Nature*, **193**, 311-314 (1962).

[72] SAMPSON, D. N. and WRIGHT, A. E., Quarter degree sheet 183, "Morogoro", 1:125,000: Geol. Surv. Tanganyika (1961).

[73] SEGGERSON, E. P. and BAKER, B. H., Post-Jurassic erosion-surface in eastern Kenya and their deformation in relation to rift structure: *Quart. J. Geol. Soc. London*, **121**, 51-72 (1965).

[74] SELBY, J. and MUDD, G. C., Quarter degree sheet 104, "Kondoa", 1 : 125,000: Geol. Surv. Tanzania (1965).

[75] —— and THOMAS, C. M., Quarter degree sheet 103, "Balangida Lelu", 1 : 125,000: Miner. Resour. Div. Tanzania (1966).

[76] SHIMAZU, Y. and KÔNO, Y., Unsteady thermal convection within the upper mantle and tectogenesis (I) (in Japanese with English abstract): *Zisin (Earthquake)*, Ser. II, **16**, 115-122 (1963).

[77] —— and ——, Unsteady thermal convection within the upper mantle and tectogenesis (II) (in Japanese with English abstract): *Zisin (Earthquake)*, Ser. II, **17**, 148-157 (1964).

[78] STOCKLEY, G. M., The pre-Karroo stratigraphy of Tanganyika: *Geol. Mag.*, **80**, 161-170 (1943).

[79] SUTTON, G. H. and BERG, E., Seismological studies of the Western Rift Valley of Africa: *Trans. Am. Geophys. Union*, **39**, 474-481 (1958).

[80] SUWA, K., Geology of Ethiopia (in Japanese): *Nagoya Chigaku (Nagoya J. Geol.)*, **18**, 13-25 (1963).

[81] —— and UEMURA, T., Geology of the African rift valley and the Olduvai Gorge (in Japanese with English abstract): *Africa Kenkyu (J. Afr. Stud., Japan. Assoc. Africanists)*, **3**, 18-48 (1966).

[82] ——, Precambrian system of the African continent, I (in Japanese): *Chikyu Kagaku (Earth Sci.)* No. 84, 39-48 (1966).

[83] ——, Precambrian system of the African continent, II (in Japanese): *Chikyu Kagaku (Earth Sci.)*, **21**, 32-44, (1967).

[84] TAYLOR, M. H., Geologic structures in the Ethiopian region of East Africa: *Tran. New York Acad. Sci.*, Ser. II, **14**, 220 (1952).

[85] TEMPERLEY, B. N., REEVE, W. H. and KING, A. J., Quarter degree sheet 163, Mpwapwa-south B 37/M I, 1: 125,000: Geol. Surv. Tanganyika (1953).

[86] THOMAS, C. M., Quarter degree sheet 84, "Hanang", 1 : 125,000: Miner. Resour. Div. Tanzania (1966).

[87] THOMPSON, A. O., Geology of the Kijabe area (Degree sheet 43, S. E. Quarter, 1 : 125,000): *Minist. Nat. Resour., Geol. Surv. Kenya, Rept.*, **67**, 52 pp. (1964).

[88] —— and DODSON, R. G., Geology of the Naivasha area (Degree sheet 43, S. W. Quarter, 1 : 125,000): *Minist. Nat. Resour., Geol. Surv. Kenya, Rept.*, **55** (1963).

[89] UNESCO, Explanatory note of the International tectonic map of Africa 1 :5,000,000: UNESCO, Paris (1969).

[90] VENING MEINESZ, F. A., Thermal convection in the Earth's mantle: Cont. Drift, edited by S. K. Runcorn, Chapt. 6, 145-176, Academic Press. New York and London (1962).

[91] VON HERZEN, R. P., Geothermal heat flow in the Gulfs of California and Aden: *Science*, **140**, 1207-1208 (1963).

[92] WADE, F. B. and OATES, F., An explanation of Degree Sheet No. 52 (Dodoma): Dept. Lands and Mines, Geol. Div., Tanganyika (1938).

[93] WHITEMAN, A. J., A summary of present knowledge of the rift valley and associated structures in Sudan: *Rept. UMC/UNESCO Seminar, East Afr. Rift System*, 34-46 (1965).

[94] WHITTINGHAM, J. K., Quarter degree sheet 53 N. E. "Mlali", 1 : 125,000: Geol. Surv. Tanganyika (1958).

[95] ——, Quarter degree sheet 53 S. E. "Kilosa", 1 : 125,000: Geol. Surv. Tanganyika (1959).

[96] ——, Quarter degree sheet 215, "Iringa", 1 : 125,000: Geol. Surv. Tanganyika (1962).

[97] ——, Quarter degree sheet 234, "Chombe", 1 : 125,000: Geol. Surv. Tanganyika (1963).

[98] WILLIAMS, L. A. J., Petrology of volcanic rocks associated with the rift system in Kenya: *Rept. Geol. Geophys. East Afr. Rift System*, 33-39 (1965).

[99] ——, Geology, Nairobi-City and Region: edit. by W. T. W. Morgan, Oxford Univ. Press. Nairobi, 1-14 (1967).

[100] YAIRI, K. and MIZUTANI, S., Fault system of the Lake Tanganyika Rift at the Kigoma area, western Tanzania: *J. Earth Sci. Nagoya Univ.*, **17**, 71-96 (1969).

Fault system of the Lake Tanganyika rift at the Kigoma area, western Tanzania

Kenji YAIRI and Shinjiro MIZUTANI

Department of Earth Sciences, Faculty of Science, Nagoya University

(Received 16 August 1969)

ABSTRACT

The African rift valley traverses the east Africa over 6000 km with approximately north-south trend. It bifurcates into the eastern and the western rift valley at the equatorial area. A rift along Lake Tanganyika, called the Lake Tanganyika rift, belongs to the western rift valley.

Geotectonic study on the fault systems of the Lake Tanganyika rift was carried out at the Kigoma area, western Tanzania. Structural analyses of the fracture systems had led to a conclusion that the fault systems consist of N-S trending fracture system and E-W trending one. The former is much more predominant than the latter, and is attributed to tension fractures, whereas the latter is shear fracture with horizontal displacement. Judging from their interrelationship, it is concluded that both of them occurred simultaneously. It may be given as a mechanism of the rift formation that the fault systems of the Lake Tanganyika rift are composed of combination of the E-W trending transform fault along older weak lines and the N-S trending tension faults, both of which occurred concurrently under the same regional tensile stress field.

INTRODUCTION

The African rift valley running through the African continent over 6000 km with approximately north-south trend bifurcates into the eastern and the western rift valley at the equatorial Africa. Along the western rift valley, there can be seen a link of lakes such as Lake Albert, Lake Edward, Lake Kivu, Lake Tanganyika and Lake Rukwa from north to south. It forms an arc convex to the west and, therefore, its trend takes NE-SW at the northern part, N-S at the middle and NW-SE at the southern one. The rift along Lake Tanganyika is called in this paper the Lake Tanganyika rift, whose general trend is NNE-SSW to NNW-SSE.

In the Lake Tanganyika rift area and its environs are developed the Archeozoic Ubendian system, and the Proterozoic Karagwe-Ankolean and Bukoban system (Fig. 1). Previous works by Stockley [13] and Halligan [10] had been carried out on the Proterozoic rocks and on stratigraphy of south and west Tanzania, respectively. Geological Survey of Tanganyika

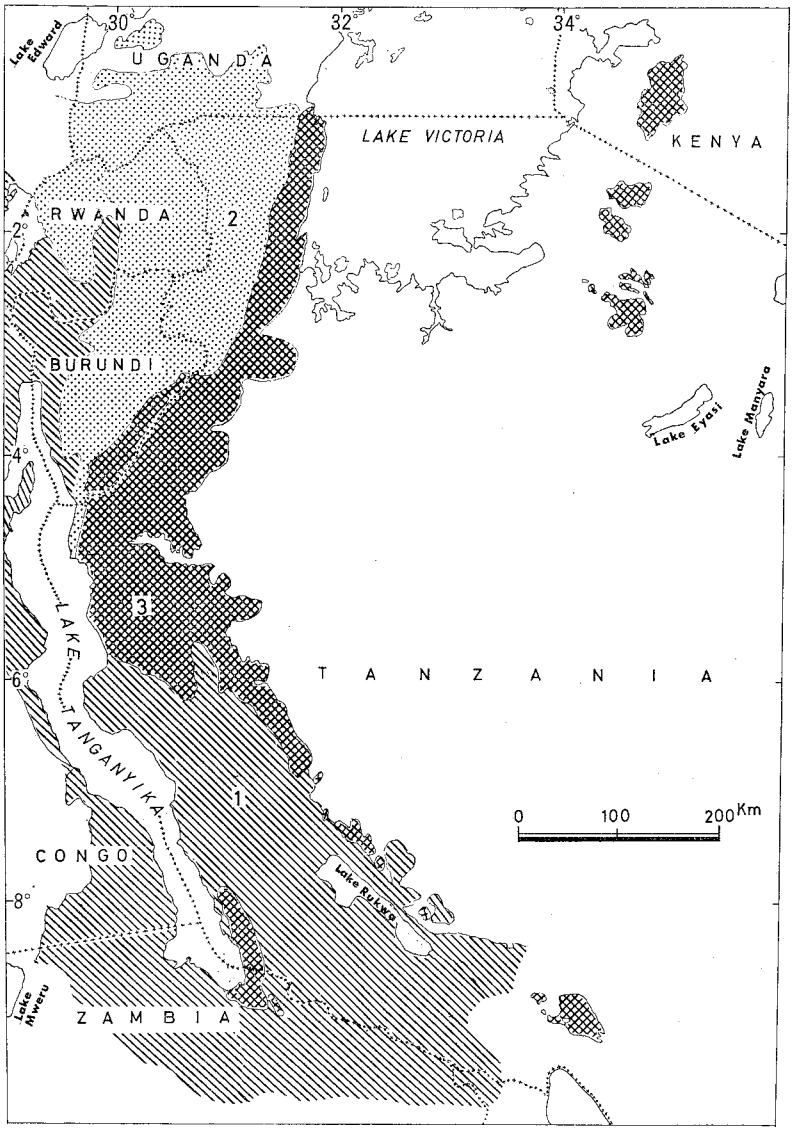

FIG. 1. Map showing geological distribution of Ubendian, Karagwe-Ankolean and Bukoban system (Compiled from L. Cahen and N. J. Snelling 1966). 1: Ubendian system, 2: Karagwe-Ankolean system, 3: Bukoban system.

had published six sheets of the geologic map (1 : 125,000) surveyed by Halligan [4, 5, 6, 7, 8, 9] in west Tanzania.

General discussions and hypotheses on the African rift valley and related structures had been presented by many authors [2, 3, 11, 12]. Information of faults or fracture systems themselves resulting from the rift movement is,

however, not necessarily available for our interpretation. In the present work carried out in summer of 1968 at the Kigoma area on the eastern shore of Lake Tanganyika, we made detailed survey especially on fracture systems found in the Proterozoic rock formations. In this paper, we describe some evidences obtained during our field investigation and present a result of photogeologic analysis of areal lineament, which provides us with a clue for understanding of regional patterns of the fracture systems.

PHYSIOGRAPHY

There are twenty regions in Tanzania. They are subdivided into sixty-six districts. The Kigoma district is situated in the westernmost Tanzanian country, and is bordered by Lake Tanganyika in the west. Kigoma town, which was a base of our field investigation, is situated at lat. 4°53′ S and long. 29°38′ W, and is known as an important port town on the eastern shore of Lake Tanganyika. Kigoma is also the terminal station town of East African railway traversing the Tanzanian country from east to west over 1,100 km from Dar es Salaam city, a capital of Tanzania. Ujiji, 7 km southeast of Kigoma, is well known as an earlier civilized site.

Topographic maps and airphotographs of various scales have been published by Survey Division of the Ministry of Land, Settlement and Water Development, Tanzania. The maps available for our survey at Kigoma and its environs are as follows: a sheet of Y 742 series "92 III" (1 : 50,000 non-contoured), eight sheets of township map series "Kigoma and Ujiji" (1 : 125,000 contoured), and a sheet of IMW series 1301 "Tabora" (1 : 1,000,000 contoured). Forty-six sheets of 1240 series (1 : 10,000 airphotograph) and a compiled mosaic of airphotograph "Kigoma" (1 : 10,000) were also used for photogeologic analysis of lineament.

Lake Tanganyika extends from the Burundi-Congo border through the Tanzania-Congo border to the Tanzania-Zambia border. Its dimensions amount to 660 km in length, 50 km in the mean width, 773 m in altitude above sea level, and 1,000 m or more in depth below the lake level (Fig. 19). The external shape of Lake Tanganyika forms longitudinally elongated one with a gentle curve convex to the west, that is, NNE-SSW to N-S trend in the north and NNW-SSE trend in the south, its medial part being somewhat crooked. Mountain ranges of some 2,000 m high above sea level are developed along the eastern side of the lake. Further eastern territory is occupied by an extensive plateau 1,000 m above sea level, which is called geologically the Tanganyika Shield.

In the Kigoma and Ujiji area, the mountain range along the lake is dissected and eroded by the Ruiche river running from east to west, and presents a rolling-hill scenery 800-1,000 m in altitude including such a drainage area as the Malagarasi river about 40 km south of Kigoma. The mountain range extending from Burundi to the south reaches the Mtanga and Kagongo

area north of Kigoma bay, where the altitude is about 1,500–1,600 m above sea level.

In the Katongwe point about 9 km north of Kigoma and further northward, the shoreline generally trends NNE–SSW. South of the point, however, it is not always a simple straight line but a composite one made up of combination of NNE–SSW, NNW–SSE and WNW–ESE trending lines, which delineate bays and headlands. Some hamlets and a town such as Kigari, Kagongo, Remba, Kigoma and Katabe are situated around these bays, and the Katongwe point, Nondwa point, Luansa point, Bangwe point and Kitwe point are so named from the proper names of the hamlets.

Topographic features such as shorelines or escarpments are greatly controlled by the geologic structure, and lots of them have been left unmodified and represent fault escarpments (Plate VI, Fig. 2). For example, the cliffs along the shoreline in the western and the southern part of the Bangwe peninsula are made of approximately N–S and E–W trending fracture planes. Some river systems developed in the mountain range also show parallelism to the geologic structures as is recognized by NNE–SSW and WNW–ESE trend in the north of Kigoma bay. Many swamps and wet land are seen on a flat low land spreading from the east of the Kitwe point to the south of Ujiji.

GEOLOGY

Outline of geology

The Proterozoic Karagwe-Ankolean and the Bukoban system in western Tanzania unconformably rest on high-grade metamorphic rocks of the Archeo-

TABLE 1. GEOLOGIC SUCCESSION IN WESTERN AND NORTH-WESTERN TANZANIA BY HALLIGAN (1962)

Bukoban	Bukoba Sandstone	
	Uha Group	Manyovu Red Beds Ilagala Dolomitic Limestone Gagwe Amygdaloidal Lavas
	Kigonero Flags	
	Busondo Group	Malagarasi Sandstone Nyanza Shale Uruwira Sandstone and Igenda Flags
	Masontwa Group	Mkuyu Sandstone Mokuba Shales
Pre-Bukoban	Itiaso Group	Makamba Formation Mapeta Basal Quartzite
Karagwe-Ankolean	Kigoma Quartzites	
Archaean	Ubendian gneisses, schists, granulites	

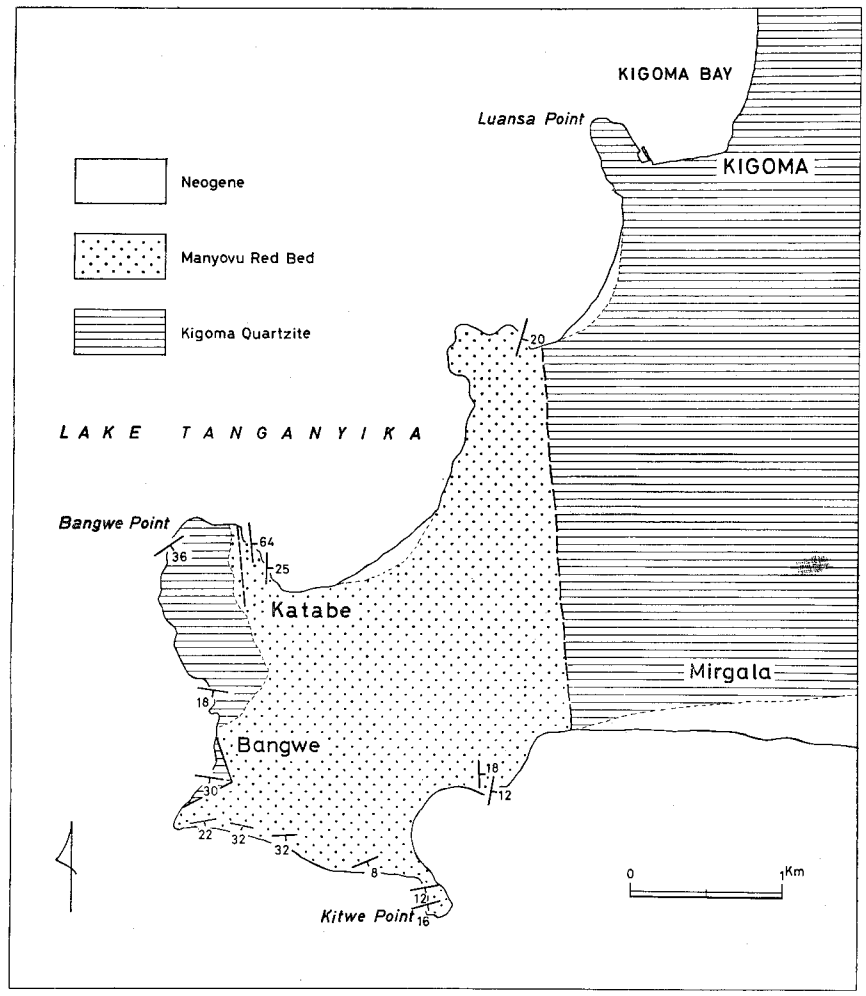

FIG. 2. Geologic map of the Kigoma area.

zoic Ubendian system. The Proterozoic rocks surround the Tanganyika Shield in the west, and their distribution is subparallel to the Lake Tanganyika rift zone (Fig. 1). Halligan's succession of the Proterozoic rocks in western Tanzania is shown in Table 1.

In the Kigoma area and its environs surveyed by the present authors are distributed the Kigoma quartzite refered to the Karagwe-Ankolean system, the Manyovu red bed refered to upper part of the Bukoban system and lake bed of Neogene by Halligan [9], as shown on the geologic map (Fig. 2).

Kigoma quartzite

In western and northwestern Tanzania the Karagwe-Ankolean system,

which unconformably overlies the Ubendian system, is a thick formation composed of grey, blue-grey, brown and red phyllitic shales, and thick, grey, blue and white quartzite (Halligan [9, 10]). Its distribution extends southwards from the northwestern borderland of Tanzania through Ruanda-Burundi to the Kigoma area on the eastern shore of Lake Tanganyika.

A formation of the Karagwe-Ankolean system in the Kigoma area is called the Kigoma quartzite, which consists mainly of white or grey medium- to coarse-grained orthoquartzitic sandstone and sometimes intercalates intraformational rounded pebble to cobble conglomerate. It is partly metamorphosed to metaquartzite as is observed in Kigari and its environs. It frequently turns red or reddish brown, and its appearance looks like the Manyovu red bed, especially in a place where the Kigoma quartzite is covered by the red bed.

Manyovu red bed

The Bukoban system is extensively developed in western Tanzania, and its distribution extending southwards from Bukoba through Kasulu, Kigoma, and east of Mpanda, to the east of Mbeya, is approximately parallel to the western rift valley (Fig. 1). The Manyovu red bed is an uppermost formation of the Uha group of the Bukoban system, and it is characterised by red to red-maroon fine-grained sandstone with the thickness of 2,000-3,000 feet in all [10].

In the Kigoma area, rounded boulder to cobble conglomerate is well developed, and it seems to be basal facies of the Manyovu red bed (Plate I, Fig. 1). It occupies almost all of the Bangwe peninsula. Arkosic red sandstone facies is seen near the Kitwe point, and alternation of red sandstone and cobble to pebble conglomerate facies is found in the northeast of the Kitwe point (Plate I, Fig. 2).

The Kigoma quartzite is generally covered by the Manyovu red bed with unconformity, and the contact is observed on the shore at the Katabe and Bangwe village.

GEOLOGIC STRUCTURE

Outline of geologic structure

The western rift valley runs southwards from Lake Albert on the Uganda-Congo border through Lake Edward and Lake Kivu with NE-SW to NNE-SSW trend and Lake Tanganyika on the Tanzania-Congo border with N-S to NNW-SSE trend to Lake Rukwa with NW-SE trend and ultimately reaches Mbeya, where it meets the eastern rift valley. It draws an arc convex to the west, the radius of curvature being about 900 km. Regional structural trend of the Archeozoic and the Proterozoic system along the Lake Tanganyika rift is concordant with the rift trend, and what's more significant is that the elongated direction of Proterozoic sedimentary basin is subparallel to the trend.

General structural trend of the Kigoma quartzite and Manyovu red bed to the north of Kigoma is nearly N-S and almost concordant with the regional one in western Tanzania. In the south of Kigoma and the Bangwe peninsula, however, local structure of beds has nearly E-W strike and dips to S (10°-30°), and it forms a uniform monoclinal structure as a whole. The Manyovu red bed is generally in contact with the Kigoma quartzite by the rift trending fault (N-S) in the area north of Kigoma bay, but the relation is nearly parallel uncomformity in the Bangwe peninsula, where N-S trending structures are

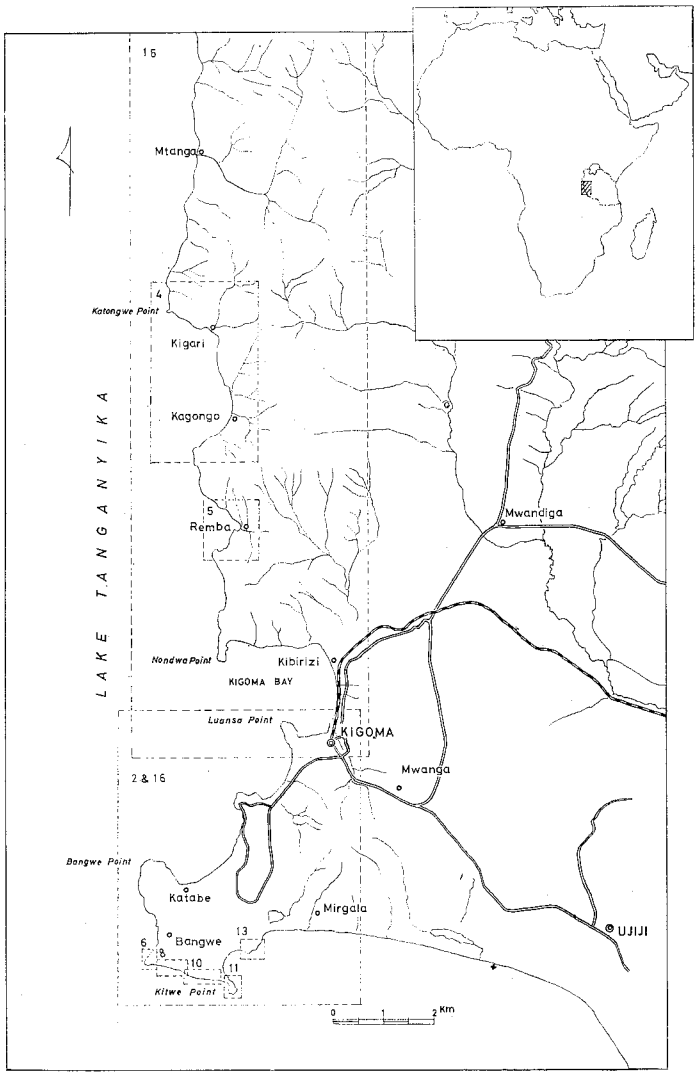

FIG. 3. Index map showing localities of the investigated area; location number corresponds to the number of text-figure.

observed in places.

Orientations of fault or joint system were measured chiefly in the Bangwe peninsula. Two characteristic fracture systems, N–S and E–W trend, are distinguished. Interestingly enough, these two are invariably recognized irrespective of rock facies and of structure of the Kigoma quartzite and Manyovu red bed. The directions of these two fracture systems are designated as R-direction (Rift direction) for N–S fracture systems and T-direction (Transform fault direction as will be mentioned later) for E–W ones, respectively. Existence of both systems is well reflected upon topographic features, which are analyzed by using the topographic maps as well as airphotographs, and both trends greatly control the most recent shoreline pattern of Lake Tanganyika.

Investigated area (Fig. 3)

Kigari and Kagongo.—General structure of the Kigoma quartzite and Manyovu red bed has nearly N–S strike dipping to E at the Kigari and Kagongo area about 7 km north of Kigoma. Geologic sketch map of this area is shown in Fig. 4. In fracture patterns, three distinguishable trends, that is, NNE–SSW, NNW–SSE, WNW–ESE, are found there, and they are

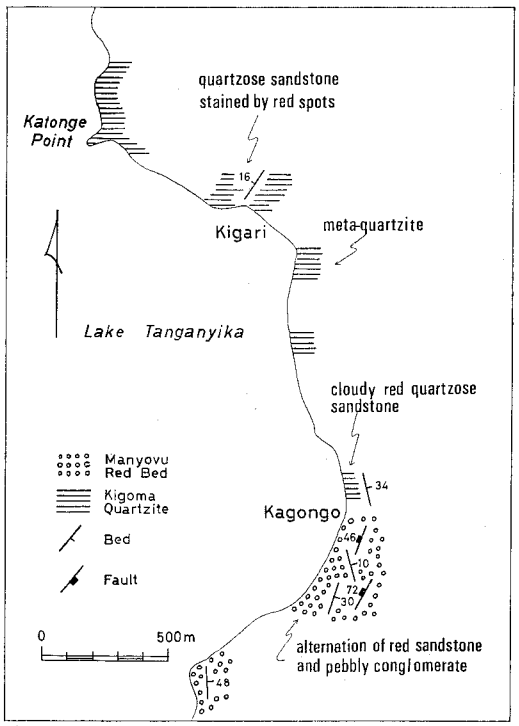

FIG. 4. Geologic sketch map of the Kigali and Kagongo area.

reflected on shoreline features and river systems in the mountain range as shown in Fig. 15.

Outcrops of faults cutting alternation of red sandstone and pebbly conglomerate referable to the Manyovu red bed are observed at two points at Kagongo. The trends of them are N 28°E dipping 72° to W and N 20°E dipping 46° to W, respectively, and a striation measured on a fault plane plunges 44° to N 86°W. It apparently suggests a normal fault whose western side was thrown down.

Remba.—At Remba and its environs are distributed orthoquartzite probably correlatable to the Kigoma quartzite and alternation of red siltstone and sandstone of the Manyovu red bed as shown in Fig. 5. Some lineaments on airphotographs display remarkable NNW–SSE trend, which strongly governs drainage systems. The Manyovu red bed is in contact with the Kigoma quartzite by faults which may belong to R-direction fault system, and they are apparently cut by T-direction fault system. On the other hand, Halligan [10] described on the repetition of two formations that "..... on the coast

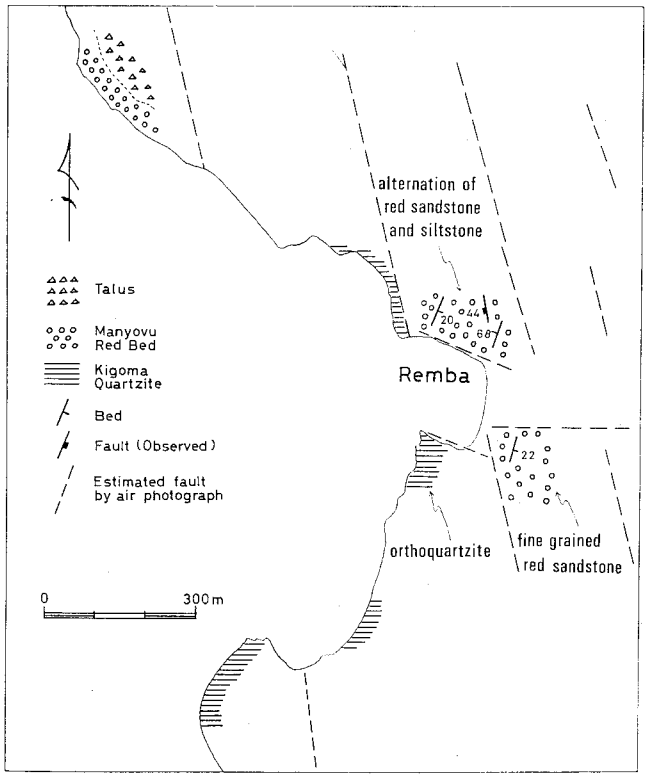

FIG. 5. Geologic sketch map of the Remba area.

just north of Kigoma, overfolding to the east was seen in more argillaceous sequence". A fault cutting the Manyovu red bed is measured and its strike and dip are N 10°W and 44° to W on the fault plane with a striation plunging at 55° to N 86°W, which may suggest a normal fault. Talus deposits on the Manyovu red bed are found at an exposure about 600 m northwest of the Remba village.

Area northwest of Katabe village.—Conglomeratic facies of the Manyovu red bed is distributed at an area about 400 m northwest of the Katabe village, where the beds strike N–S and dip to E, though general structure in the Bangwe peninsula has strike of E–W and dip to S. In places, the structure is disturbed by another minor faults developed near unconformity between

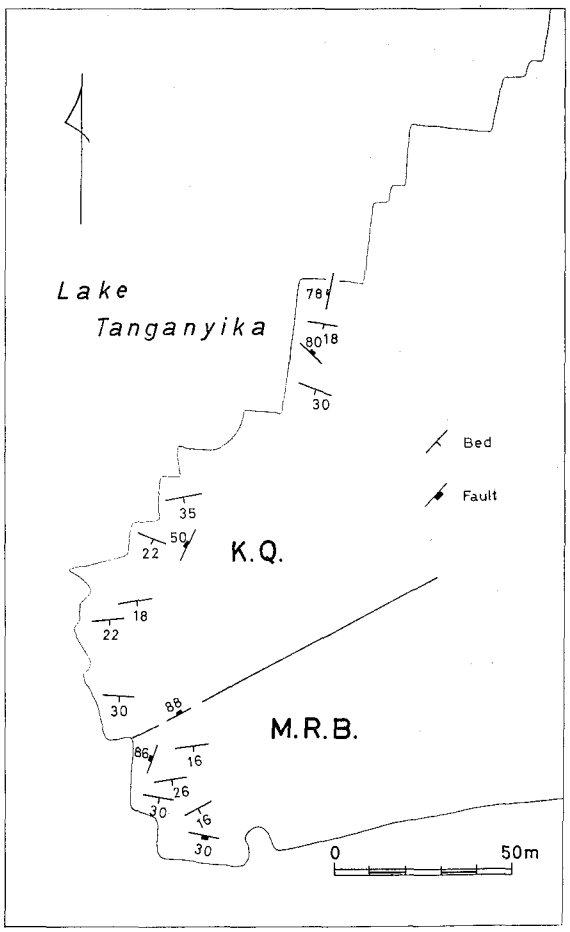

FIG. 6. Geologic sketch map of the point southwest of the Bangwe village. M.R.B.: Manyovu Red Bed and K.Q.: Kigoma Quartzite.

the Manyovu red bed and the Kigoma quartzite. The relation of unconformity between them is also found at a shoreside area west of the Bangwe village. Cliffs, distinctly observable on the shoreline westwards from the Katabe village to the Bangwe point, are formed by both fractures of R-direction and T-direction (Plate II, Fig. 1).

Point southwest of Bangwe village.—General structure of the Manyovu red bed and the Kigoma quartzite near the point to the southwest of the Bangwe village (Fig. 6) has strike of E-W (N 70°W ~ N 80°E), and gently dips to S (16° to 30°). The Kigoma quartzite to the southwest of the Bangwe village is in contact with the Manyovu red bed by two faults (see Fig. 2), one of which strikes N 20°W and dips 80° to E and the other N 64°E and 88° to N (Plate II, Fig. 2). The structure of both formations is not disturbed by these faults. There is observed a low angle fault subparallel, though slightly waving, to the bed of the Manyovu red bed on which is seen a striation plunging 8° to N 60°W. This fault is cut by joint systems of R-direction and T-direction. It is likely, therefore, that the fault is older than the rift fault systems (Plate III, Fig. 1).

Fig. 7 is an equal-area projection for the poles of the fracture planes

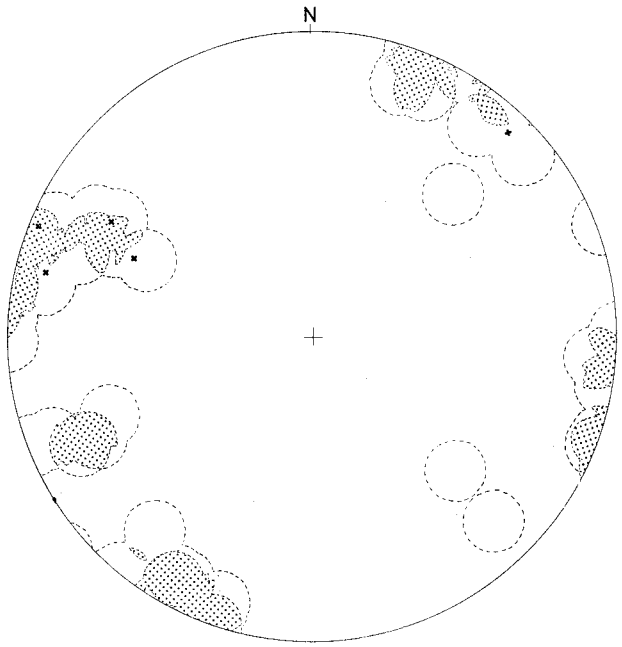

FIG. 7. Equal-area projection for the poles of 52 fracture planes measured at an exposure 400 m north to the point southwest of the Bangwe village. Dotted line: 2% contour line; dotted area: more than 6% area; cross mark: pole of minor fault.

measured at a place 400 m north from the point. It is shown that the joints are concentrated at N 25°E•80°W, N 25°W•70°W and N 65°W•80°S, and the former two may be refered to R-direction and the latter one T-direction. Several minor faults have the same tendency as the joints. These fracture systems in this area are characterized by the joints without sheared plane, and generally clearly cut pebbles or cobbles in conglomeratic facies of the Manyovu red bed. No displacement along the fracture plane is observed. Some physiographic features along the shorelines are also greatly controlled by the R-direction and T-direction fracture systems as shown on the sketch map of Fig. 6.

Lake-shore area east of a point southwest of Bangwe village.—Cobble conglomerate of the Manyovu red bed, sometimes intercalating thin red sandstone layers, crops out at lake-shore area east of a point southwest of the Bangwe village (Fig. 8). The present authors observed faults and joint systems along the shore for 700 m eastwards from the point. The Manyovu red bed strikes approximately E–W dipping about 30° to S, whereas almost all faults and joints strike N–S ~ NNE–SSW steeply dipping to the east or west. In all probability, they belong to the fracture system of R-direction. Fault planes are generally observed at an interval of a few meters to several ten meters and they are sometimes associated with shear zone (Plate III, Fig. 2). However, it is considered that almost all of the fractures are essentially tension fracture, because they are in general associated with no or little displacement along the plane and no fault clay or breccia accompanied with (Plate IV, Fig. 1). The orientation of the fault and joint developed in this area is concentrated to N 15°E•85°E as shown in Fig. 9. It is of much interest that the fault systems cut both of cobbles and matrix in the conglomerate, but the joint systems cut exclusively cobbles (Plate IV, Fig. 2). Moreover, difference of density of development between them are also remarkable; for instance, one

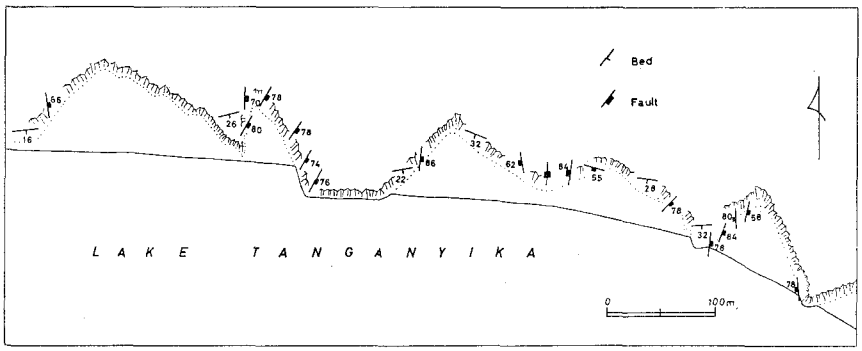

FIG. 8. Geologic sketch map of lake-shore area east to the point southwest of the Bangwe village.

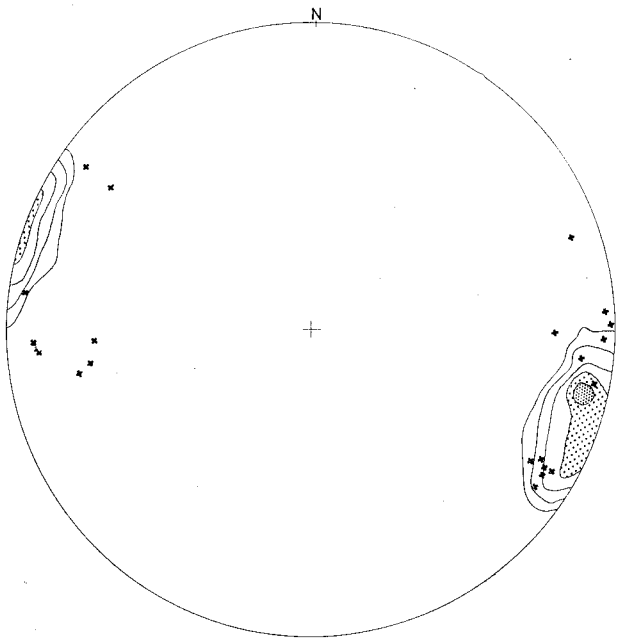

FIG. 9. Equal-area projection for the poles of 70 joint planes measured at an exposure east of the point southwest of the Bangwe village (see Plate IV, Figs. 1 and 2). Contour lines: 5.1%, 10.3%, 15.4%, 20.6%, 25.7%; cross mark: pole of fault.

fault is found in every two or three meters width, while one joint in every two or three centimeters width. The fracture system of R-direction is more consipicuously developed than that of T-direction, which latter is reflected on the topographic feature, especially on approximately E–W trending shoreline (Plate VI, Fig. 1).

Area west of the Kitwe point.—A shoreline west of the Kitwe point trends WNW–ESE, along which conglomeratic facies of the Manyovu red bed crops out well (Fig. 10). Cliffs along the shore about 700 m west of the Kitwe point trend approximately E–W and are made of fault planes themselves; slickensides on the shear planes are observable (Plate V, Figs. 1, 2). The fault planes are measured at five points and their strikes and dips are N 80°W and 85°S (with a horizontal striation), N 70°E and 70°N, N 70°W and 70°N, N 68°W and 85°N, and N 70°E and 65°N (with a striation plunging at 7° to S 76°W). Let's call a direction represented by the faults mentioned above T-direction. On the other hand, R-direction is tentatively defined as the direction of a nearly vertical plane striking N 20°W to N 20°E. It is noticeable that some joints of R-direction cut only cobbles in the Manyovu red bed in this area.

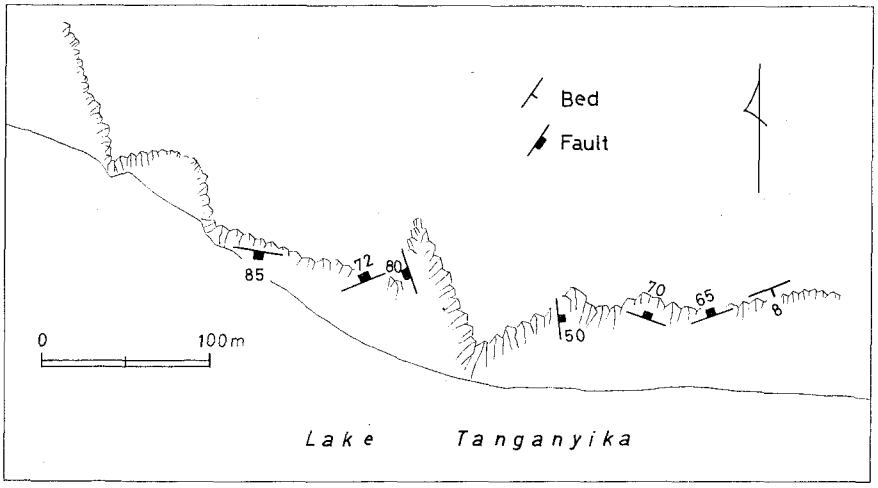

FIG. 10. Geologic sketch map of the area west of the Kitwe point.

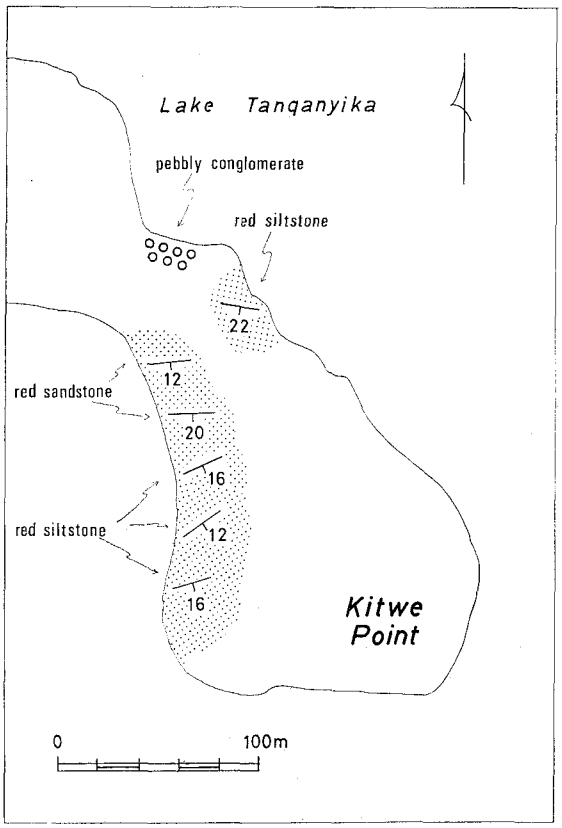

FIG. 11. Geologic sketch map of the Kitwe point and its environs.

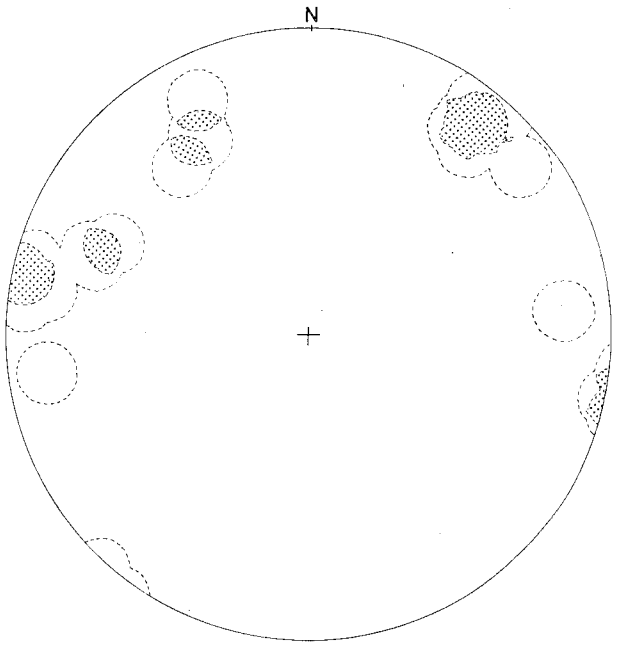

FIG. 12. Equal-area projection for the poles of 23 joint planes measured at the Kitwe point. Dotted line: 4% contour line; dotted area: more than 13% area.

Kitwe point and its environs.—At the Kitwe point and its environs are distributed pebbly conglomerate and laminated red sandstone or siltstone, which may be stratigraphically correlated to the upper part of the conglomeratic facies to the west (Fig. 11). They generally trend approximately E-W dipping 16° (12° to 22°) to the south. Joints are developed in the sandstone facies, and three modes of concentration, that is, N 50°W•80°E, N 60°E•65°NW and N 15°E•75°W, are recognizable on the equal-area projection for the poles of joint planes (Fig. 12). The last one is undoubtedly referred to R-direction. Topographically, the Kitwe point area appears to be a tilted block plunging at 8° to the north.

Area northeast of Kitwe point.—On the shoreline about 800 m northeast of the Kitwe point crop out red sandstone and conglomerate referable to the Manyovu red bed, and they strike N-S to NNE-SSW dipping 12°E (Fig. 13). This structural trend is different from the general trend found in the Bangwe peninsula. Althouth the stratigraphic relation between this and the western area is not well known, the existence of faults of R-direction may be implied by discontinuous change of strike.

Topographic features of shorelines are made of conbination of cliffs of two directions, that is, R-direction and T-direction (Figs. 13 and 14).

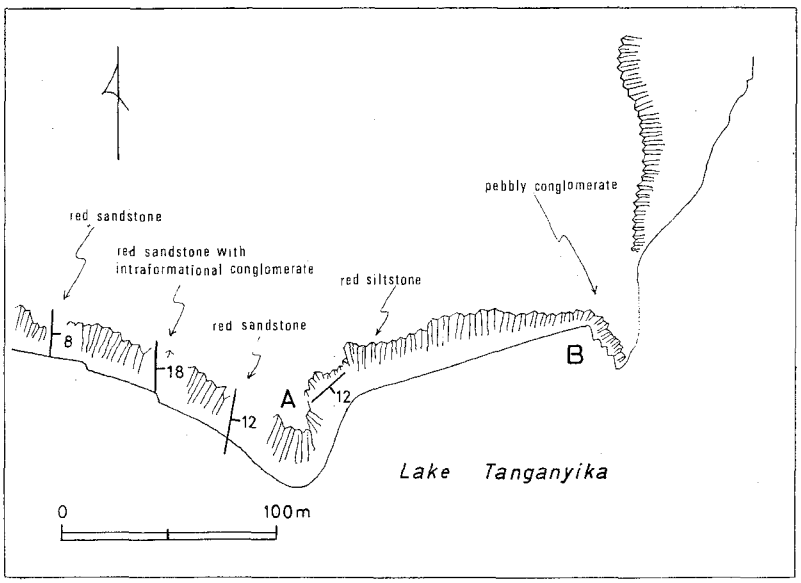

FIG. 13. Geologic sketch map of the area northeast of the Kitwe point.

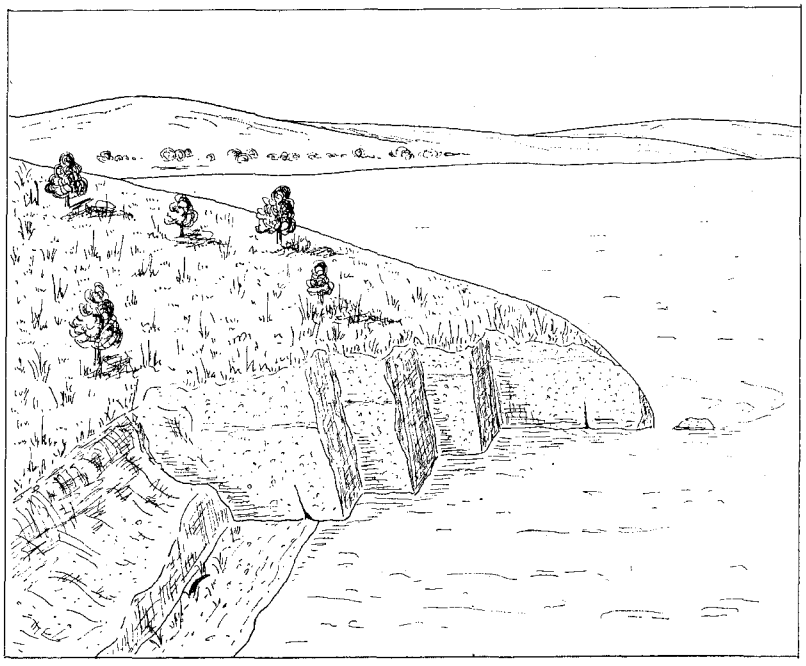

FIG. 14. Sketch of a view from point A to point B in Fig. 13.

Fault and fracture systems

As mentioned above, two characteristic fracture systems were recognized in the authors' field observation. One approximately trending N-S is described as R-direction, and the other nearly perpendicular to that is described as T-direction. In order to obtain regional generality of each system, a photogeologic investigation was carried out on lineaments of these areas (Figs. 15 and 16). The result shows that approximate N-S and E-W trending lineaments are predominant (Fig. 17), and their trends are not contradictory to the result of the field observations. There is a fundamental difference on the occurrence of fracture between two systems; the fracture system of R-direction is mainly composed of an opened fracture and that of T-direction is a shear fracture with horizontal displacement. The system of R-direction is further discriminated into the following three types,

1) opened vertical joint swarm developed at intervals of a few centimeters,

2) well developed vertical and long fracture found at intervals of ten meters or so,

3) normal fault, generally dipping 50° to 70° to the west.

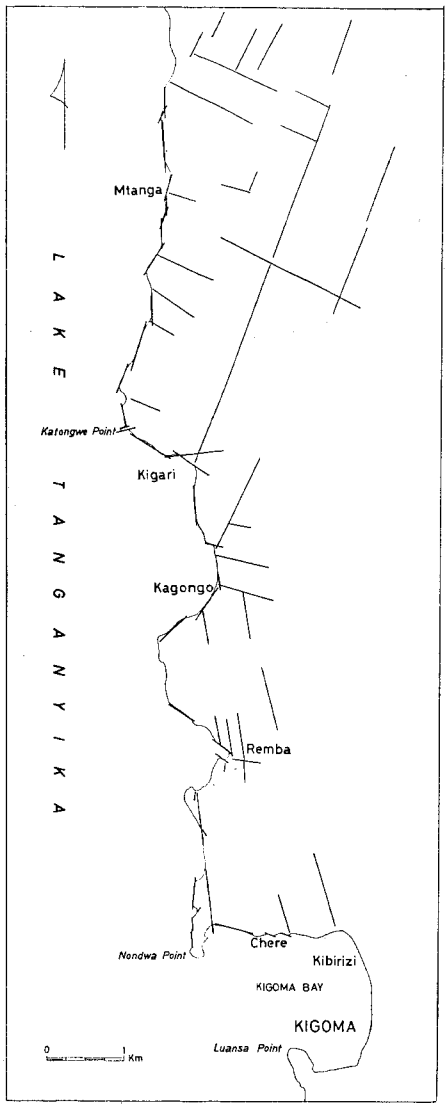

FIG. 15. Photogeologic lineament in the area north of Kigoma.

The former two types might occur under such stress system as E-W horizontal minimum and N-S horizontal maximum principal stress, and the last one E-W horizontal minimum and vertical maximum. The former two obviously gave an incipient effect of rift formation, and they were probably formed under the tensile stress field. The last one is considered to have been formed at a marginal zone of the rift area, and the gravitational downthrowing had to occur after the rift area was opened in a large extent.

On the other hand, the fracture system of T-direction is also an important

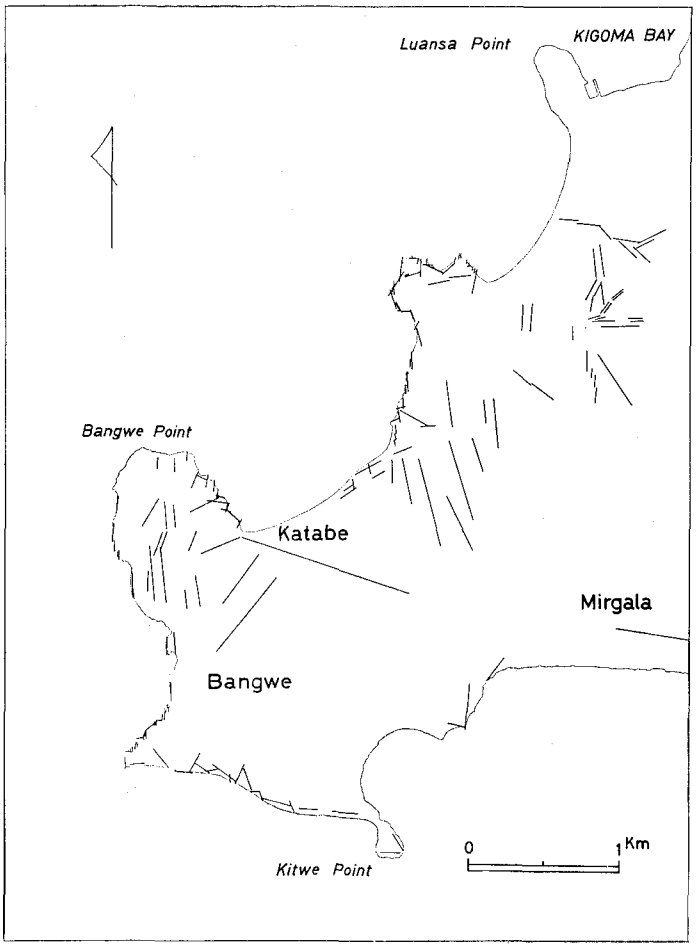

FIG. 16. Photogeologic lineament in the area south of Kigoma and Bangwe peninsula.

constituent of rift fault systems, though it is less predominant than that of R-direction. It is clearly distinguished by nearly horizontal displacement along the sheared plane as already described. Judging from the interrelationship between both fracture systems of R-direction and T-direction, they are considered to have been formed simultaneously. It is very difficult to find a stress field under which these two different fracture systems occur simultaneously. However, if the concept of transform fault as defined by Wilson [16] is introduced, a plausible explanation of the fracture systems found in this area can be made.

The attitude and interrelationship of both systems observed in the Kigoma area offer sufficent evidences to explain them by mechanism of formation of

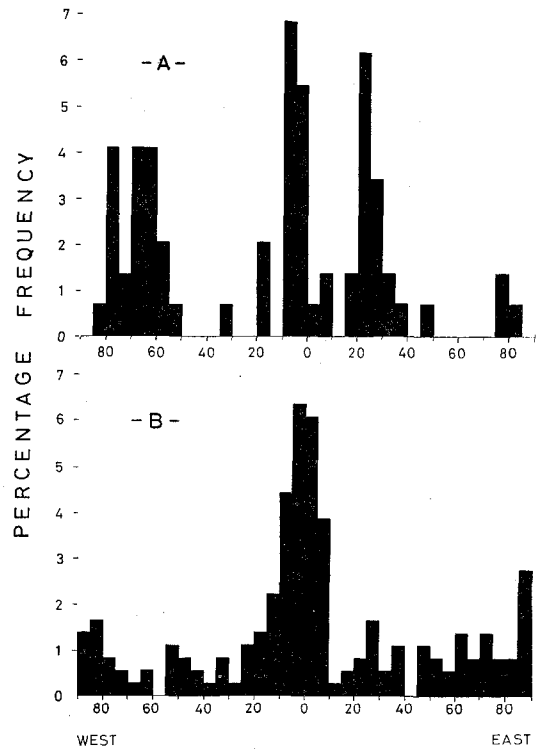

FIG. 17. Histogram of direction of lineament; **A** for 73 data in the area of Fig. 15 and **B** for the 177 data in the area of Fig. 16.

transform fault as follows.

1) Almost all fractures of R-direction are supposed to have occurred under the tensile stress field. The rift fault proper may reach considerable depth of the crust as suggested by gravitational data.

2) As observed in some faults of T-direction, the horizontal displacement is much larger in amount than the vertical one along the fault plane.

3) Apparent sense of lateral displacement between two blocks in both sides of the fault of T-direction could not be clarified in the field; however, the apparent relative displacement is implied by the topographic discontinuity found in topographic maps or airphotographs. It is also strongly suggested by the bent of external shape of Lake Tanganyika in its medial part as will be mentioned in the next chapter.

4) The occurence of transform fault requires an older weak line along which the lateral movement is rejuvenated. Drainage system shown in Fig. 18 suggests such dormant weak line in the direction of approximate E-W.

It is very interesting problem to discuss when the rift formation began. Fracture systems of R-direction and T-direction strongly control the present

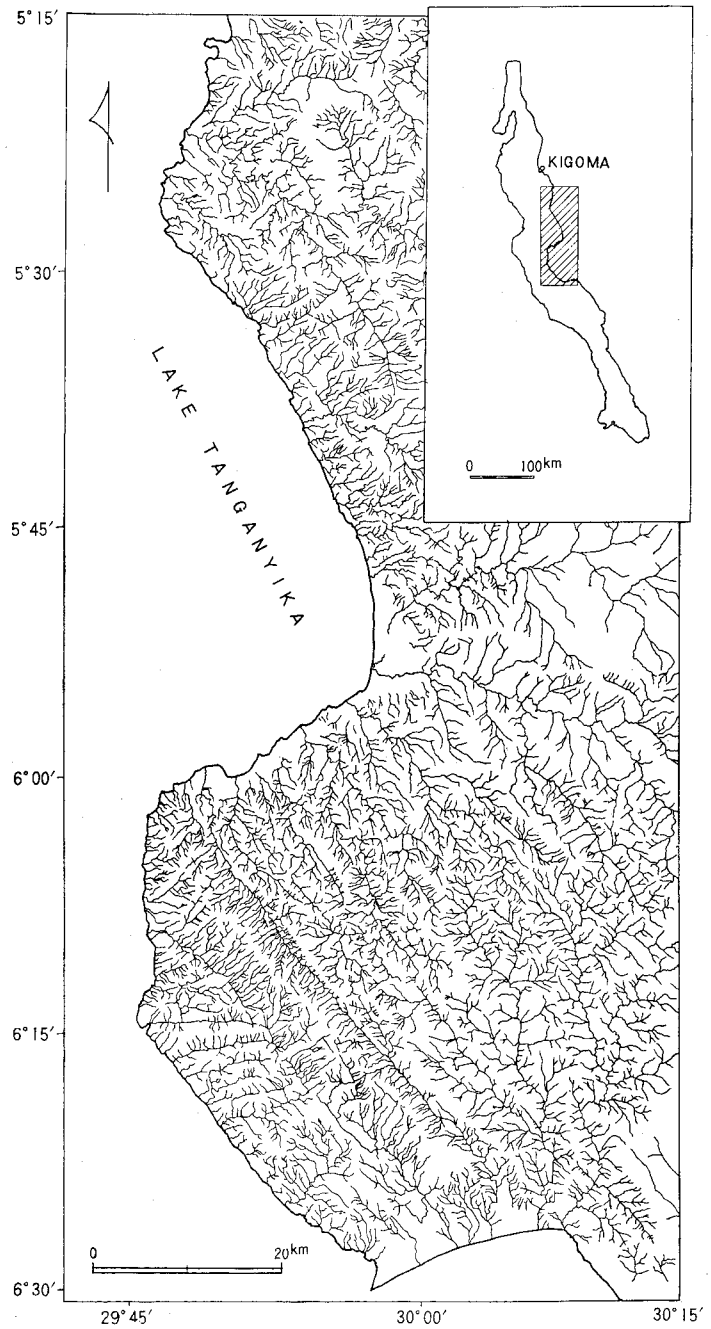

FIG. 18. Drainage system of the eastern shore area in the medial part of Lake Tanganyika, compiled from ten sheets of the topographic maps of series Y 742 published by the Survey Division, Ministry of Lands and Surveys, Tanzania (1 : 50,000).

shape of shoreline of Lake Tanganyika. This fact suggests that they occurred more recently than all the other structures. Since the distribution of the Bukoban system in western Tanzania, however, is concordant with the trend of the Lake Tanganyika Rift, the origin of the rift of R-direction may well date back to the time when the Bukoban sedimentary basin was formed.

LAKE TANGANYIKA RIFT

On a basis of field observations and geomorphological investigations of the Kigoma area, it is concluded that both fracture systems of R-direction and T-direction occurred simultaneously under the same regional tensile stress field.

The shape of Lake Tanganyika itself is very suggestive to the possibility of the transform fault crossing the medial part of Lake Tanganyika, though a right-lateral transcurrent fault may be supposed from its appearance. This assumption is further supported by the displacement of steep slope below the lake level. As shown in Fig. 19, the distance between opposite shorelines is about 40 km. However, the interval of the deepest part across the south latitude 6° and its neighbourhood amounts about 15 km. This difference may be attributed to a modification by gravity faulting near the marginal part of the rift, though it may be more or less concealed by sediments supplied from river systems. Therefore, it is reasonable to estimate the amount of displacement by the transform fault being about 15 km. It is of much interests that Bloomfield [1] described the sinistral transform fault across the middle part of Lake Malawi near the south latitude 12°.

Van Andel *et al.* [15] stated that the ridge crest is offset more than 300 km along the E–W trending Vema

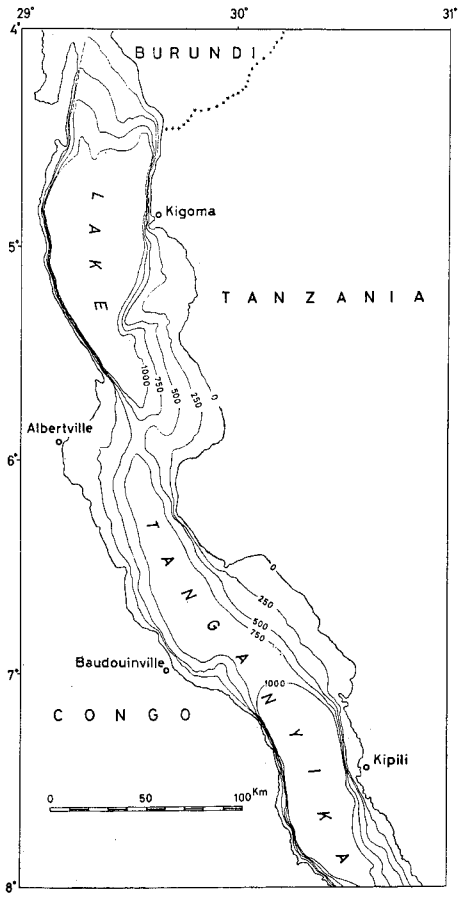

FIG. 19. Bathymetric chart of Lake Tanganyika, compiled from the topographic map "Tabora" (1 : 1,000,000), a sheet of series 1301, published by Directorate of Overseas Surveys for Republic of Tanganyika and Zanzibar, 1964.

fracture valley in the north Atlantic. A geometrical model proposed by them is very similar to the shape of Lake Tanganyika. In transform faults, the direction of ocean-floor spreading coincides with the direction of the pre-existing weak line as shown in the Romanche fracture zone on the mid-Oceanic ridge described by Sykes [14]. On the other hand, the Vema fracture zone trends obliquely to the direction of the spreading, and the attitude of the zone along the weak line may be opened. The Tanganyika rift fault system has much the same properties as the Romanche Zone and the Vema fracture zone, and it may be probably said that both properties are displayed in the topographical features closely related with variously trending dormant weak lines. The existence of the weak line was revealed by the lineaments shown in the river system (Fig. 18), in which E-W trending lineaments are found to be remarkable, though they are not necessarily cropped out as dislocation zone at present as shown on Halligan's map.

As already mentioned the fracture systems of R-direction are discriminated into various types, one of which is joint swarm developed at intervals of a few centimeters, and another one is the fault developed at intervals of ten meters or so. The interval of two fracture planes may well be indicative of the density of development. The relationship between the length of continuity of lineament and the interval of each lineaments was investigated on the photogeologic lineaments of larger dimensions belonging to R-direction. The present authors can obtain the data distinguishable into six groups by each dimensions by means of field observation, airphotograph and topographic map of various scales (Table 2). By plotting these data on the logarithmic paper, it is found that they are almost on a straight line (Fig. 20). Rift formation involves many problems to be solved, and this linear relation between the interval and continuity of fracture or order of the dimension of fracture is thought to be one of the essential features of the rift of the Lake Tanganyika Rift.

This significant feature probably implies the fundamental structure finely or moderately modified by the simultaneous movement along the major rift

TABLE 2. RELATION BETWEEN INTERVAL AND CONTINUITY OF FRACTURE SYSTEM

Order	Interval	Continuity	
1	1~4 cm	2~8 cm	Field Observation
2	10~15 m	20~60 m	
3	50~250 m	150~800 m	Airphotograph, Fig. 15, 16
4	0.5~2 km	1.0~5 km	
5	6.5~10 km	24~60 km	Topographic Map, Fig. 18
6	33~50 km	130~400 km	Topographic Map, Fig. 19

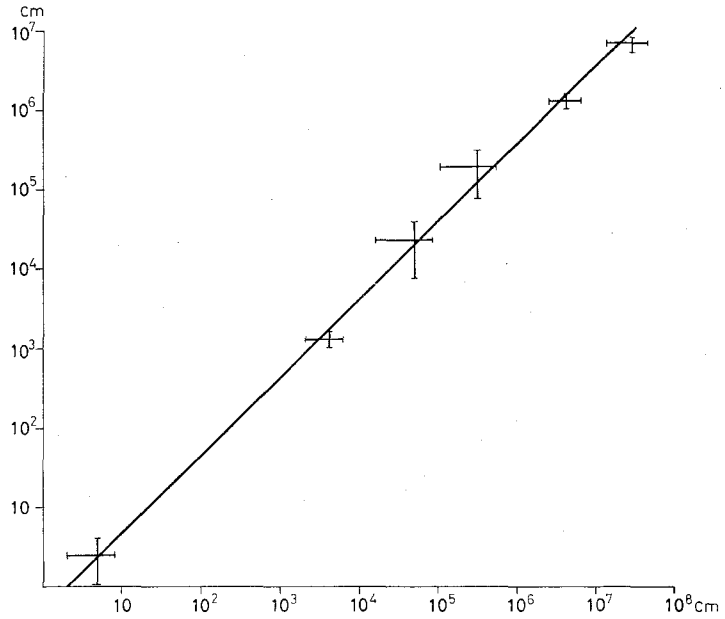

FIG. 20. Relation between interval and continuity of fracture system.

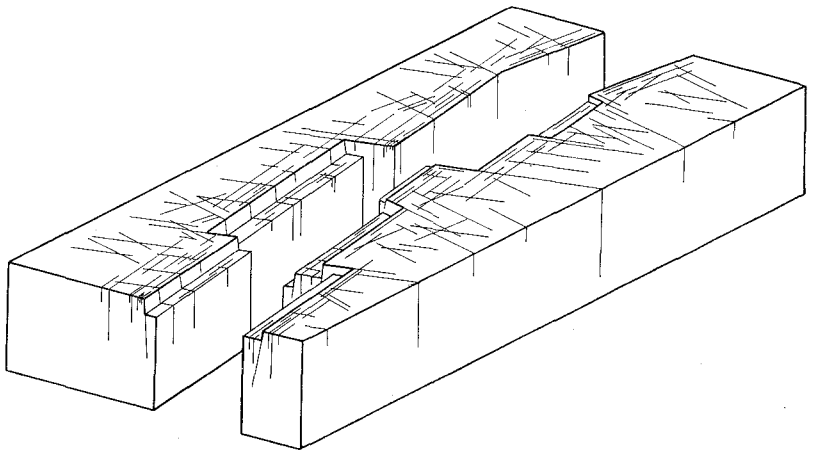

FIG. 21. Schematic illustration of fault system of Lake Tanganyika rift.

fault. Fig. 21 illustrates the schematic model of the Lake Tanganyika rift fault system by considering some characteristic attitude or disposition as mentioned in this chapter.

SUMMARY

1) In the Kigoma area, the Kigoma quartzite of the lower Proterozoic

Karagwe-Ankolean system and the Manyovu red bed of the upper Proterozoic Bukoban system are well exposed as shown in Fig. 2.

2) General structure of these formations is approximately E-W in the Kigoma area, though it trends generally N-S in western Tanzania.

3) Among characteristic fractures found in this area two remarkable fracture systems are recognized; one is N-S trending tension fracture and the other is E-W sheared fracture with horizontal displacement. The former is designated as the fracture system of R- (rift) direction and the latter as that of T- (transform) direction.

4) Some specific features of the fracture system of T-direction may indicate the possibility of transform fault.

5) It is suggested that the fracture patterns and the fault system of the Lake Tanganyika rift are made up of combination of two systems of R-direction and T-direction.

ACKNOWLEDGEMENTS

The authors are greatly indebted to Prof. Emeritus Dr. Isao Matsuzawa of Nagoya University who gave them encouragement in all phases of this work. The authors express their sincere thanks to Prof. Dr. D. G. Osborne of University College Dar es Salaam and to Dr. G. Luena of Mineral Resources Section of Tanzania at Dodoma, who gave the permission to stay and study in Tanzania. Thanks are extended also to many persons in the Kigoma district: Mr. Siyoberwa, Regional Commissioner of Kigoma, Mr. M. Abdallah, Administral Secretary of Kigoma, Mr. Kihampa, Educational Commissioner of Kigoma, and J. K. Kaneno, District Educational Officer of Kigoma, gave us many facilities during our stay and study in Kigoma, and Mr. Gerald Kasimba, the young man of Katabe village, rendered help for surveying by boat. The authors would like to thank Dr. H. Kurimoto and Dr. G. Omi of the members in our party for their helps.

REFERENCES

[1] BLOOMFIELD, K., A major east-north-east dislocation zone in central Malawi: *Nature*, **211**, 612-614 (1966).

[2] CAHEN, L. and SNELLING, N. J., The geochronology of equatorial Africa: North-Holland Publ. Co., Amsterdam (1966).

[3] DESWARDT, A. M. J., GARRARD, P. and SIMPSON, J. G., Major zones of transcurrent dislocation and superposition of orogenic belts in part of central Africa: *Geol. Soc. Am. Bull.*. **76**, 89-102 (1965).

[4] HALLIGAN, R., Quarter Degree Sheet 131, Mgambo: Geol. Surv. Tanganyika (1962).

[5] ——, Quarter Degree Sheet 132, Kakungu: Geol. Surv. Tanganyika (1962).

[6] ——, Quarter Degree Sheet 113, Uvinza: Geol. Surv. Tanganyika (1962).

[7] ——, Quarter Degree Sheet 112, Ilagala: Geol. Surv. Tanganyika (1962).

[8] HALLIGAN, R., Quarter Degree Sheet 93, Kasulu: Geol. Surv. Tanganyika (1962).

[9] ——, Quarter Degree Sheet 92, Kigoma: Geol. Surv. Tanganyika (1962).

[10] ——, The Proterozoic rocks of Western Tanganyika: *Geol. Surv. Tanganyika, Bull.*, No. 34 (1962).

[11] MATSUZAWA, I., Formation of the African Great Rift System: *J. Earth. Sci. Nagoya Univ.*, **17**, 11-70 (1969).

[12] SPENCER, E. W., Introduction to the structure of the earth: McGraw Hill Book Co. (1969).

[13] STOCKLEY, G. M., The geology of parts of the Tabora, Kigoma, and Ufipa districts, northwest Lake Rukwa: Depart. Lands and Mines Geol. Division, Tanganyika (1938).

[14] SYKES, L. R., Mechanism of earthquakes and nature of faulting on the mid-oceanic ridge: *J. Geophy. Res.*, **72**, 2131-2153 (1967).

[15] VAN ANDEL, T. H., PHILLIPS, J. D. and VON HERZEN, R. P., Rifting origin for the Vema fracture in the north Atlantic: *Earth Planetary Sci. Letters*, **5**, 296-300 (1969).

[16] WILSON, J. T., A new class of faults and their bearing on continental drift: *Nature*, **207**, 343-347 (1965).

PLATE I

FIG. 1. Rounded boulder and cobble conglomerate of the Manyovu red bed at an exposure west of the Kitwe point (Photo by S. M., 31 VIII 1968).

FIG. 2. Arkosic red sandstone in the Manyovu red bed at the Kitwe point (Photo by S. M., 2 IX 1968).

FIG. 1

FIG. 2

PLATE II

FIG. 1. Cliffs on the shore line west of the Katabe village formed by fractures of R-direction and T-direction (Photo by S. M., 31 VIII 1968).

FIG. 2. A fault (N 64°E•86°N) between the Kigoma quartzite (left) and the Manyovu red bed (right) at an exposure southwest of the Bangwe village (Photo by S. M., 5 IX 1968).

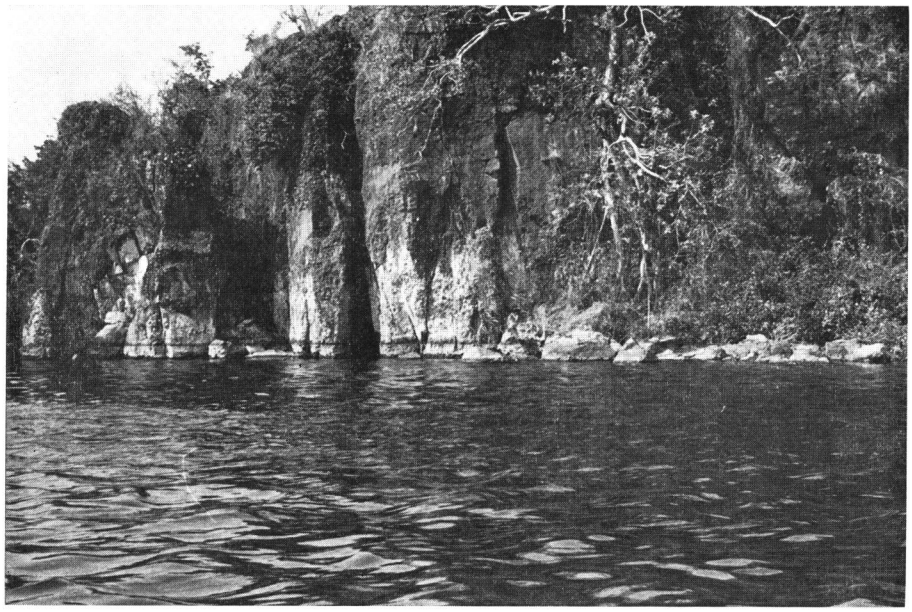

FIG. 1

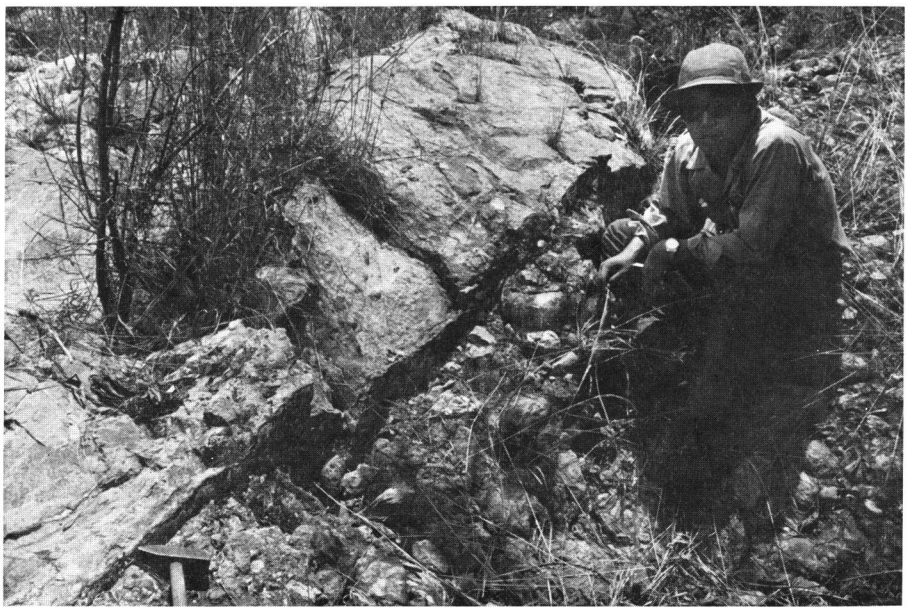

FIG. 2

PLATE III

FIG. 1. Low angle fault subparallel to bedding of the Manyovu red bed at the point southwest of the Bangwe village (Photo by K. Y., 31 VIII 1968).

FIG. 2. Fault of R-direction associated with shear zone at an exposure east of the point southwest of the Bangwe village (Photo by K. Y., 31 VIII 1968).

FIG. 1

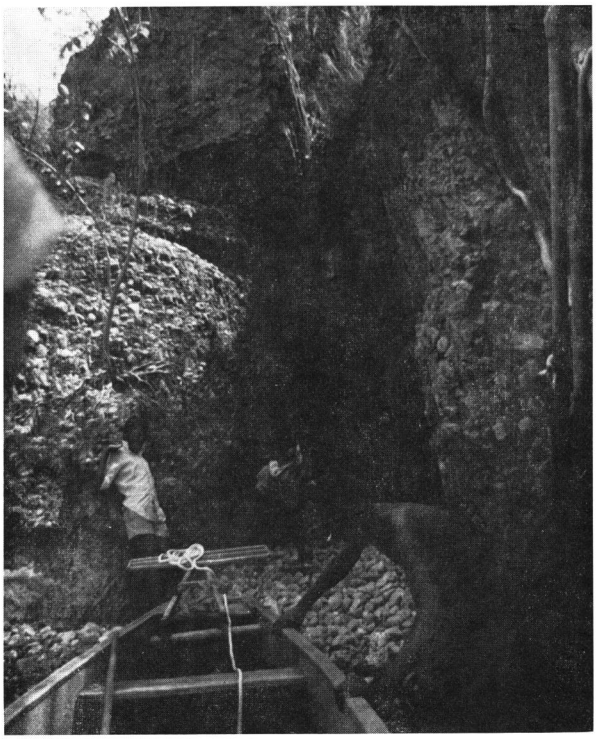

FIG. 2

PLATE IV

FIG. 1. Minor faults cutting both of cobbles and matrix, and joints cutting exclusively cobbles in conglomerate at an exposure east of the point southwest of the Bangwe village (Photo by K. Y., 4 IX 1968).

FIG. 2. Joints cutting exclusively cobbles in conglomerate at an exposure east of the point southwest of the Bangwe village (Photo by S. M., 5 IX 1968).

FIG. 1

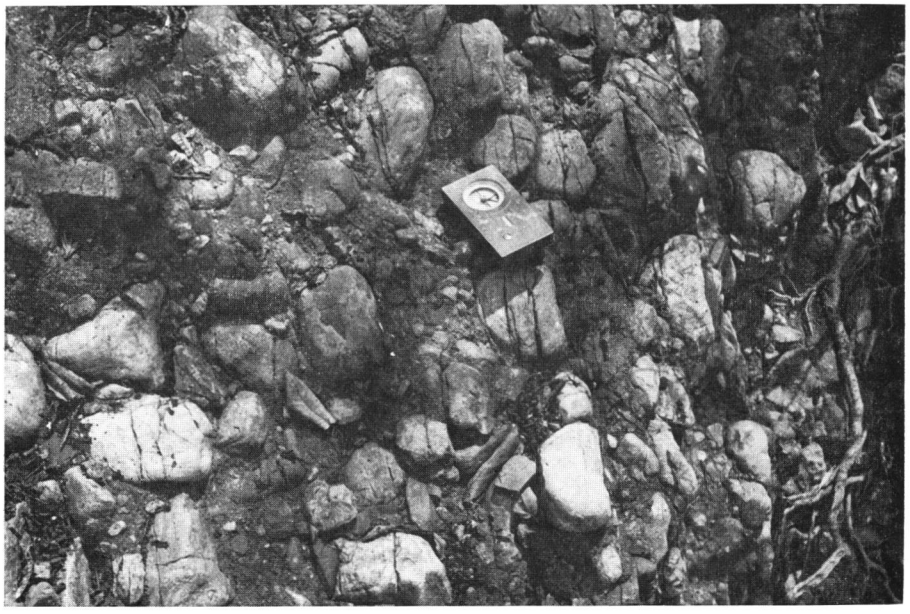

FIG. 2

PLATE V

FIG. 1. Fault of T-direction with approximately horizontal striation on the slickenside at a cliff of the fault plane along the shore about 700 m west of the Kitwe point (Photo by S. M., 2 IX 1968).

FIG. 2. Distinct horizontal striation enlarged from a part of the fault plane shown above (Photo by K. Y., 2 IX 1968).

FIG. 1

FIG. 2

PLATE VI

FIG. 1. Lake-shore feature governed by the fracture system of R- and T-direction, viewed from the west to the east; E-W trending cliffs are of T-direction, and N-S trending ones of R-direction (Photo by K. Y., 2 IX 1968).

FIG. 2. Fault escarpment along the shoreline viewed northward from the Katabe village (Photo by S. M., 31 VIII 1968).

FIG. 1

FIG. 2

Metamorphic rocks of the North Pare Mountains, Tanzania

Kunihiko MIYAKAWA

Department of Earth Sciences, Nagoya Institute of Technology

Kanenori SUWA

Department of Earth Sciences, Faculty of Science, Nagoya University

Isao SHIIDA

Department of Geology, College of General Education, Nagoya University

(Received 16 August 1969)

ABSTRACT

Metamorphic rocks of the North Pare Mountains have been tentatively assigned to the Usagaran System of Precambrian age. They consist mainly of granulites. Granulites of the area are grouped into three groups: acid, intermediate and basic, based on the proportion of felsic to mafic constituent minerals. Petrographically, hornblende is quantitatively an important constituent of the rocks of intermediate as well as basic composition and coexists with both clinopyroxene and orthopyroxene. The composition of hornblende is usually close to that of hastingsite. Orthopyroxene occurs wide-spreadly in rocks of different compositions. The dominant rock-type is hornblende-pyroxene granulite of intermediate division. The mineral paragenesis indicates that the North Pare metamorphic rocks have been metamorphosed in the lower-temperature zone of the granulite facies.

INTRODUCTION

The North Pare Mountains are a fault block about 65 km long and from 12 to 20 km wide, elongated in a north-north-west to south-south-east direction. They are composed almost entirely of granulites and related rocks. The South Pare Mountains are their southern extension. The geology of this area was first outlined by McKinlay [11] and then was investigated in more detail by Bagnall [1, 2]. Metamorphic rocks of the North Pare Mountains and the surrounding area are assigned to the Usagaran System of Precambrian age by Quennell *et al.* [12]. They are believed to have been originally a thick series of arenaceous, argillaceous and calcareous sediments with intercalated basic and intermediate igneous rocks. Specifically rocks of the Usagaran System are distributed in an orogenic belt called the Mozambique Belt [5, 10], which extends northward into Kenya and southward into the Mozambique.

A road runs from Mwanga through Ghogho to Butu across the northern part of the North Pare Mountains. It is suitable for a grasp of the geological

outline of the area. The present authors had an opportunity to observe metamorphic rocks along the route from Mwanga to Ghogho for a few days in October, 1968. This paper is a preliminary report on the North Pare metamorphic rocks along the above route.

GEOLOGY

The metamorphic rocks of the North Pare Mountains are composed mainly of granulites of intermediate composition closely associated with those of basic and acid composition. Bands of different composition bring about the well-developed foliation. They have a fairly constant trend parallel to the elongation of the Mountains. Crystalline limestone is scarcely found in the Mountains. A geological sketch map along the route is shown in Figs. 1 and 2. The regional strike of the foliation is N 15°–30° W and the dip is generally 30°–55° NE. Contrasted with the surroundings, rocks have been intensely folded and disturbed at one locality 3.5 km east of Mwanga. This structural disturbance extends for a width as much as 20 meters. It appears to be situated on a supposed northern continuation of an unnamed thrust which runs parallel with the Changube thrust. Many small dikes of pegmatite, usually

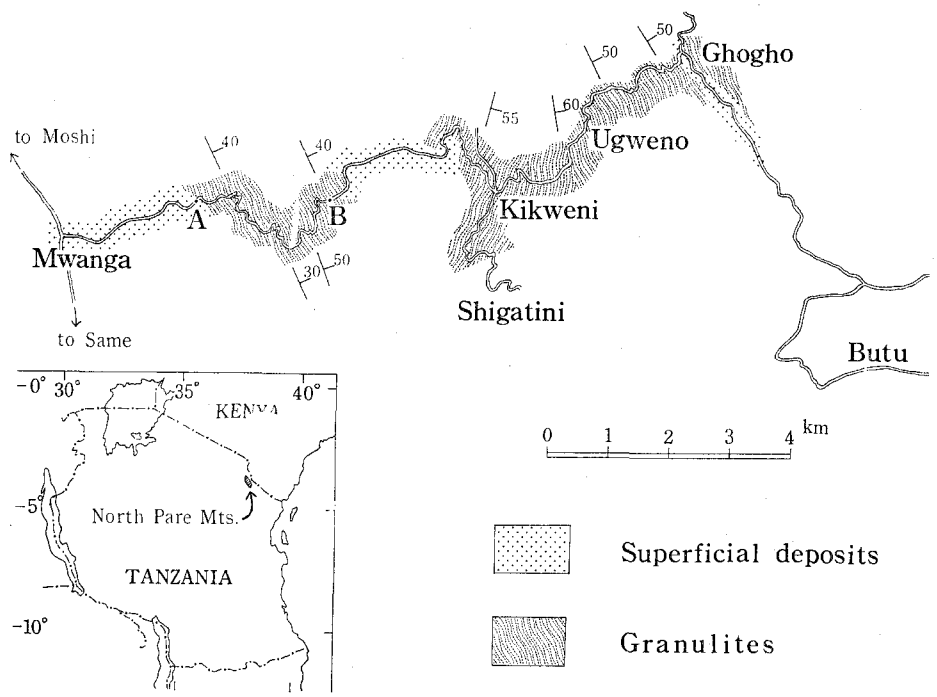

FIG. 1. Geology along the road between Mwanga and Butu in the North Pare Mountains.

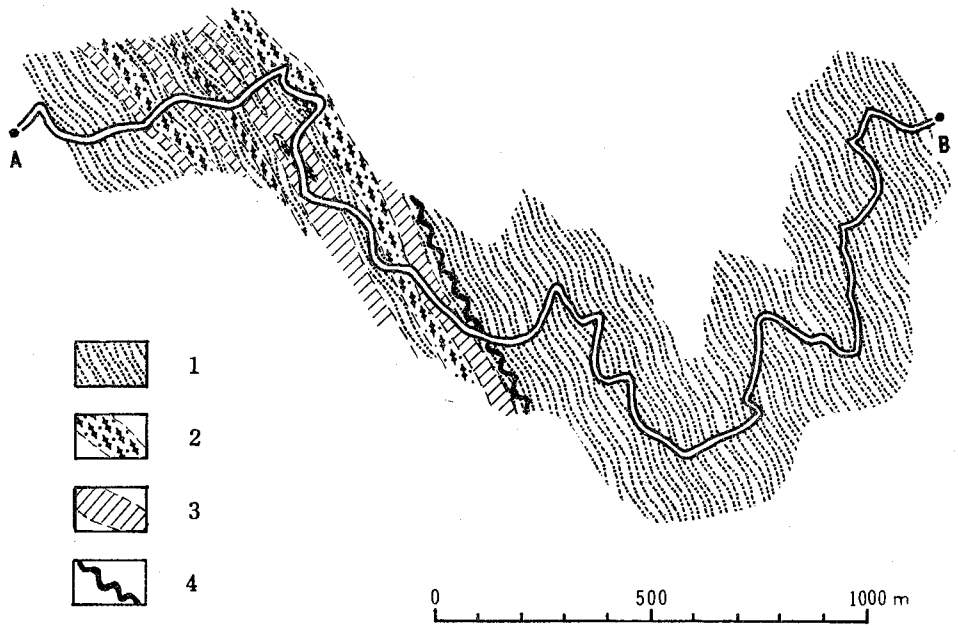

1. Intermediate granulites predominate.
2. Basic granulite layers and lenses are abundantly associated with intermediate granulites.
3. Acid granulites are abundantly associated with intermediate granulites.
4. Zone of structural disturbance.

FIG. 2. Geology between A and B in Fig. 1.

less than a half meter thick, cut the North Pare granulite complex. Their intrusion is later than the regional metamorphism.

In this paper some rock-types of granulites and related rocks will be treated descriptively. They are tentatively grouped into the following three divisions based on their mineral composition: acid granulites, intermediate granulites, and basic granulites. Acid granulites are composed principally of quartz and feldspar with minor amounts of orthopyroxene and/or garnet. Intermediate granulites contain large percentages of plagioclase and mafic minerals (some of hornblende, orthopyroxene and clinopyroxene, or all) with subordinate quartz. Potassium feldspar is present in a negligible amount. Generally felsic minerals exceed mafic ones in amount. Basic granulites consist essentially of mafic minerals and plagioclase. Quartz is absent or negligible. Plagioclase may be less than mafic minerals in amount.

Acid granulites

Acid granulites are leucocratic, fine- to medium-grained, and foliated. These rocks usually form light-colored bands which are interbedded with darker bands of intermediate division. The light- and dark-colored bands con-

stitute banded granulites as a whole (Pl. I-1, 2). The acid granulites consist principally of feldspar and quartz and subordinately of orthopyroxene, garnet, biotite, iron ore, apatite, and zircon. Secondary sericite, calcite and chlorite are usually present in small amounts. Quartz and plagioclase which are always predominant are usually light-colored but in some specimens they are darker. Potassium feldspar may or may not predominate. Foliated structure is well shown by the development of platy quartz in more leucocratic rocks (Pl. I-3). The felsic constituent minerals show signs of deformation such as cracks and wavy extinction. The composition of plagioclase ranges from An_{19} to An_{30}. Twinned plagioclase is common. Though twinning is ordinarily multiple, one group of lamellae is frequently more slender in shape and smaller in number compared with the other group. The composition plane parallel to (010) or (001) is common. Sometimes plagioclase is polysynthetically twinned in two directions. Antiperthite is present, though not so common (Pl. I). A small amount of albite is often well-developed in perthite. Potassium felpspar never occurs in simple twins such as Carlsbad twinning. Microcline structure is lacking but, in part, moiré appearance is occasionally found between crossed nicols. Hair perthite is quite common (Pl. II-1). According to the U-stage measurement, the potassium feldspar is supposedly monoclinic and has a fairly constant optic axial angle varying from $2V_X$ 55° to $2V_X$ 61° in different rocks. Myrmekite occurs at boundaries between potassium feldspar and plagioclase. Garnet is a dark red variety with the naked eye. It is usually concentrated in layers and sometimes it becomes a major constituent with increasing the amount (Pl. II-2). Garnet crystals are very irregular in outline and sieved in structure on account of numerous irregular inclusions of quartz. Orthopyroxene is strongly pleochroic (X=pale brownish red, Y=pale brownish yellow, Z=pale green, $Y \geqq Z > X$) and is similar to that of intermediate granulites. Zoned grains of zircon are found to occur rarely (Pl. II-3). The core part is well-rounded in shape and dusty in appearance. The rim is of a prismatic outline and is very perucid. This suggests that detrital zircon was overgrown with newly deposited material during the metamorphism. Biotite seldom exceeds 1 per cent in amount, although acid granulites have a little higher content of biotite than intermediate and basic granulites. Frequently it is semi-radial in shape and has vermiform quartz inclusions. The pleochroism is X=pale yellow, Y=Z=brown. Some flakes of biotite which are paler in color are a product due to later alteration. Examples of modal analysis in volume percent of these acid rocks are given as follows:

	Qu	Plag	K-feld	others
A:	37	58	—	5*
B:	43	21	33	3**

A: 3-681026-146 C, B: 3-681026-167 A

* Includes iron ore, K-feldspar, biotite, etc.
** Includes iron ore, biotite, garnet, etc.

Intermediate granulites

Intermediate granulites are of the most predominant type in the North Pare Mountaines. These rocks are fine- to medium-grained, dark, foliated rocks and are generally non-garnetiferous. They contain various percentages of plagioclase and mafic minerals in addition to the variation of mineral assemblage. Such heterogeneity is frequently found even in a hand specimen. Foliated and banded structures result mainly from different mineral compositions in different layers or bands and in part from the preferred orientation of some constituent minerals (Pl. II-4). The rocks are composed mainly of plagioclase and either some of hornblende, orthopyroxene and clinopyroxene, or all, with subordinate quartz, iron ore, potassium feldspar, biotite, apatite and zircon. Occasionally garnet is found as a major constituent.

Hornblende is one of the most important constituents of intermediate granulites in this area but sometimes it is scarce or absent. The commonest variety is brown-green in color and probably is close to hastingsite in composition as is suggested by the optical properties. An example is as follows: $\alpha=1.669$, $\beta=1.682$, $\gamma=1.689$, $2V_X=72°$, X=yellow, Y=yellowish brown, Z=green with a brown tint, $Y \geqq Z > X$. Prismatic crystals of hornblende are roughly parallel to the foliated structure. Either orthopyroxene or clinopyroxene, or both are usually found in moderate amounts. In many cases, both pyroxenes occur together (Pl. III-1). Clinopyroxene (diopsidic augite) is nearly colorless to pale green and sometimes feebly pleochroic (X=pale yellow-green, Y=pale brown, Z=pale green). Orthopyroxene (hypersthene) has fairly strong pleochroism: X=pale brownish pink, Y=pale yellow, Z=pale green. Microscopic exsolution lamellae of clinopyroxene are contained in some cases (Pl. III-2). An orthopyroxene has $2V_X=59°$, $\gamma-\alpha=0.014$. The plagioclase is usually andesine. Its composition is fairly constant, ranging from An_{34} to An_{39}. Most grains of plagioclase are homogeneous and are free from antiperthitic structure. Some grains are antipethitic and have very fine thread-shaped potassium feldspar. Rarely, exsolved potassium feldspar is present as platy inclusions set in orderly array. The mode of twinning is the same as in acid granulites. Garnet, if present, is poikiloblastic and is irregular in shape under the microscope (Pl. III-3). Potassium feldspar is usually contained in very small amounts as interstitial material. It is not perthitic and does not form myrmekite in contact with plagioclase. Biotite frequently occurs only in a very small amount. There are two types of biotite. One is found as scattered flakes. It is strongly pleochroic from pale yellow to brown, sometimes to dark brown. Chloritization is rather rare. The other, which is an alteration product, is a green-brown biotite and is found along the fracture and cleavage in orthopyrox-

ene. Iron ore is always present up to a few per cent by volume. Scapolite is a rare accessory and is found in a restricted number of intermediate granulites. Volume percentages of the constituents, for example, are shown as follows:

	Hb	Op	Cp	Gar	iron ore	Pl	Qu	K-feld	others
A:	21.0	7.5	3.4	—	3.7	59.8	1.7	0.8	2.1
B:	—	—	10.5	6.4	1.6	42.6	37.6	0.2	1.1*
C:	1.5	6.2	7.1	—	1.4	66.6	14.1	2.7	0.4

A: 3-681025-144, B: 3-681025-147, C: 3-681026-159.
* Includes hornblende.

Basic granulites

Basic granulites are fine- to medium-grained, melanocratic, foliated rocks. These rocks are interbedded with intermediate and acid granulites and form bands from a few centimeters to several meters in thickness. They also occur as irregular lenses, which are generally less than a few meters long. Plagioclase, hornblende and clinopyroxene are constantly found as major constituents and are occasionally associated with orthopyroxene or garnet. Accessary minerals are biotite, apatite, quartz, scapolite, iron ore and so on. Ferromagnesian minerals form more than 50 per cent of the rock and hornblende is first in abundance. The foliated structure of the rock is principally due to the preferred orientation of prismatic hornblende crystals and is accentuated by alternating layers with variable amounts of mafic minerals. The plagioclase shows various compositions in different rocks and ranges from An_{34} to An_{85}. Antiperthite is not found. Hornblende is usually a brown-green variety and is similar to that of intermediate granulite. For instance, it has $\alpha=1.664$, $\beta=1.677$, $\gamma=1.684$ and $2V_X=74°$. The pleochroism is X=pale yellow, Y=yellow-brown, and Z=green. The optical properties are not imcompatible with those of hastingsite. The associated plagioclase is An_{37} ($\alpha=1.547$, $2V_Z=83°$). There are also found basic granulites in which brown hornblende predominates. Pargasite occurs in a certain rock of basic division (Pl. III-4). The pargasite found has the following properties: $\alpha=1.638$, $\beta=1.650$, $\gamma=1.659$, $2V_Z=83°$, X=pale yellow, Y=pale yellow-green, Z=yellow-green. According to Deer, Howie and Zussman's diagram [6], the composition is approximately $100\,Mg/(Mg+Fe^{+2}+Fe^{+3}+Mn)=82$. Plagioclase associated with it is bytownite (An_{85}) in composition, as is indicated by $\alpha=1.570$, $\beta=1.577$, $\gamma=1.582$, and $2V_X=81°$. Clinopyroxene is more ubiquitous than orthopyroxene in basic granulites. Both pyroxenes are similar to those of intermediate granulites. Biotite is always found only in a very small amount. It is strongly pleochroic from pale yellow to brown with a red tint. Iron ore is generally less plentiful in basic granu-

lites than in intermediate ones. The following modal analyses (by volume) are given:

	Pl	Hb	Cp	Gar	Scap	iron ore	others
A:	30.5	55.5	6.9	—	3.4	1.0	2.7
B:	39.8	30.3	21.1	3.5	—	1.5	3.8

A: 3-681025-146 B, B: 3-681027-186.

MINERAL ASSEMBLAGES

The following assemblages are found in the North Pare metamorphic rocks. Minerals in parentheses are minor constituents.

Acid granulites:

1. Quartz-plagioclase-potassium feldspar (-orthopyroxene-biotite)
2. Quartz-plagioclase-potassium feldspar (-garnet-biotite)
3. Quartz-plagioclase (-potassium feldspar-biotite)
4. Quartz-plagioclase-garnet (-clinopyroxene-sphene-biotite)

Intermediate granulites:

1. Quartz-plagioclase-hornblende-clinopyroxene-orthopyroxene (-potassium feldspar-biotite with or without scapolite)
2. Quartz-plagioclase-hornblende-orthopyroxene-garnet (-potassium feldspar)
3. Quartz-plagioclase-clinopyroxene-orthopyroxene-garnet (-hornblende -biotite)
4. Quartz-plagioclase-clinopyroxene-garnet (-potassium feldspar -hornblende-biotite)
5. Quartz-plagioclase-orthopyroxene-garnet (-potassium feldspar-biotite)
6. Quartz-plagioclase-clinopyroxene-orthopyroxene (-hornblende-biotite)

Quartz is often subordinate in amount.

Basic granulites:

1. Plagioclase-hornblende-clinopyroxene (-scapolite-biotite-quartz)
2. Plagioclase-hornblende-clinopyroxene
3. Plagioclase-hornblende-clinopyroxene-orthopyroxene (-biotite)
4. Plagioclase-hornblende-clinopyroxene-garnet (-biotite)

Anhydrous minerals such as garnet, orthopyroxene and clinopyroxene may be characteristic of these mineral assemblages. Sillimanite and kyanite are reported to occur in a certain kind of aluminous rocks and quartzite [2]. There are also found hydrous minerals, hornblende and biotite. The latter, however, is in a very small amount. Hornblende is one of the most important constituents of the North Pare metamorphic rocks. It is stably associated with orthopyroxene and/or clinopyroxene in basic members of granulite and intermediate ones as well. The rocks of basic composition contain a plenty of

hornblende which exceeds other ferromagnesian constituent minerals quantitatively, and the assemblage plagioclase-hornblende-clinopyroxene (without orthopyroxene) is most common. On the other hand, there also occurs the assemblage plagioclase-hornblende-clinopyroxene-orthopyroxene, which is the assemblage of the granulite facies. Intermediate granulites usually contain considerable amounts of hornblende as a stable mineral and sometimes are practically lacking in it. The hornblende is generally of brown-green color and strongly pleochroic. Such feature is characteristic of hornblende of most granulite terranes. Quantitatively biotite is a negligible constituent, even though most assemblages carry it. It is supposed that biotite has decreased even to the point of elimination with rising metamorphic grade. Of course secondary biotite is excepted. Sphene is invariably absent except in a garnetiferous variety of acid granulite, in which it is associated with quartz, plagioclase, clinopyroxene and garnet. Under the border condition between the amphibolite facies and granulite facies sphene breaks down and all of liberated titanium oxide are absorbed into pyroxene and/or amphibole in the case where titanium is not enough to form rutile. This case is the same in the North Pare metamorphic rocks, with respect to the rare occurrence of rutile. Scapolite is associated with plagioclase in some granulites of intermediate as well as basic divisions. Potassium feldspar of acid granulites is characterized by a fine microperthite structure in the same manner as that of other granulite terranes. Antiperthite is not well-developed and its occurrence is restricted to acid and intermediate rocks. The granulite facies as defined by Eskola [8] is characterized by the assemblages of anhydrous minerals. In many granulite terranes (for example, Lapland [9], Adirondack [4, 7], Broken Hill [3], Lützow-Holmbukta [13], etc.), however, the presence of hornblende in the rocks of appropriate composition is rather common. With rising metamorphic grade, the quantity of hornblende in these rocks tends to decrease at the formation of clinopyroxene and/or órthopyroxene. Ultimately hornblende disappears and hydrous assemblages give place to anhydrous ones. The characteristic of granulite facies assemblages is the ubiquitous presence of orthopyroxene rather than the assemblages of anhydrous minerals, as contrasted with the amphibolite facies. Based on the petrographical evidences observed, the North Pare metamorphic rocks have been metamorphosed under the condition which is prevailing in the granulite facies. It is probable that they belong to the lower temperature part of the granulite facies for the most part.

ACKNOWLEDGEMENTS

We wish to express our appreciation to Dr. Isao Matsuzawa, Emeritus Professor of Nagoya University, who made every efforts to organize the Nagoya University African Rift Valley Expedition and led us to the study of African geology. We should also like to express our thanks to Professors Takeo

Watanabe and Kōkichi Ishioka of Nagoya University for their advice and encouragement. We gratefully acknowledge the assistance and kindness given by the Geological Survey of Tanzania and the government offices concerned during our stay in Tanzania. The field work was made possible by the Grant-in-Aid for Overseas Scientific Researches from the Ministry of Education, Japan, to which we express our thanks.

REFERENCES

[1] BAGNALL, P. S., Geological map of North Pare (Lake Jipe), Quarter Degree Sheet 73: Geol. Survey Tanganyika (1962).

[2] ——, The geology of the North Pare Mountains: *Rec. Geol. Survey Tanganyika*, **10**, 7-16 (1963).

[3] BINNS, R. A., The mineralogy of metamorphosed basic rocks from the Willyama Complex, Broken Hill district, New South Wales, Part I Hornblendes: *Mineral. Mag.*, **35**, 306-326 (1965).

[4] BUDDINGTON, A. F., Isograds and the role of H_2O in metamorphic facies of orthogneisses of the northwest Adirondack area, New York: *Bull. Geol. Soc. Am.*, **74**, 1155-1182 (1963).

[5] CAHEN, L. and SNELLING, N. J., The geochronology of Equatorial Africa: North-Holland, Amsterdam (1966).

[6] DEER, W. A., HOWIE, R. A. and ZUSSMAN, M. A., Rock-forming minerals, Vol. 2 Chain silicates: Longmans, London (1963).

[7] ENGEL, A. E. J. and ENGEL, C. G., Progressive metamorphism and granitization of the major paragneiss, northwest Adirondack Mountains, New York, Part II Mineralogy: *Bull. Geol. Soc. Am.*, **71**, 1-58 (1960).

[8] ESKOLA, P., Die metamorphen Gesteine, *in* T. F. W. Barth, C. W. Correns, und P. Eskola: Die Entstehung der Gesteine, Springer, Berlin (1939).

[9] ——, On the granulites of Lapland: *Am. J. Sci.*, Bowen Vol., Part 1, 133-171 (1952).

[10] HOLMES, A., The sequence of Precambrian orogenic belts in south and central Africa: Intern. Geol. Congr. 18th, London, 1948, Rept. 14, 254-269 (1951).

[11] MCKINLAY, A. C. M., The North Pare area: *Rec. Geol. Survey Tanganyika*, **2**, 13-21 (1952).

[12] QUENNELL, A. M., MCKINLAY, A. C. M. and AITKEN, W. G., Summary of the geology of Tanganyika, Part I Introduction and Stratigraphy: *Geol. Survey Tanganyika Mem.* 1, 1-264 (1956).

[13] SUWA, K., Petrological studies on the metamorphic rocks from the Lüzow-Holmbukta area, east Antarctica: Intern. Geol. Congr. 23rd, Prague, 1968, Proc. Sect. 4, 171-187 (1968).

EXPLANATION OF PLATES

PLATE I

1. Banded granulite from roadside between Mwanga and Kikweni. Banding is due to alternating acid and intermediate granulites.
2. Intermediate granulite with banded structure. Banding is due to varying mafic mineral contents. Roadside between Mwanga and Kikweni.
3. Long platy quartz in acid granulite (3-681025-150 B). Roadside between Mwanga and Kikweni. Crossed nicols, ×28.
4. Antiperthite in actd granulite (3-681025-146 A). Roadside between Ghogho and Kikweni. Crossed nicols, ×28.

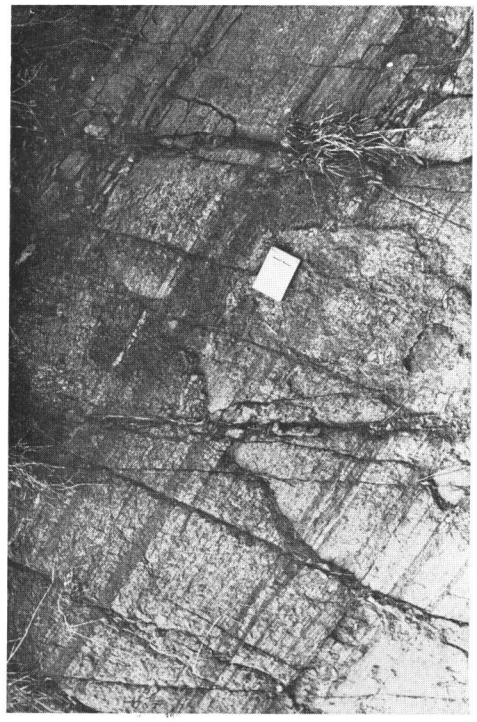

2

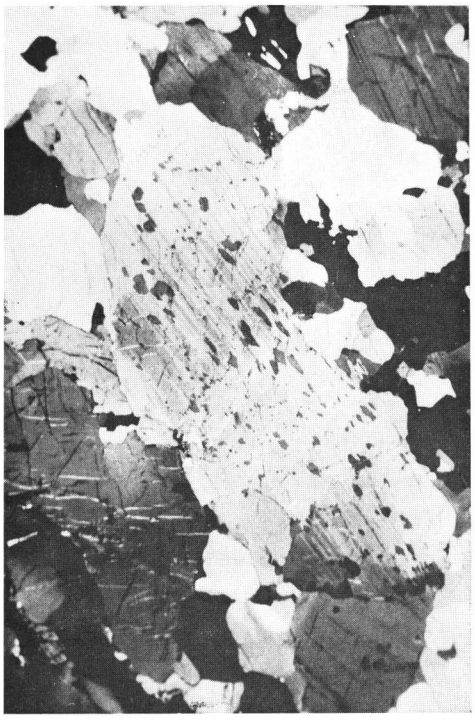

4

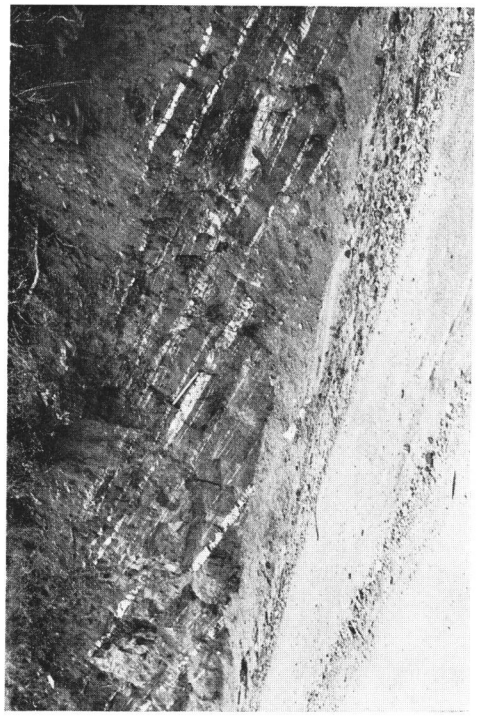

1

3

PLATE II

1. Perthite characteristic to acid granulite (3-681026-167 A). Between Mwanga and Kikweni. Crossed nicols, ×33.
2. Acid granulite (white band of the middle part) with garnet-concentrated layers. The same outcrop as Plate I-1.
3. Zoned zircon in acid granulite (3-681026-167 A). Between Mwanga and Kikweni. Crossed nicols, ×135.
4. Orthopyroxene-clinopyroxene-hornblende granulite of intermediate division (3-681025-150 A). Between Mwanga and Kikweni. One nicol, ×28.

2

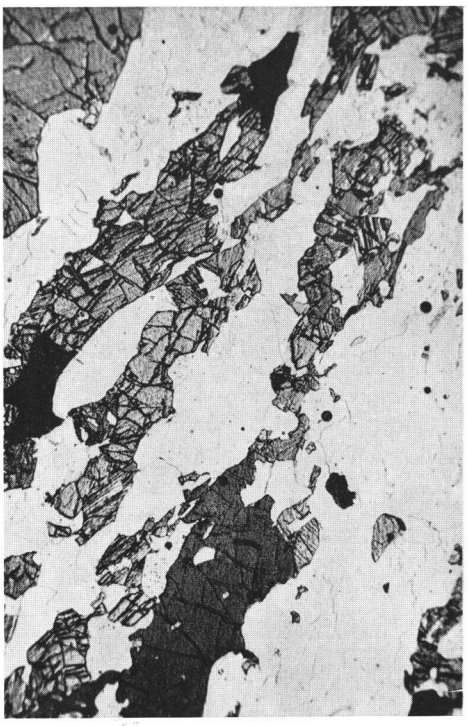

4

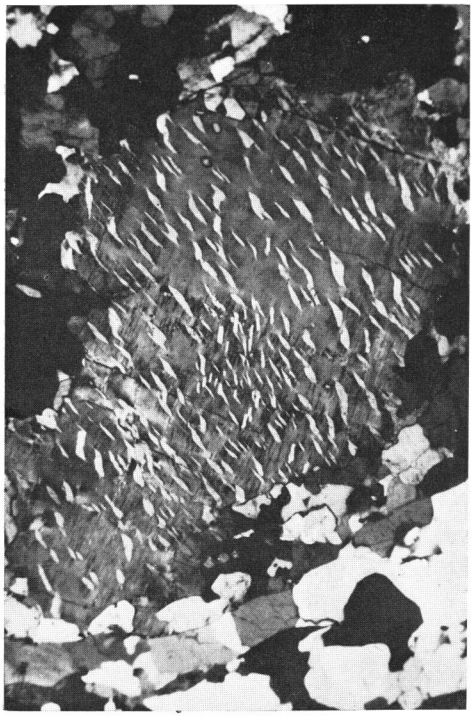

1

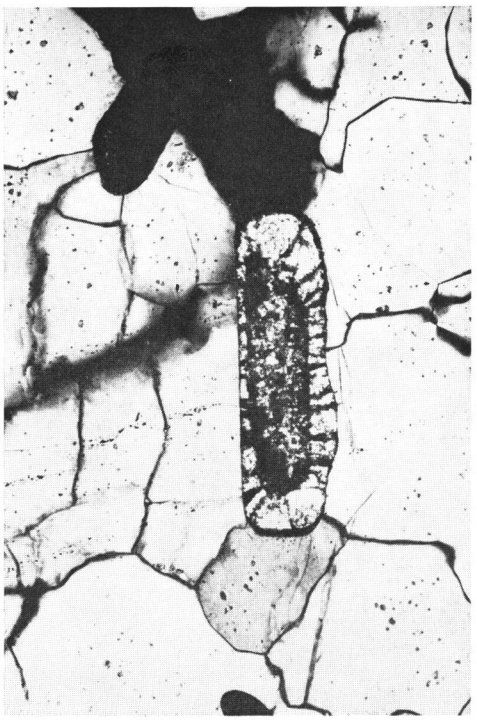

3

PLATE III

1. Orthopyroxene (middle and upper-left) and clinopyroxene (lower-right) in hornblende-clinopyroxene-orthopyroxene granulite of intermediate division (3-681026-152 A). Between Mwanga and Kikweni. One nicol, ×69.
2. Clinopyroxene lamellae in orthopyroxene in garnet-pyroxene granulite (3-681025-148). South of Kikweni. Crossed nicols, ×146.
3. Poikiloblastic garnet in intermediate granulite (3-681025-147). Between Ghogho and Kikweni. One nicol, ×58.
4. Pargasite in basic granulite (3-681027-185). Between Mwanga and Kikweni. One nicol, ×69.

2

4

1

3

Tectonic sketch of the Mbeya area, southern Tanzania

Shinjiro MIZUTANI and Kenji YAIRI

Department of Earth Sciences, Faculty of Science, Nagoya University

(Received 22 November 1969)

ABSTRACT

The African Great Rift Valley is split into two in East Africa, and the western rift represented by the Lake Tanganyika Rift and the Lake Rukwa Rift appears to join with the eastern one in the Mbeya area, where the Precambrian granitic and metamorphic complex of the Ubendian and the Ukingan epoch is widely distributed in highland and mountainous area unconformably overlain by the Bukoban sedimentary rocks. Segments of the Karroo and the Cretaceous system occur along the Rukwa and the Nyasa Rift, whereas large amounts of volcanic and pyroclastic rocks of the Tertiary age fill the northern part of the Lake Nyasa Rift. On the basis of the tangible features observed in the field investigation and the present topography of the Mbeya area, the four remarkable fracture systems are discriminated; the NNE-SSW direction represented by the Usangu Escarpment, E-W direction by the Buhoro Escarpment, NW-SE direction by the Lake Rukwa Rift, and NNW-SSE direction by the Lake Nyasa Rift. Tectonic development of the Mbeya area is summarized with special reference to birth and development of the rift structure together with the brief description of the local geology. It is considered that the Precambrian structure plays an important role in the development of the rift structure, and tectogenic movement in a part of the present rift valley is traceable back to the Proterozoic age, and possibly earlier.

INTRODUCTION

The African Great Rift Valley bifurcates in Equatorical Africa, and the eastern valley running through the central part of the Tanzanian country joins with the western one in the Mbeya area. This is geomorphologically displayed by development of Lake Rukwa and depressions of its tributaries northwest of Mbeya, and extends southeasterly to Lake Nyasa where the Livingstone Mountain represents a typical fault escarpment east of the lake. The Usangu Escarpment bordering the Buhoro Flats in the west is considered to be the southern extension of the eastern rift valley in the Tanzanian country. These geological structures come across with each other in the Mbeya area.

The Mbeya area and its geology have been investigated not only for a geotectonic interest of the rift structure but from an economical standpoint of mineral deposits, and many publications including geological maps, Quarter

Degree Sheet, 1 : 125,000, have been issued in these decades by Geological Survey of Tanganyika and Mineral Resources Division of Tanzania (Grantham and others [6]; Harkin and Harpum [8]; Harpum [9]; Harpum and Brown [10]; Kennerly and others [11, 12]; Macfarlane and others [13, 14, 15, 16]; Teale and others [22]). All of these maps were very instructive for our field investigation. During our stay in Mbeya, the present authors surveyed several districts in this area aiming at a tectonic investigation of birth and development of the rift system. In the other parts of this volume, the authors present another paper on the rift structure of Lake Tanganyika in Kigoma, western Tanzania (Yairi and Mizutani [23]), and Dr. Aoki reports a result of geophysical researches made by himself in this country (Aoki [1]). These papers will be helpful to fully understanding of our investigation on the rift structure in Tanzania.

PHYSIOGRAPHY

From Mbeya to the east, a highway called Great North Road leads to Dar es Salaam *via* Iringa and Morogoro. This highway runs at the foot of the Buhoro Escarpment along the southern margin of a plain named the Buhoro Flats. Many rivers and their upper reaches originating from the Poroto and Kipengere Mountains debouch into the flat plain cutting through the Buhoro Escarpment, and they flow into the Great Ruaha River. While the south of the Buhoro Flats is bounded by the Buhoro Escarpment, the west of the plain is also bordered by another steep topography called the Usangu Escarpment; thus, the Buhoro Flats form an angular basin and its height is about 3500 feet above sea level at the central part of the plain of the surveyed area. Geomorphologically, the Buhoro Flats show a marked contrast to the other part of the Mbeya area, and a large part of it is such a mountainous highland area as represented by Mbeya Peak (9272 feet high) in the Usangu Mountain or by Rungwe Volcanic Mountain (9713 feet high), Mt. Mtorwi (9711 feet high), Mt. Ngozi (8598 feet high) and Mt. Chaluhangi (9623 feet high) in the Poroto Mountain. Surface of the Buhoro Flats is exclusively covered by superficial alluvial deposits which were laid down on the flood plain at the time of rainy seasons.

The Poroto and Kipengere Mountains are a highland area south of the Buhoro Flats. Though remarkable the Buhoro Escarpment is, the inland parts of the mountain range show a rather gentle topography with hilly landscape. As implied by presence of the steep escapment, a discontinuous relief difference between these inland parts of the mountains and the Buhoro Flats suggests that the Poroto and Kipengere Mountains form a faulted block gently tilting to the south. This block is bounded on the north by the Buhoro Escarpment, on the west by the Rungwe Volcanics and on the south by the Lake Nyasa

Rift.

The Usangu Mountain occupies a plateau area northwest of Mbeya, and it is bounded in the east by the Usangu Escarpment and in the south by the Lake Rukwa Rift. These remarkable topographical features are represented by Mbeya Peak (9272 feet high) on the northeastern escarpment of the Lake Rukwa Rift on one hand and by World End's View (8000 feet high) and by the Highest Point of all main roads in Tanzania (8050 feet) on the Usangu Escarpment on the other. Inward to these escarpments, a large part of the Usangu Mountain, though more or less excavated by many small streams, is rather plain area, and the mountain forms, as a whole, a faulted block gently tilting to the north or northwest.

To the southwest of the Usangu Mountain are found many parallel lineaments trending NW–SE. Many streams running in this direction flow into the Songwe River, which courses in lowland area to the northwest and into Lake Rukwa. This topography represents a rift valley called the Lake Rukwa Rift. It is said that the water level of Lake Rukwa (about 2600 feet above sea level) is considerably fluctuated annually. Since large amounts of detrital materials are now trapped in the lake, the lowest level of the basement complex in the Lake Rukwa Rift is thought to be much lower than estimated on the topographical maps. The rift is bounded on the southwest by the Mbozi Plateau in which we can find a similar lineament structure running northwesterly in the basement complex. Parallel arrangement of the above-mentioned lineaments suggests that there may be a step-like structure especially on the southwestern part of the Lake Rukwa Rift.

In the southeastern extension of the Lake Rukwa Rift occurs the Lake Nyasa Rift, its northeast being bordered by the Nyasa fault at the foot of the Kipengere and Livingstone Mountains. However, there is not found such a topographical feature as valley near the Tukuyu area, because enormous amounts of volcanic materials erupted from the Rungwe, the Ngozi and the Kiejo volcanoes are extensively found to occur. They are distributed on basement rocks and cover the rift structures between Lake Nyasa and a town area of Mbeya. Volcanic activities and their products are the youngest geological events in the Mbeya area, and there are now developed volcanic mountains accompanying a volcanic crater on their tops. Lake Wentzel Heckerman, about 6700 feet high, is one of the representatives of these volcanic craters. The greatest and most remarkable topographical feature in the Lake Nyasa Rift is Lake Nyasa itself (about 1570 feet above sea level), and there are typical fault scarps forming the Livingstone Mountain northeast of the lake.

Concealed by the volcanic rocks of younger ages, the basement structure of the Lake Nyasa Rift in an inland area cannot be directly observed, and it is only traceable along the Nyasa Fault at the foot hill area of the Kipengere Mountain northwest of Lake Nyasa. Probably many lineaments trending NW–

SE, almost parallel to the elongation of Lake Nyasa, may be found under the thick volcanic covers. As will be discussed later, these volcanic areas are thought to be downthrown again after the volcanic eruption, and these areas form, as a whole, relatively lowland areas of the post-volcanic rift.

GEOLOGY

Most extensively distributed in a mountainous part of this area are, in the order of age, the Precambrian rocks of the Ubendian, the Ukingan and the Bukoban epoch. Metamorphic rocks of the Ubendian and the Ukingan epoch occur in the Usangu and the Poroto and Kipengere Mountains, whereas sedimentary formations of the Bukoban system is found in the Poroto and Kipengere Mountains. The Ubendian metamorphic complex consists mainly of granite, granitic gneiss and migmatite. In the northeast of the Usangu Mountain of this area, basic and ultrabasic rocks are found to occur; this basic complex consisting of peridotite, lherzolite, pyroxenite, troctolite, and olivine gabbro found in the Nsamya Hill is called the Nsamya ultrabasic body (Teale and others [22]). Calcareous complex belonging to the Ubendian metamorphic system occurs in the eastern part of the Poroto Mountain, where marble, dolomitic marble and skarn are intercalated in amphibolite. In the southwest of the Mbeya area, many lenticular bodies and ring-shaped intrusion of basic rocks named the Mbozi syenite-gabbro complex are distributed in an alignment in the granitic gneiss (Macfarlane and others [14]). General trend of these lenticular bodies is almost parallel to gneissose structure and also to the trend of the Lake Rukuwa Rift. In fact, there runs a fault relevant to formation of the Lake Rukwa Rift; this is called the Ufipa fault. It is described that the Mbozi syenite-gabbro complex is probably Proterozoic and its intrusion post-dates the regional metamorphism of the Ubendian rocks; radiometric age on biotite in biotite perthosite of this complex is 743 ± 30 m.y. (Cahen and Snelling [4]). It is very noticeable that the positive gravity anomaly is observed by Dr. H. Aoki, a member of Nagoya University African Rift Valley Expedition, in a traverse on this gabbro complex. He discusses its geophysical significance in his paper on the geophysical research carried out in the Tanzanian country [1].

According to Cahen and Snelling [4], the radiometric age determination on the Ubendian rocks shows that the Ubendian cycle is a major and widespread one in Equatorial Africa, and it dates in a range 2150–1650 m.y. For example, K–A ages of muscovite and biotite from greisen associated with post-orogenic granite intruding Ubendian gneisses (Chunya District, 8°12′30″ S, 33°13′30″ E) and from porphyritic biotite-granite intruding presumed Ubendian gneisses (Chunya District, 8°01′35″ S, 32°37′34″ E) date 1800 ± 70 and 1825 ± 70 m.y., respectively.

On a mountainous area southwest of the Lake Rukwa Rift, general gneissose structure and the other foliation trend almost parallel to the Rift; similarly, northeast of the Lake Nyasa Rift, they show a direction parallel to that of the Lake Nyasa Rift. On the other hand, in the northwestern part of the Usangu Mountain the trend of the Ubendian rocks takes rather variable strikes, in which the predominant one is almost parallel to the Lake Rukwa Rift. In the northeastern part of it, however, there is found a latitudinal trend represented by a foliation of metasediments and a zone of intense shear and cataclasis (Kennerly and others [11] and Macfarlane and others [16]).

Together with the Ubendian rocks, the later metamorphic rocks of the Ukingan epoch comprise a part of the Usangu Mountain and the Poroto and Kipengere Mountains. As is observed on the geological maps of the Kipengere Mountain (Harpum [9]), the Ukingan metamorphic complex occurs intimately connected with the Ubendian one. In other words, there is no structural difference between the Ubendian and the Ukingan metamorphic rocks northeast of Lake Nyasa, and they have a general strike NW–SE parallel to the direction of the Lake Nyasa Rift. Northwest of the Mbeya town, there occur also metamorphic rocks referrable to the Ukingan, and they also trend almost parallel to the Lake Rukwa Rift. These rocks are, in the approximate order of relative abundance, granitic gneiss, mylonitic rock, phyllonite, and amphibolite; and in the Kipengere Mountain there is found to occur a granitic rock, designated as the Ndyuda granites and migmatites by Harpum [9], its distribution being almost parallel to the trend of the metamorphic rocks described above. At Chimala of the Buhoro Escarpment of the Poroto Mountain, there is distributed granitic rock, called the Chimala granite; this occurs as a massive boss apparently discordant to the metamorphic trend and is considered to be a post-orogenic granite. According to Cahen and Snelling [4], the Ukingan epoch is included in the Kibaran–Burundian–Karagwe-Ankolean Cycle, the date of which ranges from 1290 m.y. to 850 m.y., and the Ukinga Series itself is probably younger than 1800 m.y. but older than 1300 m.y. The radiometric age of the Chimala granite is recorded as 1300 ± 50 m.y. on hornblende in the granite (Chimala, 8°52′ S, 32°02′ E). Age determination by means of K–A method is now carried out in Japan on some samples of the Ukingan system, and its result will be reported in near future.

The youngest Precambrian rocks cover unconformably the Ubendian and the Ukingan metamorphic rocks, and they occupy the northern part of the Poroto and Kipengere Mountains. Probably they belong to sedimentary formations of the Proterozoic era called the Bukoban system in East Africa. This system in this area consists mainly of quartzite, red sandstone and shale intercalating thin lenses of limestone, conglomerate and basic lava, and these clastic formations are overlain by basic rocks called gabbro eruptives (Harpum and Brown [10]). All of these rocks as well as the Ubendian and the Ukingan

metamorphics are intruded by many dikes of dolerite. These dolerite dikes are considered to be igneous activity of the Bukoban age. By summarizing many results of radiometric age determination, Cahen and Snelling [4] stated that the Bukoban sedimentation was after the Chimala granite (probably about 1300 m.y.), and the latest Precambrian orogenic cycle called "Katangan" was 1300 m.y. to 450 m.y. The sedimentary formations cropping out along the Great North Road show a gentle dipping structure and form a synclinal or basinal structure, the long axis of which runs approximately north to south. However, the southern part of the system in the Kipengere area underwent a strong diastrophism as is shown on the geological map (Harpum [9]), showing intensive folds such as isoclinal and recumbent folds sometimes accompanied by low-angled thrust.

Scattered outcrops of the Karroo sediments are found in foot hills of mountainous areas southwest of the Lake Rukwa Rift and the Lake Nyasa Rift. The Karroo System consists of coarse clastic materials of continental deposits, and it is distributed in a narrow and long strip almost parallel to the rift valley. The system, more or less inclined, is uncomformably underlain by the Precambrian metamorphic rocks, and sometimes cut by younger faults of the rift system. Probably, the birth and deformation of the Karroo basin in this area had been related with the development of the Lake Rukwa Rift and the Lake Nyasa Rift.

There is found to occur the Cretaceous group also in the mountainous area southwest of Mbeya. It is composed exclusively of sandstone and occupies an elongated, but detached, area along the rift valley. North or northwest of Kiwira, sandstone of the Cretaceous group is most extensively distributed, and it is unconformably covered by Tertiary volcanics. It is lithologically correlated to the Cretaceous group found to the west of the Mbeya town, where the Dinosaur's egg buried in sediments was discovered by Dr. W. G. Aitken (Grantham and others [6]).

One of the most interesting rock species in this area is carbonatite. It occurs either occupying a long and narrow zone bordered by faults parallel to the Lake Rukwa Rift or forming an oblong area as the Panda Hill south of the Mbeya town. According to Grantham and others [6], it contains such rare metal as niobium and it is economically investigated in some detail. The intrusion of the carbonatite is considered to date Cretaceous on a basis of the radiometric age determination made on phlogopite (113 ± 5 m.y.), biotite (96 ± 9 and 101 ± 12 m.y.) and potash feldspar (100 ± 10 m.y.) from rocks related to carbonate rocks of the Mbeya area (Cahen and Snelling [4]). Petrological and petrochemical investigation of the carbonatite collected from the Panda Hill is done, and the result is reported in a separate paper in this volume written by the petrological group (Suwa and others [21]).

All of these geological formations described above are covered by the

volcanic lava and ash of the Tertiary age. Volcanic activity is also displayed by the topographical features, especially by the presence of volcanic craters. According to petrological charateristics and stratigraphical distribution of these eruptives and pyroclastics, they are discriminated mainly into two, younger and older; the former constructs the Rungwe, the Mbozi and the Tukuyu volcanoes and the latter the basal part of these volcanic terrain. These volcanic rocks are chemically basic and alkalic such as basalt, phonolite, tranchyandesite, and their pyroclastics. The volcanic activity is considered to be most violent in the Lake Nyasa Rift, and the rift valley area is almost wholly covered with its products. Recent report on the ages of volcanic activities in East Africa described by some English geologists (Bishop and others [2]) suggests that volcanic eruptions have two acmes in the rift valley areas of Equatorial Africa. If the dates are tentatively correlated to the volcanic activities of the Mbeya area, the Tertiary eruption dates either 23–18 m.y. or 15–11 m.y. The exact correlation will be made, when the radiometric age determination is done. After the Tertiary volcanic rocks were erupted, thin but extensively distributed blanket of pumice ash overlies on whole of the Mbeya area irrespective of the topographical natures. It was produced by the Quaternary volcanic activity. The latest eruption in this area was observed at the Kiejo volcanoe during last century (Harkin and Harpum [8]).

From the geological history briefly summarized above, it is interpreted that the formation of the rift valley is traceable back to the Cretaceous or much older age. McConnel [17] stressed that the present rift valley of African Continent is geologically related with the Precambrian geology and the birth and development might be commenced in the Precambrian age. In addition, Matsuzawa [19] stated that the African rift valley was formed in the Miocene age, its structural pattern being arranged almost parallel to foliation of the Precambrian rocks. During our stay in Mbeya, the authors visited and studied several parts within this area in detail aiming at clarifying structural features which are related to the formation of the Tanzanian Rift Valley.

Kimani River area:–About 50 miles east of Mbeya, Kimani River runs from the Poroto Mountains to the north crossing the Great North Road. There are distributed sedimentary formations of the Bukoban age assuming a gently dipping basin in the upper reaches tributary of the Kimani River. The Bukoban system occuring in the Kimani River area consists of red slate, sometimes intercalating calcareous layers, and orthoquartzitic sandstone called the Gofio quartzite. Red slate is chocolate brown in color and easily foliated parallel to the slaty cleavage. In this slate are interbedded several layers of ferruginous siltstone about 0.5 m in thickness. The ferruginous rock is heavy, its density measuring about 3.74, and contains dense assemblage of hematite. The Gofio quartzite is well exposed under the bridge of the Great North Road, where

massive white orthoquartzitic sandstone is found to occur. It is composed exclusively of well rounded quartz grains showig secondary enlargement of quartz in optical continuity, by which all grains are tightly cemented. To the south of the Great North Road, green slate sparsely intercalating calcareous

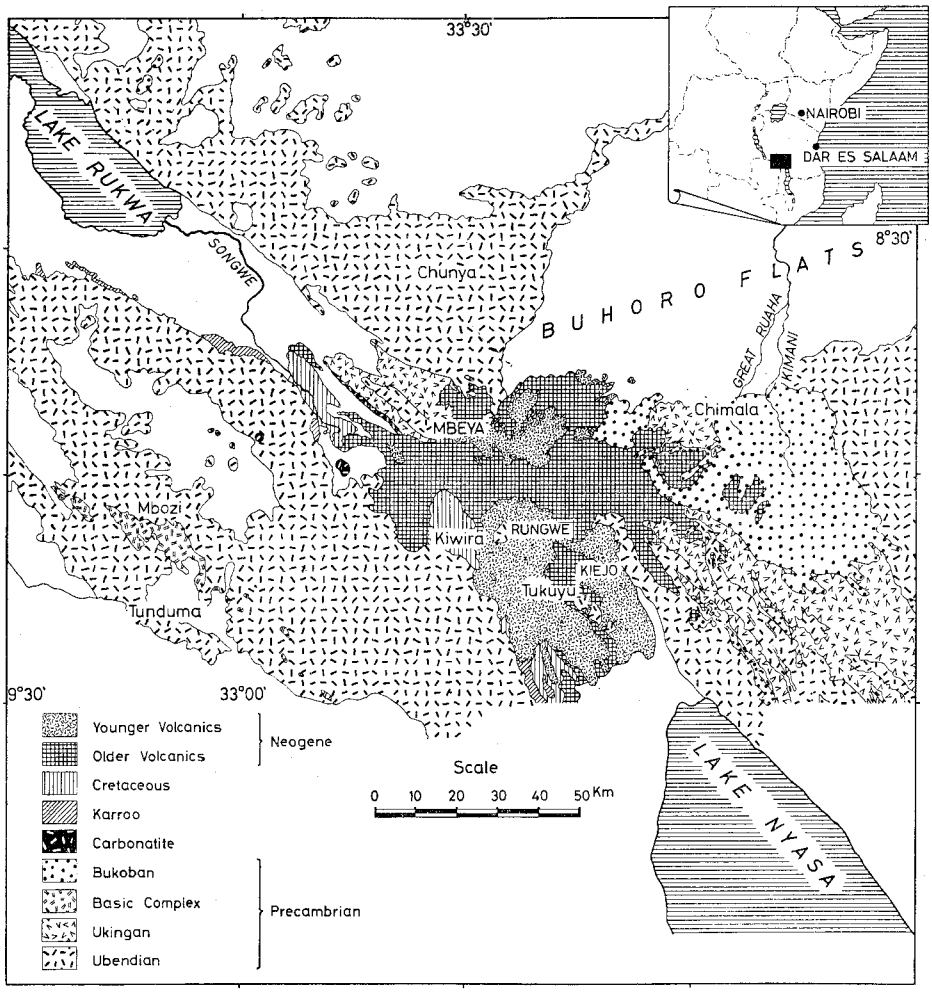

FIG. 1. Geologic map of the Mbeya area compiled from Quarter Degree Sheets (No. 227-"Luika", Macfarlane, Macdonald, Grantham and Skerl [15]; No. 228-"Makongolosi", Macfarlane, Mudd, Orridge, Teale, Eades and Grantham [16]; No. 229-"Shoga", Kennerly, Teal and Eades [11]; No. 243-"Itaka", Kennerly, Spence and Spurr [12]; No. 70 SW= 244-"Mbeya", Grantham, Teale, Spurr, Harkin and Brown [6]; No. 245-"Irambo", Teale, Eades, Harkin, Harpum and Horne [22]; No. 71 SW=246-"Chimala", Harpum and Brown [10]; No. 257-"Tunduma", Macfarlane, Brock and Spurr [13]; No. 258 and 258 S-"Itumba", Macfarlane, Harkin, Horne, and Spurr [14]; No. 78 EN=259-"Tukuyu", Harkin and Harpum [8]; No. 79 NW=260-"Kipengere", Harpum [9]).

layers crops out widely together with red slate. All of these dip gently to the east or west and form a syclinal structure, the axis extending to the south.

Many fractures are observed in these Precambrian rocks. Among them, the authors descriminated two directions of the fracture planes; one is almost parallel to the present topography of the Buhoro escarpment so that it is called here the Buhoro direction or abbreviatedly B-direction. A picture shown in Plate I, Fig. 1 presents an example of fractures of the B direction developed in the Gofio quartzite. Irrespective of the horizon of strata or their trend, these fractures run parallel to each other. The other fracture system occurs almost perpendicular to that of the B-direction, and takes nearly N-S trend, or parallel to the trend of the Lake Nyasa Rift. Here, it is called the Nyasa direction or N-direction. The fractures of B-direction and of N-direction are frequently found to be associated with each other in an outcrop as is shown in Plate I, Fig. 2. In the Kimani River area, nearly vertical fractures of the B-direction trend ENE-WSW~ESE-WNW and those of the N-direction is NNE-SSW~NNW-SSE. Almost all of the fractures of the B-direction neither show any displacement along their planes, nor accompany sheared plane and slickenside. Furthermore, no remarkable opening is observable along these fractures, though papery thin openings are sometimes found there. These fractures may well be called a kind of the extension fracture. In addition to these extension fractures, there are found to occur many minor faults also taking the B-direction (Plate II, Figs. 1 and 2). One of exposures of such minor faults along the Great North Road reveals that red slate of the Bukoban

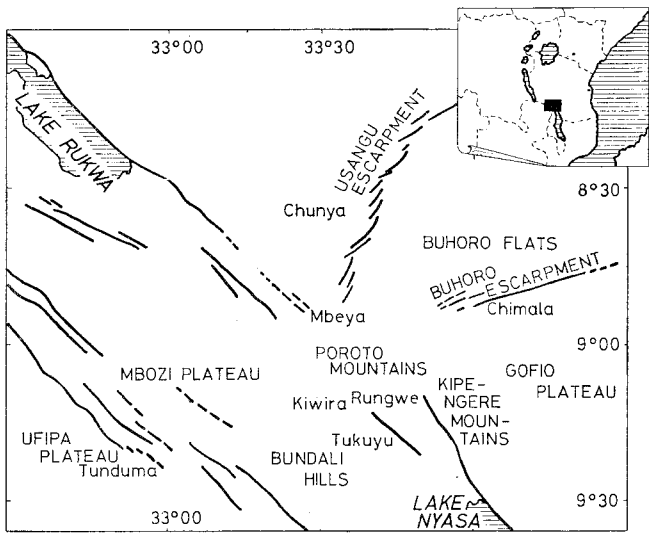

FIG. 2. Sketch map of the Mbeya area showing physiographic features, lineaments and fracture patterns.

system is cut, displaced or rotated by the faults and some of them display a contorted broken structure. It is highly probable that the present topography of the Buhoro Escarpment was produced by accompanying such minor faults.

Another fracture system designated as the N-direction almost perpendicular to the B-direction shows neither vertical nor lateral displacement along the fractures of that direction. Inasmuch as observed in each exposure in this area, there is no indication to testify which fracture was earlier. It is considered that the fracturing of the N-direction probably occurred at the time of formation of the Lake Nyasa Rift, and the fractures form the Mbeya Crux together with those of the B-direction.

Irambo area:–Tertiary eruptives are widely distributed in the Lake Nyasa Rift, and lava and pyroclastics expose along the Great North Road to the east of the Mbeya town. Younger volcanic series of phonolite, trachybasalt, trachyte and olivine basalt constitute hilly land. Tongue-shaped flows of these volcanic rocks sometimes invade into the Buhoro Flats, and the western extension of the remarkable topography of the Buhoro Escarpment is covered by them, so that morphological features are obscure in this area. Pre-Tertiary formations are unconformably overlain by these volcanic and pyroclastic rocks; the stratigraphically uppermost part is occupied by pyroclastic layers consisting of pumice ash of the Quaternary age.

About 25 miles east of the Mbeya town, there are found outcrops of alternation of volcanic rocks and pyroclastic layers. They dip gently to the east or northeast, and there are developed, though sporadically, fractures of the Buhoro direction as well as of the Nyasa direction. At road sides of the Great North Road, the authors observed a fault cutting the volcanic and pyroclastics rocks almost vertically. The fault runs north to south to cross the road, and it is well exposed at its both sides. As is presented by the photograph of Plate III, Fig. 1, the volcanic rock is clearly cut by the fault which occurs in association with fault breccia derived from agglomeratic tuff found to the west of the fault. The fault plane measurable at the sharp end of the trachytic rock trends N–S dipping 70° to the west, and the western side is seemingly downthrown. The trend of this fault is nothing but the Nyasa direction, and this suggests that the rift movement was active again after the Rungwe and other volcanic eruption occurred in the Lake Nyasa Rift. A part of the pyroclastic rock is covered by weathered coarse ash, that is probably of much younger age, but it is undetectable whether the fault is covered by this weathered ash or cuts and displaces it.

Buhoro Flats:–Bordered by the Usangu and the Buhoro Escarpment, the Buhoro Flats extend to the northeast forming, as its name implies, a wide flat plain, where the Great Ruaha River gathers its tributaries from mountainous parts of the Mbeya area. Superficial part of the Buhoro Flats consists of clay

and silt laid down at rainy seasons and their weathered equivalents. In the plain are found many brooks and streams even in a dry season, and they denudate the plain to make small and low precipice. As far as observed at these small vertical cliffs along the streams, the thick pumice ash, partially weathered, lies under the thin blanket of recent clay and silt. A picture in Plate III, Fig. 2 shows that layering of ash is flat and horizontal. It is probably conceivable that volcanism releasing large amounts of pyroclastic materials was still active after formation of the present topography of the Buhoro Flats.

Highland area of the Poroto and Kipengere Mountains:–Areas south of the Buhoro Escarpment are higher than 5000 feet in altitude. There are found rather gentle topographical natures represented by flat plateau and rolling hills. Except for volcanic topography in the Lake Nyasa Rift area, it seems likely that a part of the Poroto and Kipengere Mountains shows an elevated peneplain partly upheaved by such a movement as block faulting. The Precambrian rocks are the main constituents of the basement of this area, among which sedimentary and igneous rocks of the Bukoban system are widely distributed. Just south of Chimala, gabbro eruptives, so called in Quarter Degree Sheet "Chimala" (Harpum and Brown [10]), expose on steep slopes of the Buhoro Escarpment. It is massive course-grained gabbro, and under the microscope it has a typical ophitic texture. Judging from the distribution of the gabbroic rock, it seems to form sill or sheet, but there are found no rock formations which overlie it.

In the eastern part of the Poroto Mountain, a higher ridge of the Kipengere Mountain extends from the south-southeast to north-northwest. There are found sedimentary formations such as red slate and quartzose sandstone of the Bukoban system. Red slate is composed of thin or laminar alternation of red slate and siltstone and trends northwest and dip to the southwest. Frequently, this slate displays a minor folding as is shown in Plate IV, Fig. 1. Though red slate is more or less sheared there, the minor folding reveals a plastic nature of deformation and is ascribed to be formed by slumping at the time of or just after deposition. The red slate changes upwards to alternation with sandstone, and to quartzose sandstone. This is stratigraphically called the Gofio quartzite. It dips southwesterly or northeasterly, and forms a folded structure. Scenic view of the folds is shown in Plate IV, Fig. 2. Fold axes or axial traces of this Gofio quartzite run a little obliquely to the ridge of the Kipengere Mountain, and they trend approximately N 20°~30° W. Interestingly enough, this structural trend is almost parallel to the Lake Nyasa Rift, whose morphological features are now concealed by volcanic rocks of later age and obscure though. The fold structure of the Bukoban system of this ridge of the Kipengere Mountain shows a marked contrast to that of the Kimani River area, where the whole successions dip very gently assuming a basinal structure.

Basement rock formations are widely covered by volcanic rocks, especially tuffaceous materials. The youngest ash falls are chiefly pumiceous, and their distribution conforms to the present topography. In other words, erosional surface of the basement rock and older volcanic rocks governs the distribution and thickness of the pumiceous ash. A picture in Plate V, Fig. 1 shows an ash layer dipping gently covering an ancient slope, and the present topography itself is conformable to the ancient one. Ash falls and features of their layerings are well observed at a cutting along the Tukuyu Road where alternate occurrence of ash falls and erosion gave rise to apparent folding structure (Plate V, Fig. 2). Anyway, it is evident that the youngest ash fall occurred after the recent topography was formed.

Kiwira area: To the northwest of Kiwira is found to occur a weakly indurated coarse sandstone sporadically intercalating red shale. Lithologically this clastic formation is correlatable to the Cretaceous system in the Songwe River area west of the Mbeya town where the Dinosaur's egg fossils were discovered by Dr. W. G. Aitken (Grantham and others [6]). Sandstone found in the Kiwira area is pale yellow brown composed of clastic particles of quartz and feldspar, and rarely it contains fragments of schistose rocks. Most of the clastic grains are more or less fringed by newly grown minerals, same as their cores in composition, in optical continuity. Deficient in caly matrix, the rock may well be classified to arkose sandstone. The cross-stratification is very remarkable, and in places small fragments of shale are contained in a medial part of a bed. Accompanied by them, much coarser facies occurs intraformationally. On a basis of the fabric relation between bedding plane and cross-stratification, it is possible to obtain the paleocurrent direction of the Cretaceous system. Stereographic reconstruction of cross-bedding shows that the original attitudes of four cross-bedding measured in this area dip 16°, 16°, 10° and 10° to N 83°W, N 62°W, N 24°W and N 33°W, respectively. This result suggests that the paleocurrent direction is variable and the condition of transportation or deposition is rather complicated by a localized drainage system. Generally the Creraceous sandstone of this area dips gently 20~30° to the north and intruded by small dikes of andesite. These rocks are overlain unconformably by tuff, and further upwards the pumice ash covers unconformably. Many minor faults and fractures are developed in the Cretaceous system of this area. The authors descriminated two groups of the faults and fractures, the one trending N 20°W–S 20°E and the other N 30°E–S 30°W. The latter group takes a direction almost parallel to the Usangu Escarpment, while the former is parallel to the Lake Rukwa Rift. Here, let us designate the former as the fracture of the R-direction and the latter that of the U-direction. All of the faults and fractures cut not only the Cretaceous sandstone but the older tuff, and some of them cut also the younger pumice ash. Consequently, both groups of the faults

and fracture occurred after the older volcanic activity and before the younger ash, and the youngest faults and fractures were formed after the younger ash fall. Since the fractures of the R-direction are more frequently developed in the younger pumice ash layers and the faults of the same direction displace fractures of the U-direction, it is probably interpreted that the latest tectogenesis is the formation of the fracture of the R-direction. An assumption that these two groups of fractures, the U-direction and the R-direction, constitute a set of conjugate fractures is possibly conceivable in this Kiwira area, but the authors could not find any evidence to support this assumption.

TECTONIC DEVELOPMENT OF SOUTHERN TANZANIAN RIFT AREA

As was briefly described in the preceeding chapter, physiographic features of the Mbeya area represent conspicuous tectonic patterns, whose constituents are the Lake Rukwa Rift, the Lake Nyasa Rift and the Buhoro Flats. The Usangu Escarpment and the Buhoro Escarpment border the Buhoro Flats in the west and in the south, respectively. The Usangu Escarpment extends northeasterly and seems to be connected to the Eastern Rift of the Tanzanian country; therefore, the escarpment is considered to be a southwestern extension of the Eastern Rift, though it shows echelon pattern of faults in the Mbeya area. Judging from these fundamental structure of the basement, the Mbeya area has been noticed to be an area where two great rifts come to cross each other. Brock [3] depicted a structural pattern of the African Rift insisting that many faults are found in a peripheral zone of basement blocks and the birth and development of the African Rift can be ascribed to the differential movement occurring in and between the blocks. In the Mbeya Crux, so he called, many faulted structures encounter and converge, and this tectonic peculiarity triggered eruptions of the Rungwe and related volcanoes. A part of the volcanic activity is said to have been observed in a recent age. As was described in the preceeding sections of geology of the Buhoro Flats and the Highland area of the Poroto and Kipengere Mountains, a blanket of the latest ash falls cover the older rock, and its distribution and thickness conformable to the present topography suggests that the present physiographic features were already formed, when the ash falls overlay on them. However, it is evidenced in the Kiwira area that the Lake Rukwa Rift and the Usangu Escarpment are partly rejuvenated very recently. In other words, the fractures and the minor faults of the U- and R-direction were formed or reactivated after the latest ash falls. To summarize the tectogenesis of the Mbeya area in recent ages, fractures and faults of the Usangu and the Buhoro Escarpments, the Lake Rukwa Rift, and the Lake Nyasa Rift, all of which characterize the present topography of this area, were formed along with fall of the latest ash accompanying rejuvenation or reactivation of some of the fractures and faults.

In the Irambo and the Kiwira area, the older lava flow and older tuff are cut by faults trending the U-, R- and N-directions. Furthermore, as is clearly observable in the Lake Nyasa Rift area, the present topography shows that the northern extension of Lake Nyasa was subsided after the Tertiary volcanic formations filled the faulted trough. Although there are found rising peaks of the late Tertiary or Quarternary Volcanic cones, it is doubtless that fractures and faults of the N-direction or the Lake Nyasa Rift, of the U-direction or the Usangu Escarpment and of the R-direction or the Lake Rukwa Rift were formed after the older volcanic activity and before the younger pumice ash. The exact age of these movements is unknown, and supposedly it might be late Tertiary to early Pleistocene.

All of the movements mentioned above are thought to be rather of subsidiary nature, and the greatest events happened probably in the early Miocene. At that time, the Lake Nyasa Rift and related trough were produced in the southeastern part of the Mbeya area. To the west and southwest of the Kipengere Mountain, Precambrian rocks emerge under volcanic formations and they represent a remnant of a basal part of the faulted trough. Though no geological evidence is found, it is highly probable that a part of the Lake Rukwa Rift and the Usangu Escarpment were produced together with formation of the Lake Nyasa Rift. Thus, an intensive volcanism occurred in the Mbeya Crux pouring trachytic, phonolitic and basaltic lavas into the trough. Tectogenesis of this time was the most conspicuous one in the Mbeya area in magnitude and in nature, and it was also traceable not only to all over the African Rift Valley but to the Red Sea and Dead Sea Rift (Girdler [5], Quenell [20]). Formation of the Rift Valley in the Miocene age is characterized by its intensiveness and world-wide nature; this fact suggests that the rift valley and the orogenic belt are genetically related with each other, its fundamental cause being attributed to the convection current underneath the crust (Matsuzawa [19]).

Judging from geological, lithological and petrographical properties of the Cretaceous system in the Mbeya area, it follows: The sedimentary basin of the system should be an elongated one in shape almost parallel to the Lake Rukwa Rift and to the Lake Nyasa Rift, clastic materials trapped in this basin were transported in relatively short distance from surrounding Precambrian basement, and paleocurrent direction suggests the localized variable drainage system. These facts imply that birth of the Cretaceous basin was controlled by a tectogenic movement producing the long strip of lowland area in which the Cretaceous clastic particles were laid down. The explanation of the apparent distribution of the Cretaceous system lies in an assumption that the birth of the Lake Rukwa Rift and the Lake Nyasa Rift can be traced back to the Cretaceous age. Similar interpretation is possible for the sedimentation of the Karroo system in this area, because the areal distribution of the Karroo sediments is also limited in an elongated area along the Lake Rukwa Rift and

the Lake Nyasa Rift. It is quite unknown whether the rift or the faulted trough took the same shape as the present rift valley at the Cretaceous or the Karroo time. But it is very likely that the tectonic lineament of the Rukwa and Nyasa direction was already formed at the time of the Karroo sedimentation.

On the Proterozoic history, we can treat the Bukoban system and deformation structure as the late Precambrian record. According to Halligan [7], the Bukoban sedimentary rocks are distributed in long and narrow areas of the Tanzanian country from Lake Victoria to Lake Nyasa through Lake Tanganyika. The Bukoban geosyncline was, therefore, situated on the western rift of the Tanzanian Country or, at least, parallel to it, embracing the basement of the Archaeozoic complex. Its general spatial relation suggests that the fundamental block structure as stressed by Brock [3] was achieved at the Proterozoic era by birth of the Bukoban geosyncline. Tectonically, the assumption that gentle upwarping of the Tanzanian Anticlise supplied clastic materials into the Bukoban geosyncline which surrounded the Anticlise in the west is plausible for elucidation of the distribution of the Bukoban system in the Tanzanian country. In the Mbeya area, an extensive distribution of the system is found in the mountainous area east of the Lake Nyasa Rift. It forms a large basinal structure or gentle syncline, the axial trace of which runs almost in the direction of the Lake Nyasa Rift. On the other hand, the slumping structure is observed in the system at the northern part of the Kipengere Mountain, where the Gofio quartzite is folded and forms synclinal and anticlinal structure together with red slate. Here, we may consider that the Bukoban geosyncline probably occupied this part of the area, and the deformation of the Bukoban system was more or less governed by the tectogenic movement such that the resulting folding axes trended almost parallel to the present Lake Nyasa Rift. Namely, it may be said that even in the Proterozoic era the tectonic trend of the Tanzanian rift was prevailing and had an effect on deformation of the system as well as on birth of the Bukoban geosyncline.

To the northeast of Lake Nyasa, metamorphic complex of the Ukingan and Ubendian epoch occupies the Kipengere Mountain and the northern part of the Livingstone Mountain. This metamorphic complex trends in the main northwesterly parallel to the Lake Nyasa Rift. In fact, one of the main faults bordering the northeastern escarpment of the Lake Nyasa Rift is nothing but a bedding fault in the foliated metamorphic rocks. It is said (Harkin and Harpum [8]) that an intense folding of the Bukoban system was accompanied by rejuvenated movement along many tectonic zones such as mylonite zones, sheared belts, and faults. However, the tectonic pattern of pre-Bukoban age had, at least in the Kipengere Mountain northeast of Lake Nyasa, almost the same attitude as the present one. This suggests that the Ukingan and/or the Ubendian metamorphism and granitization were generated probably along with shearing parallel to the Lake Nyasa Rift. Coincidence of the Precambrian foliation with

the rift structure is surely a basis of an argument that fundamental structure of the African Rift Valley may be attributed, above all, to the Archean diastrophism. Anyway, as is stressed by McConnel [17, 18], it is probable that a part of the Archean metamorphic zone was developed along a trend almost parallel to the present African Rift Valley.

SUMMARY

In the Mbeya area of the southern Tanzanian Country are distributed granitic and metamorphic complex of the Ubendian and the Ukingan epoch unconformably overlain by the Bukoban sedimentaries. These Precambrian rocks constitute the main part of mountainous area, namely, the Usangu, Mbozi, Poroto, and Kipengere mountains. The Lake Rukwa Rift and the Lake Nyasa Rift occupy the western and southern part of this area, and the depressions of these rifts forms the Mbeya Crux together with the Usangu Escarpment. Surrounded by the Buhoro and the Usangu Escarpment, the Buhoro Flats are situated in the northeastern part of the Mbeya area, whereas volcanic rocks of late Tertiary and Quaternary in age fill depression of the Lake Nyasa Rift north of Lake Nyasa.

The authors investigated geology of this area, especially the Kimani River area, Buhoro Flats, the Irambo area, a part of the Poroto and Kipengere mountains, and the Kiwira area. Among various structural features, they observed four remarkable fracture systems found in the Bukoban, Cretaceous, and Cenozoic volcanic rock formations as well as in the present topography of this area. They are those of the U-direction of the NNE–SSW trend represented by the Usangu Escarpment, the B-direction of the E–W trend by the Buhoro Escarpment, the R-direction of the NW–SE trend by the Rukwa Rift and N-direction of the NNW–SSE trend by the Nyasa Rift. From the sequential relation and areal development of these directions, the authors reached a conclusion as follows: 1) the N-direction was genetically related with, if not all, a part of the Ubendian and the Ukingan orogeny, and probably both of the N- and the R-direction were generated by accompanying the Ubendian orogeny and by rejuvenation at the Ukingan epoch; 2) birth and development of the Bukoban geosyncline and ensuing deformation were connected with reactivation of the Ubendian and the Ukingan belt in the Western Tanzanian Rift Valley; 3) commenced at the Precambrian age, these rift zone was, thereafter, spasmodically and intermittently active at the Karroo and the Cretaceous age; 4) tectogenic movement of the Lake Nyasa Rift and the Lake Rukwa Rift was most intense at the Miocene age and the volcanic activity of the Rungwe and others occurred together with the tectonic framework of the U- and the B-direction. It was probably a time of block-faulting of the Tanganyika Shield; 5) very recently, all of the directions mentioned above

became active again and the present topography was formed. Minor modification after the latest pumice ash fall is also observed.

ACKNOWLEDGEMENTS

The authors are greatly indebted to Prof. Emeritus Dr. Isao Matsuzawa of Nagoya University for his leadership and encouragement given in all phases of this study. It was a experience of great delight to have such an opportunity to carry out the geological investigation of the Tanzanian Country. The authors express their sincere appreciation to many people in the Country, especially to Prof. Dr. D. G. Osborne of University College Dar es Salaam and to Dr. G. Luena of Mineral Resources Section of Tanzania at Dodoma, who gave the permission to stay and study in Tanzania. Their acknowledgements extend also to Mr. O. Marwa, Regional Commissioner of Mbeya, and Mr. W. Magurusa, Regional Mining Officer of Mbeya, who gave us many facilities during our stay in Mbeya. Ambassador M. K. Yoshida and the other members of Japanese Embasy in Dar es Salaam, Mr. K. Tomita, representative of Japanese Peace Corps in Dar es Salaam, Mr. T. Fujiwara, managing director of Blankets Manufactures Limited in Dar es Salaam and Miss M. Shirai and Miss I. Oda, Japanese Peace Corps in Mbeya, encouraged us throughout our research in this country; the authors would like to thank to all of them.

REFERENCES

[1] AOKI, H., Gravity measurements of rift valleys in Tanzania: *Jour. Earth Sci., Nagoya Univ.*, **17**, 169-188 (1969).

[2] BISHOP, W. W., MILLER, J. A., and FITCH, F. J., New potassium-argon age determinations relevant to the Miocene fossil mammal sequence in East Africa: *Am. Jour. Sci.*, **267**, 669-699 (1969).

[3] BROCK, B. B., The rift valley craton. The World Rift System: Geol. Surv. Canada, Paper **66-14**, 99-123 (1965).

[4] CAHEN, L. and SNELLING, N. J., The geochronology of equatorial Africa: North Holland Pub. Co., 195 pp. (1966).

[5] GIRDLER, R. W., The relationship of the Red Sea to the East African Rift System: *Quart. Jour. Geol. Soc. London*, **114**, 79-102 (1958).

[6] GRANTHAM, D. R., TEALE, E. O., SPURR, A. M. M., HARKIN, D. A., and BROWN, P. E., Quarter degree sheet No. 70 S. W. "Mbeya": Geol. Surv. Tanganyika, 1 : 125,000 (1958).

[7] HALLIGAN, R., The Proterozoic rocks of western Tanganyika: *Geol. Surv. Tanganyika, Bull.*, No. 34, 34 pp. (1962).

[8] HARKIN, D. A. and HARPUM, J. R., Quarter degree sheet No. 78 N. E. "Tukuyu": Geol. Surv. Tanganyika, 1 : 125,000 (1957).

[9] HARPUM, J. R., Quarter degree sheet No. 79 N. W. "Kipengere": Geol. Surv. Tanganyika, 1 : 125,000 (1958).

[10] —— and BROWN, P. E., Quarter degree sheet No. 71 S. W. "Chimala": Geol. Surv.

Tanganyika, 1 : 125,000 (1958).

[11] KENNERLY, J. B., TEALE, E. O., and EADES, N. W., Quarter degree sheet No. 229 "Shoga": Geol. Surv. Tanganyika, 1 : 125,000 (1962).

[12] ——, SPENCE, J. and SPURR, A. M. M., Quarter degree sheet No. 243, "Itaka": Geol. Surv. Tanganyika, 1 : 125,000 (1963).

[13] MACFARLANE, A., BROCK, P. W. G., and SPURR, A. M. M., Quarter degree sheet No. 257, "Tunduma": Mineral Res. Div. Tanzania, 1 : 125,000 (1966).

[14] ——, HARKIN, D. A., HORNE, R. G., and SPURR, A. M. M., Quarter degree sheet No. 258 & 258 S. "Itumba": Mineral Res. Div., Tanzania, 1 : 125,000 (1966).

[15] ——, MACDONALD, A. S., GRANTHAM, D. R., and SKERL, A. C., Quarter degree sheet No. 227 "Luika": Geol. Surv. Tanzania, 1 : 125,000 (1964).

[16] ——, MUDD, G. C., ORRIDGE, G. R., TEALE, E. O., EADES, N. W., and GRANTHAM, D. R., Quarter degree sheet No. 228 "Makongolosi": Geol. Surv. Tanganyika, 1:125,000 (1963).

[17] MCCONNELL, R. B., The East African Rift System: *Nature*, **215**, 578-581 (1967).

[18] ——, The association of granites with zones of stress and shearing: *Geol. Soc. Am. Bull.*, **80**, 115-120 (1969).

[19] MATSUZAWA, I., A study on the formation of the African rift valley: *Jour. Earth Sci., Nagoya Univ.*, **14**, 89-115 (1966).

[20] QUENNELL, A. M., The structural and geomorphic evolution of the Dead Sea Rift: *Quart. Jour. Geol. Soc. London*, **114**, 1-24 (1958).

[21] SUWA, K., OSAKI, M., OANA, S., SHIIDA, I., and MIYAKAWA, K., Isotope geochemistry and petrology of the Mbeya carbonatite, south-western Tanzania, East Africa: *Jour. Earth Sci., Nagoya Univ.*, **17**, 125-168 (1969).

[22] TEALE, E. O., EADES, N. W., HARKIN, D. A., HARPUM, J. R., and HORNE, R. G., Quarter degree sheet No. 245 "Irambo": Geol. Surv. Tanganyika, 1 : 125,000 (1962).

[23] YAIRI, K. and MIZUTANI, S., Fault system of the Lake Tanganyika Rift at the Kigoma area, western Tanzania: *Jour. Earth Sci., Nagoya Univ.*, **17**, 71-96 (1969).

PLATE I

FIG. 1. Fractures with E-W trend (Buhoro direction) developed in the Bukoban Gofio quartzite near a bridge of Great North Road over the Kimani River (Photo by S. M., 4 X 1968).

FIG. 2. Two sets of nearly vertical fractures with E-W trend (Buhoro direction) and with NNW-SSE trend (Nyasa direction) in the Bukoban green slate at an exposure west of upper reaches of the Kimani River (Photo by S. M., 27 IX 1968).

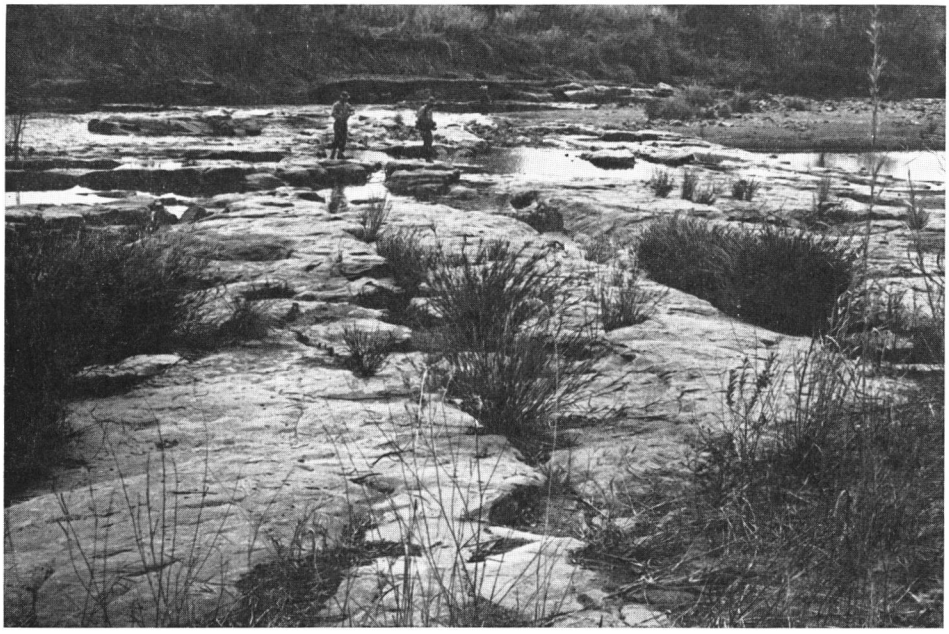

FIG. 1

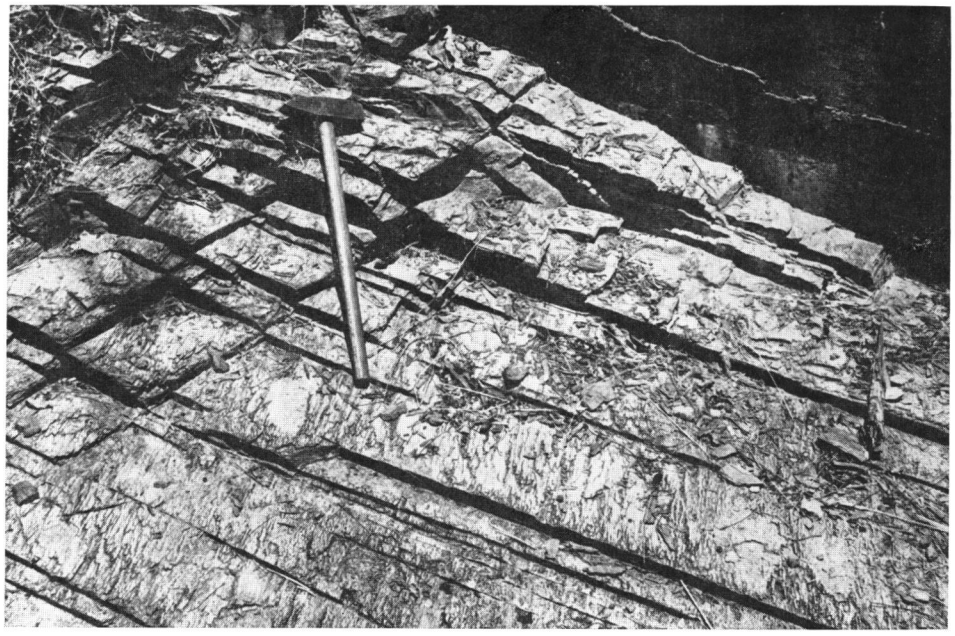

FIG. 2

PLATE II

FIG. 1. Fractures with E-W trend (Buhoro direction) in the Bukoban red slate along Great North Road near the Kimani River (Photo by K. Y., 25 IX 1968).

FIG. 2. Fractures and minor faults with E-W trend (Buhoro direction) in the Bukoban red slate along Great North Road near the Kimani River (Photo by S. M., 25 IX 1968).

FIG. 1

FIG. 2

PLATE III

FIG. 1. Faults with N-S trend (Nyasa direction) in the Tertiary volcanics along Great North Road about 25 miles east of the Mbeya town (Photo by S. M., 4 X 1968).

FIG. 2. Thin blanket of recent clay and silt covering pumice ash deposits in the Buhoro Flats. (Photo by S. M., 1 X 1968).

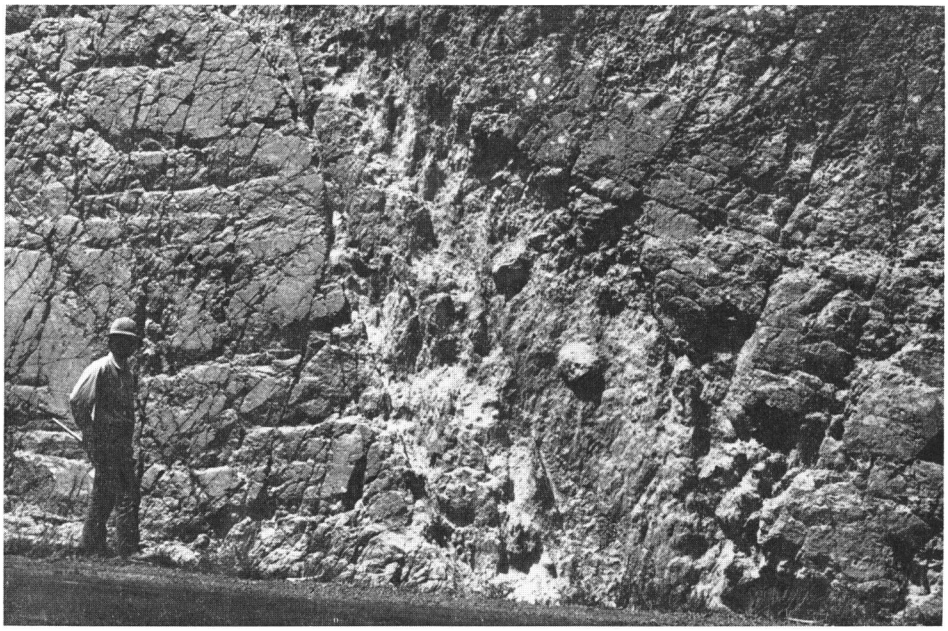

FIG. 1

FIG. 2

PLATE IV

FIG. 1. Synsedimentary minor folding in the Bukoban red slate at the northern part of Kipengere Mountains (Phcto by S. M., 3 X 1968).

FIG. 2. Anticline of the Bukoban Gofio quartzite with NNW-SSE trend at the northern part of Kipengere Mountains (Photo by K. Y., 3 X 1968).

FIG. 1

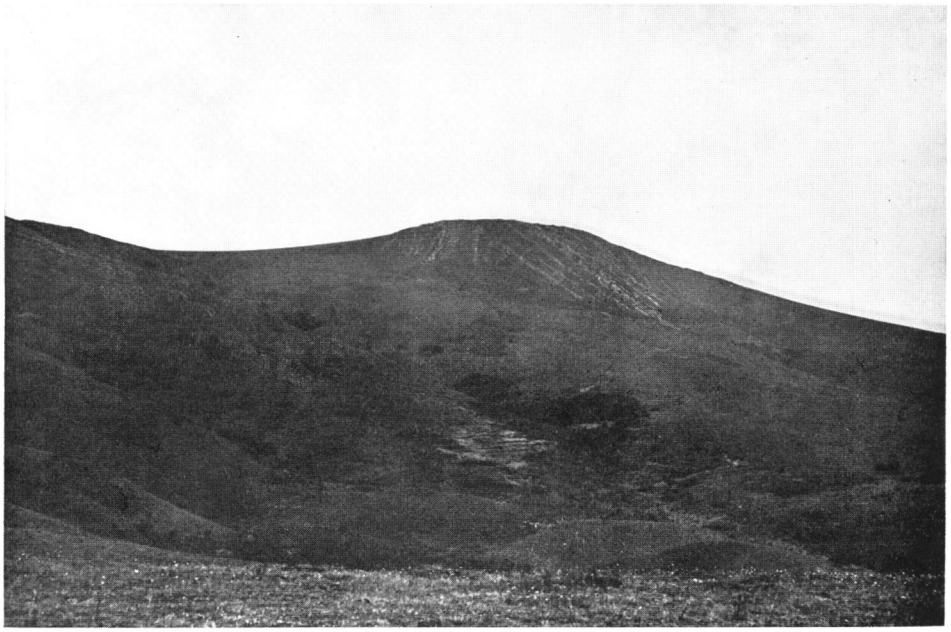

FIG. 2

PLATE V

FIG. 1. Gently dipping ash layers laid down on an ancient slope at the northwestern part of Kipengere Mounains (Photo by S. M., 3 X 1968).

FIG. 2. Layering of ash beds laid down on an uneven surface at a cutting between Tukuyu and Mbeya (Photo by S. M., 18 IX 1968).

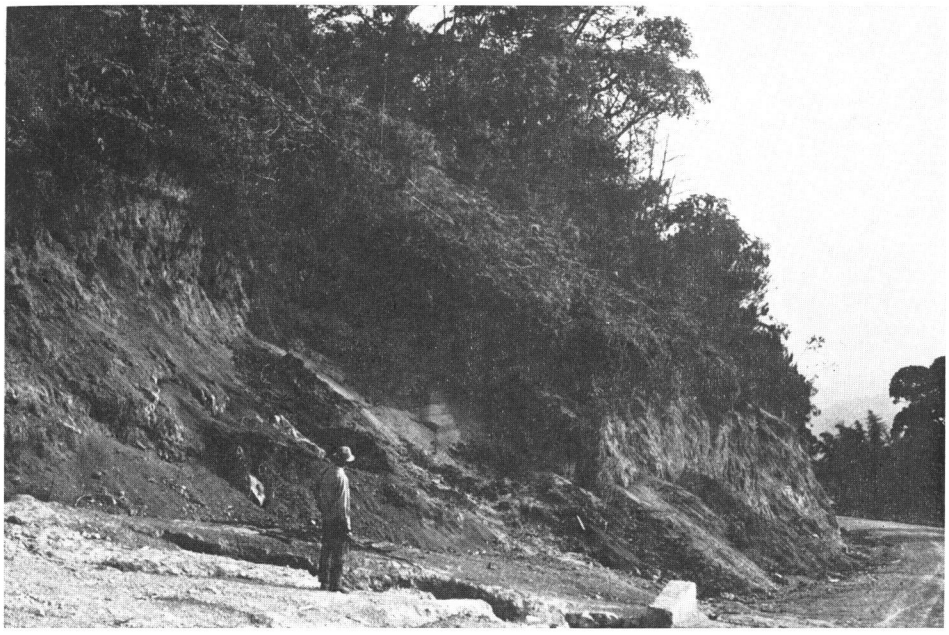

FIG. 1

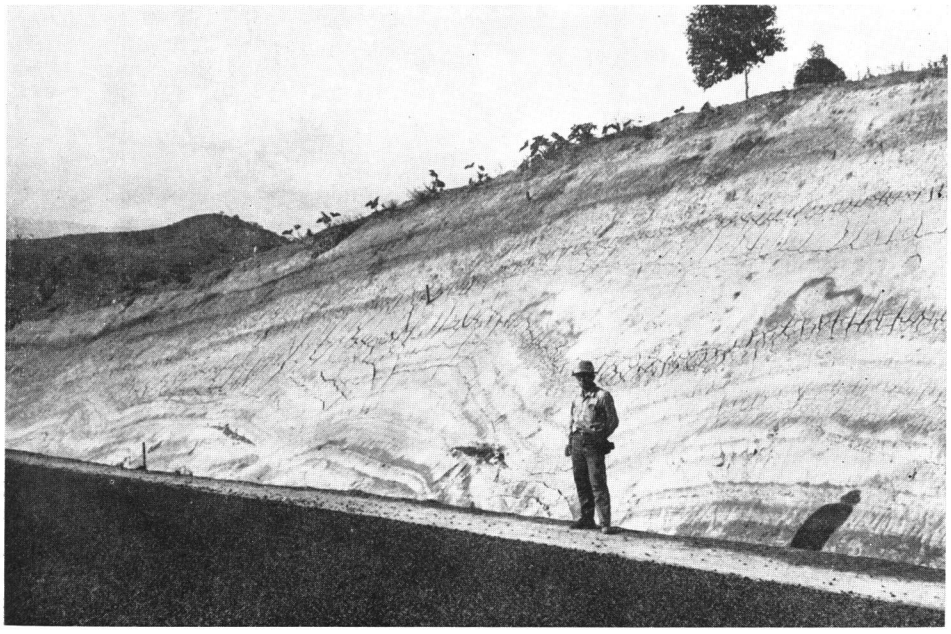

FIG. 2

Isotope geochemistry and petrology of the Mbeya carbonatite, south-western Tanzania, East Africa

Kanenori SUWA*, Susumu OSAKI*, Shinya OANA*,
Isao SHIIDA** and Kunihiko MIYAKAWA***

* *Department of Earth Sciences, Faculty of Science, Nagoya University*
** *Department of Geology, College of General Education, Nagoya University*
*** *Department of Earth Sciences, Nagoya Institute of Technology*

(Received 5 December 1969)

ABSTRACT

The Mbeya carbonatite (Panda Hill and Sengeri Hill) is located near the south-west border of Tanzania, and is Cretaceous in age. The Panda Hill sövitic carbonatite mass has a crudely circular outcrop with a maximum diameter of 1.8 km and consists of a central plug and an outer ring. It was emplaced in Precambrian gneisses and is surrounded by a fenitized and shattered zone. At Sengeri Hill, beforsitic carbonatite dikes cut fenitized Precambrian gneisses.

The carbonatite samples examined include sövite (4), beforsite (2), carbonatitic pseudotrachyte-breccia (1), carbonatitic mixed-breccia (1), and carbonatized pseudotrachyte (1). The petrography and mineralogy of these carbonatites are fully described in order to elucidate the geochemical behaviour of carbon and oxygen isotopes and petrogeny.

Thirty-three carbonate samples (20 calcites and 32 dolomites) from these carbonatites were analysed isotopically. The δC^{13} value of calcites ranges from -5.3 to $+3.1‰$ and that of dolomites from -5.6 to $+1.2‰$. The δO^{18} value of calcites ranges from 5.9 to 25.5‰ and that of dolomites ranges from 6.0 to 24.1‰. The data lie in a wide range, but show some regularities:

(1) There is a hiatus in δO^{18} values between 9.7 and 11.8‰ for the carbonates. Thirteen out of 20 calcites and 5 out of 32 dolomites are enriched in O^{18} and these are altered and/or formed in relation to one or more cycles of younger hydrothermal activity, brecciation and mixing accompanied by explosive activity, opaque mineral concentration, and weathering. This shows also that δO^{18} of calcite is easily affected but that of dolomite is hardly affected by alteration.

(2) Twelve dolomites lie in the field high in δC^{13} and low in δO^{18}. No calcites are found in this field. These dolomites are affected by a later stage of alteration and frequently coexist with barite and/or fluorite. A process which involves enrichment only in C^{13} may not be possible without contamination and/or thermal effect after hydrothermal alteration.

(3) Five calcites and 15 dolomites lie in a small field low in δO^{18} (from 5.9 to 7.7‰) and low in δC^{13} (from -3.6 to $-5.3‰$) All 5 calcites came from unaltered sövite. Eleven out of 15 dolomites are from unaltered sövite and beforsite, and 4 dolomites are considered to be related to later hydrothermal alteration though

they appear to be practically unaffected by hydrothermal alteration.

A field considered to represent primary Mbeya carbonatite is delineated in Fig. 17. It is similar in δO^{18} and a few per mil higher in δC^{13} compared with the probable field of primary igneous carbonatite proposed by Taylor *et al.* (1967).

(4) Two calcites lie in the field low in δC^{13} and slightly high in δO^{18}. Carbonates coexisting with abundant metal oxides become enriched in δO^{18}.

(5) The isotope ratios of primary Mbeya carbonatitic carbonates are substantially different from those of sedimentary carbonates, and it is difficult to imagine a natural process (*e.g.* assimilation) which would change the isotope ratios of sedimentary carbonates to those of carbonatitic carbonates.

(6) The oxygen isotope ratios of carbonatitic carbonates can be explained by the assumption that the carbonatitic magma originated by partial melting or fractional crystallization from a primary mafic or ultramafic magma in the lower crust or upper mantle.

(7) The fractionation factors of oxygen isotope between the coexisting calcites and dolomites in the primary Mbeya carbonatite range from 0.1 to 0.6‰, suggesting that the carbonates crystallized at temperatures above 400°C.

(8) δC^{13} of diamonds are almost identical to those of carbonatitic carbonates. If diamonds are similar in δC^{13} to the material in the lower crust or upper mantle, δC^{13} of carbonatitic carbonates indicates that carbonatitic magma may be formed at temperatures above 1,000°C.

(9) δC^{13} of diamonds and carbonatitic carbonates from Africa, including Mbeya, is higher than values obtained from other regions, *e.g.* Siberia. This is perhaps indicative of heterogeneity in the lower crust or upper mantle, and of characteristic of an African setting.

INTRODUCTION

The African rift valleys form part of a world-wide fracture zone, extending from the Red Sea and Gulf of Aden through Ethiopia, Kenya, Uganda, Rwanda, Burundi, Tanzania, Malawi and Mozambique to the Indian Ocean to link up with the mid-oceanic ridges, whose median parts are often occupied by similar structures. Various evidences suggest a tensional origin for the rift valleys.

The pattern of alkaline igneous activity shows a remarkable correspondence to the rift pattern, and may probably be ascribed to the same major process. The occurrence of carbonatites is perhaps the most striking petrological feature found in the region of the Rift System. The Mbeya carbonatite, which is the subject of the present paper, is close to the junction of the Western and Eastern rifts near the south-western border of Tanzania.

The carbonatites have at one time or another been suggested to be igneous differentiates, melted or altered limestones, plastic intrusion of limestone caused by crustal movement, and/or deposits from hydrothermal solutions.

The field evidence that many carbonatites are intrusive and possibly

magmatic was generally considered to be incompatible with available experimental data until Wyllie and Tuttle [37] demonstrated that liquids in the system CaO-CO_2-H_2O precipitate calcite at temperatures down to 640°C through a wide pressure range. At about that time, the active volcano Oldoinyo Lengai (meaning Mountain of God in the Masai language, altitude 9,650 feet) in the Gregory Rift 10 miles south of Lake Natron in Tanzania, yielded lavas rich in alkali carbonate (lengaite) during the eruption of October 1960 [8], and thus became one of the outstanding items of field evidence of igneous carbonatite activity.

Recently several additional experimental studies on systems more complex than CaO-CO_2-H_2O have been undertaken in efforts to elucidate two problems: the physical and chemical nature of carbonatite magmas, and the petrogenetic relationships between carbonatites and associated alkalic igneous rocks. Reviews of the experimental results so far obtained were published recently [36] and at the same time two books on carbonatites, which review the various hypotheses for the origin of carbonatites and describe the field occurrence of almost all the known carbonatites of the world, were published [17, 30]. Furthermore, there has been increasing awareness in recent years of possible genetic links between kimberlites and carbonatites [34]. Recent experimental studies on carbonatites have been extended to pressures corresponding to conditions in the upper mantle, where kimberlites probably originate [38].

On the other hand, in recent years oxygen isotope studies have been made on a variety of igneous rocks and minerals, and determinations have been made of equilibrium constants for oxygen isotopic exchange among certain minerals at high temperatures. The general principles of isotopic fractionation at magmatic temperatures and of isotopic variations during crystallization are fairly well understood. These previous investigations provide a background for further detailed studies on carbonatites whose origin is a subject of controversy. Previous isotopic studies of C^{13}/C^{12} and/or O^{18}/O^{16} in carbonatites were carried out by Von Eckermann *et al.* [34], Baertschi [1], Vinogradov *et al.* [33], Taylor *et al.* [29] and others. Recent detailed studies of O^{18}/O^{16} and C^{13}/C^{12} on unaltered carbonatites and related rocks by Taylor *et al.* [29] deal not only with carbonates but also with associated silicate minerals from, in particular, the Laacher See. They show the uniformity of O^{18}/O^{16} (6.0 to 8.5‰) and C^{13}/C^{12} (-5.0 to -8.0‰) in the Laacher See carbonatite, indicating that it is a primary igneous carbonatite. Those carbonatites and related rocks, however, are not found as an intrusive or extrusive mass but as ejectites (bombs) in the Selbergit Tuff located on the margin of the Riedener Kessel.

In the present study, we set out to elucidate in detail the O^{18}/O^{16} and C^{13}/C^{12} variations in the various kinds of carbonatites of the Mbeya region, *e.g.* sövite, beforsite, carbonatitic pseudotrachyte-breccia, carbonatitic mixed-breccia and carbonatized pseudotrachyte; to elucidate these variations in rocks

which have been subjected to various kinds of alteration, *e.g.* younger hydrothermal alteration, brecciation and mixing accompanied by explosive activity, opaque mineral concentration, and weathering; to determine the conditions of formation of the Mbeya carbonatite; and to come to firm conclusions about the ultimate origin of carbonatite.

The field evidence that the Mbeya carbonatite is intrusive and probably magmatic is fully accepted, and both the geology and mineralogy on the Mbeya carbonatite are probably much better known than those of any other African carbonatite. In considering the isotope ratios of primary igneous carbonatite, such established field evidence is most important. The petrography and mineralogy of the carbonatites are fully described in order to elucidate the geochemical behavior of carbon and oxygen isotopes and petrogeny. The carbonatite samples examined were collected by Shiida, Suwa and Miyakawa during our second scientific expedition to Africa in 1968, organized by the Association for African Studies of Nagoya University. Studies of the petrography and mineralogy were chiefly carried out by Suwa, and measurement of oxygen and carbon isotopes was performed by Osaki and Oana with a mass spectrometer at the Institute for Thermal Spring Research, Okayama University. The isotope geochemistry and petrology have been discussed by all the present authors.

GEOLOGICAL SETTING OF THE MBEYA CARBONATITE

A. Carbonatites in Tanzania

The carbonatites of Tanzania are grouped geographically under the headings northern, eastern, and southwestern.

a) Northern Tanzania represents the southern end of the extensive lava fields associated with the Eastern (Gregory) Rift. In the northern Tanzania volcanic field, two petrologic types of volcanoes occur: trachytic (*e.g.* Lemagrut and Olomoti) and nephelinitic-carbonatitic (*e.g.* Oldoinyo Lengai, Malanja, Oldoinyo Dili, Kerimasi and Mosonik). All except Oldoinyo Dili are of the same age range (Pliocene-Pleistocene), and the two types belong to the same volcanic cycle.

b) In eastern Tanzania, carbonatites occur at Wigu Hill, Maji Ya Weta, and Luhombero and Pangani Gorge of Morogoro District. The Wigu Hill carbonatite is characterized by an unusually high concentration of rare earth minerals.

c) In southwestern Tanzania near the northern end of Lake Malawi (formerly Lake Nyasa), carbonatites occur at Sangu, Ngualla, Songwe Scarp, Musensi, Mbulu, Mbeya (Panda Hill and Sengeri Hill), Nachendezwaya and Nankwale as shown in Fig. 1. Here also the Rungwe volcanic field (alkali basalts and related lavas) is situated on the junction of the Western and Eastern Rifts. The Songwe Scarp and Musensi Hill carbonatites are both

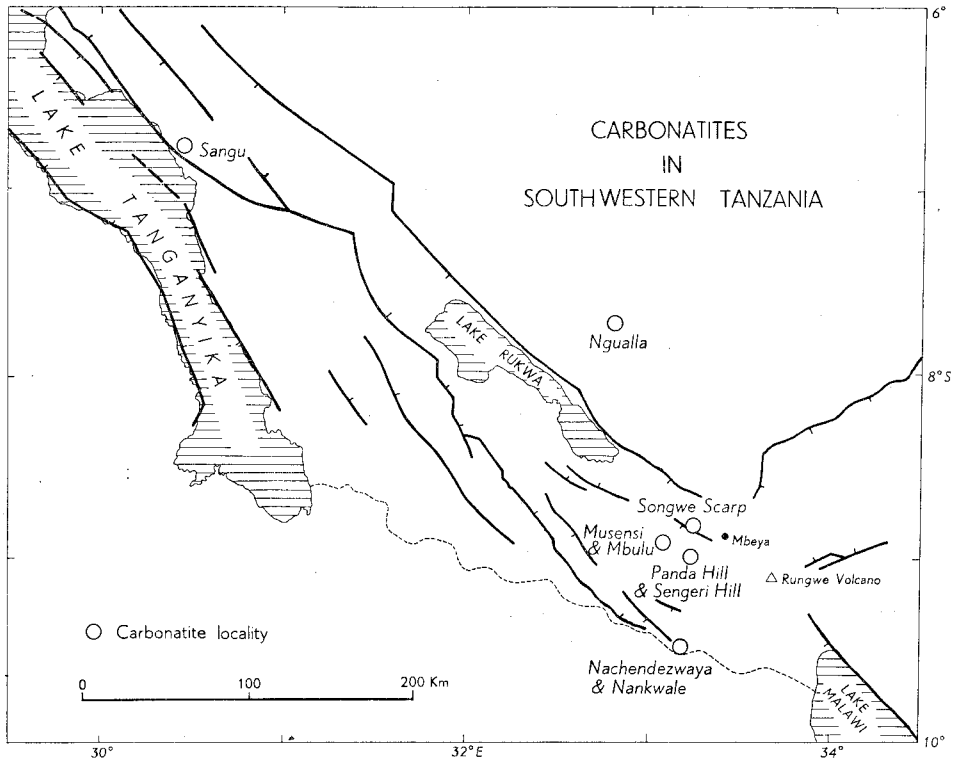

FIG. 1. Carbonatites in southwestern Tanzania.

Cretaceous in age, according to a K-Ar age determination on the feldspar and the biotite respectively [20]. The Mbeya carbonatite is on the edge of the Rukwa trough. Dating of the Mbeya carbonatite depends on the age interpretation of sediments that truncate a carbonatite dike. Fawley and James [10] regarded the carbonatite as probably Jurassic or early Cretaceous in age; Fick and Van der Heyde [11] concluded that the carbonatite is older than a pre-Cretaceous sedimentary formation and younger than doleritic dikes of assumed pre-Karroo age. According to a K-Ar age determination on the phlogopite, the Panda Hill carbonatite is Upper Cretaceous in age (113±6 m.y.) [26]. Age determinations have also been made by the uranium-lead method on two samples of pyrochlore from the Panda Hill carbonatite complex by Schurmann, *et al.* (cited by [26]). The ages as calculated are discordant, and range from 68 to 273 m.y. These same two pyrochlore samples, which can safely be assumed to be of the same age, were analysed later by Snelling [26]. Snelling's results are still discordant and range from 73 to 185 m.y. and he considered that one or both of these pyrochlores have suffered chemical alteration, and that no other geological significance can be attached to these results.

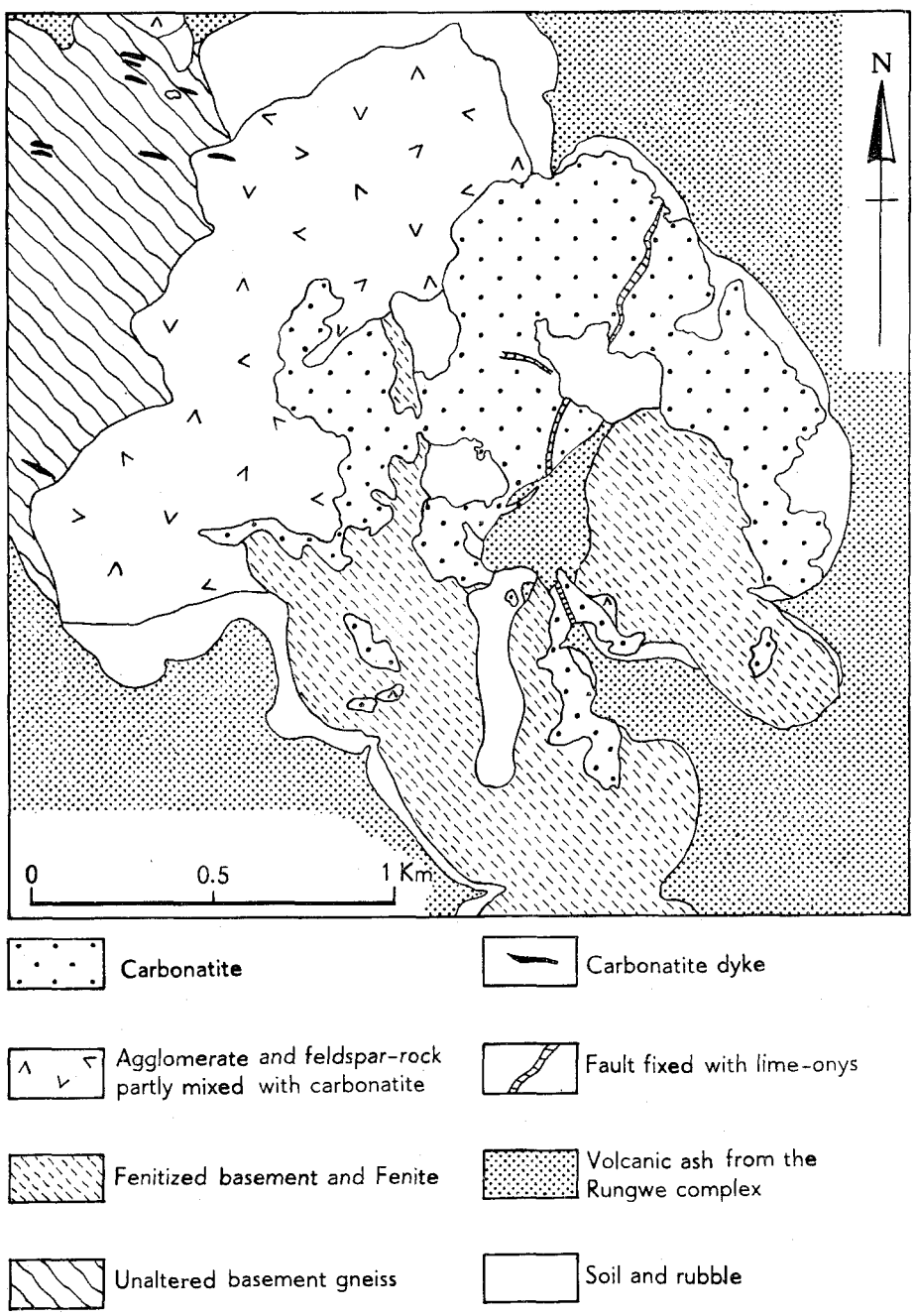

FIG. 2. Geological Map of the Panda Hill carbonatite (According to Fawley and James, 1955; and Fick and Van der Heyde, 1959). "Fault fixed with lime-onys" should read "Fault fixed with lime-onyx".

B. Mbeya Carbonatite (Panda Hill and Sengeri Hill)

a) Panda Hill

The Panda Hill carbonatite is near the south-west border of Tanzania about 20 km west-southwest of Mbeya at latitude 8°59′ S and longitude 33°14′ E. It is crudely circular with a maximum diameter of 1800 m and consists of two units rising respectively 330 and 270 m above the floor of the Rukwa trough (Fig. 1, 2 and 3). The carbonatite mass, consisting of an outer ring and a central plug, was emplaced in Precambrian gneisses and is surrounded by a zone of fenitized and shattered gneisses. The Precambrian rocks are predominantly garnet-bearing augen gneisses and banded gneisses. Structurally they may be characterized by one major plane of fissility parallel to the banding of the augen gneiss with a northwesterly strike and a dip to the southwest of around 45°. In the fenitized zone, alteration of garnet into phlogopitic pseudomorphs, decrease in quartz content, hydration of feldspar, formation of microperthite, growth of orthoclase and infiltration of calcitic or dolomitic carbonates can be observed. Bodies of feldspathic breccia (carbonatitic pseudotrachyte-breccia) sometimes intervene between the central plug of carbonatite and the surrounding fenites. The breccia fragments consist of altered basement gneiss, potassium feldspar and pseudotrachyte, locally scoriaceous. The fine-grained matrix is carbonatitic, but locally feldspathic, or siliceous.

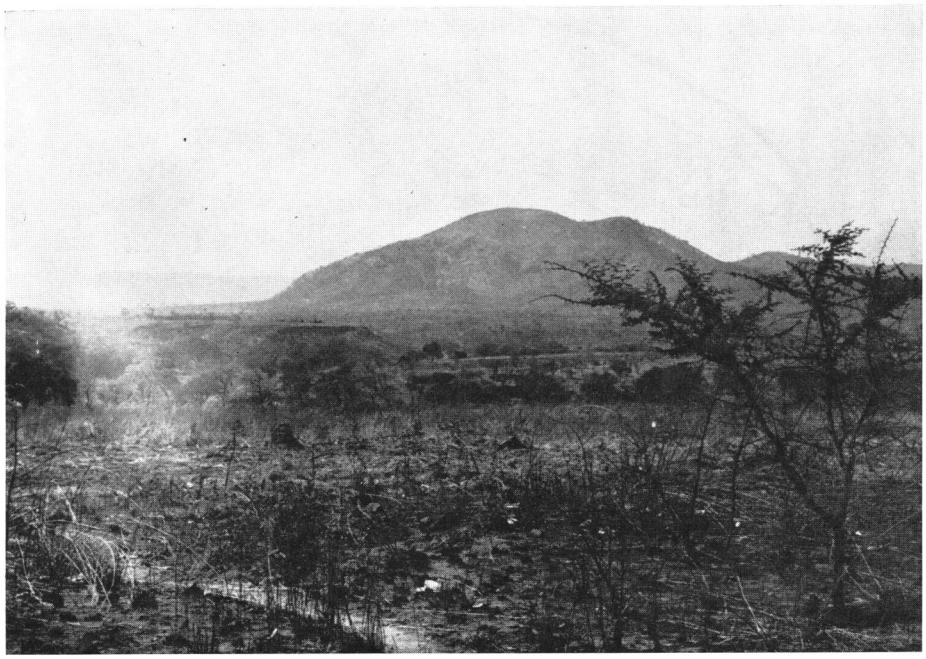

FIG. 3. Panda Hill (lat. 8°59′ S., long. 33°14′ E.) in the background, the floor of the "Rukwa Trough" rift valley in the foreground (Photo. by K. Suwa, Sept. 25, '68).

FIG. 4. Sövite with a well-defined flow feature marked by apatite-rich and magnetite-rich streaks. Eastern part of Panda Hill carbonatite (Photo. by K. Suwa, Sept. 23, '68).

The plug of carbonatite is a white sövite (calcitic carbonatite) with a well-defined flow feature, which in the peripheral parts tends to be more or less parallel with the contacts, but in the centre shows little regularity or continuity. The flow feature is marked by apatite-rich and magnetite-rich streaks (Fig. 4), having a steep inward dip at 85 degrees. The flow lines in the carbonatite suggest that the magma was plastic at least during the later stage of emplacement. At the eastern contact many xenoliths of Precambrian gneisses occur in the carbonatite. Flow features bend around these xenoliths which are altered to fine-grained feldspar in a phlogopite-calcite matrix. At

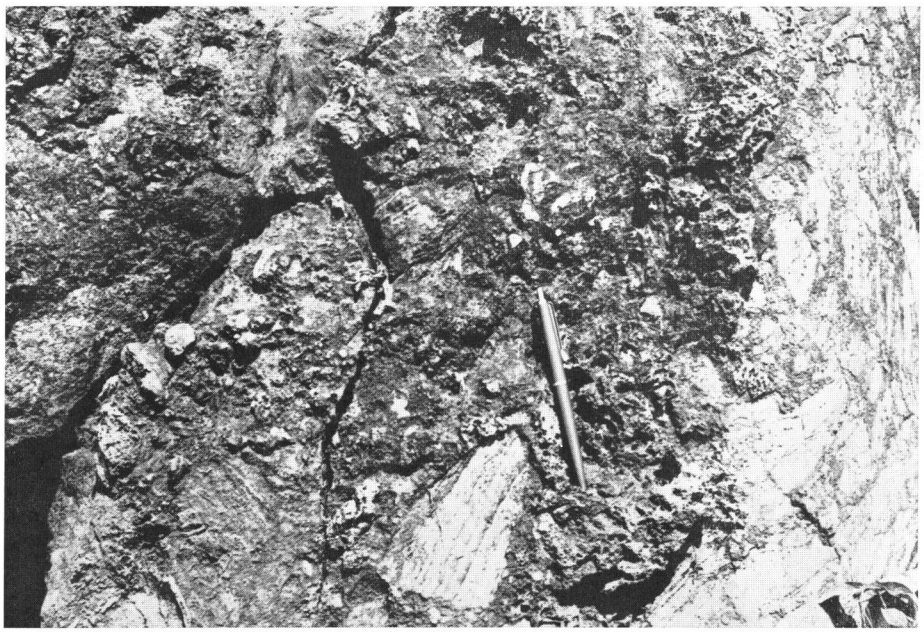

FIG. 5. Ochreous carbonatitic mixed breccia. Eastern part of Panda Hill carbonatite (Photo. by K. Suwa, Sept. 23, '68).

the northern and western contacts the carbonatite is separated from the gneisses by feldspathic agglomerate as shown in Fig. 2. The agglomerate and breccia do not represent ejected fragments formerly rolled down a slope of a crater-rim, but are intrusive and intimately related to the carbonatite. As will be described later, this agglomerate and breccia are carbonatitic mixed-breccia or pseudo-trachyte-breccia.

The carbonatite is dominantly calcitic, but it frequently contains some dolomite. A chemical and spectrographic assay of the average carbonatite from the centre of the plug is: SiO_2 5.1, TiO_2 0.60, Al_2O_3 0.78, Fe_2O_3 5.8, FeO 1.5, MnO 0.60, MgO 3.8, CaO 40.5, SrO 0.33, BaO 0.20, Na_2O 0.1, K_2O 0.1, Nb_2O_5 0.32, P_2O_5 4.2, CO_2 31.9, F 1.2, H_2O +1.2, ZrO_2<0.1 [11].

Fine-grained dolomitic carbonatite, which occurs as dikes and irregular masses commonly intersecting sövite flow lines, contains more quartz and fluorite but less magnetite and apatite than sövite. Some of the gray dolomitic dikes are in turn transected by narrow dikelets of white aphanitic carbonatite. Carbonatized alnöitic dikes transect sövite in several places. Segregations of ankerite, siderite, and manganese carbonates also occur. Fluoritic replacements are widely distributed, some being localized along very fine fractures and along margins of dolomitic lenses.

The presence of a rauhaugite (massive dolomitic carbonatite) body at

depth is indicated at the north-central part.

The pyrochlore shows various types of alteration: alteration to pandaite (Ba-Sr-pyrochlore), alteration to fersmite, and replacement by columbite marginally and along cracks. Carbonatite that contains the altered pyrochlores shows various extensive deuteric changes: dolomitization, corrosion and replacement of biotite and alkali amphibole by carbonate-limonite-quartz mixtures, replacement of large siderite grains by quartz and platy limonite, development of abundant secondary quartz, some in veinlets, and alteration of magnetite by quartz-carbonate-leucoxene.

The three larger explosion vents are situated along a remarkably straight line trending NNW-SSE. This is the general direction of the Western rift valley faulting and the vents may be situated along one of these fractures. Several faults contain banded fillings of secondary calcite ("lime-onyx").

b) *Sengeri Hill*

Sengeri Hill is 6 km northwest of Panda Hill. Two large and numerous small carbonatite dikes trending NE-SW cut fenitized Precambrian gneisses. These carbonatites are dolomitic, the principal accessory minerals being pyrite, magnetite, pyrochlore and barite.

There are numerous dikes of carbonatite suite between Sengeri Hill and Panda Hill and to the southeast of Panda Hill. They are less than one metre wide, have chilled margins, altered xenoliths, and are flow-banded parallel to their walls. Fluorite veins and quartz veins crosscut some of the smaller dikes. In their vicinity Precambrian gneiss has been completely kaolinized. In the same area as the dikes there are small explosion vents along a NW-trending line parallel to the main rift faulting. These are filled with a breccia made up of highly altered angular and rounded fragments of the Precambrian gneiss in a carbonate matrix.

PETROGRAPHY OF THE MBEYA CARBONATITE

The carbonatite samples examined were collected from the eastern part of the Panda Hill carbonatite area and from the southern part of the Sengeri Hill area. They include four sövites, two beforsites, one ochreous carbonatitic pseudotrachyte-breccia, one ochreous carbonatitic mixed-breccia and one carbonatized pseudotrachyte.

2-68092301 : Sövite, Panda Hill (Fig. 6: 01-A, 01-B)
2-68092302 : Sövite, Panda Hill (Fig. 7: 02-A, 02-C)
2-68092303 : Sövite, Panda Hill (Fig. 8: 03-A, 03-B)
2-68092304 : Sövite, Panda Hill (Fig. 9: 04-A, 04-B, 04-D, 04-E)
2-68092305 : Ochreous carbonatic mixed breccia, Panda Hill (Fig. 10: 05-A, 05-F, 05-G, 05-H, 05-I)
2-68092306 I: Beforsite, Panda Hill (Fig. 11: 06 I-A, 06 I-A″, 06 I-C,

06 I-D, 06 I-E)
2-68092306 II: Beforsite, Panda Hill (Fig. 12: 06 II-A, 06 II-A′, 06 II-A″)
2-68092307 a: Carbonatized pseudotrachyte, Panda Hill (Fig. 13: 07 a-D, 07 a-L, 07 a-M, 07 a-N)
2-68092307 b: Carbonatized pseudotrachyte, Panda Hill (Fig. 14: 07 b-A, 07 b-D, 07 b-M, 07 b-N)
2-68092310 : Ochreous carbonatitic pseudotrachyte breccia, Sengeri Hill (Fig. 15: 10-D, 10-J, 10-K)
2-68092311 : Beforsite with small amounts of orthoclasite and pseudotrachyte, Sengeri Hill (Fig. 16: 11-A, 11-A′)

Photographs and sketches near natural size of these samples and their mineral assemblages are shown in Figs. 6-16. From thirty-three parts (*e.g.* A, B, C, etc.) of these carbonatite samples carbonate samples were picked out and twenty calcites and thirty-two dolomites were analysed isotopically.

For brevity, the following abbreviations of specimen number shown on the figures are used: *e.g.* 01: 2-68092301, 07 a: 2-68092307 a.

In sövite specimens (01, 02, 03, and 04) from Panda Hill, Part A indicates white-coloured sövite with accessory dolomite, biotite, apatite, pyrochlore, magnetite and hematite; PartB is pale brown-coloured sövite having a streak of apatite-zoned pyrochlore-hematite-magnetite, with accessory dolomite, biotite, amphibole; Part C is brown-coloured sövite rich in magnetite and pyrochlore, with accessory amphibole, dolomite, apatite and pyrite; Part D is a white-coloured late calcite veinlet; Part E is a fine-grained creamy white-coloured hydrothermally altered dolomite-rich part with apatite, barite and fluorite; the boundary between Parts A and B is studded with many fine-grained square-shaped dolomite grains (see Plates I, II, III, IV, VI and IX).

In beforsite specimens (06 I, 06 II) from Panda Hill, Part A is white or cream-coloured hydrothermally altered beforsite with calcite, quartz, apatite, magnetite, hematite, fluorite and barite; this part is characterized by the aggregate of medium-grained anhedral dolomite with ambiguous outline and very fine-grained anhedral dolomite, calcite, apatite, fluorite and barite grains (see Plate V-3). This carbonate texture is in strong contrast to that of carbonates in sövite (01, 02, 03, 04) and beforsite (11), and this Part A is also characterized by the presence of spotted quartz aggregates; Part A′ is pale greyish black-coloured beforsite and Part A″ is pale brown-coloured beforsite: these Parts A′ and A″ are also hydrothermally altered and are similar to Part A in their mineral assemblages and textural features; Part C is brownish black-coloured magnetite beforsite with apatite, pyrochlore and tremolite; Part D is a white-coloured younger calcite-dolomite veinlet with accessory quartz; Part E is a fine-grained white-coloured hydrothermally altered dolomite-rich part with accessory barite, fluorite and quartz (see Plates IV-4, V-1, 2).

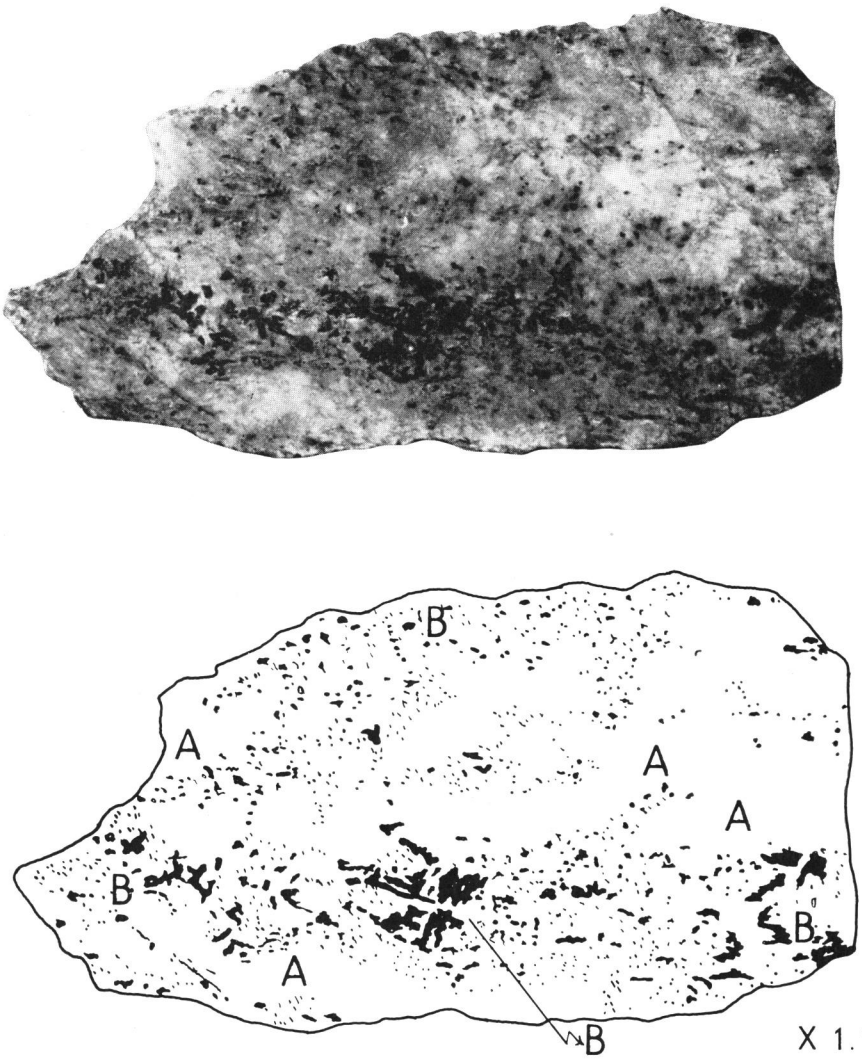

Fig. 6. 2-68092301, Sövite, Panda Hill

01-A: White-colored part

Calcite ≫ dolomite > biotite > apatite ≥ magnetite & hematite = pyrochlore

01-B: Pale reddish brown-colored part

Magnetite & hematite > pyrochlore = calcite > dolomite = apatite = biotite

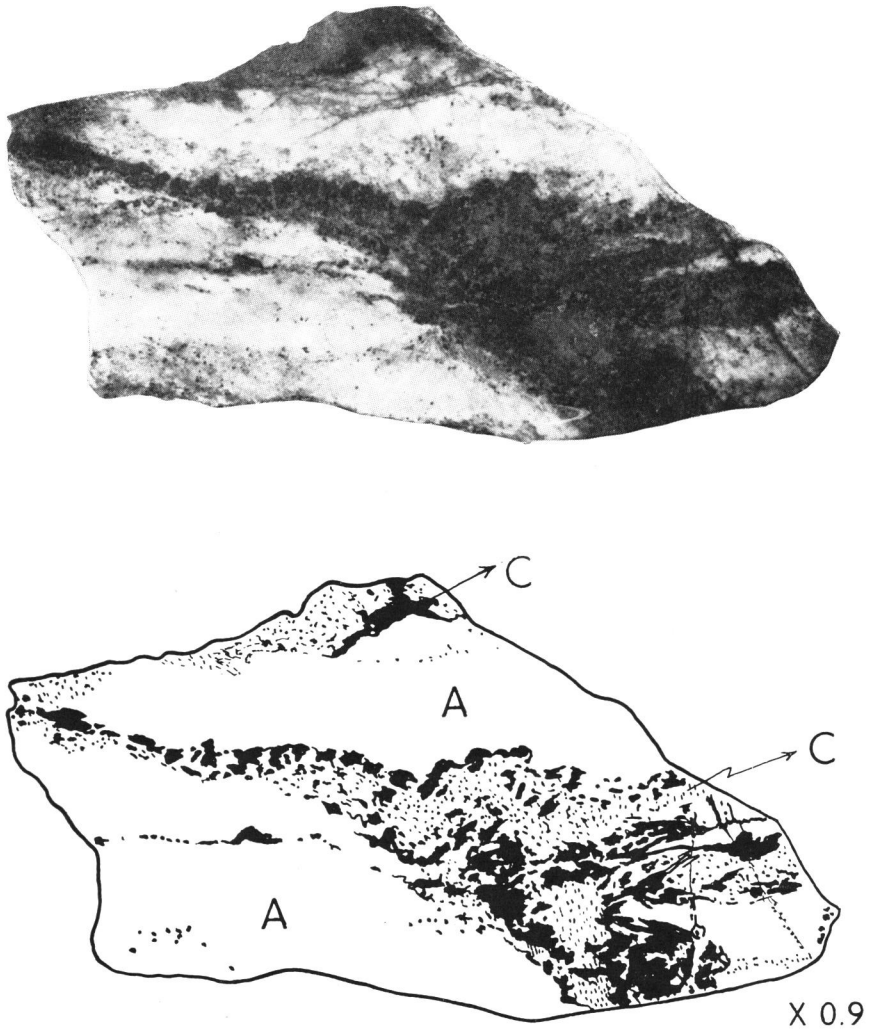

Fig. 7. 2-68092302, Sövite, Panda Hill

02-A: White-or pale pink-colored part
Calcite ≫ dolomite ≫ biotite = apatite = magnetite > pyrochlore

02-C: Brown-colored part
Calcite ≥ magnetite > pyrochlore > amphibole ≥ dolomite ≥ apatite > pyrite

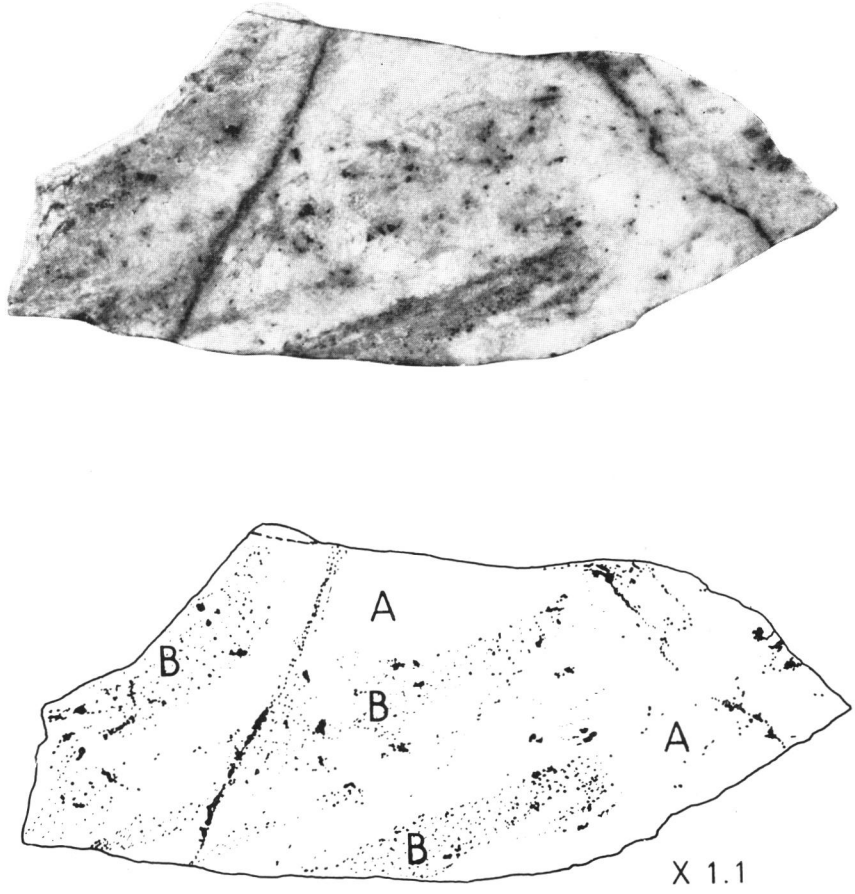

Fig. 8. 2-68092303, Sövite, Panda Hill

03-A: White-colored part
Calcite ≫ dolomite ≫ pyrochlore = apatite = biotite

03-B: Pale brown-colored part
Apatite ≥ magnetite & hematite ≥ pyrochlore ≥ calcite ≫ dolomite > biotite = amphibole

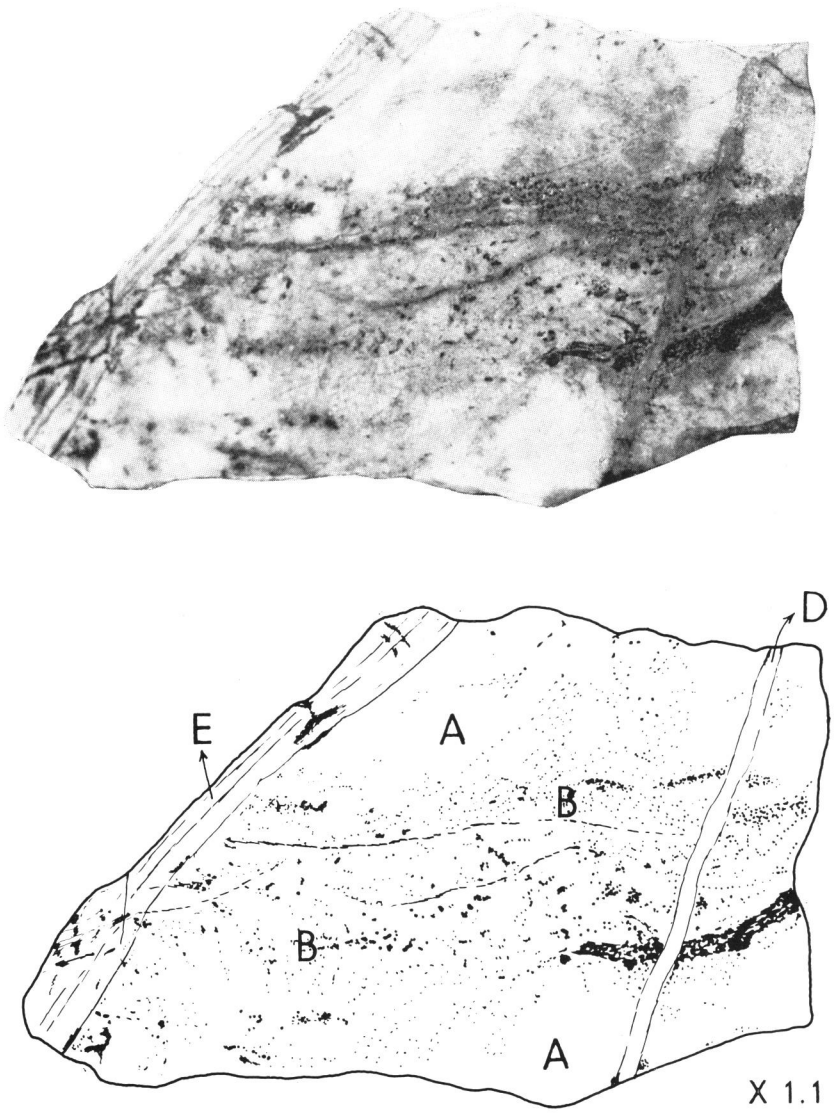

Fig. 9. 2-68092304, Sövite, Panda Hill

04-A: White-colored part
Calcite ≫ dolomite ≫ pyrochlore = apatite

04-B: Orange-brown-colored part
Calcite ≥ magnetite & hematite > amphibole = dolomite ≥ apatite

04-D: White-colored veinlet
Calcite

04-E: Fine-grained creamy white-colored part
Dolomite ≫ apatite = barite = fluorite

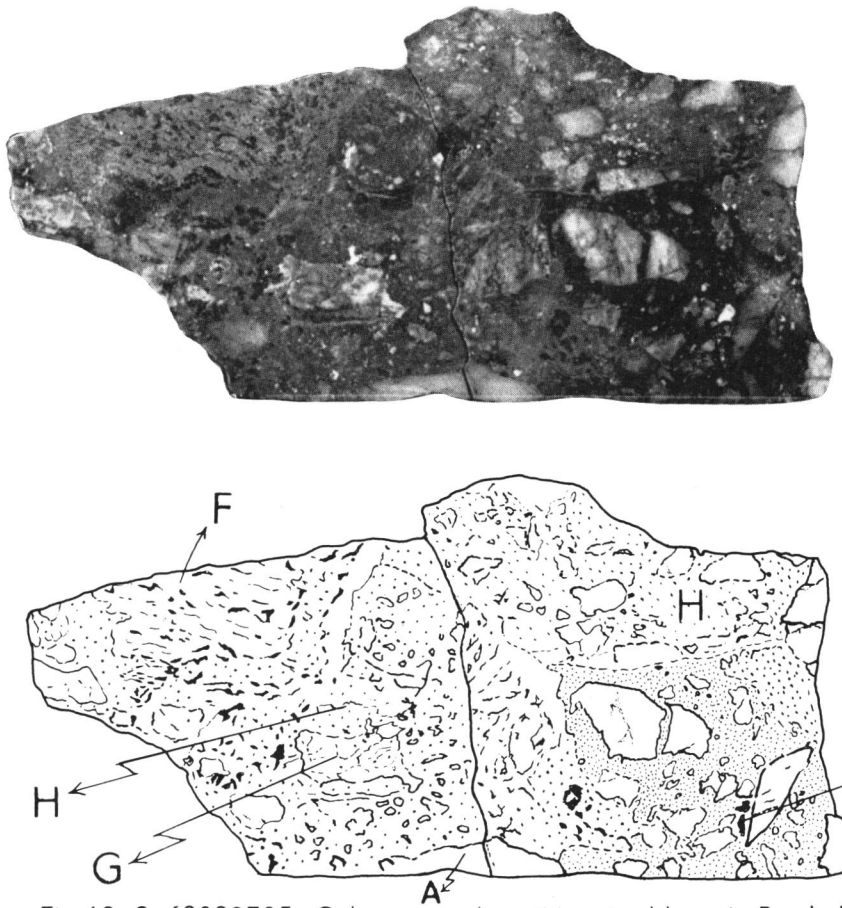

Fig. 10. 2-68092305, Ochreous carbonatitic mixed breccia, Panda Hill

05-A: White-colored fragment
Dolomite ≫ pyrochlore = apatite > limonite

05-F: Pale orange-colored fragment
Dolomite ≫ calcite > quartz > apatite > limonite

05-G: White-gray-colored fragment
Potassium feldspar > dolomite > calcite > limonite

05-H: Mixture of yellow-brown-colored matrix and fine-or medium-grained white-gray-colored fragment
Dolomite ≫ calcite > potassium feldspar ≥ apatite > limonite

05-I: Mixture of chocolate-colored matrix and medium-grained white-gray-colored fragment
Dolomite > calcite > potassium feldspar > apatite > limonite

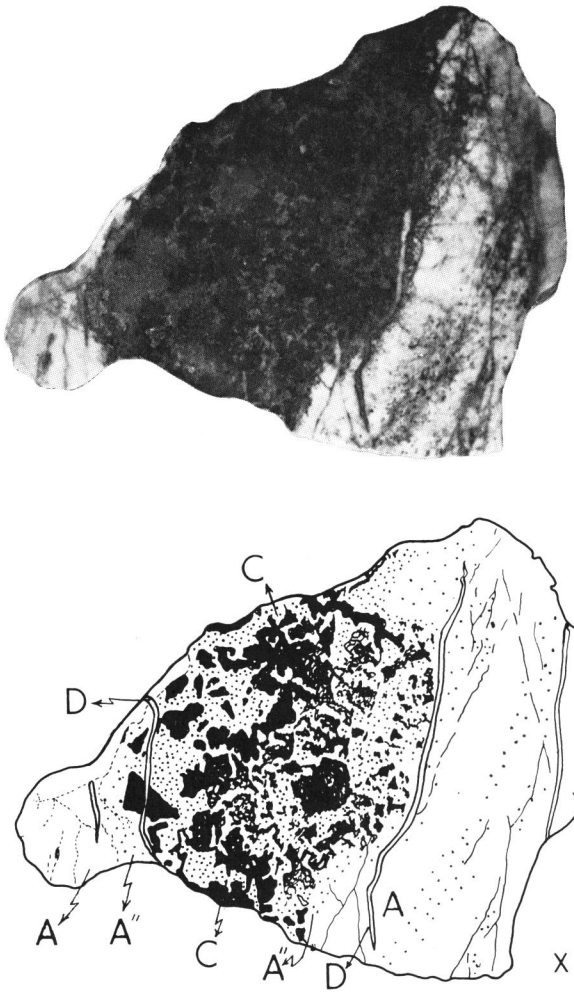

Fig. 11. 2-68092306 I, Beforsite, Panda Hill

06 I-A: White-colored part
Dolomite ≥ calcite > apatite > quartz = fluorite ≥ magnetite & hematite

06 I-A'': Pale brown tinge creamy white-colored part
Dolomite ≥ calcite > quartz > apatite > magnetite

06 I-C: Brown-black-colored part
Magnetite = dolomite > apatite = pyrochlore = tremolite

06 I-D: White- or yellow-white-colored veinlet
Dolomite > calcite ≫ quartz

06 I-E: Fine-grained white-colored part
Dolomite ≫ barite > fluorite = quartz

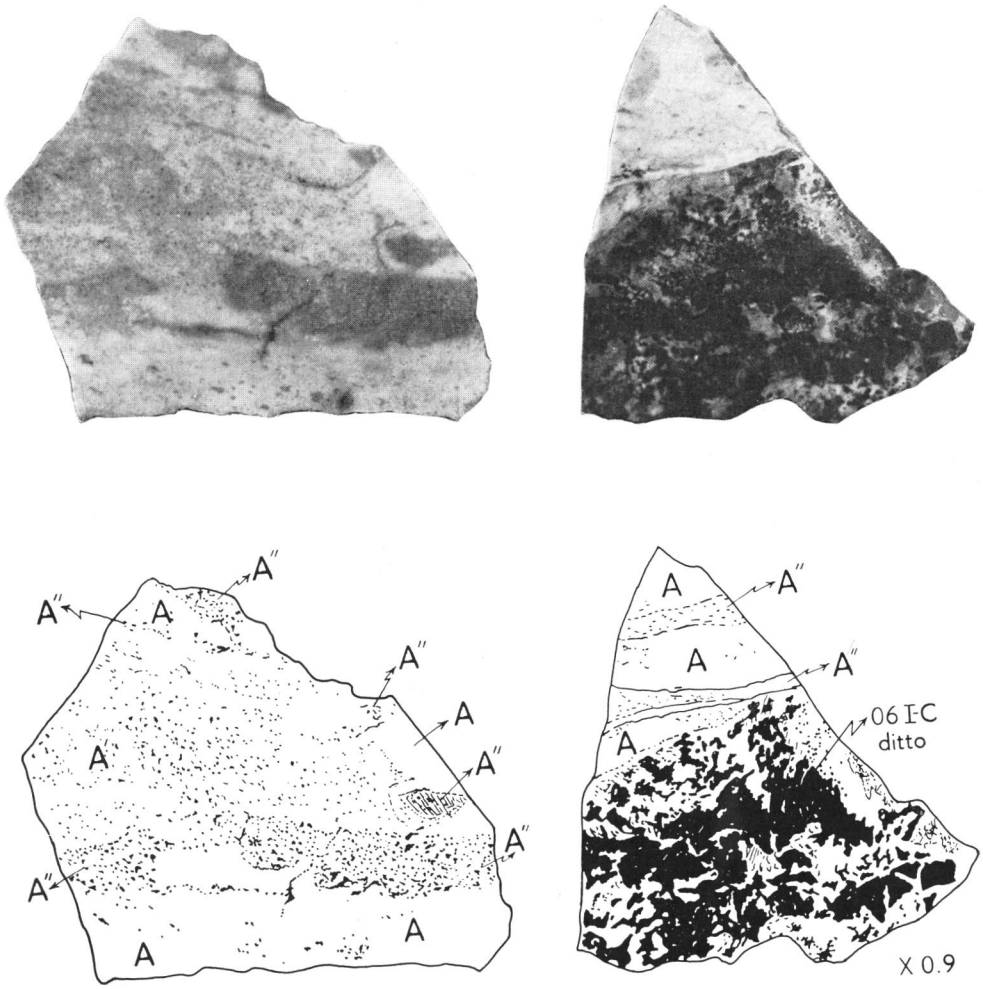

Fig. 12. 2-68092306 II, Beforsite, Panda Hill

06 II-A: White- or cream-colored part
Dolomite ≫ quartz > barite > magnetite ≥ calcite

06 II-A′: Pale grayish black-colored part
Dolomite ≫ quartz > barite > magnetite

06 II-A″: Pale brown-colored part
Dolomite ≫ quartz > barite > apatite = fluorite > magnetite

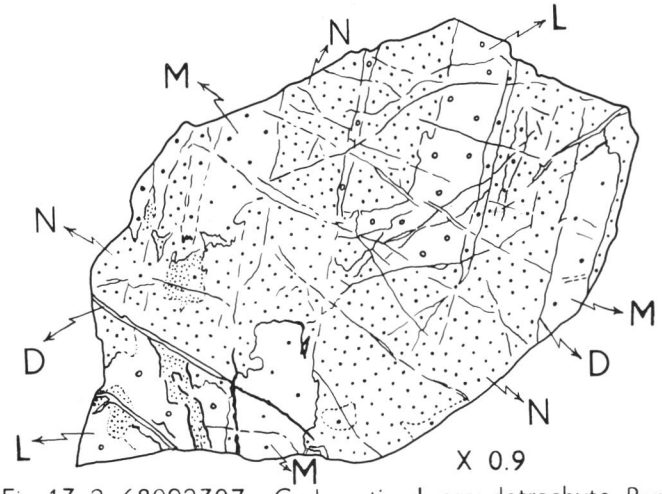

Fig. 13. 2-68092307a, Carbonatized pseudotrachyte, Panda Hill

07a-D: Brown-colored veinlet
Limonitized carbonate > potassium feldspar > quartz

07a-L: White-colored part
Potassium feldspar ≫ quartz ≒ calcite > dolomite > apatite

07a-M: Pale creamy or whity yellow-brown-colored part
Potassium feldspar > quartz > calcite = dolomite > limonite > apatite

07a-N: Brown-colored part
Potassium feldspar ≥ quartz > calcite ≒ dolomite > limonite > fluorite > hematite > apatite ≥ sphene

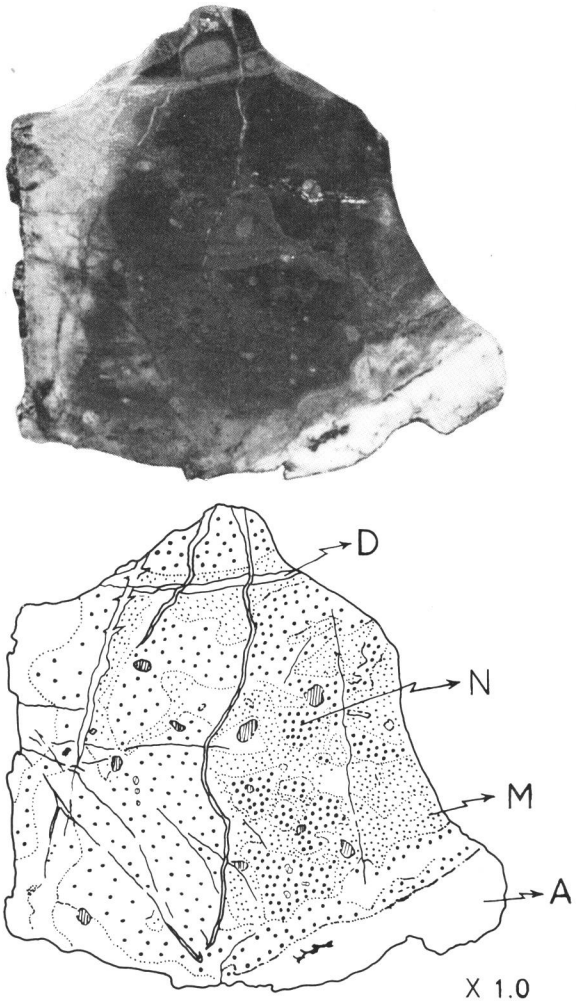

Fig. 14. 2-68092307b, Carbonatized pseudotrachyte (in beforsite), Panda Hill

07b-A: White-colored part
Dolomite ≫ quartz > fluorite ≥ apatite > magnetite & hematite > potassium feldspar ≥ limonite

07b-D: White-colored veinlet
Dolomite ≥ potassium feldspar > quartz > apatite > fluorite

07b-M: Yellow-brown-colored part
Potassium feldspar > dolomite > quartz > limonite > calcite > apatite > fluorite

07b-N: Brown-colored part
Potassium feldspar ≥ quartz > dolomite > limonite > calcite > apatite > fluorite

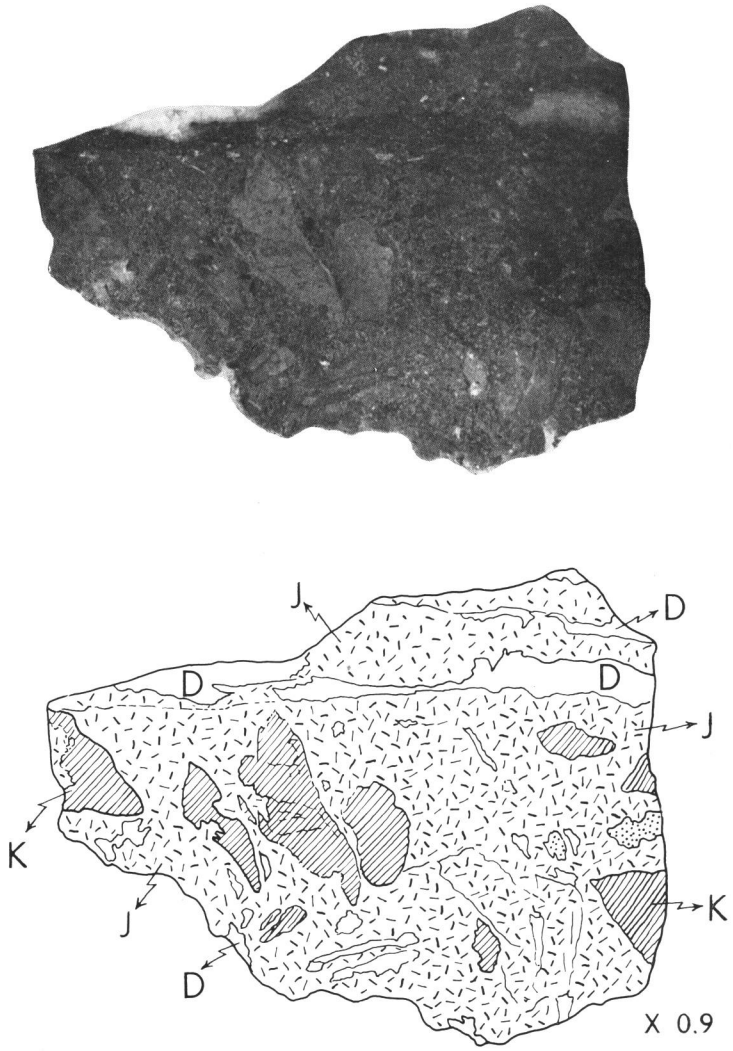

Fig. 15. 2-68092310, Ochreous carbonatitic pseudotrachyte breccia, Sengeri Hill

10-D: Transparent veinlet: Fluorite

10-J: Yellow-brown-colored brecciated matrix
Quartz ≫fluorite > dolomite ≥ kaolinite ≥ calcite ≥ apatite = potassium feldspar = limonite

10-K: Brown tinge yellow-colored fragment
Potassium feldspar ≫quartz = dolomite > limonite ≥ calcite ≥ apatite

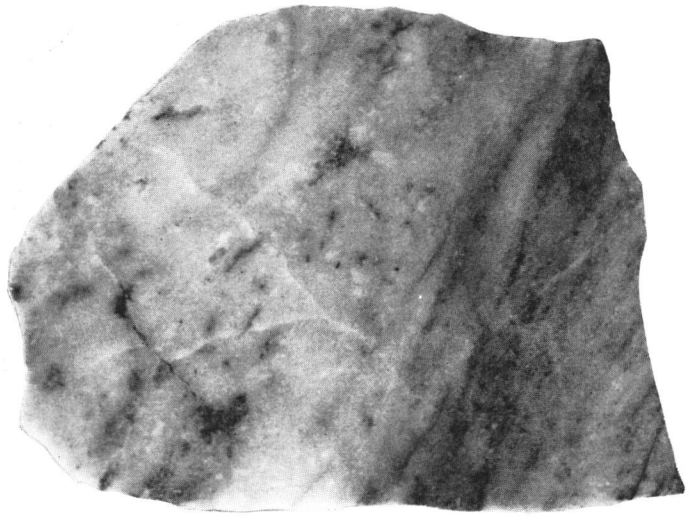

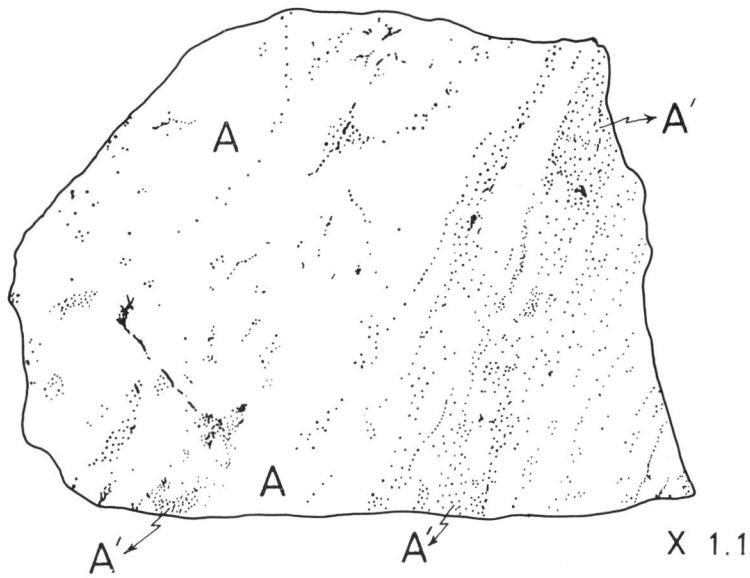

Fig. 16. 2-68092311, Beforsite with small amounts of orthoclasite and pseudotrachyte, Sengeri Hill

11-A: White-colored part
Dolomite ≫ potassium feldspar ≥ quartz ≫ pyrochlore = apatite

11-A′: Yellow tinge brown-gray-colored part
Dolomite ≫ potassium feldspar ≥ quartz ≥ limonite > pyrochlore = barite > magnetite > apatite

In beforsite (11) from Sengeri Hill, Part A is white-coloured beforsite with accessory fine-grained pyrochlore and apatite crystals and contains pseudotrachyte chips consisting of potassium feldspar, quartz, and apatite. Part A consists chiefly of phenocryst-like coarse-grained dolomite ranging from 2.0 to 3.0 mm and groundmass-like fine-grained dolomite ranging from 0.2 to 0.3 mm (see Plates V-4 and VIII-2); Part A′ is yellow tinged brown-grey-coloured limonitized beforsite with accessory pyrochlore, barite and magnetite, and contains small chips of pseudotrachyte, orthoclasite and apatite-quartz rock.

Other examples of porphyritic texture are known. Zhabin and Cherepivskaya [39] described narrow carbonatite dikes having a porphyritic and trachytoid texture with tabular calcite phenocrysts set in "microgranular granoblastic mesostasis of calcite, dolomite and apatite" occurring in the Maymecha-Kotuy petrographic province in Siberia. Those dikes also have narrow "microgranular chilled zones" along the sharp, dike-country rock contact. Johnson [19] described porphyritic beforsite from Southern Rhodesia with very large dolomite phenocrysts set in a fine-grained matrix of "fibrous dolomite". Gittins [14] also described similar textures. These are regarded as textural evidence for the existence of intrusive carbonatite magmas.

These sövite and beforsite intrusions were emplaced as magma. The numerous inclusions of altered and unaltered country rock carried in these intrusions are believed to have been transported by the movement of the enclosing fluid or dlastic material. They are volcanic breccias in which the fragments are all of pre-existing rock which have been broken and mixed by explosive activity. In addition, there is another brecciated rock accompanied by a very strong contemporaneous potassium metasomatism, and in this brecciated rock the fragment content is much more homogeneous, only fragments of country rock or altered country rock being seen.

The relations exposed at the Mbeya carbonatite are very similar to those noted at Homa Mountain in southwestern Kenya where similar breccias and feldspathic rocks are exposed [4].

The present work uses the nomenclature suggested by Sutherland [27] in which fine-grained unbrecciated rocks rich in potassium feldspar and produced by metasomatism are referred to as pseudotrachytes, and the coarse-grained variety orthoclasites. A breccia in which the fragments are predominantly pseudotrachyte in an ochreous carbonate matrix is termed ochreous carbonatitic pseudotrachyte breccia. The explosion breccia with mixed fragments is termed, using this nomenclature, ochreous carbonatitic mixed breccia.

In ochreous carbonatitic mixed breccia (05), from Panda Hill, Part A is a white-coloured beforsite fragment with accessory pyrochlore, apatite and limonite; Part F is a pale orange-coloured hydrothermally altered beforsite fragment with accessory calcite, quartz and apatite; Part G is a white-gray-coloured carbonatized pseudotrachyte fragment; Parts H and I are ochreous

mixture of fine-grained fragments of pseudotrachyte and beforsite with secondary calcite (see Plate VII-1).

In the carbonatized pseudotrachyte (07 a, 07 b) from Panda Hill, Part A is white-coloured hydrothermally altered beforsite having an apatite-rich streak with accessory quartz, fluorite, magnetite, hematite, potassium feldspar and limonite; there are two kinds of dolomite in Part A, medium-grained anhedral dolomite ranging from 0.3 to 1.5 mm and very fine-grained dolomite ranging from 0.01 to 0.06 mm; Part D is a white- or brown-coloured younger potassium feldspar-dolomite (or limonitized carbonate) veinlet with accessory quartz, apatite and fluorite; Part L is white-coloured carbonatized pseudotrachyte with quartz and apatite; Parts M and N are limonitized carbonatized quartzose pseudotrachyte with accessory apatite, fluorite, hematite and sphene (see Plate VII-2). Three kinds of potassium feldspars are observed in Parts L, M, and N, coarse-grained rounded phenocryst-like slightly sericitized potassium feldspar (2–7 mm) with apatite and quartz inclusions, ball-like aggregates (1 mm) of potassium feldspar showing radial growth around the core of fluorite-limonite-dolomite, and fine-grained potassium feldspar grains around the above phenocryst- and ball-like potassium feldspar.

In the ochreous carbonatitic pseudotrachyte breccia (10) from Sengeri Hill, Part D is a transparent younger fluorite veinlet; Part J is yellow-brown-coloured brecciated fluorite-quartzose matrix with accessory dolomite, kaolinite, calcite, apatite, potassium feldspar and limonite; Part K is a brownish yellow-coloured pseudotrachyte fragment with accessory quartz, dolomite, limonite, calcite and apatite; Part K contains tiny chips of limonitized beforsite (see Plate VIII-1).

MINERALOGICAL NOTES OF THE MBEYA CARBONATITE

A. Minerals

In polished sections, thin sections, concentrates and tailings the following minerals are observed.

a) Amphibole:

Amphibole occurs in sövite (04–A), sövite with magnetite, hematite, pyrochlore, and apatite (03–B, 04–B), sövite rich in magnetite and pyrochlore (02–C), and beforsite rich in magnetite (06 I–C). These amphiboles are altered and are replaced to some extent by alteration products such as dolomite and silica (quartz, chalcedony and/or opal?) and locally goethite. Occasionally the amphibole embedded in calcite is more strongly altered than the amphibole surrounded by dolomite. Goethite pseudomorphs after amphibole are locally present (see Plates I-4 and V-2).

Judging from the optical, X-ray, and chemical data by Fick and Van der Heyde [11], James and McKie [18] and Van der Veen [31], the amphibole may be regarded as potassic richterite. Some of the amphibole may have a

more glaucophanitic or riebeckitic composition.

b) Calcite and dolomite:

Calcite normally occurs as a granular mass of anhedral crystals up to 1 cm across, and rhombohedral cleavage is common; polysynthetic twinning is seldom observed.

Calcite occurs in several generations of which the older ones are often very cloudy. The younger and less turbid calcite occurs mostly in veins and veinlets (*e.g.* 04-A・D) (see Plate III-4). The turbidity of the calcite grains is due to minute cavities (empty or filled with liquid and/or gas), dolomite crystallites and locally to minute opaque inclusions.

Calcite has more or less replaced nearly all other minerals, except goethite and quartz, by which calcite has been replaced in many places. Calcite often occurs also as irregularly shaped patches in dolomitic areas, where calcite veinlets also occur.

Dolomite has generally a finer grain size than calcite, and is mostly clear but occasionally turbid. In some places cloudy dolomite seems to be penetrated by clear dolomite, whereas elsewhere cloudy dolomite grains are observed with a clear border. It is also observed that both dolomite types are replaced by calcite, probably belonging to a younger hydrothermal period.

Hydrothermally altered beforsite (*e.g.* 06 I, 06 II) is characterized by aggregates of medium-grained anhedral dolomite with ambiguous outline and very fine-grained anhedral dolomite. This textural feature differs greatly from that of carbonate in unaltered sövite (*e.g.* 01, 02, 03, 04) and beforsite (11).

Beforsite (11) at Sengeri Hill consists chiefly of phenocryst-like coarse-grained dolomite (2.0–3.0 mm) and groundmass-like fine-grained dolomite (0.2–0.3 mm). This is considered to be textural evidence for the existence of intrusive carbonatite magma (see Plates V-4 and VIII-2).

In the sövite, dolomite is often concentrated along bands and "schlieren" of the accessory mineral assemblage (*e.g.* 02-A・C) [18, 31]. But, in some sövites dolomite bands and "schlieren" are observed in parts free or almost free of the accessory minerals.

Van der Veen [31] reported that mutual replacement of calcite and dolomite was observed and replacement of calcite by dolomite seemed to dominate, and that other textural features which might be interpreted as exsolution of dolomite from calcite were often observed. On the calcite-dolomite relation, he reported that exsolution, as well as differentiation and replacement processes have taken place. It was impossible to establish which process dominated at Panda Hill [31].

c) Apatite:

Apatite is the most common accessory mineral in the carbonatite and occurs in all specimens examined. The apatite of the Mbeya carbonatite is a

fluorapatite with some cerium [31]. Apatite occurs in single crystals scattered throughout the carbonatite, in clusters often with lenticular shape, in "schlieren" of granular aggregates and in bands. The apatite "schlieren" and bands are often associated with pyrochlore, amphibole, magnetite, biotite, dolomite and other accessory minerals (see Plates I-1, 2 and II-3).

Apatite sometimes contains minute inclusions of amphibole needles and opaque needles, perhaps rutile (*e.g.* 02-C, 06 I-C).

d) Biotite:

Biotite occurs in sövite (01-A, 02-A, 03-A) and in sövite having magnetite, hematite, pyrochlore and apatite (01-B, 03-B) (see Plate I-2).

The biotite of the carbonatite possesses a strikingly reversed pleochroism; X=dark reddish brown, Y=Z=very pale yellowish brown to colourless. The other optical and structural data point to a mineral much resembling a Mn-rich variety of biotite [11]. Green-coloured Mn-phlogopite in which Mn^{2+} is in four-fold-coordination, synthesized by Daimon *et al.* [7], possesses a similar reversed pleochroism.

It was observed that the mica is often altered partly to carbonates, limonite, and quartz (see Plate II-1). Occasionally quartz pseudomorphs with some limonite after biotite were noticed.

e) Magnetite:

This mineral occurs in disseminated octahedra from microscopic crystal to several centimetres across (see Plates I-1, 4, II-3, III-2 and IV-1, 2). In reflected light exsolution lamellae of ilmenite, partly altered to leucoxene (rutile and/or anatase) could be observed. Magnetite is commonly partly or totally altered to hematite (martitization) and limonite. Strongly carbonatized and silicified magnetites occur locally, and original ilmenite lamellae remain behind unattacked in a field of carbonate and/or quartz (see Plates III-3 and V-2). Euhedral inclusions of amphibole, apatite and biotite occur in magnetite.

f) Pyrochlore:

The most common type of pyrochlore is greyish olive to olive-green, but all shades from dark brown to yellowish grey are also found. Pyrochlore is associated with apatite and magnetite, and these minerals are often also associated with the other accessory minerals (see Plates I-4 and II-4).

Pyrochlore may be replaced by carbonates, rutile, goethite, hematite, pyrite, fluorite, quartz, zircon, and its alteration products (*e.g.* columbite and fersmite). Locally it is so intensively replaced by calcite or dolomite that its original euhedral shape is totally destroyed. Inclusions of euhedral to anhedral crystals of amphibole, apatite, biotite and rutile were often observed.

Zonal pyrochlore is often observed (see Plate I-1). Zonal intergrowths of pyrochlore with rutile, hematite and silica are also locally observed. Needles

of fersmite, ilmenite and/or rutile distributed along two or more crystallographic directions may have been formed by alteration or exsolution [31].

g) Potassium feldspar:

Potassium feldspar occurs as the main constituent mineral of pseudotrachyte fragments in ochreous carbonatitic mixed breccia (05-G・H・I), in carbonatized pseudotrachyte (07 b-M・N), and in ochreous carbonatitic pseudotrachyte breccia (10-K) (see Plate VII). It occurs also as a minor mineral in the potassium feldspar-dolomite veinlet in pseudotrachyte (07 b-D), as an accessory mineral of hydrothermally altered beforsite (07 b-A), in the brecciated fluorite-quartz matrix in ochreous carbonatitic pseudotrachyte breccia (10-J), and as small chips of pseudotrachyte or orthoclasite in beforsite (11-A・B).

As mentioned previously, potassium feldspar originated from pre-existing Precambrian metamorphic rocks which were broken and mixed by explosive activity accompanied by a very strong contemporaneous potassium metasomatism. Albite also occurs at Mbeya (*e.g.* 07 b-M).

This evidence accords with the result of the experiments of Watkinson and Wyllie, and Koster van Groos and Wyllie [36] in the CaO-Na_2O-Al_2O_3-SiO_2-CO_2-H_2O system, indicating that physical conditions for the equilibrium coexistence of alkali feldspars and calcite have not been established.

h) Fluorite and Barite:

Fluorite occurs as an accessory mineral in the hydrothermally altered dolomite-rich parts of sövite and beforsite (04-E, 06 I-E), hydrothermally altered beforsite (06 I-A, 06 II-A″, 07 b-A), a potassium feldspar-dolomite veinlet in pseudotrachyte (07 b-D), and limonitized carbonatized quartzose pseudotrachyte (07 a-N, 07 b-M・N). It occurs also as the main mineral of the brecciated fluorite-quartz matrix (10-J) and a fluorite veinlet (10-D) in ochreous carbonatitic pseudotrachyte breccia.

Barite occurs also as an accessory mineral in hydrothermally altered dolomite-rich parts in sövite and beforsite (04-E, 06 I-E), hydrothermally altered beforsite (06 II-A・A′・A″), and limonitized beforsite (11-A′). It is noticed that barite occurs mainly in the dolomitic carbonatite, being practically unaccompanied by calcite.

Fluorite and barite seem to occur as minerals of the later hydrothermal stage (see Plates IV-3, V-3, VIII-1 and IX).

i) Quartz:

Quartz occurs as an accessory or main mineral of hydrothermally altered beforsite (05-F, 06 I-A・A″・E, 06 II-A・A′・A″, 07 b-A) and younger carbonate veinlets (06 I-D, 07 a-D, 07 b-D), and younger quartz veinlets or seggregations in altered beforsite (06 II-A). It seems to occur as a mineral of the younger hydrothermal stage (see Plates V-1, 2).

Quartz also occurs as an accessory or main mineral of carbonatized pseudotrachyte (07 a-L・M・N, 07 b-M・N, 10-K), brecciated fluorite-quartzose matrix in carbonatitic pseudotrachytic breccia (10-J), and small chips of pseudotrachyte in beforsite (11-A・A′). It seems to occur also as a remanent mineral from pre-existing Precambrian rocks (see Plates VII-2 and VIII-1).

Quartz in veinlets is often associated with fluorite, calcite, some goethite and dolomite, and occasionally with columbite and barite. Locally the rock is strongly replaced by quartz, by other silica minerals as chalcedony and opal, and by goethite. Silica also occurs as an alteration product of the amphibole.

j) Limonite (goethite):

Goethite is formed during weathering of the sulphides, iron oxides and iron bearing silicates. Sometimes goethite has completely replaced such minerals, yielding pseudomorphs after them.

B. Paragenetic mineral sequence and formation temperature of the Mbeya carbonatite

The preliminary paragenetic mineral sequence of the minerals of the Mbeya carbonatite has been established by Van der Veen [31]. According to his paper, the sequence of crystallization seems to be pyroxene, amphibole, calcite, apatite, biotite, magnetite, pyrochlore, zircon, dolomite (rutile, quartz, pyrite, goethite, barite?) in descending order. In this sequence calcite has to be placed somewhere above apatite, and whether the place of dolomite below zircon is correct is uncertain, as pyrochlore, magnetite etc. may also be formed later with euhedral shape in dolomite. Some overlapping of these sequences probably occurs as for example between pyrochlore and zircon. It is supposed that apatite was formed at least in two stages.

This assemblage, from amphibole down to and probably including zircon, points to a formation of the assemblage at the temperature generally supposed to be that of the lower amphibolite facies, indicating probably a temperature of approximately 400°C to 500°C [31]. The results of preliminary heating experiments by Brinck with apatite crystals, possessing gas-liquid inclusions, from the Mbeya carbonatite point to a formation temperature of at least 360 °C [31].

The calcite-dolomite content was computed from 74 average chemical analyses from 15 borings in the Panda Hill carbonatite. The dolomite contents vary from 0 to 100 per cent. A frequency-histogram of the relative dolomite content shows a vague bimodal distribution with modes in the 20–30% and 90–100% intervals. The mode between 90–100% is probably caused by large rauhaugitic lumps. Assuming that the flanks of the other mode located at 20–30% are caused by small to large dolomite inclusions and schlieren, this mode would represent the composition of the original magnesian calcite before

exsolution. The temperature of the solvus for this composition, that is $CaCO_3$: $CaMg(CO_3)_2$=80 : 20 to 70 : 30, is somewhere between 680°C and 800°C [16, 31].

However, this carbonatite is probably not a simple three-component system, as is evident from the presence of the other minerals, which sometimes occur in appreciable amounts (for instance apatite and amphibole). It is more likely a multicomponent system in which water and phosphorous also play a role.

The experiments by Wyllie and Tuttle [37] with the CaO-CO_2-H_2O system should make admissible the existence of carbonatite magmas at temperatures from 685°C to 640°C in the pressure interval 27 bars to 4000 bars. The experiments by Gittins and Tuttle [15] with the CaF_2-$Ca(OH)_2$-$CaCO_3$ system should make admissible the existence of carbonatite magma at a temperature of 600 °C at a pressure of 1000 bars. This means that in multicomponent carbonatitic magmas with MgO, P_2O_5, and H_2O the temperatures for exsolution of magnesian calcite into calcite and dolomite must likewise be considerably below the above mentioned temperatures.

OXYGEN AND CARBON ISOTOPE ANALYSES

Measurements of oxygen and carbon isotope ratios were made on calcite and dolomite in the carbonatite samples. The sample, ground to minus 200 mesh, was treated with 100% phosphoric acid in vacuum. The carbon dioxide evolved was purified and analysed with a McKinney-Nier mass spectrometer at the Institute for Thermal Spring Research, Okayama University. Fossil coral (CK-13) was used as a working standard, and the Akiyosi marble was used as a calibrating standard. These standards were described by Nakamichi *et al.* [21]. The results of oxygen and carbon isotope analyses are expressed as the per mil deviation of the O^{18}/O^{16} or C^{13}/C^{12} ratio from the ratio in an arbitary standard substance:

$$\delta O^{18} = \left(\frac{O^{18}/O^{16}\ \text{sample}}{O^{18}/O^{16}\ \text{standard}} - 1 \right) \times 1000$$

$$\delta C^{13} = \left(\frac{C^{13}/C^{12}\ \text{sample}}{C^{13}/C^{12}\ \text{standard}} - 1 \right) \times 1000$$

The oxygen standard is the oxygen of SMOW (Standard Mean Ocean Water; Craig [6]). The carbon standard is the carbon of the PDB—carbonate standard (*Belemnitella americana* from the Pee Dee formation of South Carolina; Craig [5]). The PDB standard is also used as the standard of the oxygen in other papers. The relationship is;

$$\delta O^{18}_{SMOW} = 1.03\delta O^{18}_{PDB} + 30.37$$

All results were corrected for O^{17} as described by Craig [5]. The dolomite data are further corrected for the kinetic fractionation in the phosphoric

acid reaction with different carbonates [25]).

A special chemical treatment was employed in order to separate dolomite from calcite in carbonatites, since physical separation is not practicable. According to the method of Epstein *et al.* [9] the carbonate samples were treated with phosphoric acid for one hour and the CO_2 thus obtained was assumed as coming from the calcite part, and the gas evolved during the period from 4 to 72 hours was collected as CO_2 from the dolomite part. The present authors determined the relative rate of reaction in order to check the result of Epstein *et al.* The outcome of the present authors' studies points to that the gas evolved during the first one hour includes CO_2 coming from 15 to 20% of the dolomite part. Therefore, to eliminate contamination by dolomite, the CO_2 formed during the first one minute was collected as coming from the calcite part only. About 65% of the calcite part reacts during the first one minute, and the isotope ratios of the CO_2 is not different from those of the CO_2 obtained by the complete reaction during about 2 hours. The CO_2 gas formed in the period from 1 minute to 4 hours of the reaction was pumped away. The CO_2 formed during the period from 4 to 72 hours was collected as coming from the dolomite part.

The analytical error is ± 0.2‰ for pure calcite and dolomite, and may become slightly higher for the mixed carbonate samples.

The calcite/dolomite ratio of the carbonatite samples was estimated semi-quantitatively by means of X-ray diffraction analyses.

ISOTOPE GEOCHEMISTRY OF THE MBEYA CARBONATITE

The analytical data are given in Table 1 and Fig. 17. The δ-values of the calcites vary from -5.31 to $+3.09$‰ for carbon and from 5.90 to 25.50‰ for oxygen. The dolomites range in δC^{13} from -5.59 to $+1.18$‰ and in δO^{18} from 6.03 to 24.06‰. The data lie in a wide range, but show some regularities.

(1) Carbonates showing high δO^{18} values:

As is clearly shown in Figs. 17 and 18, there are no δ-values for oxygen between 9.68 and 11.84‰. Thirteen of twenty calcites examined are considerably enriched in O^{18} relative to other carbonates ($\delta O^{18} > 11.84$‰). Only five of thirty-two dolomites examined are similarly enriched in O^{18}, and among these five dolomites three range in O^{18} from 11.84 to 12.78‰ and the other two from 22.04 to 24.06‰.

The thirteen calcites showing high δO^{18} values are from younger carbonate veinlets (04-D, 06 I-D), hydrothermally altered beforsite (06 I-A・A″), carbonatized pseudotrachyte fragment in ochreous carbonatitic mixed breccia (05-G), ochreous mixture of fine-grained fragments of pseudotrachyte and beforsite in ochreous carbonatitic mixed breccia (05-H・I), carbonatized pseudotrachyte

TABLE 1. THE OXYGEN AND CARBON ISOTOPE RATIOS OF CARBONATES IN THE MBEYA CARBONATITE (PANDA HILL AND SENGERI HILL)

Specimen	Calcite		Dolomite		Calcite : Dolomite, volume ratio
	δC^{13}, ‰	δO^{18}, ‰	δC^{13}, ‰	δC^{18}, ‰	
2-68092301-A	−5.30	6.85	−5.10	7.02	8 : 2
01-B	−4.94	9.01	−4.09	7.47	9 : 1
02-A	−5.31	5.90	−4.78	6.39	9 : 1
02-C	−1.13	18.11	−4.65	6.61	8 : 2
03-A	−4.80	6.03	−4.21	6.67	9 : 1
03-B	−4.45	7.67	−4.22	7.74	9 : 1
04-A	−3.82	6.21	−3.55	6.69	8 : 2
04-B	−3.96	9.66	−3.90	7.34	9 : 1
04-D	−1.94	14.67			10 : 0
04-E			−0.92	6.03	0 : 10
05-A			−5.22	5.94	0 : 10
05-F			−0.85	12.01	1 : 9
05-G	−4.62	22.07	−4.73	7.37	3 : 7
05-H	−3.13	20.50	−4.42	7.17	3 : 7
05-I	−4.29	22.17	−4.13	7.56	5 : 5
06 I-A	−1.94	13.54	−2.12	12.78	5 : 5
06 I-A″	−1.76	11.88	−2.49	11.84	6 : 4
06 I-C			−4.21	6.56	0 : 10
06 I-D	−0.80	17.66	−5.42	6.46	2 : 8
06 I-E			−1.68	8.74	0 : 10
06 II-A			−1.10	6.86	1 : 9
06 II-A′			−0.39	7.72	0 : 10
06 II-A″			−0.74	7.93	0 : 10
07 a-L	+3.09	25.02	+1.18	6.52	7 : 3
07 a-M	+1.66	25.06	−2.59	8.98	5 : 5
07 a-N	+1.93	25.50	−3.05	9.68	6 : 4
07 b-A			+0.91	6.37	0 : 10
07 b-M			−1.28	7.78	1 : 9
07 b-N			−2.37	9.15	1 : 9
10-J	−3.74	24.13	−1.65	24.06	3 : 7
10-K	−2.12	24.72	−5.59	22.04	2 : 8
11-A			−3.60	6.96	0 : 10
11-A′			−3.06	9.53	0 : 10

(07 a-L), limonitized carbonatized quartzose pseudotrachyte (07 a-M・N), brecciated fluorite-quartzose matrix (10-J) and pseudotrachyte fragment containing tiny chips of limonitized beforsite (10-K) in ochreous carbonatitic pseudotrachyte breccia, and sövite rich in magnetite and pyrochlore (02-C) as described before. These calcites are altered and/or formed in relation to one or more phases of younger hydrothermal activity, brecciation and mixing accompanied by explosive activity, opaque mineral concentration, and weathering. Consequently, these calcites became enriched in δO^{18} by alteration in a later stage.

The five dolomites showing high δO^{18} values are from hydrothermally altered beforsite fragment in ochreous carbonatitic mixed breccia (05-F), hydrothermally altered beforsite (06 I-A・A″), brecciated fluorite quartzose matrix (10-J)

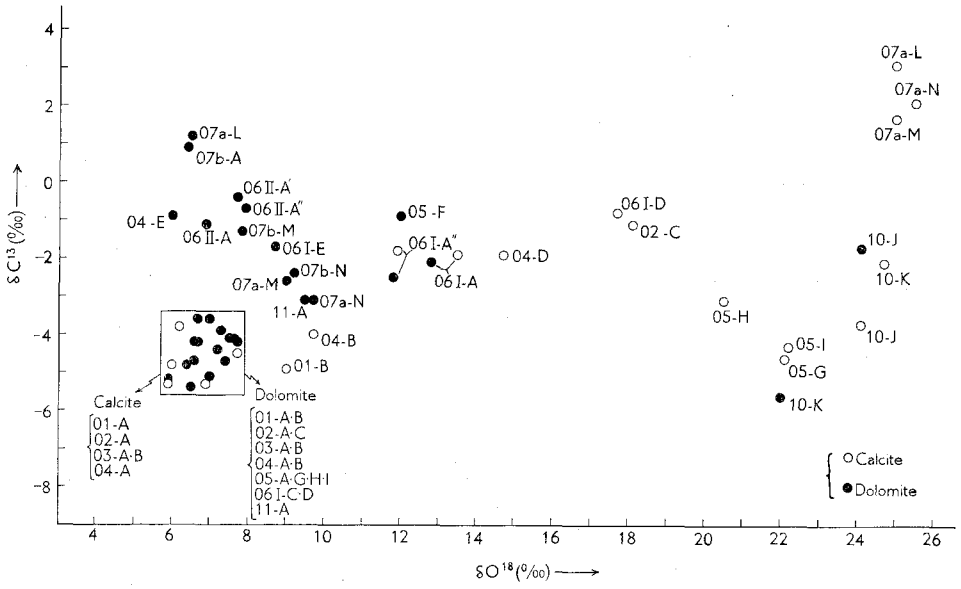

FIG. 17. The oxygen and carbon isotope ratios of carbonates in the Mbeya carbonatite (Panda Hill and Sengeri Hill). The small square represents the isotope ratios of the primary Mbeya carbonatitic carbonates.

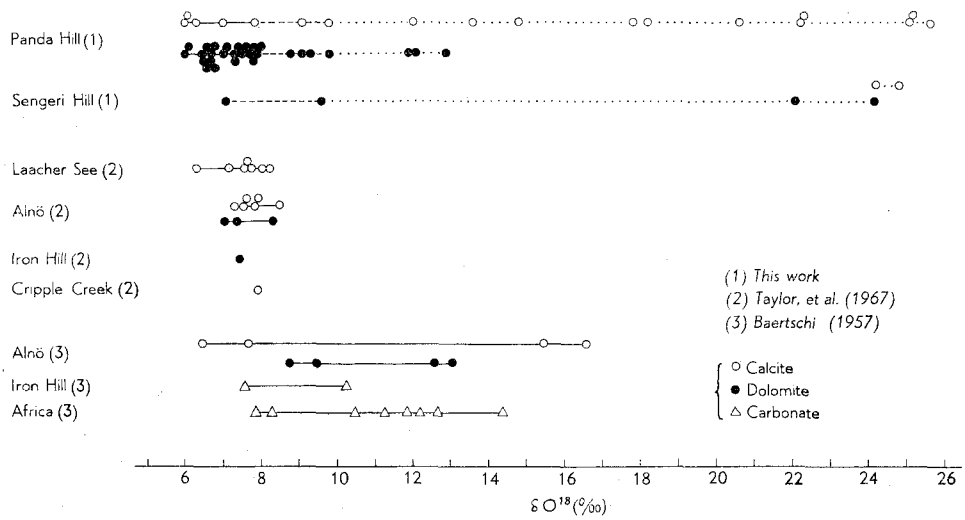

FIG. 18. The oxygen isotope ratios of carbonates in carbonatites.

and pseudotrachyte fragment containing tiny chips of limonitized beforsite (10–K) in ochreous carbonatitic pseudotrachyte breccia. These dolomites are also formed in relation to one or more phases of younger hydrothermal alteration, brecciation and mixing accompanied by explosive activity, and weathering.

Fritz [13] also showed that the oxygen isotope ratio of calcite was easily affected by weathering, but that of dolomite was practically unaffected.

The oxygen isotope ratios of most carbonate samples in carbonatites analysed by Baertschi [1], shown in Fig. 18, are spread probably by the same alteration effect.

(2) Carbonates showing high δC^{13} and lower δO^{18} values:

As shown in Fig. 17, twelve dolomites range in a higher δC^{13} region from -3.06 to $+1.18$‰ in spite of lower δO^{18} values. The oxygen isotope composition of carbonate increases in O^{18} with decrease in temperature, especially at temperatures lower than 800°C. On the other hand, the carbon isotope composition shows practically no variation at temperatures between 700°C and 300°C. The fractionation factors of oxygen and carbon isotopes are given in Figs. 20 and 21 respectively, and the present discussion is based on these fractionation factors.

Data on isotope fractionation of carbon isotope between dolomite and calcite are so far unavailable. Nevertheless, such fractionation can be expected to be less dependent on temperature than is the oxygen isotope fractionation between dolomite and calcite shown in Fig. 20. In either case, it is considered that the carbon isotope ratio varies only slightly even when the oxygen isotope ratio varies greatly.

These twelve dolomites are from hydrothermally altered dolomite-rich parts in sövite (04–E) and beforsite (06 I–E), hydrothermally altered beforsite (06 II–A・A′・A″, 07 b-A), limonitized beforsite (11–A′), carbonatized pseudotrachyte (07 a–L), and limonitized carbonatized quartzose pseudotrachyte (07 a–M・N, 07 b–M・N). Almost all these country rocks contain barite and/or fluorite. It is noticed that all six dolomites (04–E, 06 I–E, 06 II–A・A′・A″, 11–A′) coexisting with barite show high δC^{13} and low δO^{18} values.

A process which enriches only C^{13} is considered impossible without contamination and/or thermal effect after hydrothermal alteration. Contamination from wall rocks may be considered as one possibility in the cases of limonitized and/or carbonatized (quartzose) pseudotrachyte. This problem remains to be solved by further studies. It is noticed that carbonates showing high δC^{13} and lower δO^{18} values were obtained only from dolomites of the carbonatites which suffered late-stage alteration.

(3) Carbonates showing low δO^{18} and δC^{13} values:

As shown in the small square in Fig. 17, five calcites and fifteen dolo-

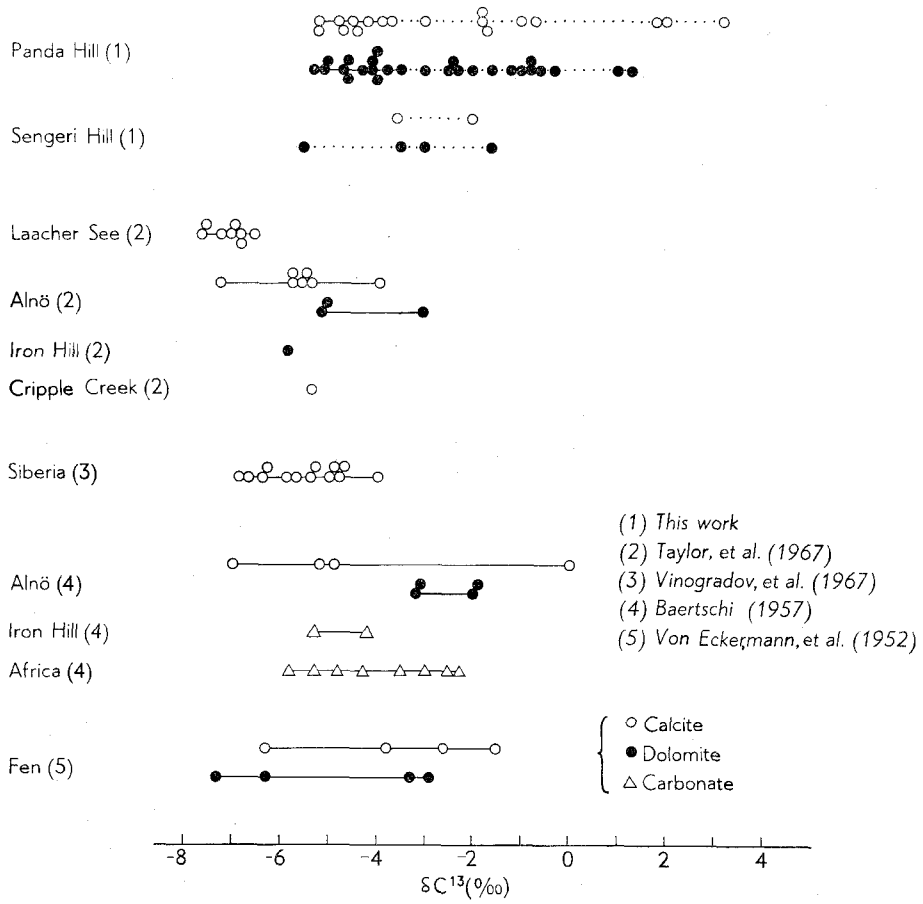

FIG. 19. The carbon isotope ratios of carbonates in carbonatites.

mites are low in δO^{18}, from 5.90 to 7.74‰, and also low in δC^{13}, from −5.31 to −3.55‰. The five calcites are from sövite consisting chiefly of calcite (01–A, 02–A, 03–A, 04–A) and sövite having pyrochlore-hematite-magnetite-apatite streak (03–B). The fifteen dolomites are from sövite consisting chiefly of calcite (01–A, 02–A, 03–A, 04–A), from sövite having apatite-pyrochlore-hematite- magnetite streaks (01–B, 03–B, 04–B), sövite rich in magnetite and pyrochlore (02–C), beforsite consisting chiefly of dolomite (05–A, 11–A), beforsite rich in magnetite (06 I–C), carbonatized pseudotrachyte fragment (05–G) and ochreous mixture of fine-grained fragments of pseudotrachyte and beforsite (05–H・I) in ochreous carbonatitic mixed breccia, and a calcite-dolomite veinlet in beforsite (06 I–D).

The five calcites are from unaltered sövite. Eleven of the 15 dolomites are from unaltered sövite and beforsite, and the other four dolomites are related to later hydrothermal alteration, though they are considered practically

unaffected by such alteration.

Four calcites from sövite poor in metal oxide are in the range of δO^{18}, from 5.90 to 6.85‰, and one calcite from sövite rich in metal oxide shows higher δO^{18}, of 7.67‰. Four dolomites from the former sövite are low in δO^{18}, from 6.39 to 7.32‰, and four dolomites from the latter sövite (rich in metal oxide) are high in δO^{18}, from 6.61 to 7.74‰.

Between the carbonates in any single carbonatite specimen, carbonate occurring in the part poor in metal oxide is always lower in δO^{18} than that from the part rich in metal oxide; *e.g.* calcite (03-A) is 6.03‰, and calcite (03-B) is 7.67‰ in δO^{18} value. It is therefore concluded that carbonate coexisting with abundant metal oxide becomes enriched in δO^{18}.

In the following discussion, the isotope ratios of the carbonates in the field delineated in Fig. 17 are considered to be of primary Mbeya carbonatites. In comparison with the probable field of primary igneous carbonatite proposed by Taylor *et al.* [29], the field of primary Mbeya carbonatite is similar in δO^{18} and a few per mil higher in δC^{13}.

(*4*) *Carbonates showing slightly high δO^{18} and lower δC^{13} values:*

As shown in Fig. 17, two calcites are slightly high in δO^{18}, from 9.01 to 9.66‰, in spite of low δC^{13} value. These two calcites are both from sövite having an apatite-pyrochlore-hematite-magnetite streak (01-B, 04-B). Metal oxides such as magnetite commonly have low δO^{18} values. According to Taylor and Epstein [28], four magnetites from the California Batholith (Quartz monzonite, granodiorite, hornblende gabbro) are low in δO^{18}, from 1.6 to 2.3‰. It is therefore considered that calcites coexisting with relatively abundant metal oxides may become slightly enriched in δO^{18}.

(*5*) *Comparison between the isotope ratios of primary Mbeya carbonatite and those of sedimentary carbonates:*

Marine carbonates are richer in heavier isotopes, and the δC^{13} values range from -3 to $+4$‰ and the δO^{18} values range from 24 to 30‰. The oxygen isotope ratio of carbonate precipitated from aqueous solution depends on temperature and δO^{18} of the water, and the carbon isotope ratio depends on temperature and δC^{13} of dissolved carbon dioxide. Carbonate becomes enriched in the heavier isotopes with decrease in temperature, especially at temperatures lower than 800°C for oxygen and lower than 300°C for carbon, as shown in Figs. 20 and 21. Since marine carbonates are precipitated in cold sea water, they are enriched in O^{18} and C^{13}. The isotope ratios of fresh water carbonates are considerably lower than those of marine carbonates, because fresh water is enriched in lighter isotopes, and biogenic CO_2, itself extremely low in δC^{13} and δO^{18}, participates in the formation of fresh water carbonate. Fresh water carbonates generally lie in the range of δO^{18} from 15 to 25‰.

The isotope ratios for the majority of ancient carbonates lie in a spread

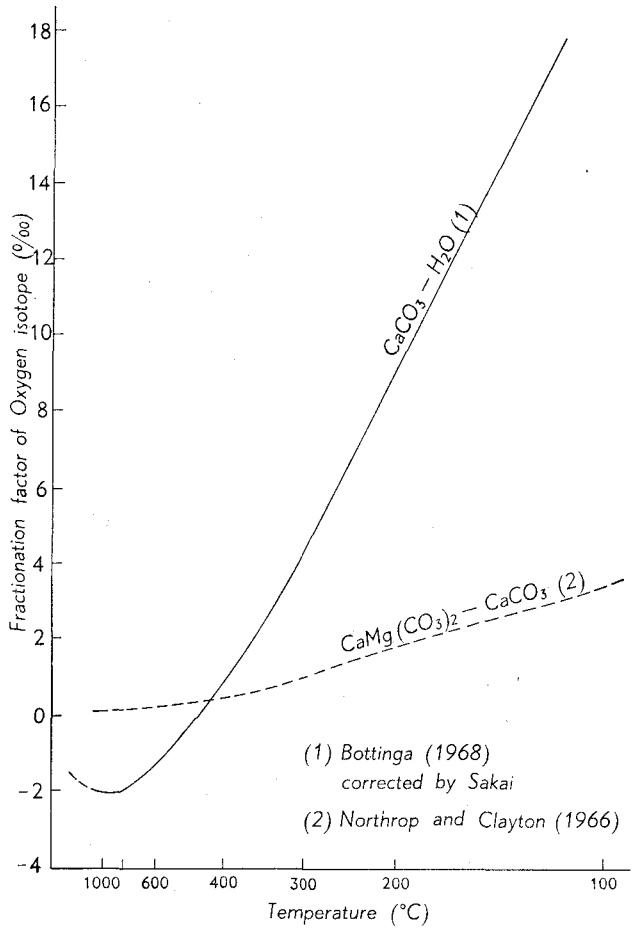

FIG. 20. Oxygen isotope fractionations between calcite and water, and between dolomite and calcite.

from those of marine carbonates to those of fresh water carbonates. Thermal metamorphism has little effect on the initial isotope ratios [12]. A few hydrothermal calcites have δ-values in the field delineated as primary Mbeya carbonatitic carbonates, but the majority of hydrothermal calcites have widely spread δ-values owing to their different physicochemical conditions and different sources of carbon.

Provided that melting of limestone has occurred in association with primary igneous rocks in the deep crust, the oxygen isotopes of the former may be exchanged with those of the igneous rocks and lowered to the value of the latter. Because the carbon content of igneous rocks is low, however, the carbon isotope ratio of the resulting carbonatite would be expected to vary considerably according to the amounts of assimilated limestone.

The isotope ratios of carbonates in carbonatites are substantially different from those of sedimentary carbonates, and it is difficult to imagine a natural process which would change the isotope ratios of sedimentary carbonates to those of carbonatitic carbonates.

(6) Oxygen isotope of carbonatitic carbonates:

The oxygen isotope ratios of the Mbeya carbonatitic carbonates show only little variation from those of specimens analysed by Taylor *et al.* [29] as shown in Fig. 18. The oxygen isotope ratios in ultramafic and mafic rocks throughout the world are relatively uniform, 6±0.5‰ [24]. As compared with this value, carbonatitic carbonates are higher in δO^{18} by 0 to 3‰. Carbonate melt may be enriched in δO^{18} relative to coexisting silicate melt by zero to a few per mil. Magmatic water holds a high concentration of δO^{18} at elevated temperatures [24]. Therefore, when magmatic water is introduced into a carbonate melt, transfer of heavy oxygen would also take place.

The oxygen isotope ratios of carbonatitic carbonates may therefore be explained by the assumption that the carbonatitic magma or CO_2-rich magma originates by partial melting or fractional crystallization from a primary mafic or ultramafic magma in the lower crust or upper mantle. The exact chemical nature of the mafic or ultramafic magma is not clear. In connection with this point, it is noticed that according to the results of some experimental studies of carbonatitic system, normal peridotite magmas are incapable of yielding a residual lime-rich carbonatite magma by crystallization processes, but there is some evidence that crystallization of an alkali peridotite magma might yield a residual alkali-rich carbonatite magma [36].

(7) Fractionation between coexisting calcites and dolomites:

The isotope fractionation among coexisting minerals can be applied to goethermometry. As is seen in Fig. 20, at high temperatures, the fractionation between dolomite and calcite is too small to infer the formation temperature. As clearly shown in Table 2, the fractionation factors of oxygen isotope between the coexisting carbonates in the primary Mbeya carbonatite

TABLE 2. THE OXYGEN ISOTOPE RATIOS OF COEXISTING CALCITE AND DOLOMITE IN THE PRIMARY MBEYA CARBONATITE (DIGESTED FROM TABLE 1)

Specimen	Calcite δO_c^{18}, ‰	Dolomite δO_d^{18}, ‰	Δ $\delta O_d^{18}-\delta O_c^{18}$, ‰
2-68092301-A	6.85	7.02	0.17
02-A	5.90	6.39	0.49
03-A	6.03	6.67	0.64
03-B	7.67	7.74	0.07
04-A	6.21	6.69	0.48

range from 0.1 to 0.6‰, suggesting that the carbonates crystallized at temperatures above 400°C.

(8) Carbon isotope of carbonatitic carbonates:

The fractionation factor between diamond and graphite is nearly zero at high temperatures, as shown in Fig. 21. Therefore, the carbon isotope ratio of diamond is often assumed to be equal to that of carbon, probably graphite, in the lower crust or upper mantle. Diamonds range in δC^{13} from −8.9 to −1.9‰ [32]. These data are almost identical to those of carbonatitic carbonates. The carbon isotope ratios of the carbonatitic carbonates are summarized in Fig. 19. In the following discussion, the data showing high δC^{13} values by the present authors, Von Eckermann, *et al.* [34], and Baertschi [1] are excluded since they have been altered from the original values by weathering or by deuteric and hydrothermal alteration.

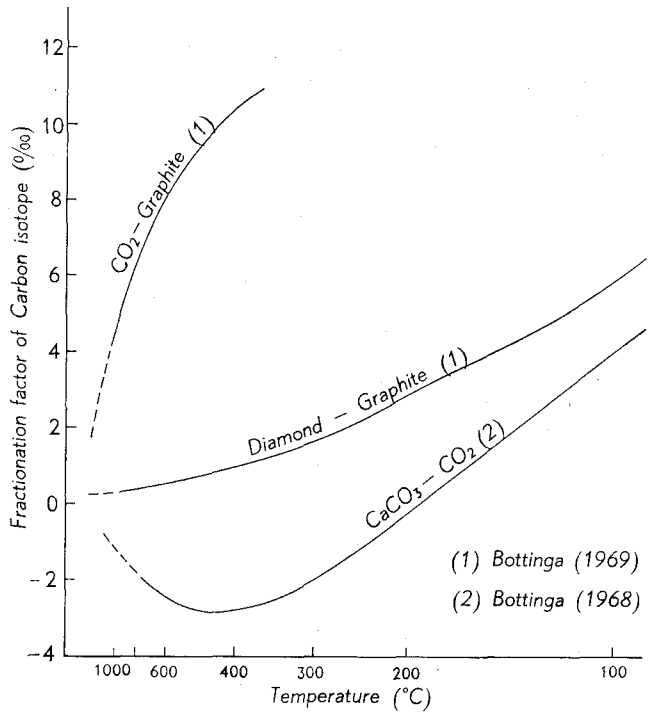

FIG. 21. Carbon isotope fractionations between carbon dioxide and graphite, between diamond and graphite, and between calcite and carbon dioxide.

Roedder [23] showed that inclusions of highly compressed, generally liquefied, nearly pure CO_2, usually with glass (presumably basaltic), were found in the minerals of every occurrence of olivine-bearing nodules in basalts through-

out the world. CO_2 is generally available in parent magmas, and in the evolution of the suites of alkalic rocks characteristically associated with carbonatites a simultaneous separation and enrichment of the CO_2 phase take place. Carbonatitic alkalic complexes represent the end products of a special set of environmental circumstances that have combined successfully to produce local, extraordinary concentrations of CO_2 and its mineral derivatives. As shown in Fig. 21, the fractionation factors of carbon isotopes can be expected to approach unity with increasing temperature. Therefore, in order to keep the original value (δC^{13}: -3.2 to -7.7‰) for carbonatitic magma, the evolution of CO_2 from original material and the concentration of CO_2 into the magma must have been accomplished at temperatures above 1000°C. But, if the processes took place at lower temperatures, the carbon isotope ratio should have varied with temperature. If diamonds are similar in δC^{13} to the material in the lower crust or upper mantle, the carbon isotope ratios of the carbonatitic carbonates suggest that carbonatitic magma may be formed at temperatures above 1000°C.

According to the result of an experimental study on the system CaO-CO_2-H_2O to 40 Kilobars pressure, the main effect of increasing pressure is to increase the solubility of the volatile components in the liquids and the compositions of the liquid and vapour phases move significantly closer together than at 1 Kb. Univariant melting reaction of $CaCO_3+Ca(OH)_2=$LIQUID occurs at 670°C under 40 Kb [38].

(9) *Regional differences in isotopic values of carbonatites:*

The carbon isotope ratios of carbonatitic carbonates from different regions of the world range from -3.2 to -7.7‰, although those from one region lie within a few per mil difference from each other. On the other hand, the oxygen isotope ratios range from 5.9 to 8.4‰ and those from different regions (Mbeya, Laacher See, and Alnö) are similarly distributed within the same range. The carbon isotope ratios of diamonds also show similar tendency with those of carbonatitic carbonates.

Kimberley diamonds are enriched in C^{13} relative to other diamonds, *i.e.*, the diamonds range in δC^{13} from -2.4 to -4.7‰ [5]. On the other hand, diamonds from Yakutia, Siberia, range in δC^{13} from -5.6 to -8.8‰ [32, 33].

Similarly, δC^{13} of carbonatitic carbonates from Mbeya and other African localities (Chilwa and Tundulu of Malawi; SE Uganda; Spitzkop and Pretoria in the Transvaal; Baertschi, [1]) are enriched in δC^{13} relative to other carbonatitic carbonates and range from -2.3 to -5.8‰. On the other hand, the Siberian carbonatitic carbonates range from -4.1 to -6.9‰ [32, 33]. This might be a mere accident, but suggests a possibility that the carbon isotope ratios in the lower crustor upper mantle are distributed heterogeneously, or that the African data described above are influenced by unknown factors peculiar to the African rift valley. Until more data are collected throughout the world, the possibility cannot be further elucidated.

ACKNOWLEDGEMENTS

The present authors would like to express their sincere appreciation to Professor Isao Matsuzawa, Director of their second scientific expedition to Africa in 1968, and to Professor Takeo Watanabe and to Associate Professor Kokichi Ishioka, all three of Nagoya University, for their advice and encouragement.

The present authors are also indebted to Professor Hitoshi Sakai of the Institute for Thermal Spring Research, Okayama University for his advice and offering his mass spectrometer to their use.

Thanks are extended to Drs. John Walsh and Martin C. G. Clarke of Mine and Geological Department, Ministry of Natural Resources of Kenya, and to Dr. L. A. J. Williams of the University College of Nairobi and Dr. Barry Dawson of the University of St. Andrews, for their advice and critical reading of the present paper in manuscript. Their thanks go to Mr. John F. Castello of Mines and Geological Department of Kenya for his assistance in drawing and to Dr. Tsuneo Sôma of Toyama University for his assistance in microphotography.

Many facilities for field work were made available by Professor W. Chagula of the University College of Dar es Salaam, by Mr. G. Luena, Assistant Commissioner of Mineral Resources Division at Dodoma, Ministry of Commerce and Industries of Tanzania, by Mr. Oswald Marwa, Mbeya Regional Commissioner of Tanzania, by Mr. William Magurusa, Regional Mining officer at Mbeya of Tanzania, by the members of Embassy of Japan at Dar es Salaam of Tanzania and at Nairobi of Kenya and by Messrs. Masoud M. Issa and Bakari s/o Mahamed at Dar es Salaam of Tanzania, to whom the authors express their deep gratitude.

This work was supported in part by the Grant-in-Aid for Scientific Research of the Ministry of Education, for which the authors would like to record their thanks.

REFERENCES

[1] BAERTSCHI, P., Messung und Deutung relativer Häufigkeitsvariationen von δO^{18} und δC^{13} in Karbonatgesteinen und Mineralien: *Schweiz. Min. Petr. Mitt.*, **37**, 73-152 (1957).

[2] BOTTINGA, Y., Calculation of fractionation factors for carbon and oxygen isotopic change in the system calcite—carbon dioxide—water: *J. Phys. Chem.*, **72**, 800-808 (1968).

[3] BOTTINGA, Y., Carbon isotope fractionation between graphite, diamond and carbon dioxide: *Earth Planet. Sci. Letters*, **5**, 301-307 (1969).

[4] CLARKE, M. C. G., The geology of the southern part of Homa mountain carbonatitic complex, western Kenya, with particular reference to the petrology of the alkaline silicate, metasomatic and melilite bearing suites: Manuscript (pp. 291 with geol. map) of a thesis presented for the degree of Doctor of philosophy in the University of Leicester, March 1968.

[5] CRAIG, H., Isotopic standards for carbon and oxygen, correction factors for mass spectrometric analysis of carbon dioxide: *Geochim. et Cosmochim. Acta*, **12**, 133-149 (1957).

[6] CRAIG, H., Standard for reporting concentration of deuterium and oxygen—18 in natural waters: *Science*, **133**, 1833-1834 (1961).

[7] DAIMON, N., SUWA, K., and YAMAMOTO, K., The synthesis of M_n^g mica (In Japanese with English summary): *J. Industry and Chemistry, Japan*, **46**, 1906-1908 (1961).

[8] DAWSON, J. B., The geology of Oldoinyo Lengai: *Bull. Volcanolog.*, **24**, 349-387 (1962).

[9] EPSTEIN, S., GRAF, D. L., and DEGENS, E. T., Oxygen isotpe studies on the origin of dolomites: Isotopic and Cosmic Chemistry (edited by Craig, H., Wasserburg, G. J., and Miller, S. L.), 169-180, North Holland (1964).

[10] FAWLEY, A. P., and JAMES, T. C., A pyrochlore (columbium) carbonatite, southern Tanganyika: *Econ. Geol.*, **50**, 571-585 (1955).

[11] FICK, L. J., and VAN DER HEYDE, C., Additional data on the geology of the Mbeya carbonatite: *Econ. Geol.*, **54**, 842-872 (1959).

[12] FRIEDMAN, I., and HALL, W. E., Fractionation of O^{18}/O^{16} between coexisting calcite and dolomite: *J. Geol.*, **71**, 238-243 (1963).

[13] FRITZ, R., Oxygen and carbon isotopic composition of carbonates from the Jura of Southern Germany: *Canadian J. Earth Sci.*, **4**, 1247-1267 (1967).

[14] GITTINS, J., Further evidence for the existence of carbonatite magmas: *Canadian Mineralogist*, **7**, 87 (1963).

[15] GITTINS, J., and TUTTLE, O. F., The system CaF_2-$Ca(OH)_2$-$CaCO_3$: *Am. J. Sci.*, **262**, 66-75 (1964).

[16] GOLDSMITH, J. R., and HEARD, H. C., Subsolidus phase relations in the system $CaCO_3$-$MgCO_3$: *J. Geol.*, **69**, 45-74 (1961).

[17] HEINRICH, E. W., The geology of carbonatites: Rand McNally and Co., 608 p., Chicago (1966).

[18] JAMES, T. G., and MCKIE, D., The alteration of pyrochlore to columbite in carbonatites in Tanganyika: *Mineralog. Mag.*, **31**, 889-900 (1958).

[19] JOHNSON, R. L., The geology of the Dorowa and Shawa carbonatite complexes,

Southern Rhodesia: *Proc. Geol. Soc. South Africa*, **64**, 101-145 (1961).

[20] MILLER, J. A., and BROWN, P. E., The age of some carbonatite activity in south-west Tanganyika: *Geol. Mag.*, **100**, 276-279 (1963).

[21] NAKAMICHI, O., KONISHI, K., and SAKAI, H., On the isotopic analyses of oxygen and carbon of marine biogenic carbonates such as corals and pelecypods (in Japanese): *Mass Spectroscopy*, **17**, 500-508 (1969).

[22] NORTHROP, D. A., and CLAYTON, R. N., Oxygen-isotope fractionation in the systems containing dolomite: *J. Geol.*, **74**, 174-196 (1966).

[23] ROEDDER, E., Liquid CO_2 inclusions in olivine-bearing nodules and phenocrysts from basalts: *Am. Mineralogist*, **50**, 1746-1782 (1965).

[24] SAKAI, H., and HONMA, H., Oxygen isotope chemistry in rock-forming processes (in Japanese with English summary): Special paper No. 5 (Isotope Petrology and Geochemistry), 9-26, Geol. Soc. Japan (1969).

[25] SHARMAN, T., and CLAYTON, R. N., Measurement of O^{18}/O^{16} ratios of total oxygen of carbonates: *Geochim. et Cosmochim. Acta*, **29**, 1347-1353 (1965).

[26] SNELLING, N. J., Age determinations on three African carbonatites: *Nature*, **205**, 491 (1965).

[27] SUTHERLAND, D. S., Nomenclature of the potassic feldspathic rocks associated with carbonatites: *Bull. Geol. Soc. Am.*, **76**, 1409-1412 (1965).

[28] TAYLOR, H. P. Jr., and EPSTEIN, S., Relationship between O^{18}/O^{16} ratios in coexisting minerals of igneous and metamorphic rocks, Part I and II: *Bull. Geol. Soc. Am.*, **73**, 461-480 and 675-697 (1962).

[29] TAYLOR, H. P. Jr., FRECHEN, J., and DEGENS, E. T., Oxygen and carbon isotope studies of carbonatites from the Laacher See district, West Germany and the Alnö district, Sweden: *Geochim. et Cosmochim. Acta*, **31**, 407-430 (1967).

[30] TUTTLE, O. F., and GITTINS, J., Carbonatites: Instersci. Publishers, 591 p., New York (1966).

[31] VAN DER VEEN, A. H., A study of pyrochlore: Verhandelingen Kininklijk Nederlands geologisch mijnbouwkundig genootschap. Geologische serie, **22**, 1-188 (1963).

[32] VINOGRADOV, A. P., KROPOTOVA, O. I, and USTINOV, V. I., Possible sources of carbon in diamonds as indicated by the C^{13}/C^{12} ratios: *Geokhimiya*, 643-651 (1965) (*Int. Geochemistry*, **3**, 495-503 (1966)).

[33] VINOGRADOV, A. P., KROPOTOVA, O. I., EPSHTEIN, E. M., and GINENKO, V. A., Isotopic composition of carbon in calcite representative of different temperature stages of carbonatite formation and the problem of genesis of carbonatites: *Geokhimiya*, 499-509 (1967) (*Int. Geochmistry*, **4**, 431-441 (1967)).

[34] VON ECKERMANN, H., VON UBISCH, H., and WICKMAN, F. E., A preliminary investigation into the isotopic composition of carbon from some alkaline intrusions: *Geochim. et Cosmochim. Acta*, **2**, 207-210 (1952).

[35] VON ECKERMANN, H., Kimberlite-carbonatite symposium: *Mineralog. Soc. India*, IMA 5, 1-148 (1966).

[36] WYLLIE, P. J., Experimental studies of carbonatite problems: The origin and differentiation of carbonatite magmas: Carbonatites (Edited by Tuttle, O. F., and Gittins, J.) 311-352, Interscience Publishers (1966).

[37] WYLLIE, P. J., and TUTTLE, O. F., The system CaO-CO_2-H_2O and the origin of carbonatites: *J. Petrology*, **1**, 1-46 (1960).

[38] WYLLIE, P. J., and BOETTCHER, A. L., Liquidus phase relationships in the system CaO-CO_2-H_2O to 40 kilobars pressure with petrological applications: *Am. J. Sci.*, Schairer Vol. **267-A**, 489-508 (1969).

[39] ZHABIN, A. G., and CHEREPIVSKAYA, G. Y., Carbonatite dikes as related to ultrabasic-alkalic extrusive igneous activity: *Doklady Akad. Nauk SSSR.*, **160**, 135-138 (1965).

EXPLANATION OF PLATES

PLATE I

1. Zoned pyrochlore (right), magnetite-hematite (left) and apatite (upper) in pale reddish brown-coloured part (01-B) of sövite (2-68092301) from Panda Hill, Tanzania; one nicol; ×35.

   01-B: Magnetite and hematite>pyrochlore=calcite>dolomite=apatite=biotite

2. Biotite (centre) and apatite (upper) in pale reddish brown-coloured part (01-B) of sövite (2-68092301) from Panda Hill, Tanzania; one nicol; ×35.

3. Calcite and dolomite in white-coloured part (02-A) of sövite (2-68092302) from Panda Hill, Tanzania; nicols crossed; ×35.

   02-A: Calcite≫dolomite≫biotite=apatite=magnetite>pyrochlore

4. Pyrochlore (upper and lower), magnetite (centre and right) and carbonatized fibrous amphibole (upper centre) in brown-coloured part (02-C) of sövite (2-68092302) from Panda Hill, Tanzania, one nicol; ×35.

   02-C: Calcite≥magnetite>pyrochlore>amphibole≥dolomite≥apatite>pyrite

1

2

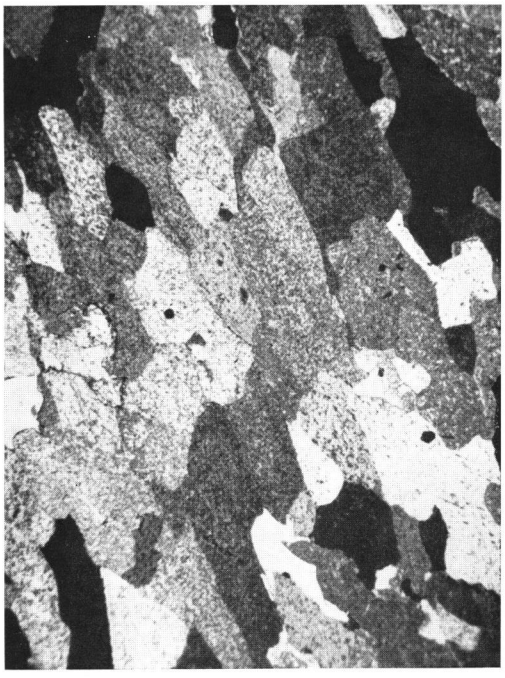

3

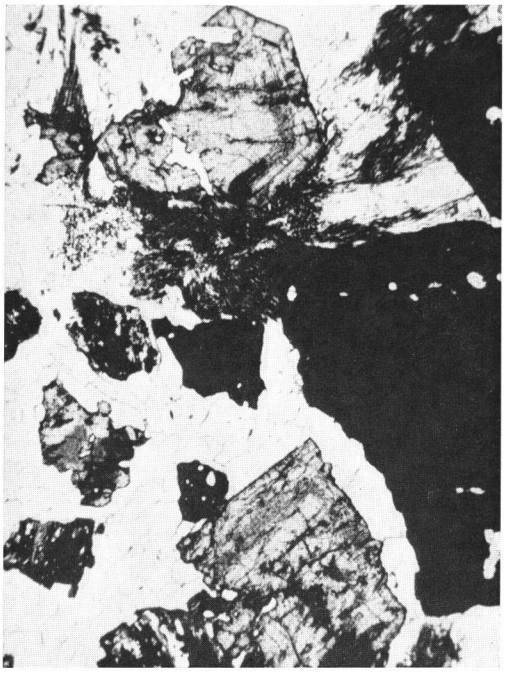

4

PLATE II

1. Carbonatized biotite (centre) in white-coloured part (03-A) of sövite (2-68092303) from Panda Hill, Tanzania; one nicol; ×35.

   03-A: Calcite≫dolomite≫pyrochlore=apatite=biotite

2. White-coloured sövite with accessory dolomite, pyrochlore, apatite and biotite (03-A) of sövite (2-68092303) from Panda Hill, Tanzania; nicols crossed; ×35.

3. Apatite (granular and white), magnetite-hematite (black), pyrocholre (central left) and carbonatized amphibole (central right) in pale brown-coloured part (03-B) of sövite (2-68092303) from Panda Hill, Tanzania; one nicol; ×35.

   03-B: Apatite≥magnetite and hematite≥pyrochlore≥calcite≫dolomite>biotite =amphibole

4. Pyrochlore (lower right) in white-coloured part (04-A) of sövite (2-68092304) from Panda Hill, Tanzania; one nicol; ×35.

   04-A: Calcite≫dolomite≫pyrochlore=apatite

1

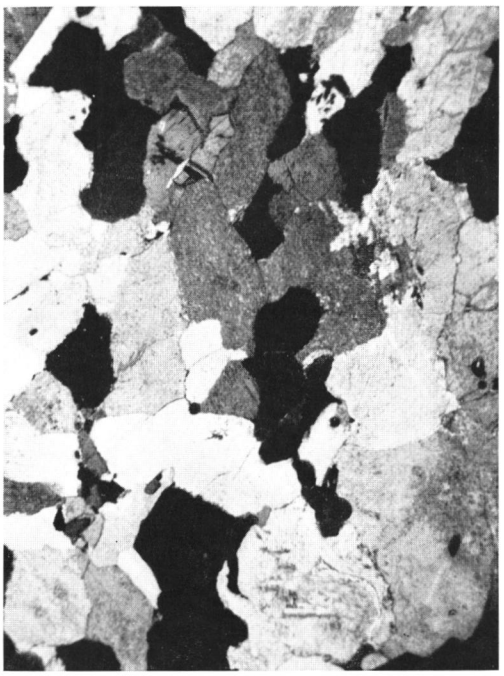

2

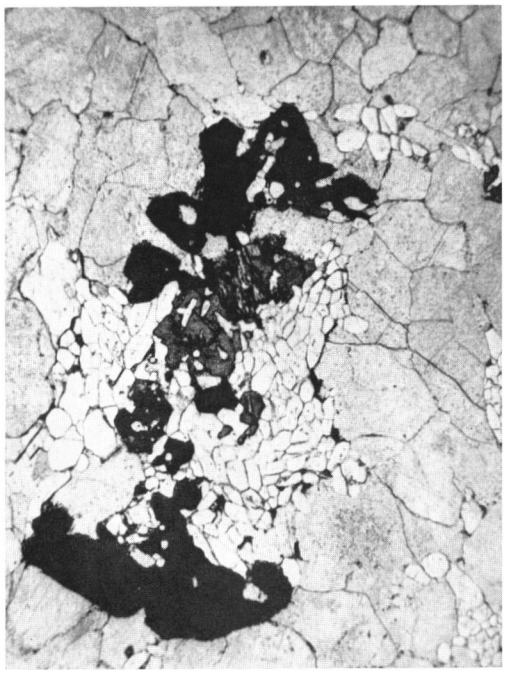

3

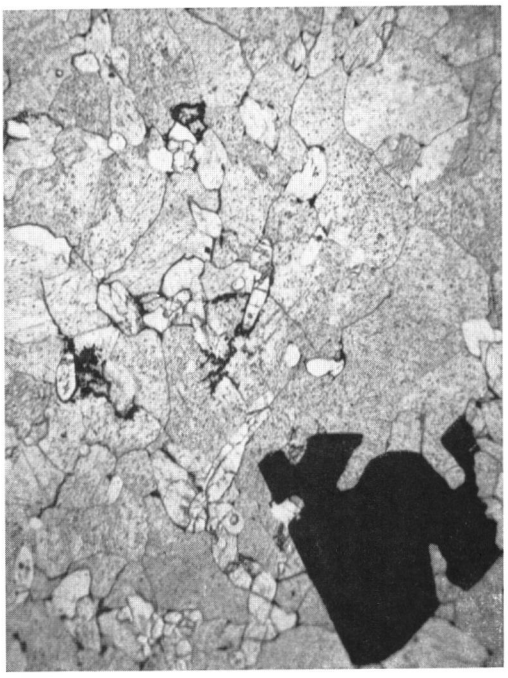

4

PLATE III

1. White-coloured sövite with accessory dolomite, pyrochlore and apatite (04-A) of sövite (2-68092304) from Panda Hill, Tanzania; nicols crossed; ×35.
   04-A: Calcite≫dolomite≫pyrochlore=apatite

2. Hematite-magnetite (black) in orange-brown-coloured part (04-B) of sövite (2-68092304) from Panda Hill, Tanzania; one nicol; ×35.
   04-B: Calcite≥magnetite and hematite>amphibole=dolomite≥apatite

3. Magnetite-hematite (black) and quartz-carbonate-leucoxene intergrowth pseudomorph after magnetite (upper and lower centre) in orange-brown-colored part (04-B) of sövite (2-68092304) from Panda Hill, Tanzania, one nicol; ×35.

4. Calcite veinlet (04-D, less turbid, from upper right to lower left) and magnetite-hematite (lower) in sövite (2-68092304) from Panda Hill, Tanzania; one nicol; ×35.

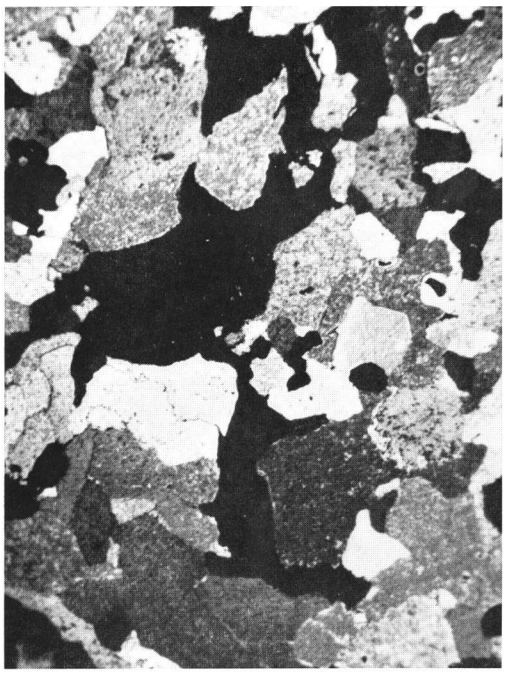

1

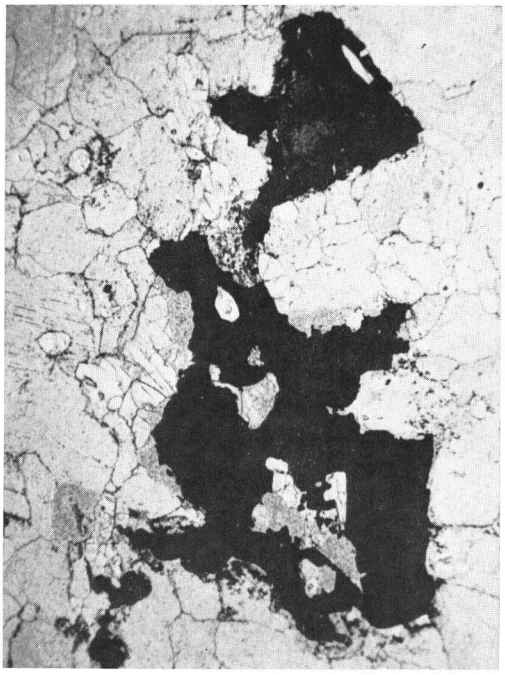

2

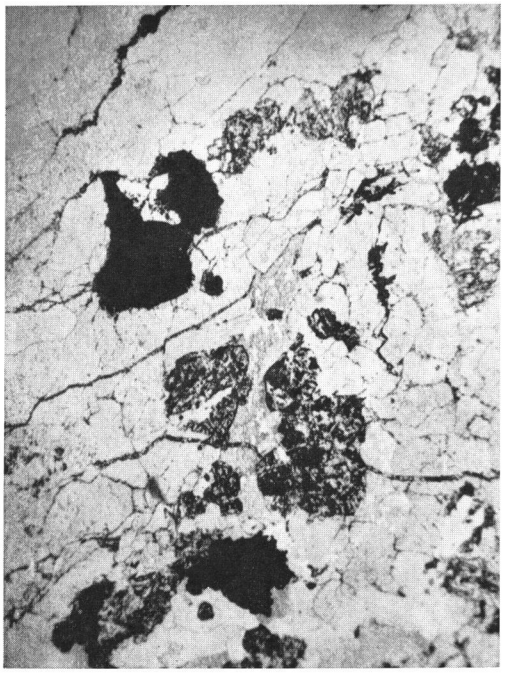

3

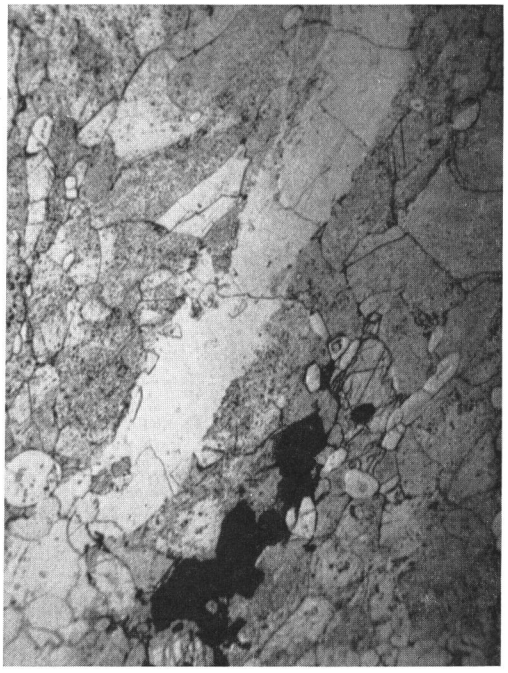

4

PLATE IV

1. Boundary between white-coloured part (04-A, left white-grey part) and fine-grained creamy white-coloured part (04-E, right dark grey part), and calcite veinlet (04-D, from upper left to lower right) in sövite (2-68092304) from Panda Hill, Tanzania; one nicol; ×35.

   04-A: Calcite≫dolomite≫pyrochlore=apatite

   04-E: Dolomite≫apatite=barite=fluorite

2. Calcite veinlet (04-D, from upper right to lower left and from upper to lower) in fine-grained creamy white-coloured part (04-E) of sövite (2-68092304) from Panda Hill, Tanzania; one nicol; ×35.

3. Fine-grained creamy white-coloured hydrothermally altered dolomite-rich part with apatite, barite and fluorite (04-E) of sövite (2-68092304) from Panda Hill, Tanzania; nicols crossed; ×35.

4. Boundary between white-coloured (06 I-A, left white-gray part) and fine-grained white-coloured part (06 I-E, right gray part) in beforsite (2-68092306 1) from Panda Hill, Tanzania; one nicol; ×35.

   06 I-A: Dolomite≥calcite>apatite>quarz=fluorite≥magnetite and hematite

   06 I-E: Dolomite≫barite>fluorite=quartz

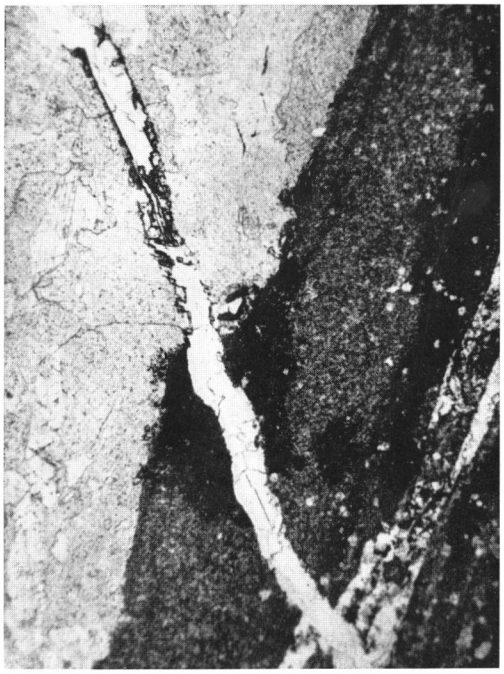

1

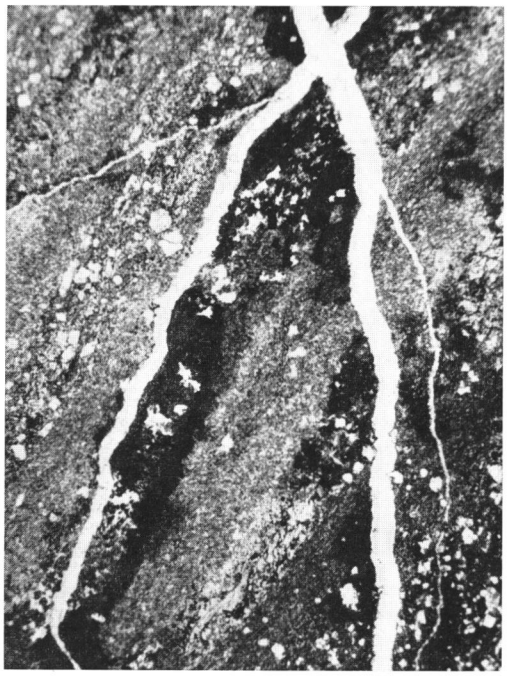

2

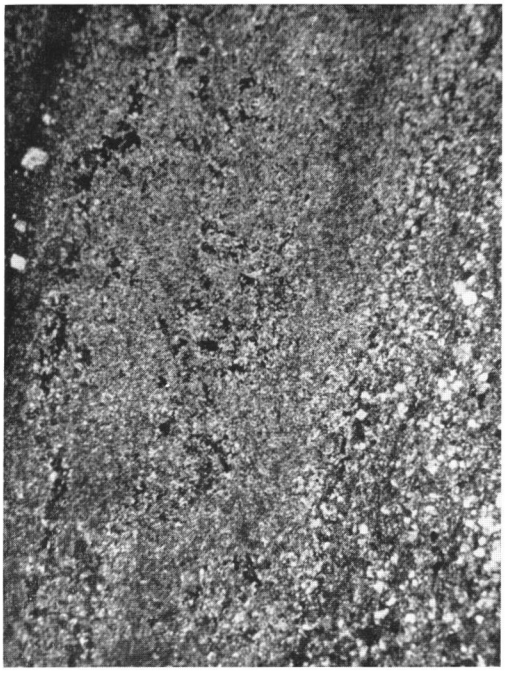

3

4

PLATE V

1. Quartz bearing calcite-dolomite veinlet (06 I-D, from upper right to lower left) through white-coloured part (06 I-A) of beforsite (2-68092306 I) from Panda Hill, Tanzania; one nicol; ×35.

   06 I-A: Dolomite≥calcite>apatite>quartz=fluorite≥magnetite and hematite
   06 I-D: Dolomite>calcite≫quartz

2. Quartz-carbonate-leucoxene intergrowth pseudomorph after magnetite (lower right and lower left) and carbonatized amphibole (upper) in brown-black-coloured part (06 I-C) of beforsite (2-68092306 I) from Panda Hill, Tanzania; one nicol; ×35.

   06 I-C: Magnetite=dolomite>apatite=pyrochlore=tremolite

3. White- or cream-coloured hydrothermally altered beforsite with quartz, barite, magnetite and calcite (2-68092306 II-A) from Panda Hill, Tanzania. This beforsite is characterized by the aggregate of medium-grained anhedral dolomite with ambiguous outline and very fine-grained anhedral dolomite, calcite and barite grains. This carbonate texture is in strong contrast to that of carbonates in sövite (01, 02, 03, 04) and beforsite (11). One nicol; ×35.

   06 II-A: Dolomite≫quartz>barite>magnetite≥calcite

4. Phenocryst-like coarse-grained dolomite (centre) in groundmass-like fine-grained dolomite in white-coloured part (11-A) of beforsite (2-68092311) from Sengeri Hill, Tanzania; one nicol; ×35.

   11-A: Dolomite≫potassium feldspar≥quartz≫pyrochlore=apatite

1

2

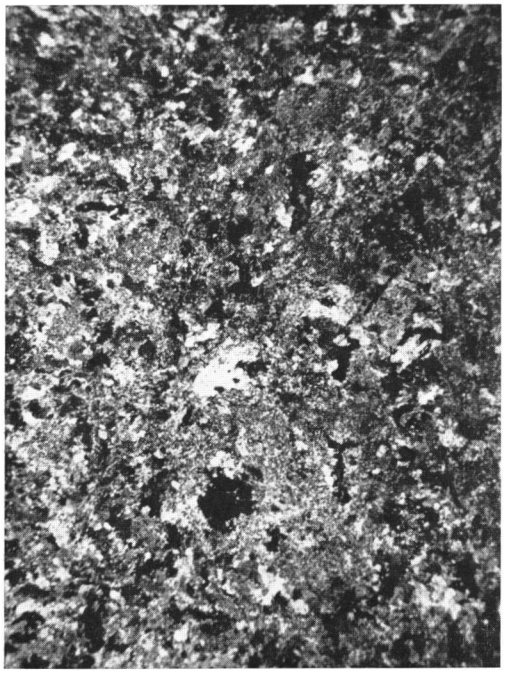

3

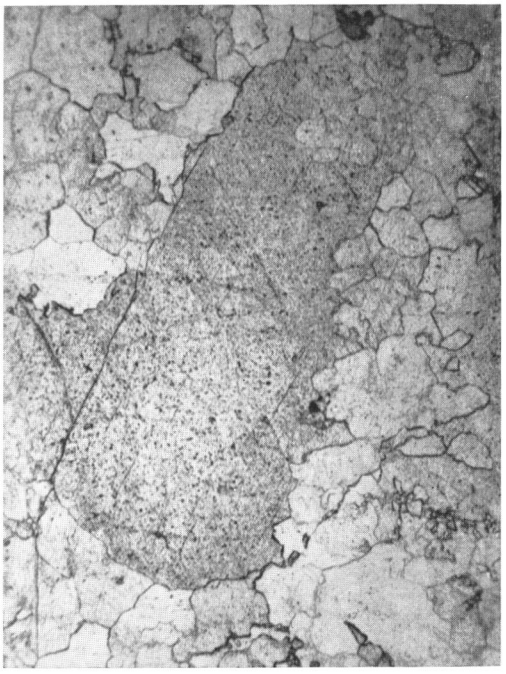

4

PLATE VI

1. White-coloured part (01-A, central left) and pale reddish brown-coloured part (01-B, right) of sövite (2-68092301) from Panda Hill, Tanzania; one nicol; ×6.

   01-A: Calcite≫dolomite>biotite>apatite≥magnetite and hematite=pyrochlore
   01-B: Magnetite and hematite>pyrochlore=calcite>dolomite=apatite=biotite

2. White-coloured part (02-A, left and central right) and brown-coloured part (02-B, central left) of sövite (2-68092302) from Pand aHill, Tanzania; one nicol; ×6.

   02-A: Calcite≫dolomite≫biotite=apatite>magnetite>pyrochlore
   02-B: Calcite≥magnetite>pyrochlore>amphibole≥dolomite≥apatite>pyrite

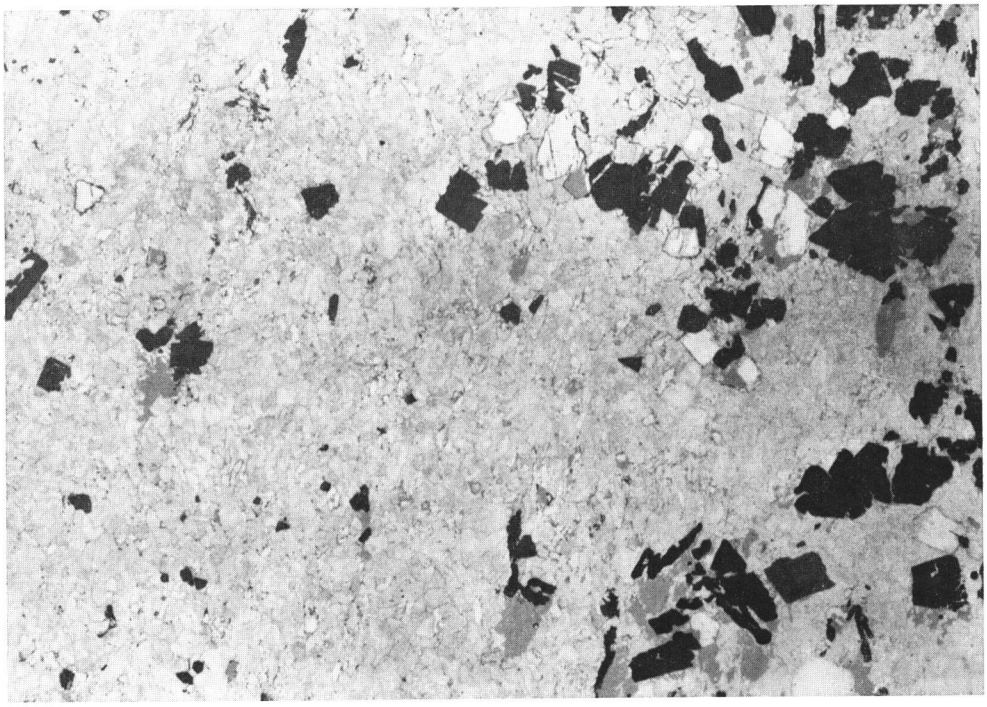

1

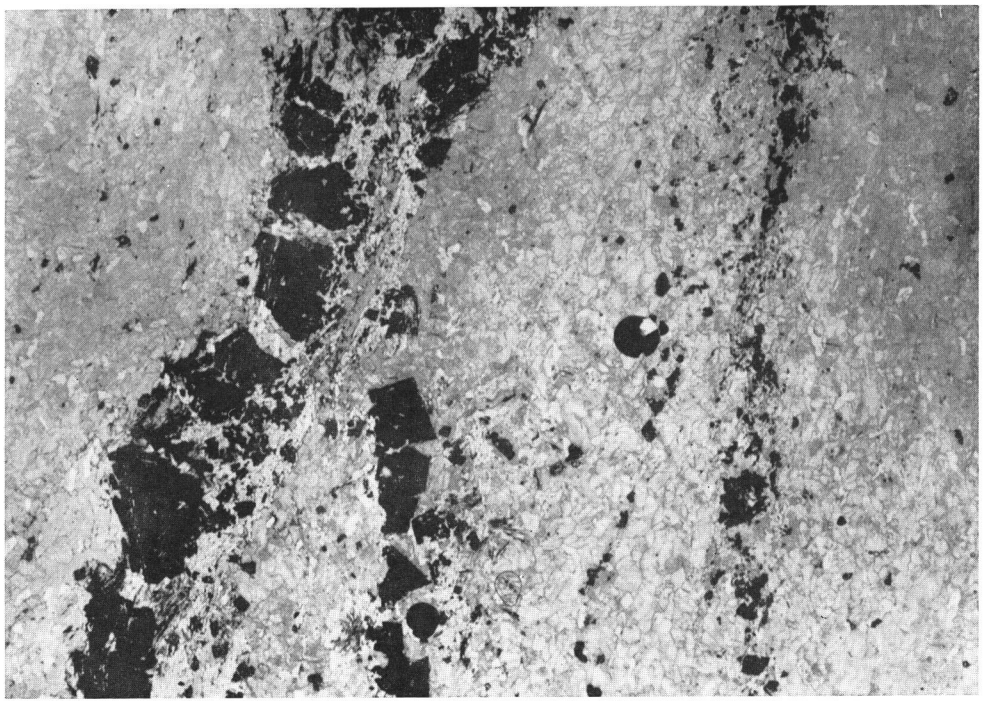

2

PLATE VII

1. White-coloured fragment (05-A, upper and lower right and upper left), pale orange-coloured fragment (05-F, central left and upper central left) and white-grey coloured fragment (05-G, upper and lower left, central and lower right, and upper central) are studded in the mixture of yellow-brown coloured matrix and fine- or medium-grained white-grey coloured fragment (05-H) of ochreous carbonatitic mixed breccia (2-68092305) from Panda Hill, Tanzania; one nicol; ×6.

   05-A: Dolomite≫pyrochlore=apatite>limonite
   05-F: *Dolomite≫calcite>quartz>apatite>limonite*
   05-G: Potassium feldspar>dolomite>calcite>limonite (some 05-G fragments contain quartz and apatite)
   05-H: Dolomite≫calcite>potassium feldspar≧apatite>limonite

2. Fine banding of white-coloured part (07 a-L, greyish black-coloured band in this photograph, *e.g.*, central right and left bands), whity yellow-brown-coloured part (07 a-M, whity grey-coloured band in this photograph, *e.g.*, central band), brown-coloured part (07 a-N, spotted whity grey-coloured band in this photograph), and fluorite-quartz-potassium feldspar-(limonitized) carbonate veinlet (07 a-D, middle left to upper right, and upper left to lower right) of carbonatized pseudotrachyte (2-68092307 a) from Panda Hill, Tanzania; nicols crossed; ×9.

   07 a-L: Potassium feldspar≫quartz=calcite>dolomite>apatite
   07 a-M: Potassium feldspar>quartz>calcite=dolomite>limonite>apatite
   07 a-N: Potassium feldspar≧quartz>calcite=dolomite>limonite>fluorite>hematite>apatite≧sphene

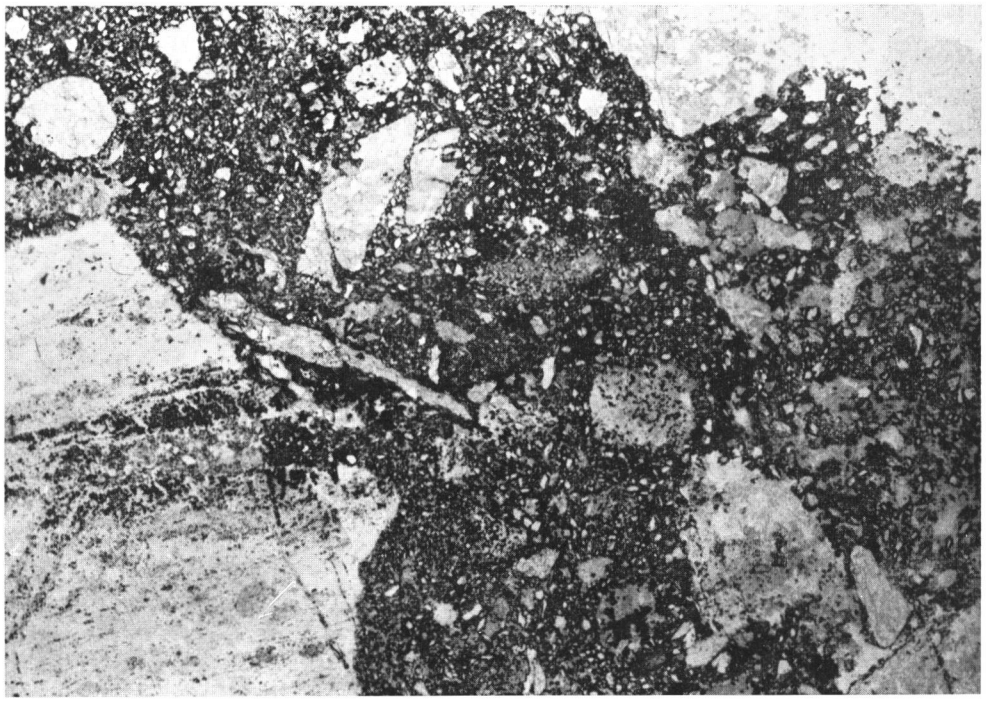

1

2

PLATE VIII

1. Yellow-brown-coloured brecciated matrix (10-J, main area in this photograph) is injected by the transparent kaolinite-quartz-fluorite veinlet (10-D, right, left and central left white-coloured part in this photograph) and is spotted by the fluorite crystal (central right and upper central white-coloured cubic crystal in this photograph). Ochreous carbonatitic pseudotrachyte breccia (2-68092310) from Sengeri Hill, Tanzania; one nicol; ×6.

   10-J : Quartz≫fluorite>dolomite≧calcite≧apatite=potassium feldspar=limonite

2. Phenocryst-like coarse-grained dolomite (upper central left and right) in groundmass-like fine-grained white-coloured part (11-A, main area in this photograph) of beforsite (2-68092311) from Sengeri Hill, Tanzania; nicols crossed; ×9.

   11-A: Dolomite≫potassium feldspar≧quartz≫pyrochlore=apatite

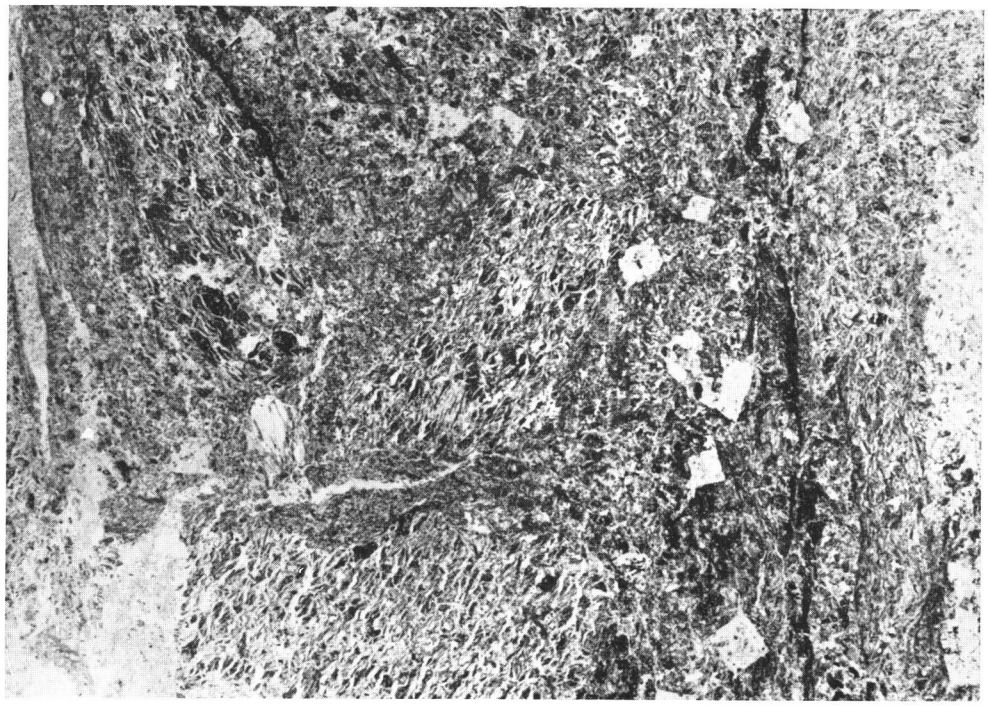

1

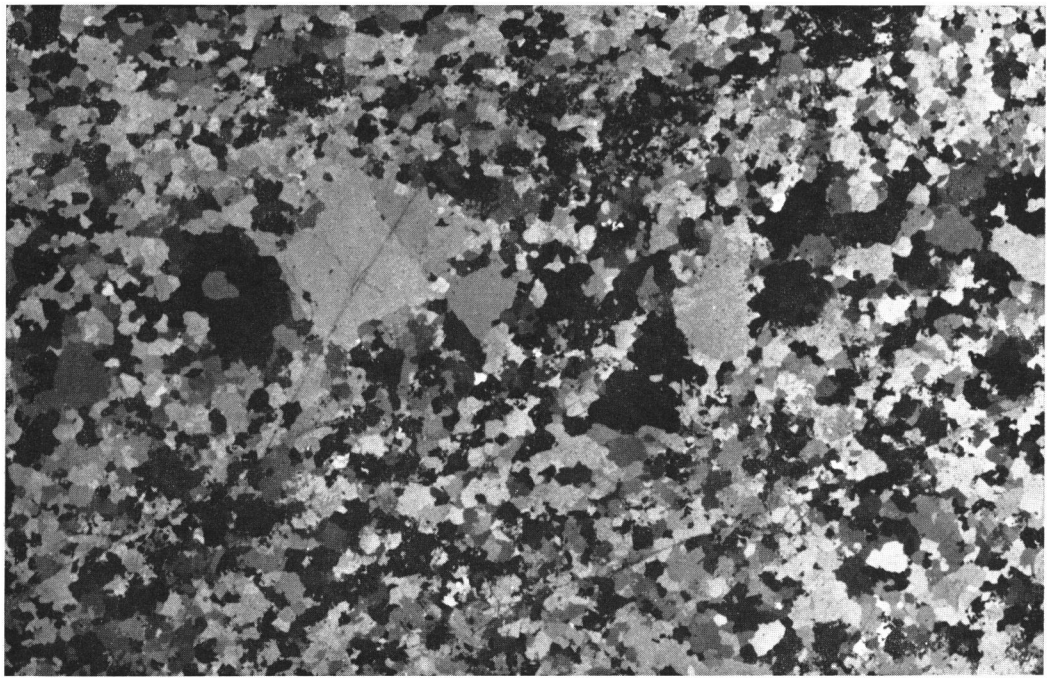

2

PLATE IX

Fine-grained creamy white-coloured part (04-E, upper part), white-coloured part (04-A, central and lower parts) and calcite veinlet (04-D, from upper right to middle left) of sövite (2-68092304) from Panda Hill, Tanzania; nicols crossed; ×9.

04-A: Calcite≫dolomite≫pyrochlore=apatite

04-D: Calcite

04-E: Dolomite≫apatite=barite=fluorite

Gravity measurements of rift valleys in Tanzania

Harumi AOKI

Department of Earth Sciences, Faculty of Science, Nagoya University

(Received 19 August 1969)

ABSTRACT

A gravity survey of rift valley in Tanzania was made over the following three areas;

1) Kigoma as one of the typical rift valleys,

2) Mbeya as the intersection of eastern and western rift systems,

3) Masange as one of the rift faults.

By dense distributions of gravity station, though within small areas, it was found that Bouguer anomalies were evidently related with surface geology as shown in Figs. 3, 4 and 6. Some of anomalies were associated with basic rocks intruded in the Precambrian basement and some were caused by unconsolidated sediments deposited in troughs of rift valleys. These local anomalies, however, may be removed from observation by a reasonable assumption of subsurface material extrapolated from the surface. The residual anomalies thus obtained seem very simple showing a feature of long waves and small amplitudes compared with those associated with sediments or basic rocks.

INTRODUCTION

Gravity observations in East Africa have been promoted for the investigation of rift valleys and their tectonic evolution in connection with the convective current in the mantle. According to Girdler [2], a positive Bouguer anomaly over Red Sea is caused by the intrusion of basic rocks from the mantle. Other typical rift valleys such as Lakes Albert, Tanganyika and Rukwa, however, seem characterized by large negative anomalies which may be attributed to thick sediments and/or to the subsidence of the crust into the mantle. From the geological view point, some of the rift valleys and associated faults in Tanzania show more complicated features compared to those of northern rift valleys. The Gregory rift in Kenya seems decline in the middle of Tanzania, and turns into a fault system till it is intersected by Lakes Rukwa and Nyasa. Big volcanoes and the intrusion of basic rocks are seen at the intersection of east and west rift systems, suggesting a complicated gavity anomaly distribution in this area.

Early gravity measurements in Tanzania had been made by the use of pendulum apparatus. Kohlschütter made gravity observations in both 1899 and 1900. Addition of gravity stations was made by Bullard [1] together with

the result of the first gravity anomaly map of East Africa.

In 1958, the number of gravity station was remarkably increased by the use of gravimeters. That is, the Overseas Geological Survey of England (O.G.S.) made an extensive gravity survey of 10 mile interval along all the main roads in Tanzania. The results were published from the Government of Tanzania in 1967 as the Geophysical Map of Tanzania. The map shows a remarkable relationship of Bouguer anomalies with rift valleys. Contour lines of Bouguer anomaly seem almost pararell to the western rift valleys but not to the eastern rift faults and negative and positive anomalies are locally distributed along western rifts.

Recently, Girdler (personal communication in 1968) made an accurate gravity measurement along the Central Rail Way and along a few routes crossing rift faults and valleys making use of an improved technique in the elevation measurement.

The purpose of the present survey is to investigate the relation between Bouguer anomalies and detailed geological features concerning to rift valleys in Tanzania. The O.G.S. gravity map revealed the distribution of large anomalies over rift zones, but was insufficient in number and in accuracy to enable any final conclusion as to the tectonics of rift valley. Consequently, a more detailed gravity survey was conducted in the dry season of 1968 at three small areas of Kigoma, Mbeya and Masange.

Kigoma is located at the shore of Lake Tanganyika where the gravity anomaly due to single rift valley is expected. On the contrary, Mbeya is located at the intersection of western and eastern rifts. Some information concerning to the relation between two rifts might be obtained through the gravity survey. At the end of the survey, Masange, located 100 miles north of Dodoma, was selected to observe the gravity anomaly associated with the escarpment which was supposed to be a part of the eastern rift fault.

ELEVATION MEASUREMENT

In any area having no precise leveling route, the accuracy of gravity anomaly depends largely on the method of elevation measurement, in which altimeters are frequently used with a suitable correction of atmospheric pressure change. O.G.S., for example, used the leapfrog technique, that is, the simultaneous reading of altimeters between successive two stations along a route. According to Girdler, however, three pairs of altimeter of different design are desirable in order to increase the reliability of elevation measurement.

The method employed here is the combined use of a theodolite and a Thommen altimeter (3 B 4 type) together with a barometer of continuous recording at a primary base station. In order to avoid an instrumental error,

measurements were tried more than twice within a short time as well as at different time and day. This method was successfully applied in many cases, because the survey was limitted in a small area having a dense distribution of gravity station, except a few routes where repeated measurements were difficult or secondary base stations measured by the theodolite were very few in number.

The variation of atmospheric pressure with time and horizontal distance is very important, since its effect on the measurements is as large as several times of a reading error. As to the daily variation of pressure, its regional difference is fortunately small in such a tropical district as Tanzania. The atmosphere in this country seems stable enough to enable the elevation measurements by the use of altimeters. The pressure varies very slowly and smoothly showing peaks twice a day, about 9 A.M. and 9 P.M. of local time. As shown in Plate I, high frequency disturbances are surprisingly small in Mbeya, but slightly observed in Kigoma. Parameters of daily variation in some districts are tabulated in Table 1. Although any significant difference is hardly seen in this table, it is not necessarily true that the pressure gradient is negligibly small for the height measurement by altimeters. In Mbeya, for example, an abnormal change of about 1 mb was observed at a secondary base station about 30 km east of the primary station when the latter was attacked by a light shower, though this was a rare case in a dry season. Another cause of pressure gradient was the difference in topography between two areas such as the case between Mbeya and Lake Rukwa. The details will be described later.

The other correction concerning to the deviation of air density from the standard is remarkably large in Tanzania, where the mean temperature in dry season is higher than that of standard atmosphere by 20°C on the average, which corresponds to 8% of the height difference measured by altimeters. The humidity has also an effect on the correction, though it is much smaller than that of temperature. The temperature effect was checked in Mbeya between two points having a height difference of about 1000 m. An intolerable error of about 30 m was found, even if the temperature effect was taken into

TABLE 1. TIMES OF PEAK AND TROUGH OF ATMOSPHERIC PRESSURE AND MEAN AMPLITUDE MEASURED FROM PEAK TO TROUGH

District	Peak	Trough	Amplitude	Period of observation
	Local time		mb	
Dar-es-Salaam	9, 22	3, 16	4-5	1, Aug.-20, Aug.
Dodoma	10, 0	4, 18	4-5	23, Aug.-25, Aug.
Kigoma	10, 23	3, 18	5-6	27, Aug.-5, Sep.
Mbeya	9, 23	4, 16	4	17, Sep.-8, Oct.

account. Such a big error might be caused partly by the wind existing near escarpments and partly by the effect of humidity which was neglected in the measurement, but it should be noted that the true temperature was not easy to estimate, because it was practically difficult to avoid the effect of intense radiation from the ground surface. It was found during subsequent observations that the less correction by 2% was rather reasonable if the temperature was measured near the ground surface. Therefore, in the present study, the correction factors except pressure change with time were determined by setting more than two secondary base stations of large height differences along each route, some of which were triangulation points near the route and some were connected to a suitable point of known altitude by the use of theodolite.

The detailed method applied in each area was slightly modified in consideration of topographies, qualities of available maps and the method of transportation.

Kigoma: Secondary base stations around Kigoma were as follows; Kigoma air port (816 m) and Uvinza air field (1084 m) listed in the gravity meter primary station net in East and Central Africa [6], Lake Tanganyika (773 m) and several stations determined by the use of theodolite within an error of about 3 m assuming that the locations of triangulation points and gravity stations were exactly represented on maps. Other gravity stations were connected to the nearest base station by an altimeter together with the correction of pressure change recorded at the primary base station. There were some stations along the shore of Lake Tanganyika, where gravity anomalies were measured most precisely because all the altitude along the shore were based on the water level.

It was not always possible to set a secondary base station by the use of theodolite, since three qualifications were required for a proposed site; the first was a short distance of less than 10 km in order to keep an acuracy of 3 m, the second was the small height difference because of the inaccurate horizontal distance measured on a map and the third was exact plotting of the station on the map.

Therefore, the secondary base stations should be such marked points as road intersections, junctions and bridges where the visibility of triangulation point is good.

By the reasons mentioned above, only several points were successfully used as base stations of Kigoma area. The route extending north from Kigoma had the worst accuracy of altitude. There were very few base stations. In addition, the second measurements at four stations 36, 37, 38 and 39 were unfortunately disturbed by a light shower. At the same time, an abnormal pressure change of about 1 mb was also recorded on the barometer at the Kigoma base station. Consequently, the writer could not help using single

measurements for above stations, allowing a large error of 10 to 20 m.

On the whole, however, it was found by repeated measurements that height differences were determined with an accuracy of about 3 m between adjacent two points and of about 10 m among stations of long intervals.

Mbeya: Throughout the survey in Mbeya, the elevation measurements were based on the following data; water levels of Lakes Rukwa (793 m) and Nyasa (475 m) represented on the sheet SC-36, Mbeya airport (1694 m) measured by Smith and Andrew [6] and some triangulation points represented on maps on the scale of 1 : 50,000. There were some discrepancies among maps published at different years: Small differences less than 10 ft in elevation were recognized among three sheet, 244/III, South C 36 D IIIc and the map of Mbeya on the scale of 1 : 2,500 published in 1957, though the differences were neglected in the present study.

As shown in Plate I, the atmosphere at Mbeya was very stable enough to make an accurate measurement might be possible, if repeated measurents at each station were tried until the pressure gradient which might exist around Mbeya was detected. For example, the altimeter was set at Kamsamba (No. 6) near Lake Rukwa for the examination of pressure change with time near the lake. The height difference between Kamsamba and Salt Lake (No. 5) was estimated from Fig. 1, assuming that the daily variation of atmospheric pressure was represented by a smooth curve. The comparison of this curve with that

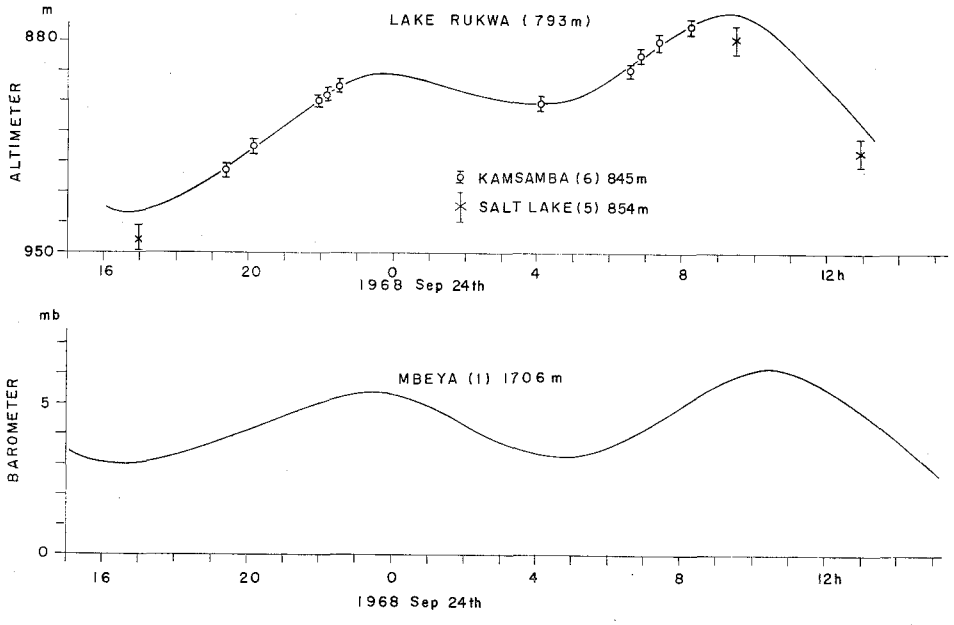

FIG. 1. Daily variation of atmospheric pressure observed at Mbeya and Lake Rukwa.

obtained by a barometer at Mbeya (No. 1) did not show any significant time lag between two curves. They were very similar in shape but not in amplitude, which might be caused by the difference in topography or by the large height difference of about 900 m between Mbeya and Lake Rukwa.

The same method for the pressure gradient observation was applied to three stations; No. 39 (1085 m) at the foot of Chimala escarpment east of Mbeya, No. 17 (1483 m) on the Mbozi plateau and No. 110 (1429 m) about 14 km south of Mbeya peak. It was likely that the pressure change with time was characterized by the respective topography but was not dependent on distance. Whenever the measurements were made on the same plain or plateau, the pressure gradient with distance was safely neglected. However, attention must be paid to the weather change even at a remote area, since it was found that a light shower gave an abnormal pressure change of about 1 mb even at the area out of the rain fall. Those observations indicating such a rapid pressure change with time were not used in the present study, but second observations were made on the other day at the same points. The detection of abnormal pressure change was not easy at stations in mountains if there were few secondary base stations. There were a number of triangulation points available for the survey on the escarpment extending north from Mbeya but were very few on the plateau northeast of Mt. Rungwe, where the measurements (No. 89–No. 98) were made along a new road, a half of which was not yet shown on the map, 259/II. The elevations along this route were determined in such a way that the mean elevation of four stations (No. 89–No. 92) which were measured on the contour map, 245/IV, was compared with that of altimeter readings after the correction of pressure change recorded at Mbeya in order to find the correction factor suitable on the plateau, then the factor was used for other stations along the new road.

In some places, gravity stations were increased in number in order to make both detailed gravity survey and the more accurate measurement of elevation by repeating it within a short time especially on the area intruded by basic rocks or on the area of complicated topography. The measurements were made with a good accuracy of about 3~5 m. However, an error of about 10 m was inevitable among stations of long intervals owing to the complicated topographic features around Mbeya.

Masange: Masange which is known as one of the rock painting sites in Tanzania consists of a curved escarpment of about 300 m high and a wide plain to the east. The escarpment is a part of the rift fault extending north of Dodoma. Only two days were spent for the examination of gravity anomaly associated with the rift fault. Elevations were measured by the use of both theodolite and altimeter together with a barometer at station No. 6, since the triangulation point TTP 104 was able to see from most of stations on the plain. The

horizontal distances necessary for the triangulation were measured on the map of Masange on the scale of 1 : 50,000. Thus determined elevations were supposed to have an error of about 5 m on the average.

LOCATION OF GRAVITY STATION

Most of longitudes and latitudes were measured on the maps on the scale of 1 : 50,000 if gravity stations were definite marks such as road intersections, junctions and bridges, though it was not always possible especially in the northern part of Kigoma beyond 4°45'S, where a geological map on the scale of 1 : 125,000 had to be used together with the milage of a car. An error of about 1 mile, in the worst case, was conjectured in such an area.

The situation was much better in Mbeya except Lake Rukwa. Most parts around Mbeya were covered with the maps of small scale (1 : 50,000) though their qualities were different according to places. In Fig. 2, showing the sheets used in the present study, those noted as "c" are contour maps, whereas others are not and poor in quality. There might be a considerable error in location in the west of Lake Rukwa owing to inaccurate representation of roads, along which distances were measured by the milage of car having an accuracy of 100 m, whereas the direction was doubtful.

It is noted here, that the revision of maps around Mbeya is not yet complete. Some discrepancies are seen between two maps of Mbeya, one is the contour map of Mbeya (South C 36/DIIId) reprinted in 1955 and the other is the sheet 244/IV published in 1954 without contours. The location of Mbeya airport, for example, is represented in different positions and neither coincides with that listed in the gravity meter primary station [6]. But only the sheet 244/IV is able to connect with other maps used in the present study. Considering the

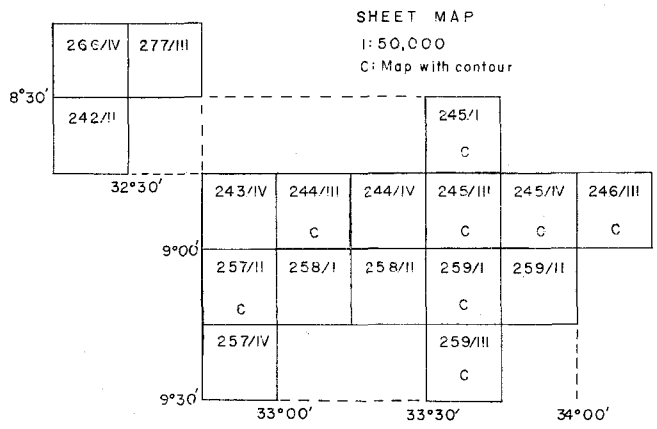

FIG. 2. Sheet index of maps used in the survey around Mbeya. The subscript c indicates the map with contour.

TABLE 2

GRAVITY MEASUREMENT — KIGOMA —

OFFSET =977000.0 DG/DZ =0.3067 mgl/m

STATION	LAT. S	LONG. E	ELEVATION m	INTERN.G mgl	G mgl	FREE AIR	BOUGUER D=2.65 g/cm³	BOUGUER D=2.67	BOUGUER D=2.69
1	4°52.6′	29°37.7′	789.0	1086.3	802.2	-41.9	-129.5	-130.2	-130.9
2	4 52.5	29 37.7	774.5	1086.2	804.1	-44.5	-130.5	-131.2	-131.8
3	4 37.5	29 38.1	773.5	1082.5	795.3	-49.9	-135.8	-136.4	-137.1
4	4 40.2	29 37.2	773.9	1083.2	789.0	-56.7	-142.6	-143.3	-143.9
5	4 54.1	29 39.5	847.5	1086.6	792.8	-33.8	-127.9	-128.7	-129.4
6	4 51.9	29 44.3	792.5	1086.1	810.4	-32.5	-120.5	-121.2	-121.9
7	4 51.4	29 53.9	1035.5	1086.0	750.9	-17.4	-132.3	-133.2	-134.1
8	4 38.2	30 8.2	1277.5	1082.7	692.2	1.4	-140.4	-141.5	-142.6
9	4 44.2	30 11.2	1147.0	1084.2	714.5	-17.8	-145.1	-146.1	-147.1
10	5 5.2	30 22.2	1043.5	1089.5	745.8	-23.6	-139.5	-140.3	-141.2
11	5 5.4	30 24.3	1084.0	1089.6	734.2	-22.8	-143.2	-144.1	-145.0
12	4 53.2	29 46.4	970.0	1086.4	773.9	-14.9	-122.6	-123.4	-124.2
13	4 50.5	29 57.4	1098.0	1085.7	731.3	-17.6	-139.5	-140.4	-141.3
14	4 50.3	29 59.8	1110.0	1085.7	729.3	-15.8	-139.0	-140.0	-140.9
15	4 50.9	29 55.4	1027.0	1085.8	748.4	-22.4	-136.4	-137.2	-138.1
16	4 53.1	29 52.1	936.0	1086.4	776.7	-22.5	-126.4	-127.2	-128.0
17	4 52.8	29 48.8	897.0	1086.3	785.8	-25.3	-124.9	-125.6	-126.4
18	4 53.3	29 46.7	954.0	1086.4	768.5	-25.2	-131.1	-131.9	-132.7
19	4 53.0	29 44.4	797.0	1086.4	807.0	-34.8	-123.3	-124.0	-124.6
20	4 51.0	29 42.3	808.0	1085.9	806.0	-31.9	-121.7	-122.3	-123.0
21	4 50.2	29 40.1	813.0	1085.7	804.6	-31.6	-121.9	-122.6	-123.3
22	4 46.3	29 36.3	773.7	1084.7	789.5	-57.8	-143.7	-144.4	-145.0
23	4 54.1	29 36.2	773.5	1086.6	800.1	-49.2	-135.1	-135.8	-136.4
24	4 54.8	29 36.7	773.1	1086.8	803.2	-46.4	-132.3	-132.9	-133.6
25	4 54.1	29 37.2	795.0	1086.6	798.5	-44.2	-132.5	-133.1	-133.8
26	4 53.2	29 38.6	857.0	1086.4	786.8	-36.6	-131.8	-132.5	-133.2
27	4 52.7	29 40.0	816.0	1086.3	801.3	-34.6	-125.2	-125.9	-126.5
28	4 55.2	29 40.3	773.3	1086.9	810.1	-39.5	-125.4	-126.0	-126.7
29	4 51.8	29 38.8	825.0	1086.1	796.7	-36.2	-127.8	-128.5	-129.2
30	4 48.5	29 39.8	871.0	1085.2	792.6	-25.4	-122.1	-122.9	-123.6
31	4 44.8	29 41.7	998.0	1084.3	761.9	-16.2	-127.0	-127.9	-128.7
32	4 45.2	29 41.1	964.0	1084.4	772.4	-16.3	-123.3	-124.1	-124.9
33	4 47.3	29 40.0	888.0	1084.9	789.9	-22.6	-121.2	-121.9	-122.7
34	4 53.1	29 37.1	773.0	1086.4	804.4	-44.8	-130.7	-131.3	-132.0
35	4 41.9	29 42.5	1012.0	1083.6	756.3	-16.8	-129.2	-130.1	-130.9
36	4 39.1	29 43.2	1307.0	1082.9	689.0	7.1	-138.0	-139.1	-140.2
37	4 37.0	29 43.7	1505.0	1082.4	645.8	25.1	-142.0	-143.3	-144.6
38	4 33.0	29 45.0	1543.0	1081.5	645.6	37.5	-133.8	-135.1	-136.4
39	4 27.2	29 46.4	1645.0	1080.1	611.1	35.6	-147.0	-148.4	-149.8
40	4 51.7	29 36.5	773.9	1086.0	801.7	-46.9	-132.8	-133.5	-134.1
41	4 50.5	29 36.6	773.3	1085.7	797.9	-50.6	-136.4	-137.1	-137.7
42	4 49.1	29 36.6	773.3	1085.4	796.7	-51.5	-137.3	-138.0	-138.6
43	4 47.9	29 35.9	773.3	1085.1	786.4	-61.4	-147.2	-147.9	-148.5
44	4 48.2	29 36.4	774.3	1085.2	793.6	-54.0	-140.0	-140.6	-141.3
45	4 45.8	29 42.9	1012.0	1084.6	763.0	-11.0	-123.4	-124.3	-125.1
46	4 47.4	29 43.6	963.0	1085.0	772.4	-17.1	-124.0	-124.8	-125.6
47	4 49.0	29 43.9	962.0	1085.4	773.8	-16.4	-123.2	-124.1	-124.9
48	4 50.3	29 43.4	925.0	1085.7	781.9	-20.0	-122.7	-123.5	-124.3

importance of relative location, the writer used the sheet 244/IV for the calculation of location, though it was not contoured.

As mentioned in the preceding section, there was a new road passing through the plateau northeast of Mt. Rungwe but not yet shown on the sheet 259/II. The accuracy of location along this route was also poor, about 2 km in the worst case.

So far the stations of poor accuracy were described. But for the most of stations it was not difficult to locate them on maps with an accuracy of about 100 m or 0.05′. Thus determined locations were listed in Tables 2, 3 and 4 with other measurements.

GRAVITY MEASUREMENT

The Worden gravimeter, No. 127 of Kyoto University, Japan, was used throughout the survey for the sake of easiness of transportation. The average

drift with this instrument amounted to 0.2~0.3 mgal during the survey of 12 hours. But its rate was not constant, occasionally showing a negative drift for a short time or a jump of about 0.1 mgal during the survey along a rough road. But the drift during the rest time was remarkably small and stable. Inspite of this fact, the check of instrumental drift was made every six hours or more in order to avoid only big errors more than 0.2 mgal, because even such a big error was sufficiently small compared to the error of elevation. Much efforts were made for the accuracy of elevation measurement in the present study. All the gravity values listed in Tables 2, 3 and 4 were based on the measurements made by Smith and Andrew [6] at four stations; Kigoma airport, Uvinza airfield, Mbeya airport and Kondoa airfield.

As for the distribution of gravity station, it was intended to make observations every 3 km not only along main roads but also along all the drive tracks so as to make an areal distribution. But it was almost impossible to cover the area with an unbiased distribution of station except very small regions, owing to the scanty number of drive tracks. Especially in the Buhoro flats, north of Chimala scarp, observations were very few owing to the damage of roads due to heavy rain in 1967, though the gravity survey in the plain was very important for the examination of the relation between west and east rifts. However, the mean interval of station was kept about 3 km if the location was clear on the map and added more stations in some routes when an abnormal change of gravity was observed.

The accuracy of the measurement was supposed to be different according to places because the resetting of the gravimeter was frequently done in mountains or the large dial of the instrument was used in a few areas distant from the primary base station of Mbeya. Therefore, the gravity values near Lake Rukwa might have an offset of about 1 mgal compared with those near Mbeya. The same error due to the use of large dial was inevitable to the station at Tunduma and a few stations near Lake Nyasa.

METHOD OF ANOMALY REDUCTION

Bouguer anomalies are most convenient to discuss the relation of local geology and underground structures in small areas, where relative values are more significant than absolute values if only the superficial structures are concerned, whereas the average density near the earth surface is very sensitive to the Bouguer reduction in particular in mountain areas such as the northern part of Kigoma where the height difference between Lake Tanganyika and the highest station is about 800 m and Mbeya where the topographic features are so complicated that a height difference of more than 1,000 m is not rare within a short distance less than 10 km. An error of 0.1 g/cm^3 in the density estimation will yield the error which is comparable to the error concerning

to the elevation measurement.

The terrain and tidal correction are not taken into account in the present study because they are negligibly small in most cases except at the edge of escarpment where the terrain correction was estimated as large as 2~3 mgals.

The basic expression of standard gravity, g_0, is given by the following international formula of 1930 as

$$g_0 = 978049\ (1+0.0052884 \sin \varphi - 0.0000059 \sin^2 2\varphi)\ \text{mgal},$$

where φ is the latitude.

The free air anomaly, g', is also calculated by the following equation, since it involves the minimum of assumptions,

$$g' = g - g_0 + 0.03067\ h$$

where g and h are the observed gravity in mgals and the elevation in meters, respectively. The coefficient of h is given by Howell [4] as the rate of change of gravity with elevation on the equator.

Then, the simple Bouguer correction which does not contain the terrain correction is applied to the free air anomaly.

$$g'' = g' - 0.0419\ \rho h,$$

where g'' is the Bouguer anomaly and ρ is the density which should be the actual mean density of the crust in studies of crustal structure. In the present study, however, three values of density, 2.65 g/cm^3, 2.67 g/cm^3 and 2.69 g/cm^3 are tentatively used in order to see some qualitative characteristics of gravity anomaly. A quantitative analysis is left in future after the measurement of densities of rocks.

RESULTS AND CONCLUSIONS

Thus obtained gravity anomalies are tabulated in Tables 2, 3 and 4. Bouguer anomaly maps based on the standard density of 2.67 g/cm^3 are also shown in Figs. 3, 4 and 6 for Kigoma, Mbeya and Masange, respectively. Contour lines in these maps are drawn with an appropriate interval easy to see and all the minor changes supposed due to errors are smoothed away.

Despite of the inaccurate measurement of elevation, regional characteristics relevant to rift valleys and geological structures are clearly observed, though they are not simple at all as will be described in the followings.

Kigoma: Fig. 3 shows the Bouguer anomaly map deduced from 48 measurements around Kigoma, where accuracies vary according to the locality. The measurements along the shore of Lake Tanganyika are most accurate and independent of the assumption of surface density. It is evident, therefore, that the contour lines near the shore are almost parallel with the trend of surface geology in

TABLE 3-1

GRAVITY MEASUREMENT — M B E Y A —

OFFSET =977000.0 DG/DZ =0.3067 mgl/m

STATION	LAT. S	LONG. E	ELEVATION m	INTERN.G mgl	G mgl	FREE AIR	BOUGUER D=2.65 g/cm³	BOUGUER D=2.67	BOUGUER D=2.69
1	8°53.4′	33°26.8′	1706.0	1172.0	676.2	27.5	-161.9	-163.4	-164.8
2	9 0.6	32 59.3	1589.0	1175.4	761.8	73.9	-102.5	-103.9	-105.2
3	8 26.3	32 35.7	793.0	1159.9	805.4	-111.2	-199.3	-199.9	-200.6
4	8 25.8	32 32.8	813.0	1159.7	826.2	-84.1	-174.4	-175.0	-175.7
5	8 25.8	32 28.7	854.0	1159.7	845.1	-52.6	-147.4	-148.1	-148.9
6	8 20.4	32 18.5	845.0	1157.4	806.6	-91.5	-185.4	-186.1	-186.8
7	8 21.3	32 22.2	849.0	1157.8	825.1	-72.2	-166.5	-167.2	-167.9
8	8 22.9	32 26.3	862.0	1158.5	828.2	-65.8	-161.5	-162.2	-163.0
9	8 32.7	32 27.3	977.0	1162.7	849.9	-13.1	-121.6	-122.4	-123.2
10	8 32.6	32 23.7	905.0	1162.7	857.9	-27.1	-127.6	-128.4	-129.1
11	8 34.9	32 18.8	855.0	1163.7	861.2	-40.2	-135.1	-135.8	-136.6
12	8 28.7	32 28.1	877.0	1161.0	860.7	-31.2	-128.6	-129.3	-130.1
13	9 34.5	33 56.6	475.0	1191.5	899.0	-146.8	-199.5	-199.9	-200.3
14	9 35.7	33 52.0	512.0	1192.1	924.3	-110.7	-167.5	-168.0	-168.4
15	9 23.6	33 42.0	765.0	1186.2	887.7	-63.8	-148.7	-149.4	-150.0
16	9 10.8	33 32.8	1307.0	1180.1	766.9	-12.3	-157.4	-158.5	-159.6
17	9 7.2	32 54.9	1483.0	1178.4	782.3	58.8	-105.9	-107.1	-108.3
18	9 18.6	32 45.8	1653.0	1183.8	704.6	27.8	-155.7	-157.1	-158.5
19	9 5.4	33 2.4	1674.0	1177.6	741.4	77.3	-108.5	-109.9	-111.3
20	8 50.8	33 29.9	2298.0	1170.9	554.2	88.2	-166.9	-168.8	-170.8
21	8 50.4	33 27.0	2332.0	1170.7	551.4	96.1	-162.9	-164.8	-166.8
22	8 49.8	33 24.2	2459.0	1170.4	538.4	122.3	-150.8	-152.8	-154.9
23	8 49.9	33 22.5	2440.0	1170.4	530.4	108.4	-162.5	-164.6	-166.6
24	8 53.6	33 26.9	1677.0	1172.1	677.3	19.6	-166.6	-168.0	-169.4
25	9 9.7	32 50.8	1513.0	1179.6	801.5	86.0	-82.0	-83.2	-84.5
26	9 9.4	32 50.0	1466.0	1179.5	808.1	78.4	-84.4	-85.6	-86.9
27	9 10.2	32 52.2	1520.0	1179.8	795.2	81.6	-87.1	-88.4	-89.7
28	9 11.9	32 51.1	1473.0	1180.6	809.0	80.2	-83.3	-84.6	-85.8
29	9 14.2	32 50.2	1378.0	1181.7	793.8	34.8	-118.2	-119.4	-120.5
30	9 8.9	32 53.0	1519.0	1179.2	795.5	82.2	-86.4	-87.7	-89.0
31	9 6.6	32 56.2	1574.0	1178.1	760.5	65.2	-109.6	-110.9	-112.2
32	8 51.9	34 10.8	1109.0	1171.4	832.1	1.0	-122.2	-123.1	-124.0
33	8 52.9	34 10.8	1114.0	1171.8	830.8	0.8	-122.9	-123.9	-124.8
34	8 51.0	34 10.4	1090.0	1170.9	833.8	-2.7	-123.8	-124.7	-125.6
35	8 47.3	34 14.7	1135.0	1169.3	828.3	7.2	-118.8	-119.7	-120.7
36	8 45.4	34 13.5	1087.0	1168.4	822.3	-12.6	-133.3	-134.2	-135.1
37	8 48.1	34 13.0	1104.0	1169.6	832.2	1.3	-121.3	-122.2	-123.2
38	8 49.1	34 11.6	1101.0	1170.1	828.9	-3.4	-125.7	-126.6	-127.5
39	8 50.1	34 10.6	1085.0	1170.5	832.5	-5.2	-125.6	-126.5	-127.5
40	8 50.4	34 8.9	1094.0	1170.7	817.5	-17.5	-139.0	-139.9	-140.8
41	8 50.5	34 8.0	1103.0	1170.7	812.8	-19.5	-142.0	-142.9	-143.8
42	8 51.0	34 6.6	1103.0	1170.9	812.3	-20.3	-142.7	-143.6	-144.6
43	8 51.2	34 5.1	1082.0	1171.0	810.6	-28.5	-148.6	-149.5	-150.4
44	8 48.4	34 8.5	1061.0	1169.8	818.6	-25.7	-143.5	-144.3	-145.2
45	8 45.7	34 8.1	1055.0	1168.5	818.1	-26.8	-143.9	-144.8	-145.7
46	8 44.1	34 9.1	1051.0	1167.8	815.0	-30.4	-147.1	-148.0	-148.8
47	8 51.6	34 3.8	1148.0	1171.2	784.7	-34.3	-161.8	-162.8	-163.7
48	8 51.5	34 1.8	1154.0	1171.2	782.2	-34.9	-163.1	-164.0	-165.0
49	8 50.0	34 3.9	1084.0	1170.5	799.7	-38.2	-158.6	-159.5	-160.4
50	8 50.4	33 59.1	1205.0	1170.7	770.7	-30.3	-164.1	-165.1	-166.1

the south but not with the shore. It is also suggested from the gradient of anomaly near the shore that a big negative anomaly exists in Lake Tanganyika. But the gradient seems to reflect a combined effect of the rift valley and a high density mass distribution near Kigoma airport, though the anomaly is somewhat complicated to represent the details with contour lines of small interval. This high density block makes a remarkable contrast with a low density mass distribution in the north which is rather in harmony with both the surface geology and the effect of Lake Tanganyika. It must be noted that both high and low density areas locate on a past geosynclinal region extending NS direction, where the upper layer consists of red sandstones of the late Bukoban and is underlain by a thick layer consisting of quartzite belonging to the Karagwe-Ankolean.

Apparently a mean density of 2.67 g/cm³ is too high in these layers but

TABLE 3-2

GRAVITY MEASUREMENT — MBEYA —

OFFSET =977000.0 DG/DZ =0.3067 mgl/m

STATION	LAT. S	LONG. E	ELEVATION m	INTERN.G mgl	G mgl	FREE AIR	BOUGUER D=2.65 g/cm³	BOUGUER D=2.67	BOUGUER D=2.69
51	8° 53.2′	33° 59.7′	2023.0	1171.9	602.1	50.7	-173.9	-175.6	-177.3
52	8 53.0	33 59.8	1990.0	1171.9	604.5	43.1	-177.9	-179.5	-181.2
53	8 51.9	34 1.4	1159.0	1171.4	780.0	-35.8	-164.5	-165.4	-166.4
54	8 51.0	34 0.3	1190.0	1170.9	774.4	-31.5	-163.6	-164.6	-165.6
55	8 50.0	33 57.0	1211.0	1170.5	764.9	-34.1	-168.5	-169.6	-170.6
56	8 49.6	33 54.2	1184.0	1170.3	772.7	-34.4	-165.8	-166.8	-167.8
57	8 49.8	33 53.0	1178.0	1170.4	766.8	-42.2	-173.0	-174.0	-175.0
58	8 49.5	33 51.2	1194.0	1170.3	767.4	-36.6	-169.1	-170.1	-171.1
59	8 46.6	33 50.4	1121.0	1168.9	787.1	-37.9	-162.4	-163.3	-164.3
60	8 45.1	33 50.2	1099.0	1168.3	796.1	-35.0	-157.0	-158.0	-158.9
61	8 48.1	33 50.9	1155.0	1169.6	778.7	-36.6	-164.8	-165.8	-166.8
62	8 49.8	33 55.9	1202.0	1170.4	767.4	-34.2	-167.7	-168.7	-169.7
63	8 53.4	33 26.8	1701.0	1172.0	675.4	25.2	-163.7	-165.1	-166.6
64	8 52.1	33 28.1	1892.0	1171.4	647.4	56.3	-153.7	-155.3	-156.9
65	8 49.8	33 32.4	2461.0	1170.4	505.8	90.3	-183.0	-185.0	-187.1
66	8 48.9	33 32.2	2443.0	1170.0	513.1	92.5	-178.8	-180.8	-182.9
67	8 48.5	33 32.0	2324.0	1169.8	543.9	87.0	-171.1	-173.0	-175.0
68	8 48.1	33 32.6	2180.0	1169.6	570.6	69.7	-172.4	-174.2	-176.0
69	8 47.7	33 33.0	2169.0	1169.4	570.1	66.0	-174.8	-176.7	-178.5
70	8 45.3	33 33.8	2054.0	1168.4	610.8	72.5	-155.6	-157.3	-159.0
71	8 43.1	33 34.3	1979.0	1167.4	621.7	61.4	-158.3	-160.0	-161.7
72	8 40.7	33 35.3	1844.0	1166.3	648.1	47.5	-157.3	-158.8	-160.4
73	8 38.2	33 33.3	1687.0	1165.2	679.6	31.9	-155.4	-156.8	-158.2
74	8 36.0	33 31.0	1641.0	1164.2	697.9	37.1	-145.1	-146.5	-147.9
75	8 34.9	33 33.2	1632.0	1163.7	692.8	29.7	-151.5	-152.9	-154.2
76	8 34.2	33 33.6	1684.0	1163.4	687.5	40.7	-146.3	-147.7	-149.1
77	8 54.5	33 30.5	1755.0	1172.5	662.2	26.0	-166.8	-168.3	-169.8
78	8 52.3	33 33.6	1654.0	1171.5	668.1	3.9	-179.7	-181.1	-182.5
79	8 50.7	33 35.3	1442.0	1170.8	710.4	-18.0	-178.2	-179.4	-180.6
80	8 48.4	33 36.3	1244.0	1169.8	748.9	-39.2	-177.4	-178.4	-179.4
81	8 46.0	33 38.3	1159.0	1168.7	777.0	-36.1	-164.8	-165.8	-166.7
82	8 45.3	33 38.3	1146.0	1168.4	779.4	-37.4	-164.6	-165.6	-166.5
83	8 43.6	33 39.1	1124.0	1167.6	782.9	-39.9	-164.7	-165.6	-166.6
84	8 42.8	33 39.4	1118.0	1167.2	773.3	-50.9	-175.1	-176.0	-177.0
85	8 46.1	33 42.0	1139.0	1168.7	781.4	-37.9	-164.4	-165.3	-166.3
86	8 47.1	33 42.5	1156.0	1169.2	777.5	-37.0	-165.4	-166.4	-167.3
87	8 49.2	33 40.9	1270.0	1170.1	752.2	-28.3	-169.3	-170.4	-171.5
88	8 51.4	33 38.2	1541.0	1171.1	692.1	-6.3	-177.4	-178.7	-180.0
89	8 55.1	33 58.6	1908.0	1172.8	630.8	43.3	-168.6	-170.2	-171.8
90	8 58.2	33 57.5	2101.0	1174.2	587.7	57.9	-175.4	-177.1	-178.9
91	8 59.9	33 54.8	2358.0	1175.0	540.0	88.3	-173.6	-175.5	-177.5
92	8 59.6	33 54.2	2543.0	1174.9	496.2	101.3	-181.0	-183.1	-185.3
93	9 1.6	33 54.1	2610.0	1175.8	486.3	111.1	-178.7	-180.9	-183.1
94	9 3.4	33 52.2	2800.0	1176.7	442.8	125.0	-185.9	-188.2	-190.6
95	9 2.2	33 49.1	2745.0	1176.1	449.6	115.5	-189.3	-191.6	-193.9
96	9 0.5	33 44.0	2623.0	1175.3	472.6	101.9	-189.4	-191.6	-193.8
97	9 0.5	33 40.7	2312.0	1175.3	522.2	56.1	-200.6	-202.6	-204.5
98	9 0.5	33 37.6	2255.0	1175.3	516.3	32.7	-217.7	-219.6	-221.5
99	8 57.0	33 35.3	2244.0	1173.7	556.0	70.6	-178.5	-180.4	-182.3
100	8 55.1	33 32.9	1818.0	1172.8	634.4	19.3	-182.6	-184.1	-185.6

the assumption of 2.6 g/cm^3 does not change the anomaly map very much. On the other hand, anomalies tend to be more neagative in the east of the high density region, in spite of the fact that the area is covered by basalts whose density is apparently higher than that of red sandstones or quartzite.

From these facts, it is concluded that a massive block of high density exists at a depth but not too shallow to disturbe the surface geology. This high density material is supposed to be related with the origin of basalts in the east and, if this is true, it is also suggested from the trend of anomaly that high density materials extend underneath from Kigoma to northeast, although the direction is not in accord with the surface geology.

Mbeya: Fig. 4 shows Bouguer anomalies and observation sites scattered around Mbeya. But the distribution of station is not necessarily uniform owing to a number of restrictions in conducting the survey. The topography is charac-

TABLE 3-3

GRAVITY MEASUREMENT — M B E Y A —

OFFSET =977000.0 DG/DZ =0.3067 mgl/m

STATION	LAT. S	LONG. E	ELEVATION m	INTERN.G mgl	G mgl	FREE AIR	BOUGUER D=2.65 g/cm³	BOUGUER D=2.67	BOUGUER D=2.69
101	8°53.6′	33°35.1′	1773.0	1172.1	645.5	17.3	-179.6	-181.1	-182.6
102	8 55.2	33 34.2	1844.0	1172.9	627.0	19.8	-185.0	-186.5	-188.0
103	8 53.7	33 34.0	1789.0	1172.2	641.7	18.3	-180.3	-181.8	-183.3
104	8 52.5	33 36.6	1646.0	1171.6	669.2	2.5	-180.3	-181.6	-183.0
105	8 46.0	33 45.7	1134.0	1168.7	789.2	-31.6	-157.5	-158.4	-159.4
106	8 47.8	35 49.0	1163.0	1169.5	778.9	-33.8	-162.9	-163.9	-164.9
107	8 54.4	33 33.7	1815.0	1172.5	634.9	19.2	-182.4	-183.9	-185.4
108	8 54.9	33 27.6	1694.0	1172.7	683.5	30.4	-157.7	-159.1	-160.5
109	8 55.4	33 23.3	1586.0	1173.0	712.8	26.4	-149.7	-151.1	-152.4
110	8 56.2	33 21.5	1429.0	1173.3	743.9	9.8	-149.7	-150.9	-152.1
111	8 55.9	33 18.8	1388.0	1173.2	734.6	-12.8	-166.9	-168.1	-169.2
112	8 56.2	33 15.9	1316.0	1173.3	751.0	-18.6	-164.7	-165.8	-166.9
113	8 57.2	33 13.5	1213.0	1173.8	789.4	-12.3	-146.9	-148.0	-149.0
114	8 57.8	33 11.3	1349.0	1174.1	775.9	15.7	-134.1	-135.2	-136.4
115	8 58.0	33 9.1	1573.0	1174.2	747.8	56.2	-118.5	-119.8	-121.1
116	8 57.9	33 6.3	1558.0	1174.1	756.7	60.5	-112.5	-113.8	-115.1
117	8 59.9	33 23.1	1654.0	1175.0	688.4	20.8	-162.9	-164.3	-165.7
118	9 2.8	33 24.1	1942.0	1176.4	631.5	50.8	-164.8	-166.4	-168.0
119	9 4.7	33 27.3	1712.0	1177.3	675.0	22.9	-167.2	-168.6	-170.1
120	9 7.4	33 30.0	1424.0	1178.5	739.5	-2.2	-160.3	-161.5	-162.7
121	9 10.3	33 32.3	1344.0	1179.9	757.6	-10.0	-159.2	-160.3	-161.5
122	9 6.6	33 33.0	1655.0	1178.1	691.5	21.0	-162.7	-164.1	-165.5
123	9 3.1	33 35.4	1913.0	1176.5	615.2	25.5	-186.9	-188.5	-190.1
124	9 1.2	33 36.5	2047.0	1175.6	565.1	17.4	-209.9	-211.6	-213.3
125	8 54.0	33 19.7	1353.0	1172.3	747.5	-9.7	-160.0	-161.1	-162.2
126	8 52.5	33 17.6	1309.0	1171.6	747.4	-22.7	-168.0	-169.1	-170.2
127	8 51.1	33 15.5	1291.0	1171.0	750.3	-24.6	-168.0	-169.1	-170.1
128	8 49.0	33 13.6	1251.0	1170.0	761.9	-24.4	-163.3	-164.3	-165.4
129	8 46.8	33 11.7	1237.0	1169.0	758.3	-31.2	-168.6	-169.6	-170.7
130	8 47.9	33 12.7	1266.0	1169.5	754.3	-26.9	-167.4	-168.5	-169.5
131	8 47.7	33 13.3	1284.0	1169.4	757.6	-17.9	-160.5	-161.6	-162.7
132	8 48.1	33 13.7	1286.0	1169.6	759.7	-15.4	-158.2	-159.3	-160.4
133	8 52.7	33 18.1	1300.0	1171.7	748.1	-24.8	-169.2	-170.2	-171.3
134	8 59.5	33 2.4	1671.0	1174.8	741.3	79.1	-106.5	-107.9	-109.3
135	9 4.6	32 57.8	1616.0	1177.2	753.5	72.0	-107.4	-108.8	-110.1
136	9 6.6	32 55.9	1571.0	1178.1	760.7	64.5	-110.0	-111.3	-112.6
137	9 8.1	32 53.8	1518.0	1178.9	779.0	65.8	-102.7	-104.0	-105.3
138	9 11.2	32 51.4	1508.0	1180.3	806.7	89.0	-78.4	-79.7	-81.0
139	9 13.2	32 51.3	1450.0	1181.3	799.5	63.1	-97.9	-99.2	-100.4
140	9 13.6	32 50.7	1437.0	1181.4	791.3	50.7	-108.9	-110.1	-111.3
141	9 16.0	32 48.7	1445.0	1182.6	751.1	11.8	-148.7	-149.9	-151.1
142	9 10.7	32 53.2	1559.0	1180.1	790.2	88.4	-84.7	-86.0	-87.3
143	9 2.4	32 55.8	1519.0	1176.2	778.5	68.3	-100.4	-101.6	-102.9
144	9 4.7	32 55.5	1573.0	1177.3	760.6	65.9	-108.8	-110.1	-111.4
145	9 8.2	32 57.9	1615.0	1178.9	750.7	67.2	-112.1	-113.5	-114.8
146	9 9.8	33 1.0	1622.0	1179.7	742.9	60.8	-119.3	-120.6	-122.0
147	9 7.3	33 1.3	1596.0	1178.5	751.3	62.4	-114.8	-116.1	-117.5
148	9 4.6	33 2.5	1640.0	1177.2	746.0	71.9	-110.2	-111.6	-113.0
149	9 19.3	33 39.4	1249.0	1184.2	781.8	-19.2	-157.9	-158.9	-160.0
150	9 23.9	33 37.3	1095.0	1186.4	842.2	-8.2	-129.8	-130.7	-131.7
151	9 15.4	33 38.5	1487.0	1182.3	714.8	-11.3	-176.4	-177.7	-178.9
152	9 13.1	33 38.4	1456.0	1181.2	732.7	-1.9	-163.5	-164.7	-166.0
153	9 12.2	33 34.9	1349.0	1180.8	752.6	-14.3	-164.1	-165.3	-166.4

TABLE 4

GRAVITY MEASUREMENT — MASANGE —

OFFSET =977000.0 , DG/DZ =0.3067 mgl/m

STATION	LAT. S	LONG. E	ELEVATION m	INTERN.G mgl	G mgl	FREE AIR	BOUGUER D=2.65g/cm³	BOUGUER D=2.67	BOUGUER D=2.69
1	4°53.6′	35°46.1′	1402.0	1086.5	652.5	-3.9	-159.6	-160.8	-161.9
2	4 43.9	35 50.0	1506.0	1084.1	627.5	5.4	-161.8	-163.1	-164.3
3	4 43.2	35 51.3	1519.0	1083.9	622.9	5.0	-163.7	-165.0	-166.2
4	4 42.4	35 52.0	1344.0	1083.7	654.8	-16.6	-165.8	-167.0	-168.1
5	4 41.4	35 52.0	1249.0	1083.5	671.4	-28.9	-167.6	-168.6	-169.7
6	4 40.3	35 52.1	1252.0	1083.2	671.4	-27.7	-166.7	-167.8	-168.8
7	4 38.5	35 50.7	1186.0	1082.8	680.5	-38.4	-170.1	-171.1	-172.1
8	4 37.1	35 49.8	1180.0	1082.4	684.1	-36.3	-167.3	-168.3	-169.3
9	4 36.2	35 48.1	1237.0	1082.2	669.7	-33.0	-170.4	-171.4	-172.5
10	4 35.9	35 48.4	1198.0	1082.1	678.6	-36.0	-169.0	-170.0	-171.0
11	4 35.5	35 49.0	1189.0	1082.1	681.9	-35.4	-167.4	-168.4	-169.4
12	4 32.6	35 46.7	1212.0	1081.4	673.3	-36.2	-170.8	-171.8	-172.8
13	4 31.0	35 47.6	1206.0	1081.0	675.0	-36.0	-169.9	-170.9	-171.9
14	4 28.5	35 49.4	1276.0	1080.4	662.8	-26.1	-167.8	-168.9	-170.0
15	4 35.9	35 45.5	1544.0	1082.1	616.0	7.5	-163.9	-165.2	-166.5
16	4 37.8	35 47.1	1646.0	1082.6	596.3	18.6	-164.1	-165.5	-166.9
17	4 40.1	35 48.2	1603.0	1083.2	605.0	13.6	-164.4	-165.8	-167.1
18	4 42.8	35 49.0	1667.0	1083.8	594.5	22.1	-163.0	-164.4	-165.8
19	4 37.9	35 53.5	1167.0	1082.6	687.5	-37.1	-166.7	-167.7	-168.6
20	4 37.9	35 55.8	1168.0	1082.6	692.2	-32.1	-161.8	-162.8	-163.7
21	4 39.0	35 57.3	1188.0	1082.9	685.6	-32.8	-164.7	-165.7	-166.7
22	4 40.9	35 57.1	1197.0	1083.4	682.5	-33.6	-166.5	-167.5	-168.5
23	4 42.8	35 56.2	1247.0	1083.8	671.9	-29.4	-167.8	-168.9	-169.9
24	4 42.7	35 54.1	1250.0	1083.8	671.3	-29.0	-167.8	-168.9	-169.9

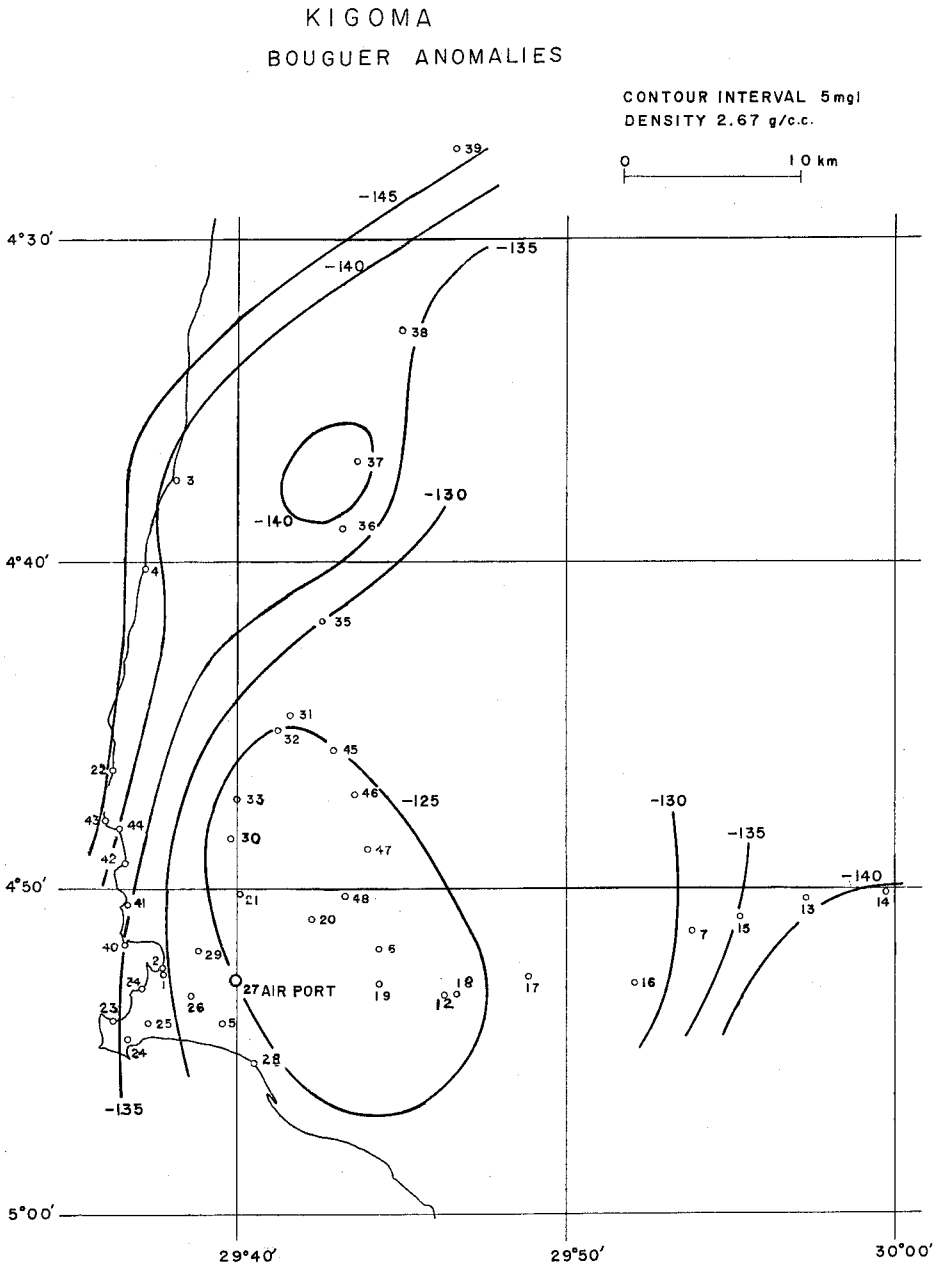

FIG. 3. Bouguer anomaly map of Kigoma, east of Lake Tanganyika.

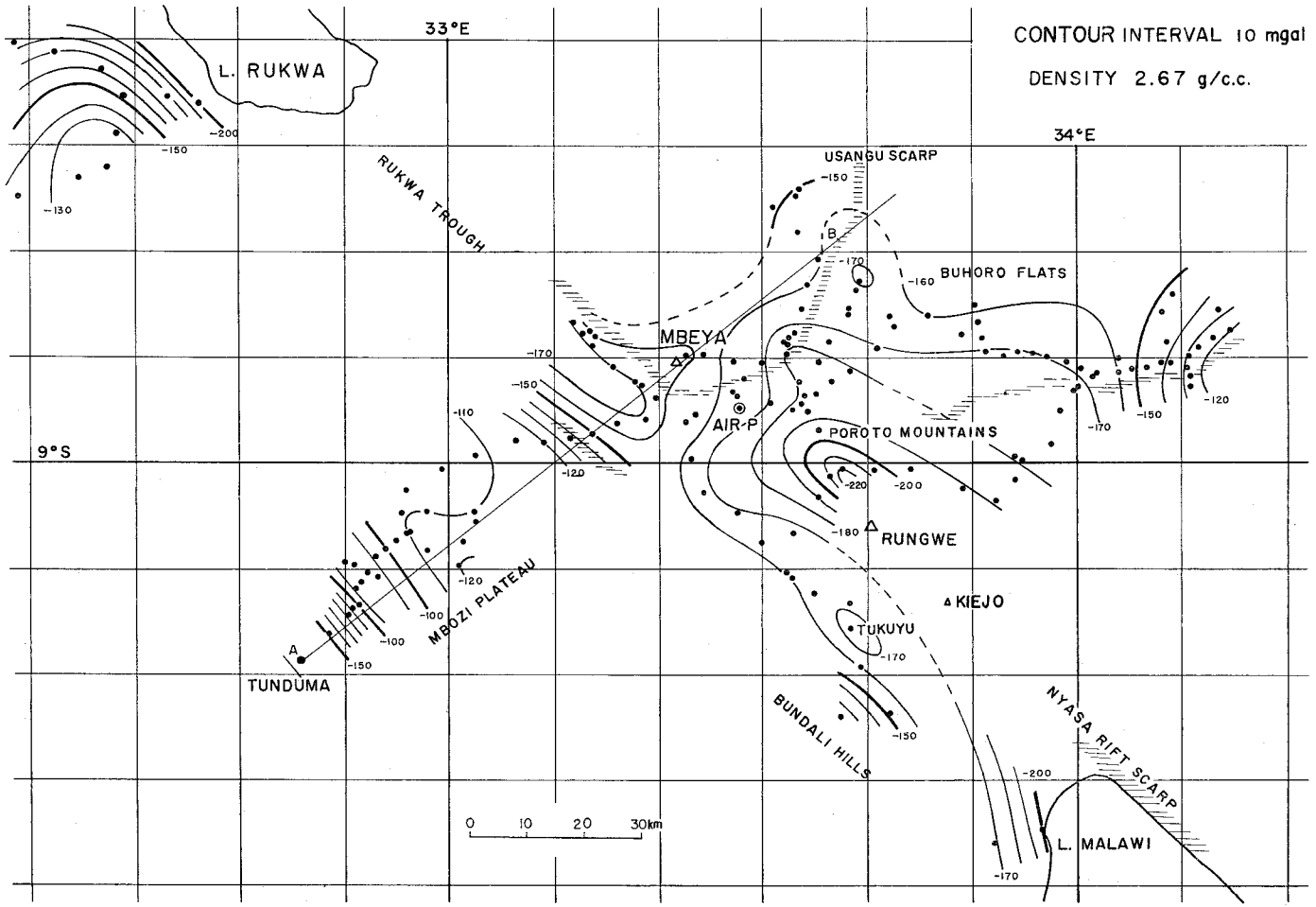

FIG. 4. Bouguer anomaly map of Mbeya, Tanzania. Hatched zones indicate escarpments. A–B is the location of profile (see Fig. 5).

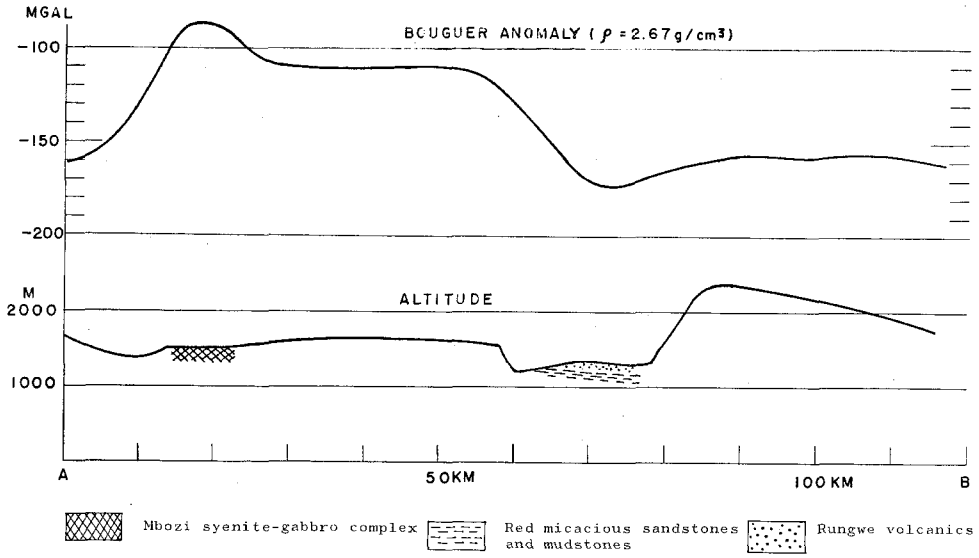

FIG. 5. Profile across the Rukwa rift valley (see Fig. 4).

terized by the distinguished rift valley extending southeastwards from the middle of Lake Tanganyika to Lake Nyasa and the Buhoro flats bordered in the west by the Usangu rift escarpment and in the south by the Poroto mountains.

Tremendous volcanics from volcanoes Rungwe and Kiejo fill the junction of two rifts and cover the western part of the Poroto mountains, so that the relation between the rift valley and the crossing rift escarpment is not known. But the existence of a big anomaly to the northwest of Mt. Rungwe is probably the effect of thick volcanic ashes deposited near the escarpment which is the extension of Nyasa rift scarp, though the continuation of the trough of Bouguer anomalies to that of the Rukwa trough is interrupted by a relatively positive anomalies around Mbeya airport, which might be due to thick basaltic lava flows filled up the escarpment or alternatively due to the lack of the escarpment in this area. The latter posibility cannot be neglected because the Usangu scarp will intercept the rift valley at the point if it is extending to the south.

Other remarkably negative anomalies are observed on the recent sediments deposited in rift valleys. Bouguer anomalies are parallel with rift valleys and are low by about 50 mgals or more compared with those on surrounding mountains. On the southwest side of the Rukwa trough, Bouguer anomalies change abruptly and become stable on the Mbozi plateau. A high value near Lake Rukwa corresponds to the outcrop of the basement rocks bordered by the Rukwa trough and a branch rift valley extending towards Tunduma. The trough of Bouguer anomaly near Tunduma is probably due to this branch rift.

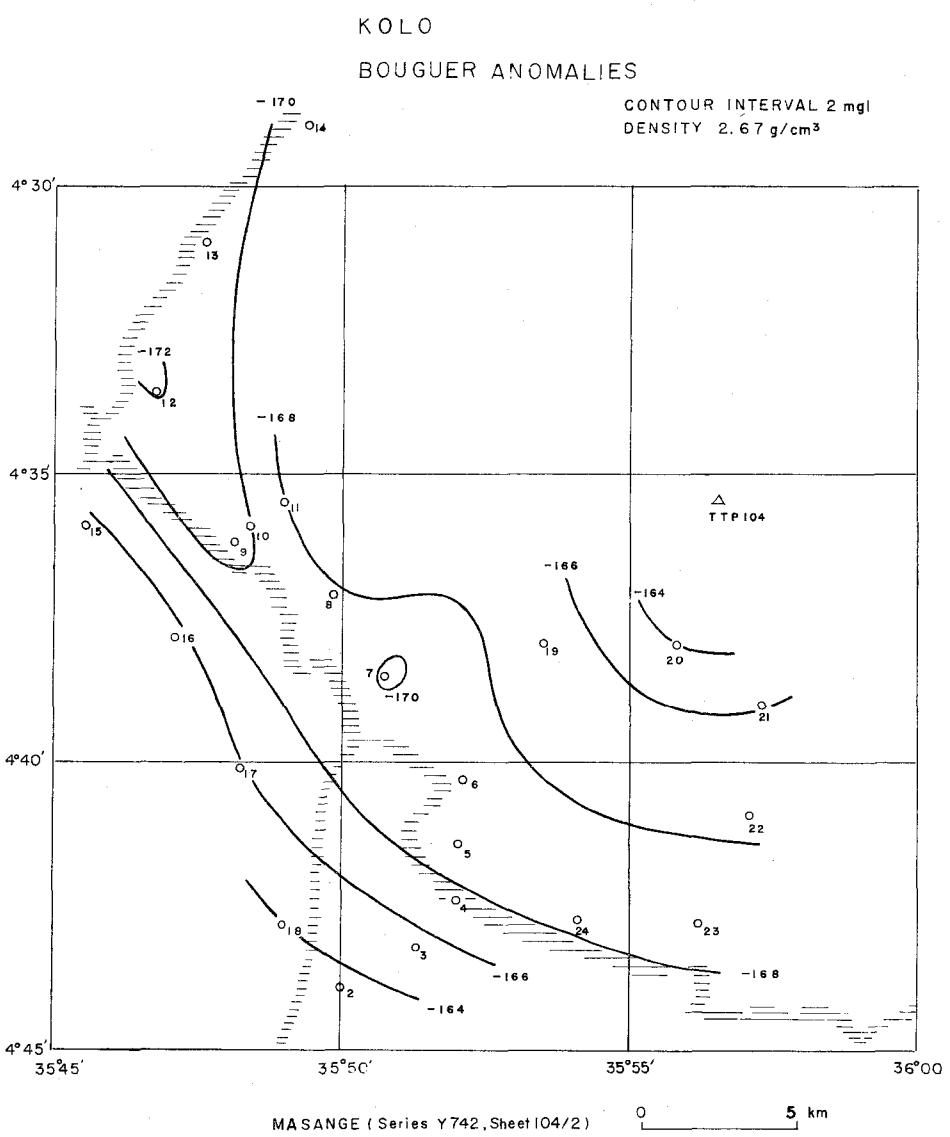

FIG. 6. Bouguer anomaly map of Masange (Kolo), north of Dodoma, Tanzania.

From the same point of view, the southwest border of the Nyasa trough is presumed to pass through the point about 10 km south of Tukuyu, because Bouguer anomalies increase abruptly towards the Bundali hills.

On the northeast side of the main rift valley, the trend of the anomaly is quite different from the other side. There is no significant difference between anomalies on the Buhoro flats and on the Poroto mountains although the height

difference between two area is as big as about 1000 m. No remarkable difference is also seen along the Usangu scarp. Consequently, it is suggested that the recent sediments and/or lake beds on the Buhoro flats are so thin near the west and south borders that the decrease of Bouguer anomaly due to light material is negligibly small. And the rift fault which forms the Usangu scarp does not show any significant effect on the Bouguer anomaly distribution. If the effects of unconsolidated sediments are removed, it might be true that most local anomalies are not related to the rift structure but to the rock type on the surface. To the east of the Buhoro flats, for example, the contour lines are roughly parallel with the geological trend of the area and an abrupt decrease of Bouguer anomaly to the west is likely caused by the thick and folded Buanji series made up of an assemblage of Bukoban sediments with lavas.

A high anomaly, a relatively positive belt of Bouguer anomaly, is clearly observed on the Mbozi plateau located to the southwest of Fig. 4.

A profile close to the great north road is shown in Fig. 5 which represents Bouguer anomalies and topography across the rift valley. As shown in Fig. 4, the profile represents well an average anomaly distribution on the southwest side of the rift but not on the other side where anomalies are disturbed by the effects of Rungwe volcanics. Nevertheless the average Bouguer anomaly is considerably lower on this side than that on the Mbozi plateau, though rock types on both sides are almost similar.

As shown in Fig. 5, a high Bouguer anomaly of about 20 mgals is apparently caused by the high density of the Mbozi syenite-gabbro complex whose outcrops are observed in a fault zone extending to the northwest. To the southwest of the ultrabasic rocks the Bouguer anomalies tend to decrease owing probably to the branch rift described already.

The other low values seen in the Rukwa trough are associated with Rungwe volcanics and Cretaceous sediments as indicated in Fig. 5. The thickness of the sediments is not known but the trough of Bouguer anomaly is apparently caused by the sediments and volcanics.

Considering these facts, it might be concluded that the Bouguer anomaly distribution is characterized by a high value on the Mbozi plateau if the effect of surface meaterials are removed. Anomalies in narrow bands in Fig. 4 are simply related to the existence of ultrabasic rocks or unconsolidated sediments and volcanic ashes deposited in the rift valley.

Masange: Fig. 6 shows the Bouguer anomaly associated with a rift fault of about 300 m high shown in the same figure by the hatched zone, by which the area is divided into two; the east side of the fault is a wide plain similar to the Buhoro flats in Mbeya district and the other side is a plateau of basement rocks. There is a small branch fault extending southward. The height dif-

ference between both sides is approximately 200 m on the average, but the writer cannot find any sign of Bouguer anomaly associated with the branch fault.

The contour lines of anomaly are almost parallel with the escarpment and the anomaly is most negative near the escarpment, though it is small in quantity. Assuming that the anomaly is mainly caused by the sediments deposited in the down thrown side of the fault, the writer estimated the thickness at about 200 m near the escarpment if the densities of the sediments and of the basement rock are 1.8 g/cm^3 and 2.67 g/cm^3, respectively.

The thickness of 200 m is quite probable in this area, since the plateau is considerably erroded near the escarpment and a most negative part in Fig. 6 locates near an outlet of a big valley made by erosion.

From the decrease of anomaly to the northeast, the sediments are supposed to thin out monotonously on the plane.

Thus it may be suggested that the rift fault in this area does not show any significant Bouguer anomaly except an anomaly due to superficial sediments deposited after faulting.

ACKNOWLEDGEMENT

The writer is grateful to the Government of Tanzania who gave him the permission to conduct a gravity survey of rift valleys in Tanzania. Thanks are due to Geological Survey Division, Dodoma, for providing data necessary for the survey and also due to directors and other officials of Regional Offices for their cooperations. The writer wishes to acknowledge the helpful advices and suggestions of Dr. R. W. Girdler of the University Newcastle upon Tyne, Professor D. G. Osborn of University College, Dar-es-Salaam, Dr. H. Suzuki of Geographical Survey Institute, Dr. A. Okada of Earthquake Research Institute, and Prof. Dr. K. Iida of Nagoya University. The writer would like to express his appreciation to Dr. J. Hatsuda and Dr. E. Abe of Kyoto University for the use of gravimeter.

REFERENCES

[1] BULLARD, SIR EDWARD, Gravity measurements in East Africa: *Phil. Trans. Roy. Soc.*, A, 235, 445-531 (1936).

[2] GIRDLER, R. W., Geophysical studies of rift valleys: Physics and Chemistry of the Earth, Pergamon Press, **5**, 121-156 (1964).

[3] HOLMES, A., Principles of physical geology: Nelson Ltd. (1965).

[4] HOWELL, B. F., Introduction to geophysics: McGraw-Hill (1959).

[5] OVERSEAS, GEOLOGICAL, SURVEYS, Gravity survey of Tanganyika, 1958: Report presented to Geological Survey Division, Dodoma (1958).

[6] SMITH, D. M. and E. M. ANDREW, Gravity meter primary station net in East and Central Africa: *Geophys. J. Roy. Ast. Soc.*, **7**, 65-86 (1962).

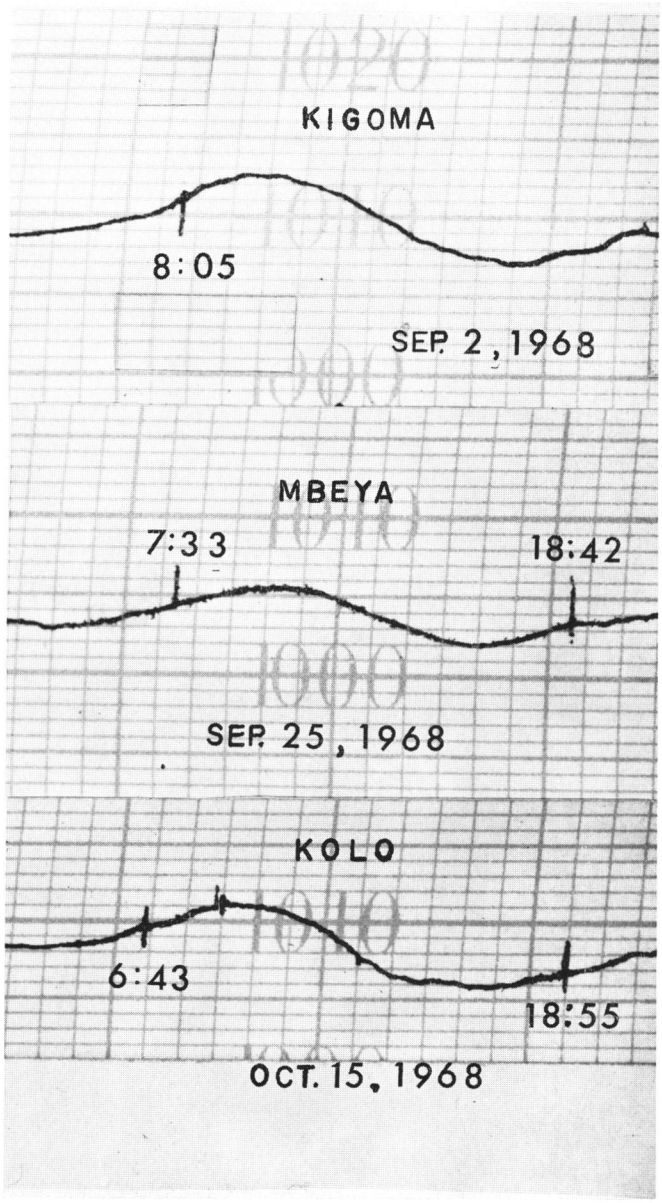

Examples of atmospheric pressure variation recorded on a barometer.

The palaeolithic site of Mgonga, Iringa District, Tanzania

Giichi OMI

Department of Archaeology, Faculty of Literature, Nagoya University

(Received 8 August 1969)

ABSTRACT

The Mgonga site is located about 7 miles north of Iringa. The Ihefu River runs through the region and forms a gully, where Quaternary sediments consisting mainly of sand and clay are exposed unconformably lying on Precambrian granitic complex and overlain by lateritic soil. This Quaternary deposits are tentatively called the Mgonga formation. A number of artifacts are found at the foot of a small cliff along the Ihefu River. Most of them are thought to have exposed from light gray clay of the upper Mgonga formation. Artifacts include many hand-axes, mostly pointed but a few almond-shaped, cleavers with a sharp transverse edge, stone balls, artificially shaped spherical stones, unmodified flakes, and flakes struck off when making tools. No fossil remains have yet been found, and excavation has not been carried out at the Mgonga site. The chronology of it can only be determined by referring to the typology of the unearthed artifacts. On that ground, the site is considered to have been formed in the Middle Acheulean period.

INTRODUCTION

It is well known that the Great Rift Valley is the important region for the study of prehistoric successions. This region has been inhabited by men since the palaeolithic age, and so it is wealthy in archaeological sites.

Prehistoric men were probably threatened in their livelihood by tectonic movements which concussed the region in the early Quaternary. Nevertheless, there is every indication that many of the palaeolithic sites concentrated in and around the Great Rift Valley. Perhaps lakes surrounded by swamps and grassy flood plains appeared on depressed ground shaped by tectonic movements. Animals came in swarm and fell in with palaeolithic men who were nomadic hunters in the lake basins. As pointed out by G. L. Isaac, "the geological conditions associated with the Gregory Rift Valley have ensured ideal preservation of fossil bones and stone artifacts".

Our party of Nagoya University African Rift Valley Expedition had an opportunity to study several famous palaeolithic sites, for example, Olorgesailie and Kariandusi in Kenya, Olduvai and Isimila in Tanzania etc. We could fortunately make an on-the-spot survey at a few sites which had not been

given out to the public. I intend to pick out one site from them —the Mgonga Site in Tanzania— and put down a preliminary report on it, and present a brief description for future work.

DISCOVERY OF THE MGONGA SITE

We visited the famous Isimila Palaeolithic Site, 13 miles southwest of Iringa, one of the greatest cities in the southern highlands of Tanzania, from October 9 to 12, 1968. At the night of October 11, Mr. Sopho Sarikas, manager of a hotel named "White Horse Inn", told us that Mr. J. R. Robert who was a geologist and teacher of Mkuwawa High School, had found a stone-age site in the north of Iringa a few days before. The next day morning, we had a time to call on Mr. Robert at the school, and we learnt that many implements of Acheulean type had been exposed on the erosion surface in a gully 7 miles north of Iringa. On that afternoon, under his and his co-worker Mr. Gerhard Bihl's guidance, we went to the site.

According to Mr. Robert, on October 5, 1968, he first discovered some stone tools lying on the floor of the gully at about 3 miles southeast of the Mgonga village. He saw lake sediments on the cliff, and he was convinced that the place was a palaeolithic site. It was 7 days before we get there. The previous year when he visited there for geological study, the place was overgrown with grasses. After that time, he said, implements had been exposed by erosion during the heavy rainy season.

TOPOGRAPHY

The site is situated about 7 miles north of Iringa, and about 2 miles west of the main Iringa-Dodoma Road (the Great North Road). There is an access road to the site from the highway. The place borders Ugongo Hill, the top of which is 6,200 ft. high, on the north, and on Ndalonga Hill, the top of which is 6,000 ft. high, on the south (Fig. 1 and Plate I-Fig. 1). There are extensively distributed red earths and weathered gneiss between the two hills [2]. A small stream called the Ihefu River runs approximately southeast to northwest through the region, and forms a gully. The head of the stream lies not far away to the southeast, and it joins with another stream at some three miles downstream from the site, and these two streams form together the Hoho River.

We can see Quaternary sediments consisting mainly of sand and clay exposed in the gully along the Ihefu River.

GEOLOGIC SETTING

The sediments unconformably lie on Precambrian granitic complex and

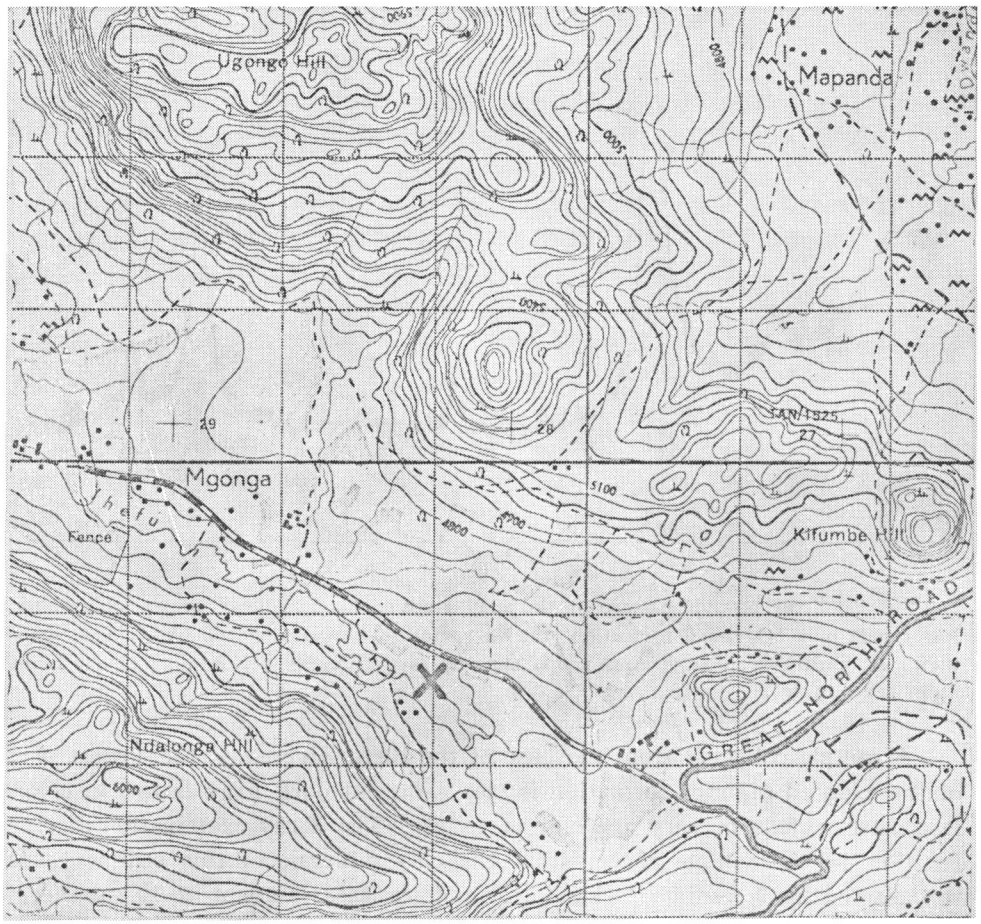

FIG. 1. Topographical map to show the position of the Mgonga Site. (Scale 1 : 50,000, Tanganyika Sheet 215/1 by the Director of Overseas Surveys).

are overlain by lateritic soil [2]. In this paper, this Quaternary formation is tentatively called the Mgonga formation, and its type locality is shown in Fig. 1. The Mgonga formation is distributed almost horizontally filling the depression along the present river (Plate I–Fig. 2), and its total thickness measured from the base of the Ihefu River to the uppermost flat surface of the formation is about 40 metres. It is composed of alternation of coarse clastic sediments such as granule sand or sand and clay, all of them being barren of megafossils. As is shown in Plate II–Fig. 1, a graded bedding is frequently observed in sandy layers, and considered to have been formed by a seasonal flood debouched into an inland lake. These sediments are rarely indurated throughout the whole succession and irregularly intercalate, especially in a lower part of the formation, many layers of caliche.

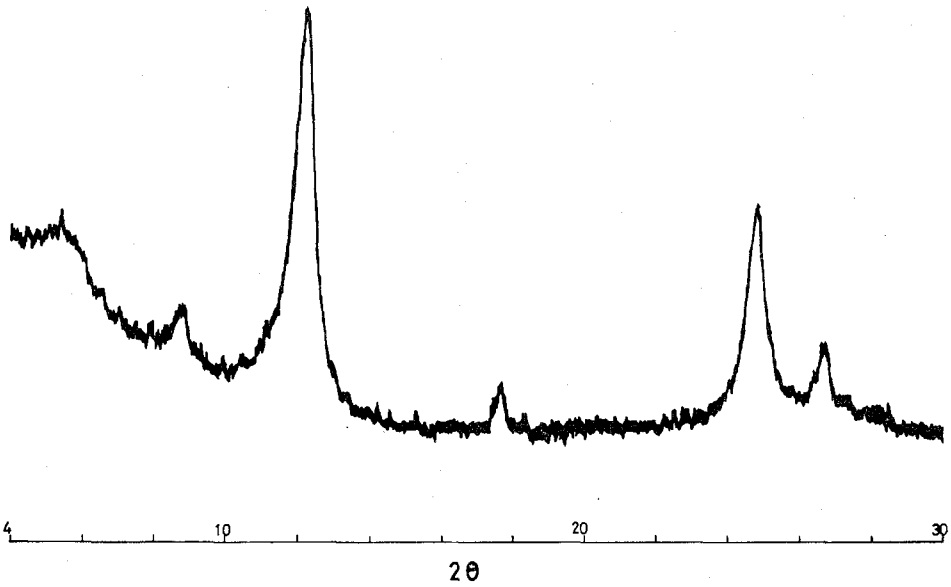

FIG. 2. X-ray powder pattern of the clay fraction in dark gray brown clay of the lower part of the Mgonga formation (Cu Kα radiation, nickel filter, 35 kV, 15 mA, scale factor 16, multiplier 1, time constant 4, canning rate 1 degree per minute, chart speed 1 cm per minute).

A sample collected from the base of the Ihefu River, *i.e.*, the lowest part of the exposed Mgonga formation is clay sediment dark gray brown in color. It consists chiefly of very fine clay particles. The X-ray examination of clay fraction in the sample reveals that the clay minerals of this sediment are represented by 7 Å-mineral (kaolinite) and by lesser amount of 10 Å-mineral (mica) as illustrated in Fig. 2. Electronmicrographs (Plate II–Fig. 2 and Plate III–Fig. 1) show that these clay minerals are very fine in size and irregular in shape; though obscure, hexagonal shape is observed sporadically. In this clay sediment is found a fragment of an organic crust that is probably diatom (Plate III–Fig. 2). It is interpreted that the inland lake in which the Mgonga formation was laid down was capable of propagation of diatom, and all the lacustrine sediments of the formation are prolific in this organism, although the remains are considerably diluted by clastic materials.

ARTIFACTS

Artifacts are found to scatter on the foot of small cliff and mixed with gravels of the upper part of the Mgonga formation. Under the laterite layer of 1.7 metres thickness, a layer of pale yellow brown sand containing large amount of rounded granule of quartz occurs which laterally thinns out and is underlain by light gray clay intermingling with sandy grains of quartz.

One of the artifacts is buried in this light gray clay about 3.25 metres lower from the base of the laterite layer (Fig. 3). Most of the artifacts are distributed now on the foot of a small cliff of the upper Mgonga formation and are thought to be washed out from the light gray clay (Plate IV–Figs. 1 and 2). The exact horizon of the artifacts cannot be determined. Judging from the present distribution of them, it is very likely that most of them are buried in this light gray clay.

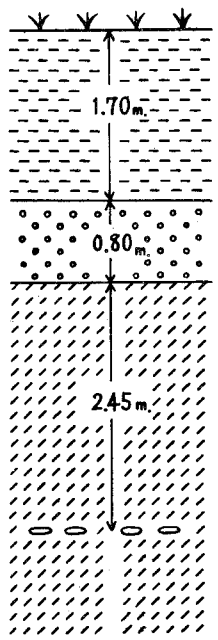

FIG. 3. Section showing the upper part of the Mgonga formation.

Artifacts include many Middle Acheulean hand-axes, mostly pointed but a few almond-shaped, cleavers with a sharp transverse edge, stone balls, artificially shaped spherical stones, unmodified flakes, and flakes struck off when making tools.

The principal stone tools —the hand-axes and the cleavers— are of simple but very characteristic type. Normal sized hand-axes are 13 to 18 centimetres long. They are fashioned from end-struck flakes, which were used almost exclusively for hand-axes, and most of the flakes were struck from prepared cores. Of the two cutting edges of them, one is very markedly more curved than the other, so that the tools form rather beak-shaped points. The butts are left almost untrimmed. There are only few almond-shaped hand-axes of flat bi-faced type and parallelogram-sectioned. They are likely to be fashioned from side-struck flakes.

The cleavers have a straight and sharp transverse edge at one end. The opposite end is roughly trimmed so as to have a rounded butt in outline. At this site, side-struck flakes were commonly used for cleavers. The primary flakes were struck off large prepared cores, and then, by only the minimum retouching, converted into well-shaped cleavers, and the edges of the primary flake were reduced to suitable proportions for grasping. In many of the implements, the bulb of percussion is flaked away. These represent the commonest forms of the cleavers at this site. However, there are a few examples of what are known as the parallelogram section cleavers. The outline of them is usually more or less rectangular, with a parallelogram cross-section. The butt-end is untrimmed and massive.

So far as we observed the raw materials of the stone tools with the naked eye on the spot, most of hand-axes and cleavers are made of hornblende porphyrite, and some made of quartzites and fine-grained granites. Most of stone balls are made of quartzite. Hornblende porphyrite supposedly occurs as dike rocks in granites and granitic gneisses, which are found to

distribute extensively in this area. Therefore, the majority of the materials of implements are available in the vicinity.

Now, we should call to mind of the famous Isimila Site of Developed Acheulean period which is about 20 miles distant from Mgonga. The following figures by the author's macroscopic discrimination are based on 74 stone tools made available to the public, which have been collected at a shelter "marked 1" (excavated by F. C. Howell of the University of Chicago in 1957–58), and show the relative proportions of the raw materials used for making those tools:

	Hand-axe	Cleaver	Core-chopper	Stone-ball
Volcanic Rock*				
alkalic volcanic rock (trachyte?)	25	9		
rhyolite	6		1	
devitrified obsidian	1			
Granite and Granitic Gneiss				
granite and granodiorite	3			1
granite gneiss	2	1		
gneissose granite	1			
quartzo-feldspathic gneiss	1			
Dike Rock				
porphyry	5	3		
porphyrite	2			
aplite	2			
diabase	1			
tourmaline-quartz rock (pegmatite)			1	
Quartz and Quartzite				
quartz (in pegmatite)	2		1	2
meta-quartzite	1			
Other				
hornblende gneiss	1			
welded tuff	1			
green phyllite (Karagwe-Ankolean?)	1			
Totals	55	13	3	3

* Some of them may be metamorphosed volcanic rocks such as metarhyolite belonging to be Karagwe-Ankolean system.

Though the implements have been collected at random and this table does not indicate accurate statistical figures, it is evident that the majority of hand-axes and cleavers are made of volcanic rocks, which are fine-grained and compact, and some are made of dike rocks, and granites and granitic gneisses. With regard to the stone balls, besides those cited in this table, we could observe many examples made of quartz and quartzites. Probably,

quartz is derived from pegmatite and quartz vein. We may understand that the Isimila Palaeolithic men chose the raw materials for each kinds of implements. Further, we should know that the alkalic volcanic rocks used predominantly for making the tools are not found in the vicinity. Thus, we can not help thinking that the greater part of the materials were brought from a distance, though dike rocks supposedly occur as dikes in the neighbourhood and granites and granitic gneisses are abundant in this area. It shows a remarkable contrast as compared with the raw materials in the Mgonga Site.

However, some stone tools, which are considered to be made of volcanic rocks, may be metamorphosed volcanic rocks. Therefore, there remains some possibility that some stone tools made of "volcanic rock" may have been originally brought from the Karagwe-Ankolean system in the neighbourhood. As already pointed out by Pickering [1], the petrology of stone tools remains to be resolved through future investigation.

CONCLUDING REMARKS

As no fossil remains have yet been found and excavation has not been carried out at the Mgonga Site, the chronology of it can only be determined by referring to the typology of the unearthed artifacts. On that ground, the site must be considered to have been formed in the Middle Acheulean period. Geologically, the upper part of the Mgonga formation was laid down probably during the Kanjeran Pluvial.

Though the uppermost laterite layer must be of post-Kanjeran Pluvial, there is no evidence except a fact that some potsherds are contained in it. By detailed examination of them, the chronology of the layer should be decided in future.

The petrology of rocks and stones in the vicinity from which materials of most artifacts must have been gathered, should be studied in detail. Scientific investigation of the interrelation between dwelling sites and stonepits in palaeolithic age is one of the most important subjects in prehistoric archaeology.

The site seems to afford great promise for archaeological excavation, and also will bring forth desirable results of geological information. And all will depend on the careful study in future.

ACKNOWLEDGEMENTS

In preparing this paper, I have received a great deal of help and advice from Drs. Kanenori Suwa, Kunihiko Miyakawa and Shinjiro Mizutani who were members of Nagoya University African Rift Valley Expedition and worked at Mgonga with me. I wish to express my deepest gratitude to

them. We are greatly indebted to Mr. J. R. Robert for his kindness to give us fruitful guidance and valuable suggestions on the Mgonga Site. His finding of artifacts at this site stimulated and enabled us to visit and study there with a great enthusiasm. I should record his name with many thanks. At last, but not least, I would like to express my thanks to Prof. Isao Matsuzawa, leader of Nagoya University African Rift Valley Expedition, and to Prof. Shoichi Sumita for their encouragement given to me throughout this study.

REFERENCES

[1] PICKERING, R., Report on the Pleistocene beds exposed on the Isimila River, Iringa District: *Geol. Surv. Tanganyika*, Rept. No. RP/4, 4 pp. (1957).

[2] WHITTINGHAM, J. K., Geological Map "Iringa" Quarter Degree Sheet No. 215: *Geol. Surv. Tanganyika* (1962).

PLATE I

FIG. 1. The Mgonga Site seen from the Iringa-Dodoma Road; Ndalonga Hill (on the left side) and Ugongo Hill (in the centre).

FIG. 2. The upper part of the Mgonga formation around the site.

FIG. 1

FIG. 2

PLATE II

FIG. 1. Alternation of graded sand and clay of the middle part of the Mgonga formation.

FIG. 2. Electron micrograph of clay of the lower part of the Mgonga formation ($\times$15,000).

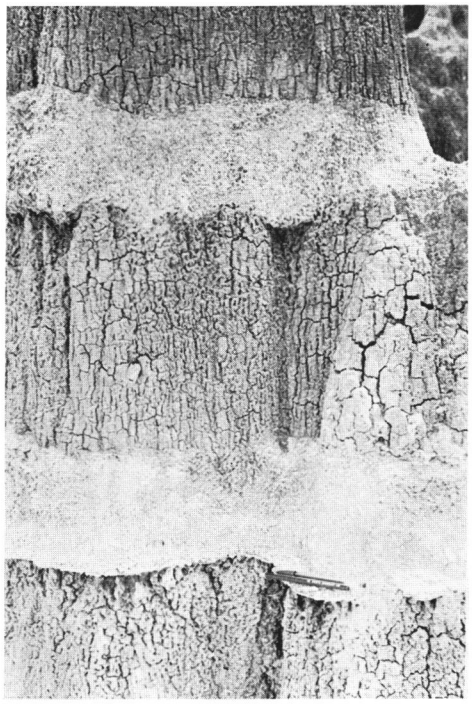

FIG. 1

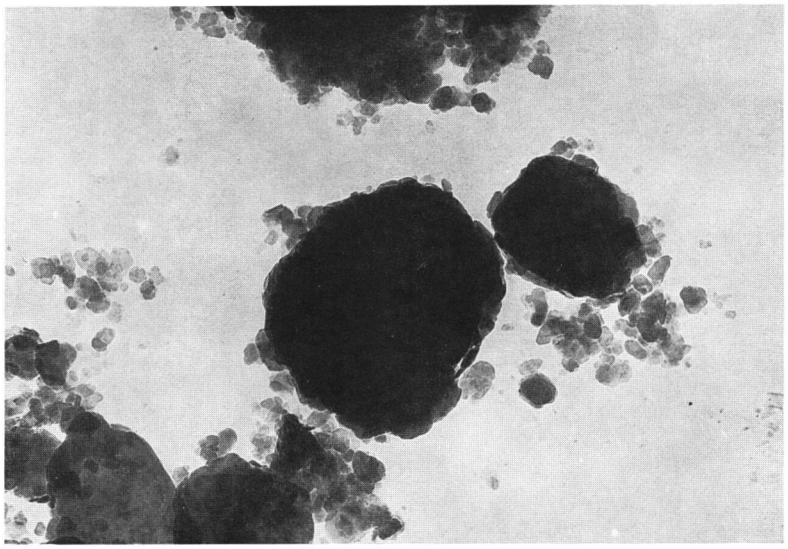

FIG. 2

PLATE III

FIG. 1. Electron micrograph of clay of the lower part of the Mgonga formation ($\times$9,000).

FIG. 2. Electron micrograph of clay of the lower part of the Mgonga formation showing a fragment of diatom ($\times$14,000).

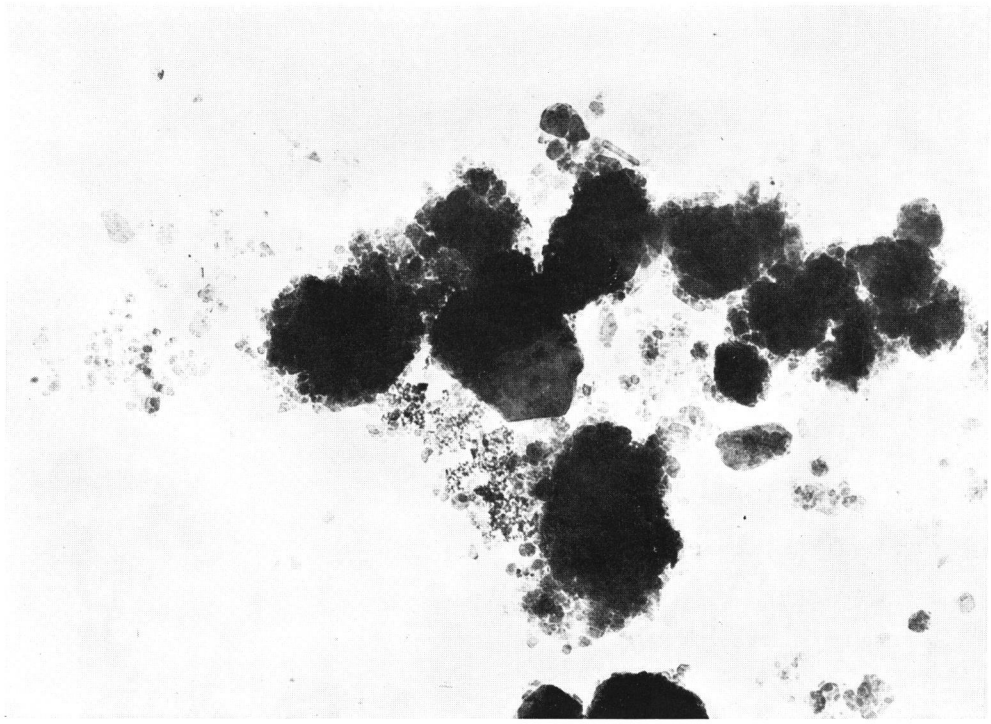

FIG. 1

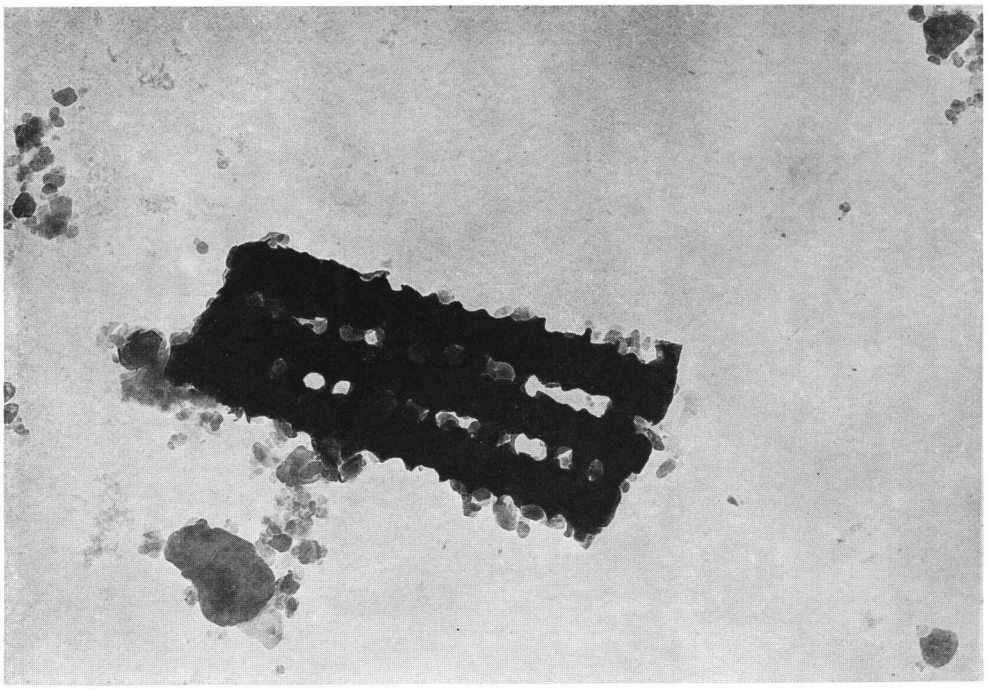

FIG. 2

PLATE IV

FIG. 1. The upper part of the Mgonga formation at the Mgonga Site.

FIG. 2. Artifacts and stones, which are found to scatter on the foot of the cliff at the Mgonga Site.

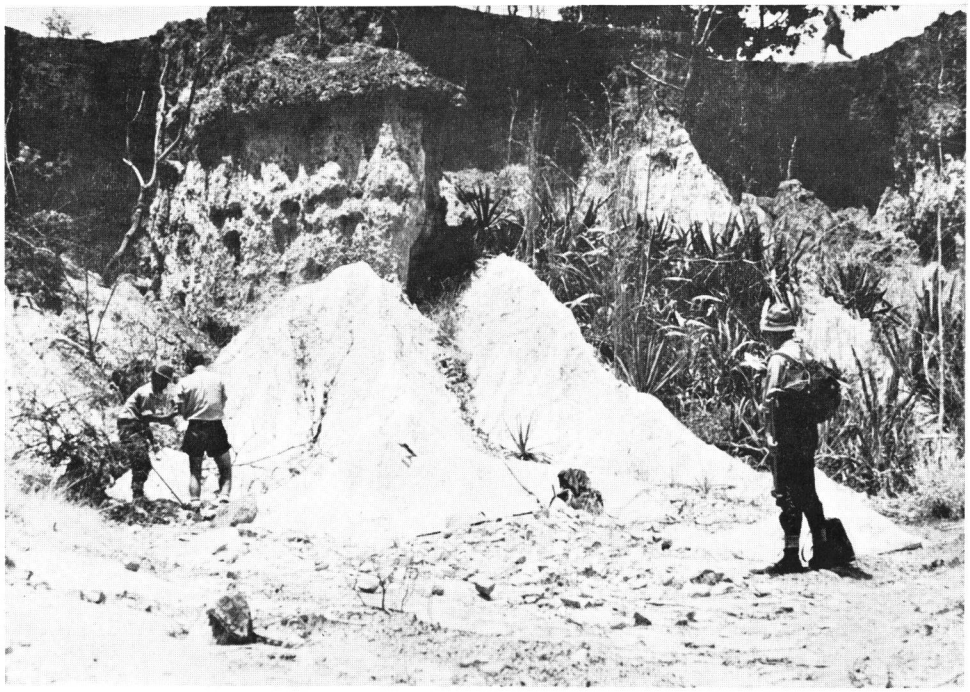

FIG. 1

FIG. 2

Tanzanian patients

Hidehiko KURIMOTO*

School of Medicine, Nagoya University

(Received 16 August 1969)

When I travelled round several regions of Tanzania, as a physician of our team, I had opportunities to visit hospitals and observe patients in this country.

Tanzania is located nearly under the equater, covering twice and a half as big area as Japan. Its climate is not so good; the half of a year being dry season, the other half wet one. But the change in atmospheric temperature is little throughout the year and, although it is very hot in the sunshine, it is more comfortable in the shade than in Japanese summer season because of low humidity.

The population of this big country is a little more than twelve millions and its population density is higher along the coast of Indian ocean and the lake-sides than in the other areas. There are only a few people living in woods, savannahs and highlands of the inland areas, for instance, in Tabora Region the number of inhabitants is only a little more than ten per square mile. Tsetse flies and wild animals are spreading in these areas, and several zones of inland are designated as for game reserves and national parks.

In 1964 Tanganyika and Zanzibar became an independent country named Tanzania. This new country is now getting more and more progressing and the government is making a great effort to establish lots of facilities to educate young people or to get rid of various diseases. The system of school education is the following; primary schools of seven years, secondary schools of four years and an university college. A schoolteacher told me that these days eighty per cent of children go to primary school, but it is only thirteen per cent that go to secondary school. At Dar es Salaam, the capital of this country, there is only one university college and it produced the first graduates of the medical course last year.

A hundred of tribes of Tanzania, most of them being the Bantu, are engaged in agriculture or semi-agriculture and semi-cattle-breeding. Their houses are made of wall of soil or burnt soil-blocks and roof of grass. Almost all houses have some small and dark rooms and a few small windows. The usual food of inhabitants is called Ugali, which is just like Japanese

* Present Adress: Department of Pathology, Cincinnati General Hospital, Ohio, U.S.A.

"dango" of maize's or cassava's flour. They eat ugali every day with beaf, matton, potatoes, mchicha, carrots etc. Banana is a usual food instead of ugali in the rainy areas. These foods for adults and young children after weaning are, however, foods of low protein. So we could find many children of mulnutrition, Kwashiorkor (Plate I, Figs. 1 and 2). But skim milk provided for them by UNICEFF is insufficient.

So many kinds of posters for medical enlightenment written in Kiswahili are hung on the walls of dispensaries and hospitals: "Mama - eat meals or eggs or fishes when pregnant", "Mosquito-net for prevention of malaria", "Have footwears on - not to get wounded", "Dusts and flies are sources of illness", "The clean air for tuberculosis - make a window" (Plate II, Fig. 1). But a remarkable improvement has not yet been made because of poor life and insufficient knowledge of hygiene. A Medical Officer's report to the government in a certain district says: "·····The maternity and child wellfare clinics were taken over by the District Council Midwife. Attendances are on the low side, mainly confined to wives and children living in the police or prison lines. With greater publicity and extra staff, more could be done".

Although each tribe has its own traditional manners and customs, each tribe, excluding the Masai, is cooperative with the government, because each understands that both education and medicine are very important. The Masai has the pride that the tribe is the one elected by God and proud highly of their own traditions. They are said to eat nothing but beaf, milk and cattle's blood. A doctor in that region told me that an old patient of Masai had drunk blood for transfusion beside the bed.

This country is still poor and comparatively low populated with the wideness of the land, and daily life is awfully inconvenient. Indeed, there are markets, but some of them are situated in the centre of uncultivated bush or tree-savannahs, and so people must walk many miles in the strong sunshine or wait long to take only a few busses, in order to get some foods, clothes and daily necessities. Along the coast of lakes people live on a narrow flat ground between cliffs and they have to row a canu for more than one hour to go to a neighbor village beyond a promontory. Such traffic condition also makes it very difficult to come to medical facilities.

Tanzania is composed of seventeen regions and sixty districts and each region has a Government Regional Hospital, where the director holds concurrently the Regional Medical Officer, and one or two doctors and two or three assistant doctors are working with him (Plate II, Fig. 2 and Plate III, Fig. 1). There is Government District Hospital in each District and in most cases, it has one doctor and one or two assistant doctors. Each district is divided into from twelve to twenty villages, which have dispensaries with one assistant doctor only. Besides these government facilities, there are fifty-four voluntary agencies including missionary and Aga-Cahn foundation, which cover half of

total beds in Tanzania and play an important role in medical services. These voluntary agencies have more staffs and are well off and generally better than the government ones. I heard some people went rather to missionary dispensary because government dispensary had few medicine. One dispensary has to cover from ten to twenty miles around, and so most patients can not come easily from so far away. Even a pregnant woman comes twenty miles on foot for delivery.

We have a rather wrong idea that Africa is infested with strange and awful diseases; however, the incidence of communicable diseases like yellow fever, small pox or cholera in this country has now decreased owing to vaccination; and 20~30 cases of yellow fever are reported a year, a few thousand cases of small pox, and recurrent fever and undulant fever are sporadic. Infection from respiratory tract, including every kind of pneumonia, occupies the highest rate of incidence. Measles and whooping cough threaten children's life and these cases are received in isolation wards. If a child becomes ill, he gets successive sequelae on the ground of imperfect nourishment and dies of pneumonia finally. The mortality of infancy is fifty-four per cent and the average span of Tanzanian life is consequently thirty-five years old. Enterocolitis as bacterial and amoebic dysentery and gonococcal infection are also common (Plate IV, Fig. 1).

People work and walk in bushes without trousers and foot gears, and get wound so often. In most cases, they are secondarily infected. There are many cases of ascariasis and ankylostomiasis, as a result of which pregnant women receive not rarely blood transfusion before delivery.

Granulomatous diseases like tuberculosis and leprosy are prevailing throughout the country and so the government has seventeen sanatoria of leprosy and four sanatoria of tuberculosis (Plate IV, Fig. 2 and Plate V, Fig. 1). Only a half of leprous cases are under medical care and I sometimes noticed some lepers among pedestrians at Dar es Salaam.

Malaria, which is a notorious protozoan disease here, seems to have invaded ninety per cent of the population. About ten per cent of cases are dealt with at hospitals and clinics as clinical malaria, and this percentage has not changed these sixty years. I noticed that a retail store in a thorn tree-sevannah of the interior sold five tablets of anti-malarial drugs for fifty yen in Japanese money, arranging soap and other daily necessities, but our driver said there were few people who could afford to buy these tablets.

The commonest causes of death reported by the main hospitals in 1966 were the followings:

	1966	1965
Pneumonia (all forms)	1,300	955
Malaria (all forms)	797	320

Gastro-enteritis (all ages)	540	373
Diseases of the heart	509	206
Tuberculosis (all forms)	495	331
Effects of violence and poisoning	494	266
Anaemia (all forms)	471	282
Tetanus	462	402
Defective nutrition	436	222
Conditions of early infancy	295	227
Pyrexia of unknown origin	281	76
Meningitis (all forms except tuberculosis)	252	156

It is regretable that we should say we cannot completely trust in the diagnoses of the cases, because most hospitals have not enouth staffs and sufficient laboratories. We, however, could know what kinds of diseases are prevailing by the above-mentioned.

African sleeping sickness and Bilharzia are well known as tropical diseases of this country. African sleeping sickness carried by tsetse flies is an endemic and is prevalent especially in the inland area on the eastern side of Lake Tanganyika. The areas infested with trypanosoma-infected tsetses extend over as wide as sixty thousand square miles, and in former days some villages in these areas had been devastated. The population density is even now very low in these areas just as being clearly seen through the cattle and tsetse distribution maps. There are check points at any border in these infected areas and the guard removes, with an insectnet, all tsetse in the cars coming out of the infested areas. The incidence of sleeping sickness is about 500 a year, the mortality being 11.8 per cent.

Bilharzia is widely spreading around lake. The water of lakes, rivers and swamps is infested with larvae and people cannot help using the infested water in daily life. Over twenty per cent of the children and more than ten per cent of the adults living near Lake Victoria show normal and healthy life superficially, but they were found that they had permanent and irreversible damage in the urinary tract through Bilharzia.

It would be a long time before to expel these endemic diseases and such simple and preventable diseases as pneumonia, enterocolitis, etc. I hope, however, that this country would make more and more progress in various fields. Even when I was there I saw farms getting gradually and steadily cultivated, roads getting well constructed, and pupils studying and playing in colourful uniforms.

I explained Tanzanian medical services and other things there. And now here in Japan, looking around us, we find most people seeking only worldly riches and absorbed in enjoying a personal life. In other words, we do merely see things and events superficially, that is, we do not try to think

over what these things and events mean really.

For instance, speaking of medical services, we see the drugs overflowing here and there, when their children have a fever, mothers would not be satisfied if they do not get an antifebrile from the doctor. Office-workers come to clinics and require an intravenous injection of so-called "eutrophic", only because of getting tired. On all occasions we would not be satisfied without drugs and are foolishly obsessed with even a fixed idea that an injection is better than an internal medicine.

We seem to be unconscious that doctors and drugs alone do not cure illnesses. In order to keep and promote health, all the member of the society should not be indifferent to medicine and they have to endeavor to take right and earnest attitude to medicine.

PLATE I

FIG. 1. An infant of kwashiorkor at Iringa - Hair discoloration, complicated scabies and general edema noticed.

FIG. 2. A mother and her two-year-old child of kwashiorkor at Kigoma - Skin dyspigmentation and reduction of quantity of hair noticed.

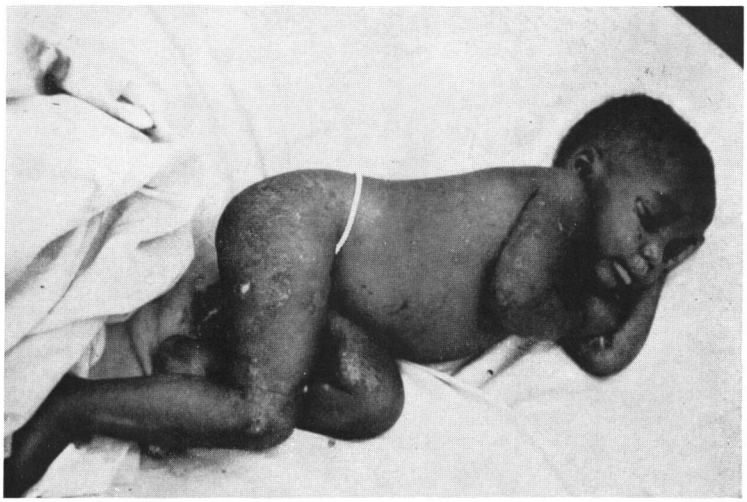

FIG. 1

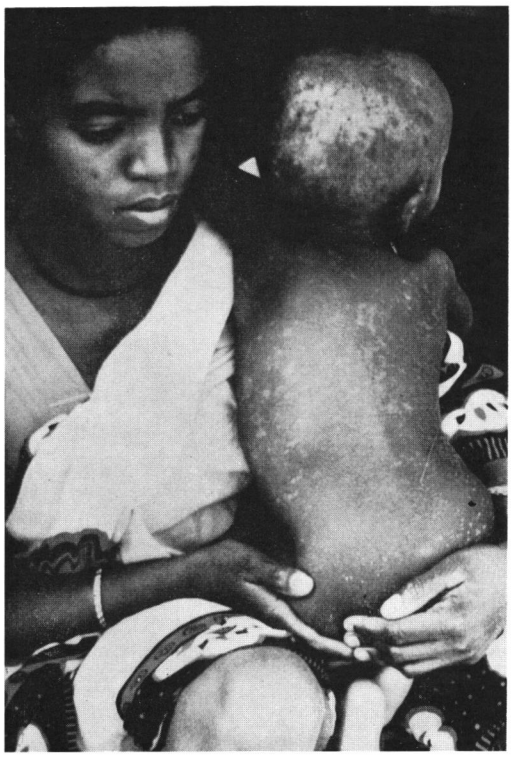

FIG. 2

PLATE II

FIG. 1. "Mama eat these foods".

FIG. 2. A ward of Kyela District Hospital in the afternoon - Every ward has mosquito-nets.


MAMA MJA MZITO
ANAHITAJI
VYAKULA
HIVI
NYAMA
SAMAKI
MAYAI
MAHARAGWE
N 42

FIG. 1

FIG. 2

PLATE III

FIG. 1. Wards of Dodoma Regional Hospital.

FIG. 2. Patients of convalescent stage at Iringa Regional Hospital.

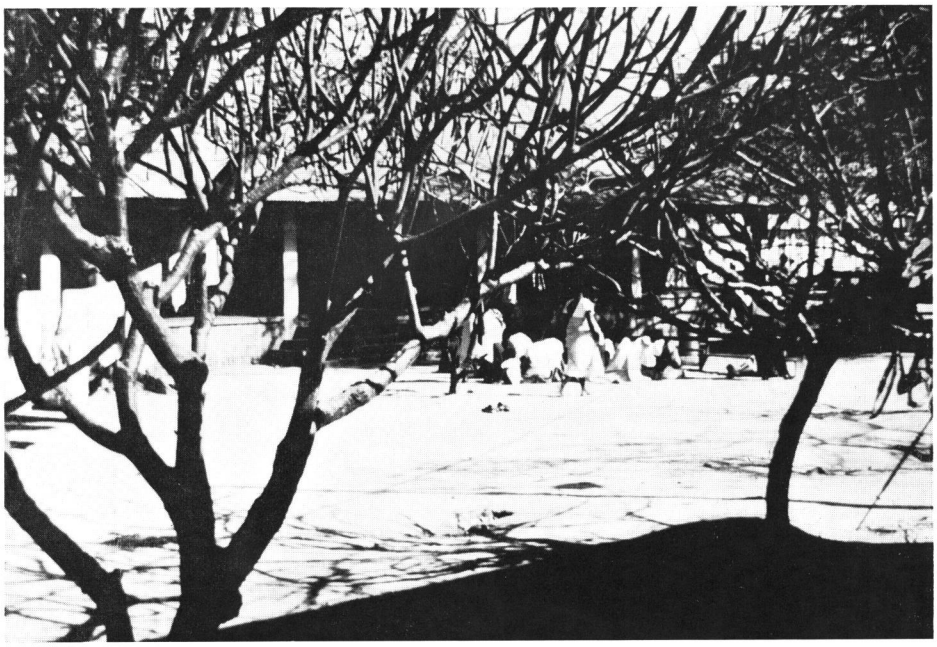

FIG. 1

FIG. 2

PLATE IV

FIG. 1. An old woman of dehydration with bacterial enterocolitis at Mbozi.

FIG. 2. Leprosy Sanatorium of Kola Ndoto.

FIG. 1

FIG. 2

PLATE V

FIG. 1. A Village at Makete where mild leprous cases are living.

FIG. 2. A check point of tsetse flies.

FIG. 1

FIG. 2